Experimental analysis of a Gene Regulatory Network underlying stable melanocyte differentiation

Vibert, Laura

Award date:
2013

Awarding institution:
University of Bath

Experimental analysis of a Gene Regulatory Network underlying stable melanocyte differentiation

Laura Vibert

A thesis submitted for the degree of Doctor of Philosophy

University of Bath

Department of Biology and Biochemistry

September 2013

Acknowledgements

I would like to acknowledge my supervisor, Prof. Robert Kelsh, for trusting me four years ago to work on a great project. This work permitted me to grow in my understanding of Genetics and Science. Thank you for helping and supporting me during these five years, through all the experiments, conferences, talks, writing up and all the frustration which can come with these activities.

Thank you very much to Prof. Melanie Welham for sharing her stock of GSK3 inhibitor with me. Thank you to Nick Parkinson for conversations and advices on qPCR experiments. Thank you to Dr Andrea Rocco for its collaboration on this project.

I would like to thank everyone in two labs in room 0.76 for scientific help and for making this experience an amazing human adventure. I would especially thank Masataka Nikaido for his precious help and patience, as well as his wisdom in approaching science. Fred, Marta, Anne, Gaby, Yolanda and Kim for their friendship and all the great moments and intense discussions we had around litres of coffee.

I would like to thank my family and my friends for support and for allowing me to escape science when necessary, none of this would have been possible without them. I would like to thank this PhD in Bath for being the excuse life found to put JB on my way.

Finally and importantly, I would like to thank University of Bath for funding... and fish for their beauty.

« Ce n’est pas assez d’avoir l’esprit bon, mais le principal est de l’appliquer bien »

René Descartes

Abstract

The study of the neural crest is fundamental in answering questions that arise in both Stem Cell Biology and Developmental Biology. This project focuses on the development of a neural crest derivative, the melanocyte. In zebrafish, melanocyte specification depends upon the Sry-related High Mobility Group box gene (*sox*) *sox10* and Wnt signalling to drive the transcription of *mitfa* (microphthalmia-associated transcription factor). However, the mechanisms involved in stable melanocyte differentiation are not fully understood. *In vivo* data suggested that *sox10* formed part of a Feed-Forward Loop repressing melanocyte differentiation and is relieved by Mitfa-dependent repression of *sox10*. Aspects of the melanocyte gene regulatory network derived from experimental data and mathematical modelling were tested with the aim of improving the understanding of melanocyte biology.

Modelling predicted an unknown factor, named Factor Y, was involved as a limiting factor for the maintenance of *mitfa* expression in differentiating melanocytes. Wnt signalling was tested as a candidate for this factor by investigating the effects of small molecule activators of the pathway during melanocyte differentiation. Resultantly, we observed increased cell dendricity, disruption of cell organisation pattern in the head of embryos and activation of *mitfa* expression. However, no other pronounced changes in cell differentiation were seen. Therefore, we suggest that maintenance of *mitfa* and of melanocyte differentiation would depend on a complex regulatory ensemble which includes factors other than Wnt signalling.

sox10 and *mitfa* expression levels were characterised through time using the Real-time Quantitative Polymerase Chain Reaction to quantify the genetic variability occurring during melanocyte derivation. The previously described decrease of *sox10* expression in melanocyte lineage was confirmed. Unexpectedly, the decrease of *mitfa* expression was observed suggesting that *mitfa* is maintained at low levels in melanocytes where stochastic effects could be important. This could also suggests the existence of a new unknown factor involved downstream of *mitfa* for melanocyte differentiation.

The role of histone deacetylase (Hdac(s)) as a candidate repressor of *sox10* expression during differentiation was investigated in melanocytes. Treating embryos with Hdac(s) inhibitor caused the regression of melanocyte differentiation and the persistence of *sox10* expression in melanocytes. These results suggested a potential role for Hdac in Mitfa-dependent downregulation of *sox10.*

Table of Contents

Chapter 1. Introduction

1.1 Developmental biology and Gene Regulatory Networks

Developmental biology aims to describe the genetics and the cellular mechanisms involved in organism development. Morphogenesis and fate restriction in multipotent cells are key processes explored in the field. These processes are organised by Gene Regulatory Networks (GRN)s which coordinate the mutual regulation between key factors to allow fate choice and specific cell type development. Understanding how different cell types emerge from multipotent and pluripotent cell populations, and how GRN regulate the developmental process for each cell type remains a challenge.

1.2 Neural crest as a model for stem cell biology and developmental biology

The Neural Crest (NC) is a dynamic and transient structure made of multipotent cells which delaminate from the neural tube and migrate throughout the embryo, giving rise to an extensive range of derivatives (Donoghue *et al.*, 2008, Sauka-Spengler and Bronner-Fraser, 2008b, Raible *et al.*, 1992, Eisen and Weston, 1993, Weston, 1970, Dupin *et al.*, 2007). Cells stemming from the NC are of two broad classes, the ectomesenchymal and the non-ectomesenchymal tissues. The ectomesenchymal tissue includes all skeletogenic cell types such as, chondrocytes, odontoblasts, osteocytes and craniofacial cartilage for instance (Cerny *et al.*, 2004, DeLaurier *et al.*, Hall *et al.*, 2006, Hanken and Gross, 2005, Schilling *et al.*, 1996, Schneider, 1999, Walker and Trainor, 2006). The non-ectomesenchymal tissue consists of all neuroglial cell types, including sensory neurons, enteric neurons, Schwann cells, but also pigment cell types, such as, black melanocytes and in zebrafish, yellow xanthophores and shiny iridophores (Baroffio *et al.*, 1991, Dupin *et al.*, 2007, Donoghue *et al.*, 2008, Bronner-Fraser and Fraser, 1991, Kelsh *et al.*, 1996a).

1.2.1 Neural crest as a model for stem cell biology

NC cells exhibit both multipotency and self-renewal which are the two properties of stem cells. Studies in chick, quail and mouse have shown that NC cells could be self-renewing (Dupin *et al.*, 2000, Stemple and Anderson, 1992, Real *et al.*, 2006, Le Douarin *et al.*, 2004, Trentin *et al.*, 2004). *In vitro* analysis of primary cultures of avian, mouse and *Xenopus* premigratory NC cells showed that cells were multipotent (Stemple and Anderson, 1992, Dupin *et al.*, 2003, Bronner-Fraser and Fraser, 1991, Baroffio *et al.*, 1988, Bronner-Fraser and Fraser, 1988, Baroffio *et al.*, 1991, Le Douarin and Dupin, 2003). Furthermore, *in vivo* analysis of single NC cell tracing using intracellular injection of

rhodamine dextran in zebrafish showed, that while migrating, the multipotent cells of the NC were differentiating in the same fates as the ones observed from NC cells in mouse, *Xenopus* and chick (Raible *et al.*, 1992). Two models can be described, the direct and the progressive fate restriction model. In the direct restriction model cells become restricted to one fate directly from the fully multipotent state and before migrating. In this case, migrating cells are committed to a fate. In contrast, the progressive restriction model suggests that cells become restricted gradually via a series of several partially restricted intermediates and that this process occurs throughout migration. Consequently, in this case, migrating cells could be partially restricted precursors.

Testing these models by investigating the existence of intermediaries and describing their heterogeneity will be of crucial importance *in vivo*. Studies analysing the potentiality of quail NC cells in clonal cultures demonstrated that pools of migrating cells consisted of heterogeneous precursors and highly multipotent cells (Dupin *et al.*, 2007). However, it remains unclear if all cells of the multipotent pool have the same potentiality prior to dispersion. Accordingly, it will be important to direct research towards resolving the relationship between individual NC cells and the NC niche *in vivo* to understand the signals responsible for the activation of factors which are involved in inducing transition between precursor intermediaries (Raible *et al.*, 1992). Consequently, the study of fate restriction and self-renewal in the multipotent pool of NC cells is a relevant model for stem cell biology.

1.2.2 Neural crest development as a model for developmental biology

In vertebrate embryos, NC development is a process of complex aspects and three characteristics together are unique to the NC: its origin at the neural plate border; its extensive migratory ability; and finally, its multipotency. Consequently, NC appears to be an excellent candidate as a model for development biology in general.

The NC developmental process is unique and happens early in the development of the embryo. It is crucial for the early structure of the embryo and the future fully developed organism as NC derived cells are involved in the establishment and development of many systems. Therefore, studying NC development is also, more broadly, a model for development in general. NC development starts during gastrulation, it is first induced at the neural plate border, between the non-neural ectoderm and the neuroectoderm, at the dorsal tips of the developing future nervous system, alongside the complex process of the neural plate induction (Figure 1.01) (Colas and Schoenwolf, 2001, Dupin *et al.*, 1993, Le Douarin, 1999). It continues through, and in parallel with neurulation and lasts until late organogenesis (Bronner-Fraser, 2003). The neurulation process is accompanied by morphogenetic changes. The paraxial mesoderm changes morphology while the neural plate folds to form the neural tube as described in Figure 1.01. In the anterior region of the embryo epithelial pleats merge to become the ectoderm epithelium and the neural tube in *Xenopus*, mouse and chick (Mayor *et al.*, 1999, Thiery *et al.*, 1982, Le Douarin, 1980, Bronner-Fraser, 2003, Hall, 2008). In zebrafish, as in all teleosts, a ventral increase of the ectoderm thickness forms a neural keel (around 10 somites/14 hour post fertilisation (hpf)) (Lamers *et al.*, 1981, Raible *et al.*, 1992, Eisen and Weston, 1993). In this case there is no

formation of neural folds. By 16 somites (17 hpf) in zebrafish, the neuroepithelium develops a central canal internally and can be referred to as a neural tube (Raible *et al.*, 1992). Subsequently, cells of the NC undergo an epithelial to mesenchymal transition (EMT), in part due to cytoskeletal re-organisation (Gammill and Bronner-Fraser, 2003, Dupin *et al.*, 1993). After delamination from the neural tube, cells of the NC acquire migratory capacities and migrate throughout the embryo in between the ectoderm and the somites or between the somites and the neural tube.

These events, altogether, are orchestrated by a complex GRNs cascade (Meulemans and Bronner-Fraser, 2004, Sauka-Spengler and Bronner-Fraser, 2006, Dupin *et al.*, 2007, Le Douarin, 2001). Experiments have proved that resolving the sequence of gene expression and factor activities involved in these processes can be conflicting when studying different model organisms due to the fact that the timing of events can vary throughout species (Sauka-Spengler and Bronner-Fraser, 2008a). Consequently, understanding the GRN coordinating the development of each NC cell derivative remains a great challenge for developmental biologists. The next step of NC development research is to determine the dynamics of the regulatory networks at play in individual cells within the NC cell population and the role of NC niche in events occurring through its development (Raible *et al.*, 1992). Below, we describe what is currently known about NC induction, NC specification, NC cell delamination and NC cells specification and migration.

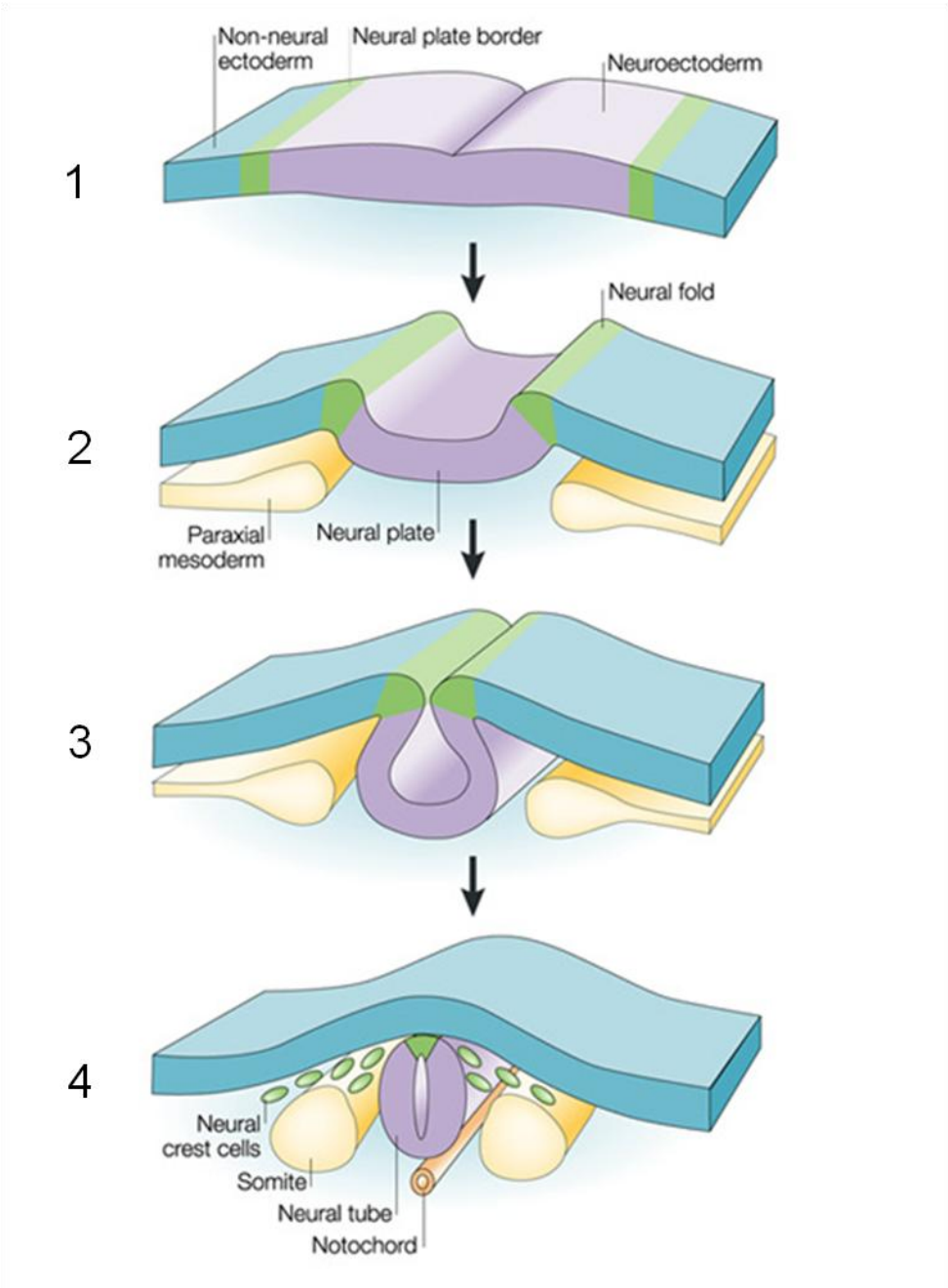

Figure 1.01: The formation of the neural crest is a dynamic process.

Neural crest cells are first induced at the neural plate border (green) (1), between the non-neural ectoderm (blue) and the neuroectoderm (purple). During neurulation, the paraxial mesoderm changes morphology while the neural plate folds (2) to form the neural tube (3). Once the neural tube is closed, cells of the NC undergo an epithelial to mesenchymal transition (3-4, not clearly represented) and migrate throughout the embryo, in between the ectoderm and the somites or between the somites and the neural tube. (reproduced with the kind permission of Gammill and Bronner-Fraser, (2003))

1.3 Evolutionary development of neural crest

In terms of evolutionary origin, the NC is described as a cell population located between the dorsal neural tube and the epidermis and it is considered to be a vertebrate novelty. However, it is crucial to understand NC in the context of its evolutionary history and to bear in mind that its complexity in vertebrates could have been built upon an ancestral genetic simplicity (Donoghue *et al.*, 2008). In the Tunicates, a population of migrating cells stemming from an area close to the neural tube was found to be comparable to the neural crest (Jeffery *et al.*, 2004). A recent study tested gene expression and derivation of the pigment cell lineage in the urochordate *Ciona intestinalis* and showed that the cephalic melanocyte lineage existed in Tunicates (Abitua *et al.*, 2012). Abitua *et al.*, (2012) showed that these cells expressed key markers of the neural plate border as well as NC specification markers such as Snail, Id or the Forkhead Box factors D (FoxD)s. In this model, induction of a mesenchyme determinant, *twist*, could reprogram cells of the ectoderm into migrating mesenchyme. Thus, the recruitment of certain factors, required for mesenchyme determination could have been a crucial event for formation of the NC cells from the neuro-ectoderm (Abitua *et al.*, 2012). The study suggested that the GRN underlying melanocyte lineage development probably existed before the divergence of Chordates and Tunicates (Abitua *et al.*, 2012).

1.4 Neural crest development is disrupted in many human diseases

Defects in NC development are called neurocristopathies. They are numerous in humans, and include the Waardenburg syndromes (WS) and Hirschprung disease. During the development they affect distinct organs and systems stemming from NC (Chen *et al.*, Lee *et al.*, 2000, Antonellis *et al.*, 2006, Bondurand *et al.*, 2000, Potterf *et al.*, 2000, Badner *et al.*, 1990, Boissy and Nordlund, 1997). Sensorineural hearing as well as myogenesis is disrupted in WS and craniofacial structure can also be perturbed. Nerve cells of the large intestine are affected in Hirschprung disease causing the aganglionic megacolon disorder. Melanocyte development is affected in neurocristopathies and disruption of melanocyte development is the cause of several specific diseases. Defects of cell specification are the cause of WS, defects of cell proliferation can be the cause of melanoma cancer, defects of cell differentiation are responsible for albinism and defects of cell survival can result in vitiligo (Lee *et al.*, 2012, Lee *et al.*, 2000, Lucky and Nordlund, 1985, Halaban *et al.*, 1988). Research which aims to understand the mechanisms involved in the development of the NC is fundamental for understanding the genetic basis for these disorders.

1.5 Melanocyte related disease in human

There are numerous melanocyte disorders in humans (Hodgkinson *et al.*, 1993, Lucky and Nordlund, 1985). Some of the main disorders are described here in order to better outline the importance of studying melanocyte development. Two generic terms often used interchangeably to denote these disorders are leukoderma and hypopigmentation, whereas several terms describe the degree of loss of melanin content. For instance, hypomelanosis designates a decrease of melanin within the skin; amelanosis suggests the total absence of melanin; and the loss of pre-existing melanin pigmentation is called depigmentation as observed in the disease vitiligo (Boissy and Nordlund, 1997, Lucky and Nordlund, 1985). Vitiligo is an idiopathic disorder defined by appearance of depigmented patches and has a worldwide incidence of less than 1 % (Lee *et al.*, 2012). Loss of melanocytes in the skin can result from several causes, including autoimmune reactions, genetic disruptions and oxidative stress (Hedstrand *et al.*, 2001, Lee *et al.*, 2012, Jin *et al.*, 2007, Pietrzak *et al.*, 2012). One therapy for vitiligo consists of exposing the skin to UVB light from UVB lamps (Don *et al.*, 2006). As alternative treatment, shown in a study from Olsson and Juhlin, (2002), found that melanocytes could be transplanted for re-pigmentation of the white skin patches, however, the longevity of cell survival was limited and variable between patients. Vitiligo is also often observed in the hereditary disorder, autoimmune polyendocrine syndrome type I (APS I), and it involves immunoreactivity against SOX10 and SOX9 (Hedstrand *et al.*, 2001). Interestingly, both *KIT* and *FOXD3* expression have also been shown to be involved in vitiligo (Goding, 2007). One hypothesis for this mechanism suggests it could involve the loss of melanocyte survival genes such as *KIT*, *MITF* or *BCL-2*. The model proposed suggested that melanoblasts containing the *FOXD3* variant promoter sequence would show increased *FOXD3* expression which would cause alterations in melanocyte development (Alkhateeb *et al.*, 2005). However, the complete role of *FOXD3* and *KIT* in the progression of vitiligo remains to be clarified (Cooper *et al.*, 2009).

Albinism is a group of related genetic disorders in which patients show not only the dilution or absence of melanin in skin but also in eyes and follicles, although melanocytes themselves are, at least initially, present (Halaban *et al.*, 1988, Boissy and Nordlund, 1997). Albinism can be caused by mutations in numerous genes such as *tyrosinase* (Summers, 2009). It is a common genetically inherited disorder with an estimated incidence in mixed populations of 1/20,000, however, in some African populations it can reach 1/1,500.

Naevi are common benign neoplasms which can be present at birth, but can also be acquired later in life, and it is a risk factor associated with malignant melanomas. Melanoma is caused by the transformation of melanocytes into a malignant tumor (Bandarchi *et al.*, 2013). Melanoma is not the most common skin cancer but it is the most dangerous as it causes death in the majority of cases. Melanoma is also widely observed in domesticated dogs, cows and horses. Cancers are complex diseases which can be driven by disruption of one or several genes and/or environmental factors. In multifactorial types of cancer, the environment can create the conditions for the

development of the disease. Malignant melanoma is a multifactorial cancer which involves both an environmental component and genetic predispositions (Bandarchi *et al.*, 2013).

The study of normal melanocyte development is fundamental for understanding the processes involved in human diseases affecting melanocyte development, but also to develop potential treatments against the progression of melanoma (Cronin *et al.*, 2009, Lister, 2012, Pathy *et al.*, 1993, Patton *et al.*, 2011, Santoriello *et al.*, 2012, Rebecca *et al.*, 2012, White and Zon, 2008, Yajima *et al.*, 2011, Yancovitz *et al.*, 2012). It would be interesting to test if gene therapy at an early stage could repair genetic disorders involving one gene, such as albinism or certain WS. Understanding the GRN involved in the melanocyte development would allow us to predict the downstream effects of disrupting any melanocyte gene and consequently better inform on the efficacy of therapeutic interventions, such as gene therapy and drug treatments.

1.6 Early neural crest development and regulation first depends on complex Gene Regulatory Networks

NC development is regulated by a succession of complex GRNs implementing internal and external signalling (Meulemans and Bronner-Fraser, 2004, Le Douarin, 2001, Bronner-Fraser, 2003, Dorsky *et al.*, 2000a, LaBonne and Bronner-Fraser, 1999). More specifically, the genetic regulation of NC development starts when the NC Induction Signals activate the Neural Plate Border Specifier genes, which in turn modify effects of the Induction Signals and allow formation of *bona fide* NC which is characterised by elevated expression of the NC Specifier genes (Le Douarin, 2008, Marchant *et al.*, 1998, Sauka-Spengler and Bronner-Fraser, 2008b, Sauka-Spengler and Bronner-Fraser, 2006, LaBonne and Bronner-Fraser, 1999, Dupin *et al.*, 2007). In turn, these NC Specifiers initiate specific cell type specification and differentiation of GRNs. Figure 1.02 summarises the succession of these events.

1.7 Important signals for neural crest induction

NC induction begins between the prospective neural and non-neural ectoderm, at the neural plate border and involves crucial signals. The bone morphogenetic proteins (BMPs), as well as Wnt signalling and fibroblast growth factor (FGF) are required for NC induction (Figure 1.02) (LaBonne and Bronner-Fraser, 1998, Sauka-Spengler and Bronner-Fraser, 2008b, Mayor *et al.*, 1995, Garcia-Castro *et al.*, 2002, Le Douarin, 1999, Steventon and Mayor, 2012, Tribulo *et al.*, 2003, Villanueva *et al.*, 2002, Schumacher *et al.*, 2011). However, the tissues secreting the induction signals in each species are not yet clearly defined. In *Xenopus* and zebrafish, NC induction at the neural plate border has been shown to be in part orchestrated by a gradient of BMP signalling (Tribulo *et al.*, 2003). The gradient of BMPs creates a gradient of activation of members of the Muscle Segment Homeobox family (MSX) which in turn activates specifiers of the NC such as *snail* (Tribulo *et al.*, 2003, Schumacher *et al.*, 2011).

Posteriorising signals, such as Wnt signalling, FGF and retinoic acid have also been shown to be required for maintenance of the NC territory (Villanueva *et al.*, 2002, Aybar *et al.*, 2003). In *Xenopus* and zebrafish, experiments of gain-of-function and loss-of-function have shown that the canonical Wnt pathway (described later) was necessary and sufficient for induction of the NC (Garcia-Castro *et al.*, 2002, Wu *et al.*, 2005, Villanueva *et al.*, 2002). In avian models, the non-neural-ectoderm could be the source secreting Wnt signalling (Garcia-Castro *et al.*, 2002). In contrast, the secretion of the Wnt factor has not yet been clearly addressed in mouse (Sauka-Spengler and Bronner-Fraser, 2008b, Lewis *et al.*, 2004). In chicks and zebrafish, studies have shown that the Delta-Notch signalling was also required for NC formation and limitation of NC to the neural plate border (Meulemans and Bronner-Fraser, 2004, Sauka-Spengler and Bronner-Fraser, 2006, Sauka-Spengler and Bronner-Fraser, 2008b). Factors involved in NC induction prepare the neural plate border for expression of the Neural Plate Border Specifiers (Sauka-Spengler and Bronner-Fraser, 2008b).

1.8 The Neural Plate Border Specifiers are required for development of *bona fide* neural crest

The Neural Plate border Specifiers are transcription factors, such as, the Paired Box (PAX) factors PAX3, PAX7, the Zinc finger protein ZIC1, the distal-less related homeobox factors DLX3 and DLX and also MSX1, MSX2, which are activated by the Induction signals as previously described. The genes coding for these factors are expressed together in combinations to define NC territory. Their expression also modifies the cellular response to BMP, Wnt and FGF signalling which allows the establishment of competence of the neural plate border and the activation of a new set of genes, the NC Specifiers (Figure 1.02) (Meulemans and Bronner-Fraser, 2004, Sauka-Spengler and Bronner-Fraser, 2008b, Sauka-Spengler and Bronner-Fraser, 2008a, Monsoro-Burq *et al.*, 2005, Mayor *et al.*, 1999). These genes seem to be expressed consistently in gnathostomes and lamprey. Furthermore, studies in the urochordate, *Ciona intestinalis*, have detected expression of homologs of neural plate border specifiers *pax3/7*, *zic*, and *msx* in the epidermal cells at the lateral tips of the forming neural plate. In Tunicates, functional analysis based on morpholino injections showed the conservation of the genetic interactions in the network, suggesting ancient roles for these genes, as well as, them being highly evolutionarily conserved (Wada and Saiga, 2002, Ma *et al.*, 1996, Imai *et al.*, 2004, Sauka-Spengler and Bronner-Fraser, 2008b).

1.9 Neural Crest Specifiers are the first factors implementing specification of the neural crest to specific derivative cell-types

The combination of Neural Plate border Specifiers and signalling, such as Wnt signalling or the BMP signalling, allows the activation of the Neural Crest Specifiers and the NC specifiers can regulate each other. Their expression is associated to the initiation of a new GRN in the NC (Figure 1.02) (Honore *et al.*, 2003, Sauka-Spengler and Bronner-Fraser, 2008b, Meulemans and Bronner-Fraser, 2004, LaBonne and Bronner-Fraser, 2000). NC Specifiers, such as, FoxD3, the Activator Protein 2 (AP-2), Twist, Snail1, Snail2, Id3, Twist and the Sry-related High Mobility Group box (Sox) factors, Sox8, Sox9, Sox10, are responsible for activation of genes involved in the specification of cell types, allowing the induction of a large number of factors which drive specification and differentiation of specific NC derivatives.

1.10 Neural crest cell delamination from the neural tube involves an epithelio-mesenchymal transition

Before gaining migratory capacity, cells leave the neuroepithelium by delaminating from the dorsal neural tube (Figure 1.02). For this, several crucial cell properties like cell morphology, cell adhesion, and cell motility, are submissive to reorganisation (Kalcheim, 2000, Dupin *et al.*, 1993, Burstyn-Cohen and Kalcheim, 2002, Kalcheim and Burstyn-Cohen, 2005, Klymkowsky *et al.*, 2010). Delamination is a process which allows NC cells to detach from the neuroepithelium by undergoing an EMT. The EMT is accompanied by major adaptations of the cytoskeleton (Garcia-Castro *et al.*, 2002). Most cells down-regulate the cell-cell adhesion complexes and modify their apico-basal polarity. The reduction of the number of tight junctions and the re-organisation of the extracellular matrix, with secretion of matrix metalloproteases implicated in the invasive behaviour can be observed. Furthermore, the control of the cell-cycle is specifically adapted for delamination (Ikenouchi *et al.*, 2003, Egeblad and Werb, 2002, Burstyn-Cohen and Kalcheim, 2002). As a result of activation of the *snail* family gene members, the expression of cadherins is adapted to enable the EMT (Nelson and Nusse, 2004, Nakagawa and Takeichi, 1995, Sauka-Spengler and Bronner-Fraser, 2008b). Finally cells show protrusive activity (Theveneau and Mayor, 2012). In zebrafish for instance, before the cells start dispersing, they enter a process of probing the dorsal surface of the somite by extending pseudopodia meanwhile the cells of the dorsal somite show active protrusive activity (Raible *et al.*, 1992).

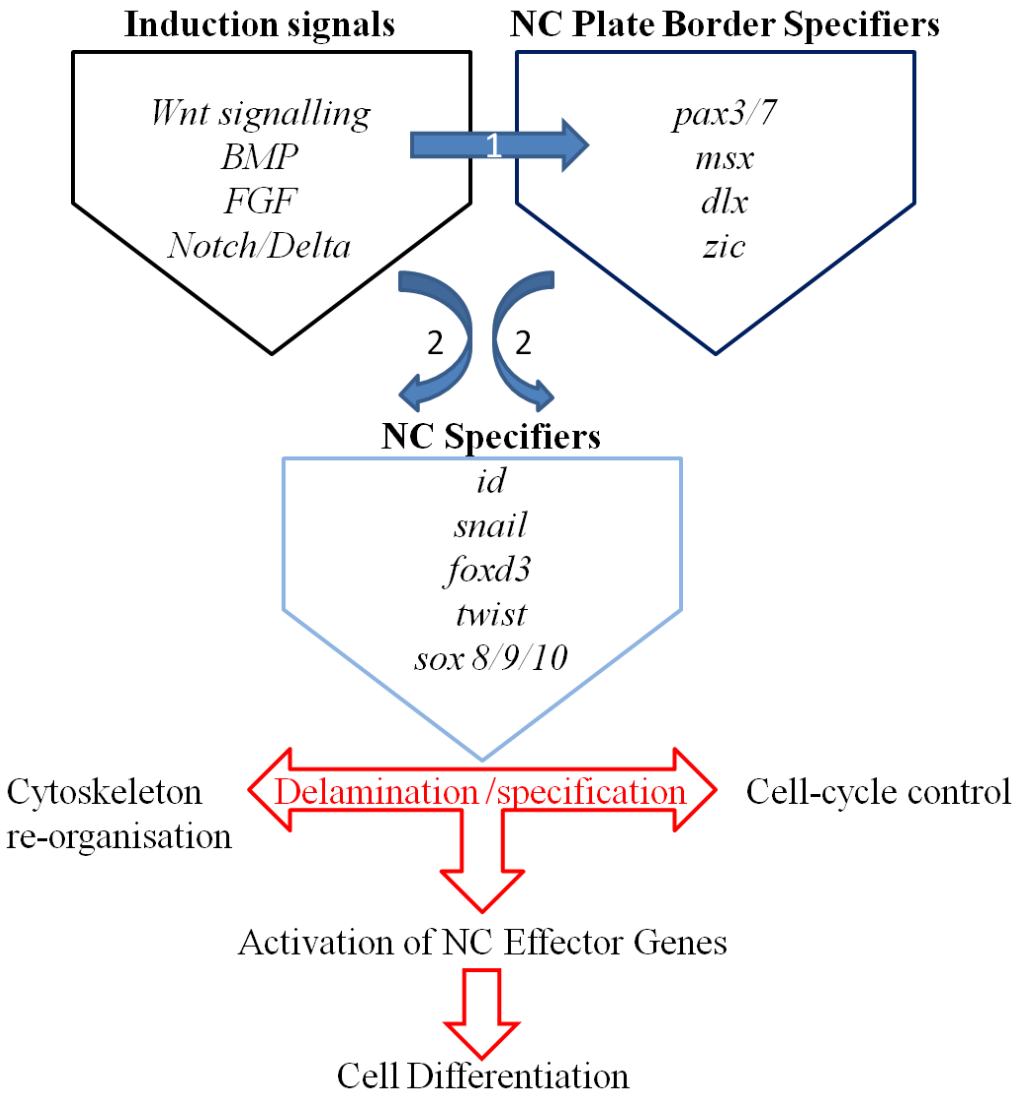

Figure 1.02: Cascade of GRNs involved in the formation of the neural crest.

The cascade of genes in play during the formation of the NC is presented here. First, NC induction is controlled by BMP, Wnt, FGF and Notch signalling for activation of Neural Plate Border Specifiers (1). The Neural Plate Border Specifiers, in turn, modify the effects of BMP, Wnt, FGF and Notch signalling to activate the expression of the NC Specifiers (2). The NC Specifiers then activate expression of genes involved in NC derivatives specific GRNs (NC effector genes). Importantly, the NC specifiers also control modification of cell aspects such as cytoskeleton re-organisation and cell-cycle arrest mediating NC.

1.11 Cell migration is associated with fate restriction

1.11.1 Cells migrate via different pathways in embryos

After delamination, NC cells migrate within the embryo and NC cell precursors lose their multipotency by becoming progressively more restricted before or during migration (Thomas and Erickson, 2008, Le Douarin and Dupin, 2003, Le Douarin *et al.*, 2004, Real *et al.*, 2006, Le Douarin, 1980). The order of dispersing, the timing and the pathway followed by different cell types for different derivative fates, can vary throughout animal models, however, the processes themselves are likely to be largely conserved (Eisen and Weston, 1993, Sauka-Spengler and Bronner-Fraser, 2008b, Serbedzija *et al.*, 1990, Raible *et al.*, 1992, Le Douarin *et al.*, 2004, Mayor *et al.*, 1995). NC cells migrate as waves following two pathways in the embryos; the lateral pathway, between the ectoderm and the somites; and the ventral/medial pathway between the somites and the neural tube. Studies in chick have suggested that signalling molecules expressed in the dorso-lateral interstice, such as, semaphorins, spondins and ephrins, could be responsible for the choice of the migratory pathway (Theveneau and Mayor, 2012). In zebrafish, NC cells migrate first via the medial pathway (Figure 1.03). Around four hours after the start of the migration, NC cells begin migrating in between the somites and the epidermis which corresponds to the lateral pathway (Theveneau and Mayor, 2012, Raible *et al.*, 1992). In *Xenopus*, the majority of cells migrate throughout the ventral pathway while a few cells follow the lateral pathway (Theveneau and Mayor, 2012). In avian and mammalian models, NC cells migrate between the developing somite and the neural tube which consists of the ventral pathway. Simultaneously in mouse and within a 24 hours delay in chick, melanocyte precursors migrate dorsally between the dorsal ectoderm and the somites (Figure 1.03) (Theveneau and Mayor, 2012). Interestingly, in this model the migratory process seemed to be orchestrated by autonomous changes, as suggested by experiments grafting NC cells and melanocytes ectopically in several parts of the trunk which showed that only differentiated melanocytes could migrate on the dorso-lateral pathway (Erickson, 1985). In zebrafish and *Xenopus*, melanocyte precursors can migrate along the two pathways, whereas, in mouse and chick, they only migrate laterally (Figure 1.03) (Kelsh *et al.*, 2009).

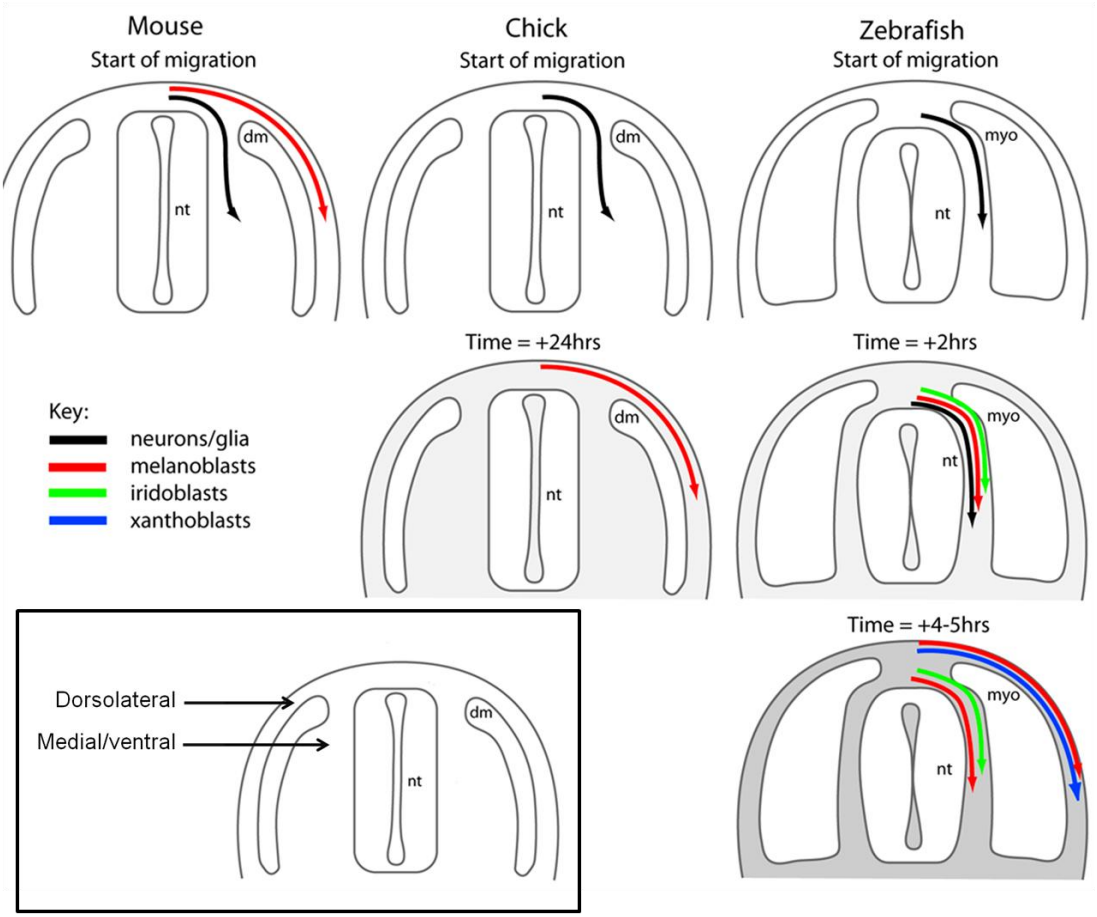

Figure 1.03: Schematic of the Neural Crest cell migration and timing in three different models.

After delamination, NC cells in the trunk and tail migrate on one of two major pathways. In all species, pathway choice and fates adopted are correlated and in some cases like melanocyte in chick, fate specification is required for correct pathway choice. In mouse, chick and zebrafish, melanocytes migrate on the dorsolateral pathway. However, in zebrafish melanocytes also migrate through the medial pathway. In mouse, melanocyte migration starts at the same time as neuronal cell migration through the ventral pathway. In chick, neuronal cells migrate first, exclusively via the ventral pathway, whereas later, melanocyte precursors migrate using the dorsolateral pathway. In zebrafish, neural cells migrate first, using only the medial pathway; then melanocytes and iridophore precursors follow the same pathway and only later, melanocyte and xanthophore precursors migrate through the dorsolateral pathway. dm: dermamyotome, myo: myotome, nt: notochord. (adapted from Kelsh *et al.*, 2009).

1.11.2 Complex interactions are involved in fate restriction during cell specification

Fate specification from the NC pool involves complex interactions. However, for each cell fate, a rather well conserved genetic network can be defined through models, showing the strong conservation of the cell types. The progressive restriction model suggests that key factors could permit fate choice in pluripotent or bipotent precursors. This hypothesis suggests that cells remain sensitive to internal and external factors until commitment.

It is crucial to understand the role of the niche which is involved in the specification of some particular cell types such as Schwann cells. Schwann cell precursors migrate via the ventral migratory pathway and differentiate along the growing nerves. A study from Adameyko *et al.,* (2011) showed that in chick, at least some NC derived Schwann cell precursors could be marked by *sox10,* however, they could also keep the potentiality to differentiate into melanocytes. Only when they specify to melanocyte, the precursors activate the melanocyte marker *microphthalmia associate factor (Mitf)*. The contacts with the nerves, which are associated with Neuregulins and ErbB3 signalling, were then critical for specification of Schwann cells in this niche (Adameyko *et al.,* 2009, Baynash *et al.,* 1994, Dupin *et al.,* 2007).

1.11.3 Fate restriction in the case of melanocyte derivation from the neural crest

The mechanisms involved in melanocyte derivation from a model to another are not fully understood. Figure 1.04 summarises melanocyte derivation from the NC pool (adapted from White and Zon, (2008)). Interestingly, studies in mouse and chick suggested that melanocytes and glial cells could be derived from a shared progenitor. Within these precursors, fate choice would involve *foxd3,* which could negatively regulate the melanocyte fate (Thomas and Erickson, 2009). *foxd3* is expressed in early pre-migrating NC and is downregulated in melanoblasts, however, molecular mechanisms involved in this process remain unknown (Curran *et al.,* 2009, Dupin *et al.,* 2007). Furthermore, it is not known if melanoblasts migrating with the first wave on the dorso-lateral pathway could also share a bi-potentiality with glial cells. In fish, the existence of a precursor restricted to all types of chromatophores has been suggested (Bagnara, 1999). The hypothesis of the existence of a chromatoblast is not contradictory to the hypothesis of the existence of a melanoglial bipotent precursor (Dupin *et al.,* 2003, Trentin *et al.,* 2004). In zebrafish, data suggested the existence, at early stages, of cells of the NC expressing four factors, the two melanoblast early markers *sox10* and *mitfa* and the potential iridoblast early markers *leukocyte receptor tyrosine kinase* (*ltk)* and *id2*. Expression of these genes could be marking chromatoglioblasts *in vivo* (Lopes *et al.,* (2008); Nikaido M, Rodrigues F, unpublished data).

A progressive model could be envisaged whereby the chromatoglioblasts would be pushed towards a specific fate by expressing certain genes and receiving specific signals at a specific time point. Investigating the existence of such precursors *in vivo* and the limiting factors for fate choice, would be crucial.

In mouse, cells known as Melanocyte Stem Cells (MSCs) are found in the hair follicle. The factors involved in the maintenance of these cells, as well as the potency of these cells *in vivo*, remains to be tested (Osawa *et al.*, 2005, Lang *et al.*, 2000, Nishimura *et al.*, 2002). Expression of *Sox10, Pax3* and *Mitf* seem to be essential for these cells. It has been shown that *Pax3*, with *Sox10*, could maintain *Mitf* expression in mouse, however, in cell culture *Pax3* was a direct repressor of *Dct* expression which acted as a factor involved in the maintenance of multipotency (Lang *et al.*, 2000, Bondurand *et al.*, 2000, Potterf *et al.*, 2001). Furthermore, Lang *et al.*, (2000) showed that Wnt signalling via β-catenin could prevent *Pax3* from repressing *Dct* on the *Dct* promoter. MSCs are mostly described in the hair follicles in mammals, although, they could also exist in the skin of adult zebrafish. The mechanisms involved in the maintenance and the properties of these cells are described in Hultman *et al.*, (2009). It is important to consider these cells when studying the renewal and the properties of melanocyte fate restriction, however, it is not investigated further in this study as it is outside the study of the GRN involved in melanocyte differentiation.

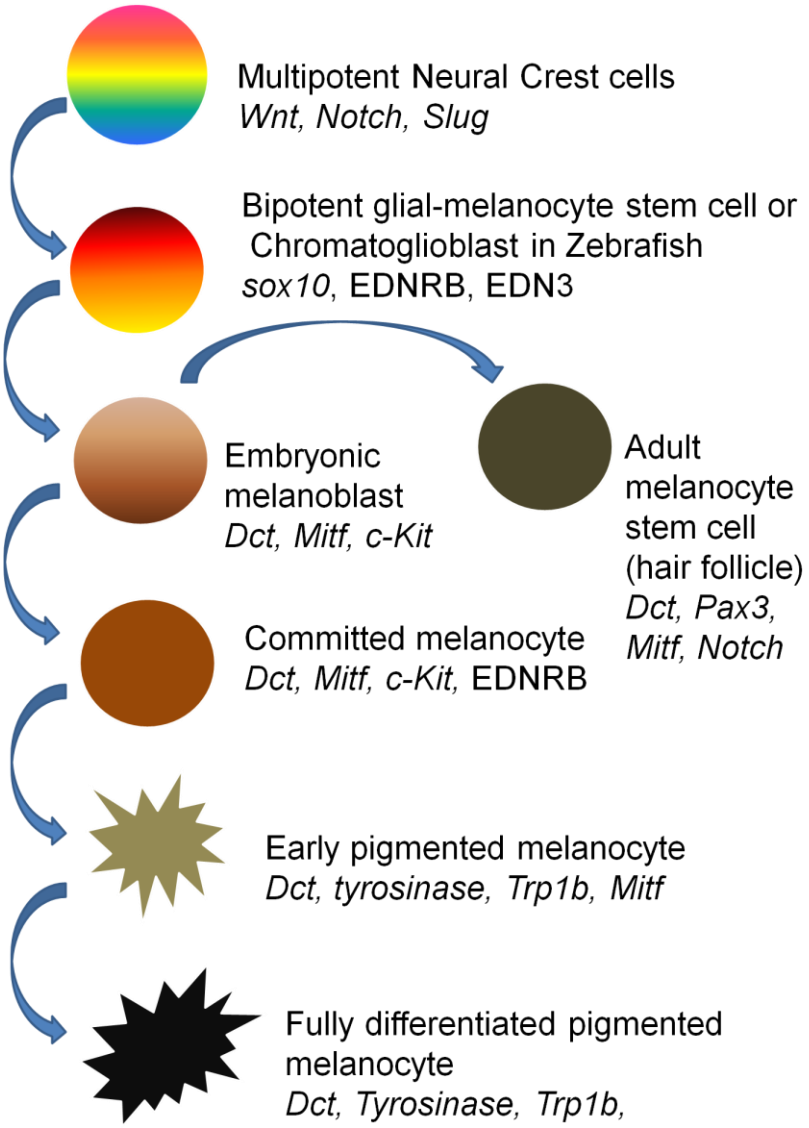

Figure 1.04: Melanocyte derivation from neural crest.

A model of the cell-types generated progressively in melanocyte specification and differentiation. At early stages, early NC specification depends upon interactions between Wnt and Notch signalling. Transcription of *Sox10* is also required for NC specification. The pool of NC cell can be marked by the expression of *crestin* in zebrafish and *Sox10*. Lineage restriction toward the melanoblast fate, through a potential melanoglioblast or even chromatoglioblast in zebrafish, is dependent upon *mitfa*. It can be marked by activation of *ednrb* and *c-kit* signalling which are not involved in fate specification. In these cells the role of *Foxd3* as a repressor of melanocytes and the contact with the nerves are crucial parameters for determining glial fate at the expense of melanocyte fate. Molecular distinction between embryonic melanoblasts and melanocyte stem cell (MSC) remains unclear, however, it has been suggested that both express *dct*. Finally, differentiating melanocytes expressed genes responsible for melanin synthesis such as *dct*, *tyrosinase* or *trp1b*.

1.12 Genetic regulation of melanocyte specification

Here, we define cell specification as events which allow the expression of factors characteristic of a specific fate; note that these cells are likely, at least initially, to remain not yet committed and sensitive to environmental factors that may switch their ultimate fate. Melanocyte development depends upon the transcription factor SOX10 and Wnt signalling to activate expression of the basic-helix-loop-helix leucine zipper transcription factor MITF (Dunn *et al.*, 2000a, Hari *et al.*, 2012, Yasumoto *et al.*, 2002, Dorsky *et al.*, 2000b, Lewis *et al.*, 2004, Takeda *et al.*, 2000a, Saito *et al.*, 2003).

Sox10 is a High Mobility Group (HMG) transcription factor described as an early stage NC cell marker. It is expressed for the first time at gastrula stage around 11 hpf in zebrafish (Kelsh, 2006a). Later *sox10* expression persists in migrating cells as they are specified and begin differentiation and is then gradually lost except in Schwann cells satellite cells (Carney *et al.*, 2006, Dutton *et al.*, 2001, Potterf *et al.*, 2001, Le Douarin *et al.*, 1991, Lang *et al.*, 2000). In *Xenopus*, zebrafish, mouse and chick, *sox10* has been shown to be required for melanocyte specification (Dutton *et al.*, 2001, Aoki *et al.*, 2010, Honore *et al.*, 2003, Southard-Smith *et al.*, 1998). In mouse, a spontaneous frameshift mutation called Dom, causes a failure to develop glial cells, neurons of the peripheral nervous system (PNS) and melanocytes (Southard-Smith *et al.*, 1999). In zebrafish, *sox10/colourless* mutants lack melanocyte pigmentation as cells fail to specify (Dutton *et al.*, 2001, Elworthy *et al.*, 2003a, Lister *et al.*, 1999). *pax3*, a paired-domain and a homeodomain containing transcription factor, with *sox10*, are expressed upstream of *mitfa* and are also necessary for NC cell derivative developments other than melanoblasts (Potterf *et al.*, 2000, Lang *et al.*, 2005, Lacosta *et al.*, 2005).

Regulation of melanocyte development depends upon *MITF*, the master gene for melanocyte development. *MITF* regulates melanocyte differentiation and lineage survival. The first mutation at *Mitf* locus was first found in mouse by Hertwig, (1942) and this bHLH leucine-zipper transcription factor was cloned for the first time by Hodgkinson *et al.*, (1993). In mammals, *Mitf* is expressed in different tissues thanks to alternative first exons regulation allowing a specific promoter to drive expression of *Mitf* in a specific tissue (Shibahara *et al.*, 2001). Only *Mitf-M* is expressed exclusively in melanocytes emerging from the NC and is considered in this study. In zebrafish, two duplicates of *mitf* exist, *mitfa* and *mitfb*. Both duplicates are homologous to one of the mammalian isoforms generated by exon splicing. Both *mitfa* and *mitfb* are involved in the retinal pigment epithelium development and their functions are redundant in the eyes. *mitfb* is also expressed in the epiphysis and the olfactory bulb, however, only *mitfa* is involved in NC derived melanocytes (Lister *et al.*, 2001). Therefore, pigmented cells of the retinal pigment epithelium (RPE), which are the only pigmented cells not arising from the NC are not discussed here (Lister *et al.*, 2001). In both mouse and zebrafish, loss of *Mitf*/*mitfa* resulted in a failure of melanoblast development (Lister *et al.*, 1999, Steingrimsson *et al.*, 2004).

In zebrafish, the melanocyte specifying factors include *sox10* and *mitfa*. Thus, in zebrafish, melanocyte specification can be defined as the series of events leading a NC cell

to first express *mitfa* and a *sox10+*/*mitfa+* precursor to maintain and perhaps enhance *mitfa* expression. *mitfa* is activated around 18 hpf by *sox10* and Wnt signalling (Figure 1.09) (Kelsh, 2006a). Experimentally, activation of β-catenin/Lef1 binding sites in the *mitfa/nacre* promoter of B16 cells as well as analysis of minimal promoter activation in the *mitfa/nacre* mutant zebrafish suggested that *mitfa* could be a direct target of the Wnt signalling *in vivo* (Dorsky *et al.*, 1998, Dorsky *et al.*, 2000b). In mouse, *Wnt1* and *Wnt3a* mutant lose pigmentation (Saint-Jeannet *et al.*, 1997b, Dunn *et al.*, 2000a). Consequently, it is well described that Wnt signalling has an important role in melanocyte specification. Melanocyte differentiation is less described however, from what is known, it could be generally defined as the series of events which are induced by this active *mitfa* expression and which result in the progression of a melanoblast into a differentiated black melanocyte. The timing of cell commitment for melanocyte fate is not clearly defined. Expression of *dopachrome tautomerase* (*dct*), around 19 hpf is considered as a marker for early melanoblast stages onwards (Figure 1.09) (Kelsh *et al.*, 2000).

1.13 Genetic regulation of melanocyte differentiation

All the NC derivatives initiate GRNs specific to their particular fate. Currently, analysing the GRNs of each NC derivative is a major area of research. For instance, *sox9* and *collagen type II α1* (*Col2α1*) have been shown to be involved in cartilage differentiation but more factors and regulatory features are being tested to describe the mechanisms involved in this process. Importantly, as suggested in Prasad *et al.* (2012), the role of epigenetic mechanisms in the regulation of chromatin state and the recruitment of transcription factors for NC cell specification, remains to be assessed (Prasad *et al.*, 2012, Le Douarin *et al.*, 1994). This study focused on the GRN involved in a NC derivative differentiation, the melanocyte.

In contrast with the mouse system, in zebrafish, the genetic regulation of melanocyte differentiation is less described than melanocyte specification. The timing of cell commitment is not described yet in melanocytes, however, first signs of pigmentation are observed around 27 – 29 hpf. Embryonic melanocytes are only mature by 72 hpf and the larval pigment pattern is complete around 4-5 dpf (Figure 1.05). As shown in Lister *et al,* (1999), ectopic expression of *mitfa* in the *mitfa*^{w2} zebrafish mutant was sufficient to rescue the main aspects of melanocyte differentiation in cells, such as production of melanin, cell morphology and location. *Mitf* expression controls the main aspects of melanocyte cell biology, via direct and indirect interactions (Johnson *et al.*, 2010, Cheli *et al.*, 2012). Mitfa is responsible for activating genes necessary for melanin synthesis such as *dct, tyrosinase,* and *tyrosinase related protein-1 (tyrp1b/trp1b*), as well as *silva* (gene encoding a structural protein) for example (Kelsh and Eisen, 2000, Lister *et al.*, 1999). It is also essential in regulating melanocyte survival and melanocyte proliferation via activation of the anti-apoptotic gene *bcl-2* (McGill *et al.*, 2002, Johnson *et al.*, 2010, Cheli *et al.*, 2012). Melanocyte shape and mobility have also been shown to be influenced by *Xn-mitf* in a study in *Xenopus* (Kawasaki *et al.*, 2008).

In contrast with mouse, experiments in zebrafish showed that *sox10* expression was gradually downregulated in melanocytes from around 24 hpf until 50 hpf, when it was not detectable anymore in melanocytes by Whole Mount *In Situ* Hybridisation (WISH) (Hou *et al.*, 2006, Greenhill *et al.*, 2011). The mechanisms involved in the decrease of *sox10* expression in zebrafish melanocytes remain unknown. It is also unclear if *mitfa* expression is maintained in cells, and if it is maintained, what factors are responsible for its maintenance needs to be identified (Greenhill *et al.*, 2011). Furthermore, the role of Wnt signalling in melanocyte differentiation has never been assessed *in vivo* in fish and in mouse (Sommer, 2011).

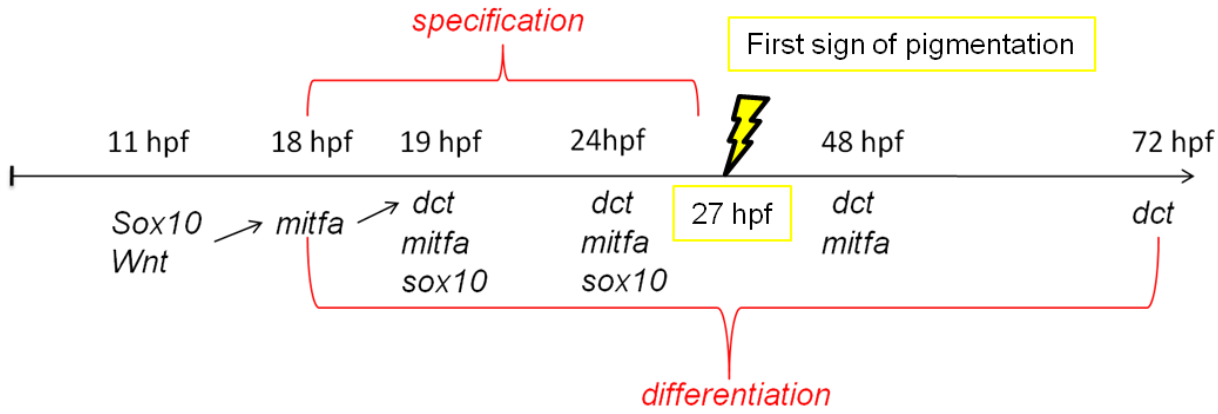

Figure 1.05: Time course of expression of *sox10, mitfa* and *dct* and timing of melanocyte specification and differentiation in zebrafish.

At 11 hpf, *sox10* is expressed in all NC cells. At 18 hpf, *sox10* and Wnt signalling activate *mitfa* expression in a subset of NC cells. However, it is unclear when exactly Wnt activation is required to allow this effect. At 19 hpf, Mitfa activates expression of several genes coding for the enzymes responsible for melanin synthesis such as *dc*t. From 28 hpf to 48 hpf, *sox10* expression decreases in melanocytes. Whether or not *mitfa* remains expressed at 72 hpf remains to be clarified. Melanocyte specification starts around 18 hpf and probably ends around 30 hpf, however, the timing is not clearly known. Melanocyte differentiation is completed by 72 hpf.

1.14 The Zebrafish is a suitable model for the study of melanocyte

The evolutionary conservation of the melanocyte cell type throughout vertebrate genetic models suggests the good conservation of the GRN responsible for melanocyte development and even melanin synthesis (Sato *et al.*, 2001, Hallsson *et al.*, 2004). Zebrafish melanocytes have been shown to be closely related to human and mouse melanocytes as most of the mammalian genes have known functional homologues in the zebrafish genome (Johnson *et al.*, 2010, Quigley and Parichy, 2002, Kelsh, 2004). Consequently, comparable melanocyte genetic development across vertebrates makes zebrafish an excellent model to better understand melanocyte-related diseases in mammals. This is important because the understanding of melanocyte genetics in zebrafish and the discovery of drugs, or treatments, in zebrafish, could then be used in the future to understand, identify and cure melanocyte-development related disorders in humans.

Zebrafish is an excellent model for the study of embryonic melanocyte development and GRN. Particularly, the transparency of embryos allows the observation of melanocytes in living embryos at sub-cellular resolution better than in any other of the main genetic models (Kelsh *et al.*, 1996a). *In vivo* study of melanocytes has a great advantage in zebrafish as cell morphology, pigmentation, size, division and migration are also very easy to observe (Figure 1.09). The rapid development of melanocytes and pigment cells gives easy and fast access to biological material and allows the precise analysis of melanocyte phenotypes (Kelsh *et al.*, 1996a). Additionally, the timing and the characteristics of embryos changes in early development are well characterized (Kimmel *et al.*, 1995). The number of cells in zebrafish NC is smaller than in any other model, however, cells are bigger and therefore easier to follow with several tracing techniques and microscopy instruments, such as Nomarski microscopy (Raible *et al.*, 1992, Eisen and Weston, 1993). Therefore, as suggested in Eisen and Weston, (1993) and in Raible *et al.*, (1992), the zebrafish model provides a system for an alternative approach to study NC development by investigating individual NC cells through their specification and differentiation.

1.15 Establishment of the pigment pattern in zebrafish

1.15.1 Embryonic pigment cells migrate and organise in stripes

The melanocyte is the only pigment cell type that exists in mammals, whereas, two other additional kinds of pigment cells can be found in zebrafish, xanthophores and iridophores. In zebrafish, the pattern of pigmentation is established during early development and is conserved and well defined (Kelsh *et al.*, 1996a). Yellow xanthophores are light absorbing pigment cells while the iridescent iridophores are light-reflecting chromatophores containing guanidine-based reflective platelets (Kelsh, 2004). In zebrafish embryos, iridophores migrate on the medial pathway, whereas xanthophores migrate only along the lateral pathway and cover the flank of fish. This study is focused on the melanocyte,

however, in zebrafish, pigment cell biology encompasses the study of these three pigment cell types.

In the mouse, as in zebrafish, it seems that melanoblasts are specified prior to migration (Hou *et al.*, 2006, Dutton *et al.*, 2001, Lister *et al.*, 1999, Parichy *et al.*, 2000b). One mechanism could involve an important receptor, tyrosine kinase *kit*, which is expressed in melanobasts in premigratory NC cells in mouse and which is important for cell migration (Hou *et al.*, 2000, Kawa *et al.*, 2005). A transient expression of its ligands, *KitL*/*kitla* is also detected in cells of the dermamyotome in mouse, and in zebrafish (Wen *et al.*, 2010, Hultman *et al.*, 2007). In zebrafish, *Kit* ortholog, *kita*, and its ligand, *kitla*, both have been shown to be required for melanoblast survival and migration (Parichy *et al.*, 1999, Rawls and Johnson, 2003, Cooper *et al.*, 2009). Melanocytes migrate ventrally along the medial and the lateral pathway. By 4-5 days post-fertilisation (dpf), embryonic melanocytes are organised in four stripes, the dorsal stripe, the lateral stripe, the ventral stripe and the yolk sac stripe (Kelsh, 2004, Odenthal *et al.*, 1996, Parichy *et al.*, 2000a, Lopes *et al.*, 2008). Figure 1.06 shows an embryo at 3 dpf with all stripes but the yolk-sac stripe which form later.

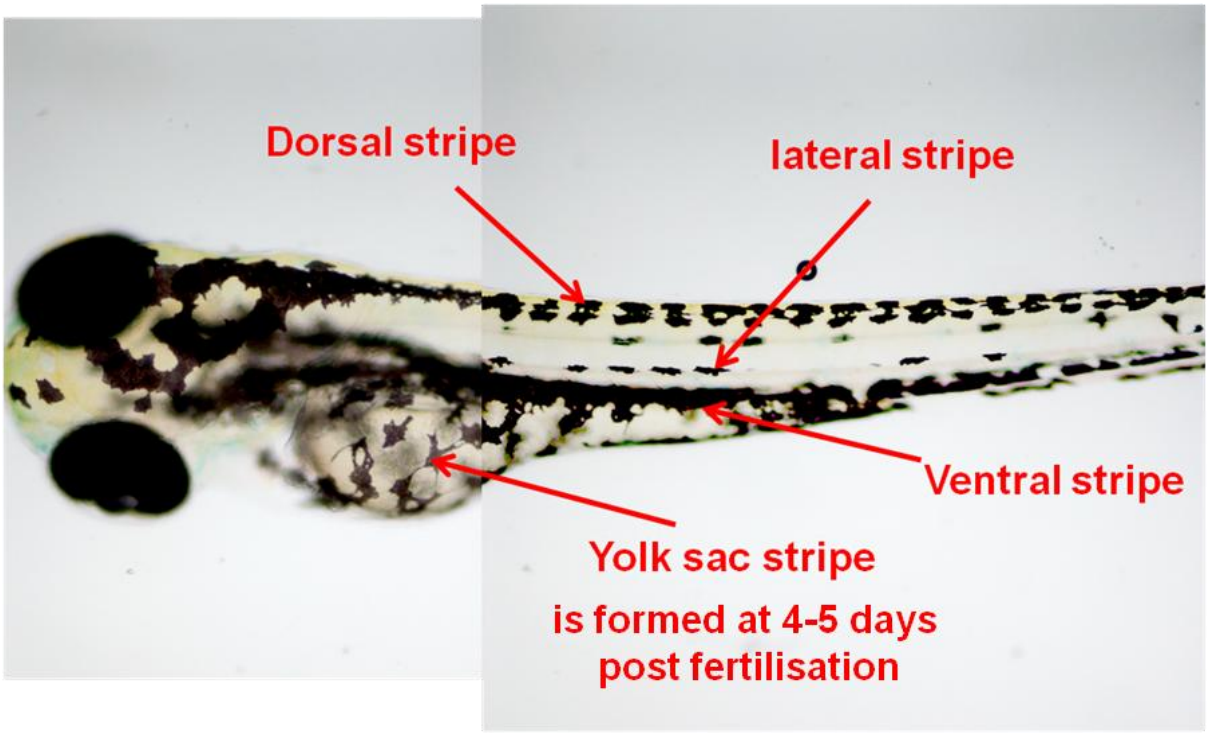

Figure 1.06: Embryonic melanocytes are organised in four stripes.

72 hpf zebrafish embryo showing organisation of embryonic mature melanocytes in four stripes, the dorsal stripe, the lateral stripe, the ventral stripe and the yolk-sac stripe which is not yet visible on the fish here as it is only formed in 4-5 days-post-fertilisation fish.

1.15.2. Melanocytes produce the black pigment melanin

Melanocytes are black pigmented cells containing the pigment, melanin, in granules called melanosomes. Mammals synthesise two different types of melanin, eumelanin and pheomelanin, whereas there is only one type of melanin in zebrafish, eumelanin (Ito and Wakamatsu, 2003). Both pigments are derived from a precursor dopaquinone (ortho-quinone or 3,4-dihydroxyphenylalanine) and an enzymatic cascade leads to the production of the black eumelanin or the reddish/brown pheomelanin (Figure 1.07) (Ito and Wakamatsu, 2008). Tyrosinase is an enzyme which catalyses two steps in the reaction to convert tyrosine to melanin. Tyrosine is first changed to dopa by Tyrosinase, which then catalyses the transformation of dopa to dopaquinone and finally dopaquinone is transformed to eumelanin (Figure 1.07) (Hearing and Jimenez, 1987, Ando *et al.*, 2007).

Two types of melanocytes can be defined, the NC derived melanocytes and the non-NC derived melanocytes. The main roles of melanocytes in organisms seem to be photoprotection and thermoregulation (Kawakami and Fisher, 2011). These roles have been well described for the NC derived cutaneous melanocytes which are found in hair, feather follicles and epidermis. However, the role of some of the NC derived extracutaneous melanocytes, such as the ones from the cochlear or the intestine, remain unclear. Interestingly, the melanocytes of the retinal pigment epithelium (RPE) in eyes are not NC derived. In zebrafish melanocytes, the pigment granules can aggregate or disperse in response to neurotransmitters, cell signals and hormones, like the Melanocyte Concentrating Hormone (MCH) and the Melanocyte Stimulating Hormone (MSH) (Takahashi and Kawauchi, 2006). NC derived melanocytes are found in the dermis, the deep layer of the skin. Black melanocytes in zebrafish embryos are shown in Figure 1.08. In adult fish, they are present on the dorsal surface where they are associated with the dermal scale (Vickaryous and Sire, 2009, Hoerter *et al.*, 2012).

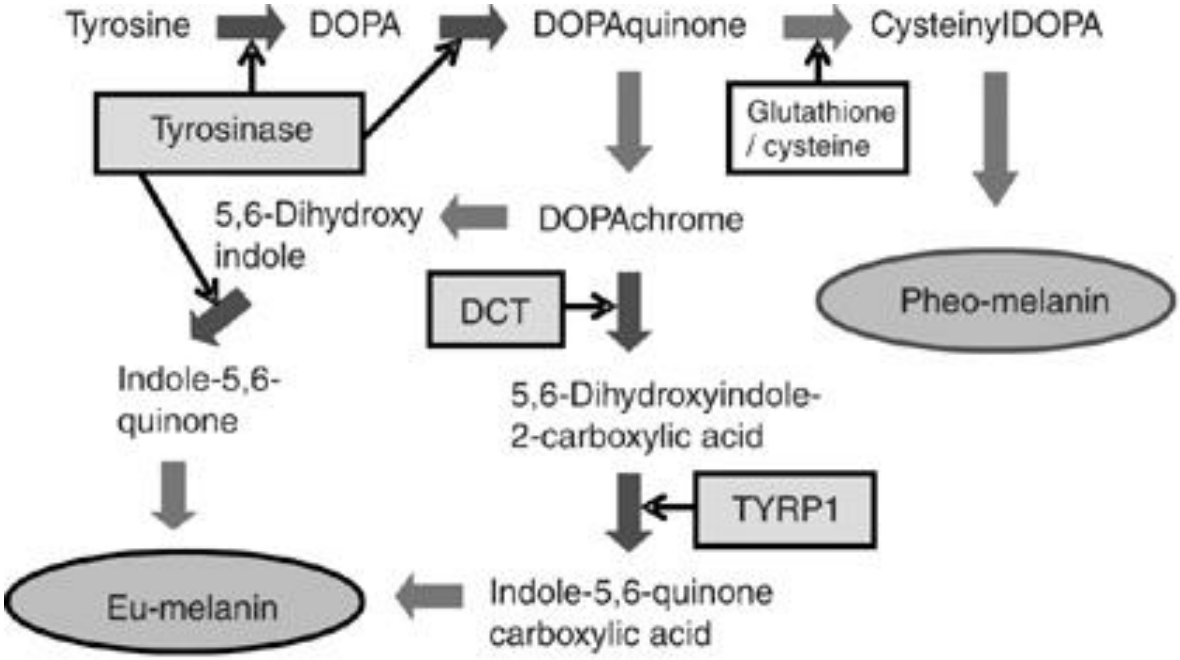

Figure 1.07: Enzymatic cascade involved in melanin synthesis.

Tyrosinase allows the conversion of Tyrosine into DOPA and DOPA into DOPAquinone. A molecule of DOPAchrome is then processed by Dct (dopachrome tautomerase) and the substrate of this reaction is processed by Tyroinase-related protein 1 (TYRP1) to become Eumelanin. Alternatively, the DOPAchrome is processed by Tyrosinase to become Eumelanin in a two steps process. DOPAquinone can also be transformed in Pheomelanin (reproduced with the kind permission of Ando *et al.*, (2007)).

1.15.3 Melanocyte differentiation is observable in zebrafish embryos

Melanocyte differentiation is a process consisting of multiple complex aspects which are observable in zebrafish and shown in Figure 1.08. These aspects include: changes in cell appearance, such as changes in cell shape, increased cell size, increased cell melanisation and divisions increasing cell number; and also, cell movements lead to positioning and organisation to form reproducible patterns. It is possible to quantify these changes in aspects although at later stages, an increase in cell melanisation can be difficult to measure due to the saturation in melanin in cells. Cell shape can be characterised by its roundness which varies through cell differentiation. Cells roundness can be measured and calculated by a formula determining a parameter called cell dendricity (R), *(R = P2/4pA, where A is the cell area and P the cell perimeter).* Increased R corresponds to increased cell dendricity (circle, R=1) (Kumasaka *et al.*, 2005). Before 55 hpf and until about 72 hpf, cell position and organisation is not clearly established in embryos. However, from 55 hpf (Figure 1.09 (A-D)), a pattern with two lines, in a "U" shape, becomes visible. By 72 hpf, this pattern is characteristic of WT embryos (Figure 1.09, (A-C)).

Melanocyte pigmentation is first observed around 27 hpf when cells show the first signs of melanisation, being grey, small and "elongated" (Figure 1.09, (E)). At 48 hpf, cells are blacker but are not yet saturated with melanin. At this stage, cells remain dendritic and not yet organised as a definitive pattern (Figure 1.09, (F)). Embryonic melanocytes are finally fully mature at 4-5 dpf, but by 72 hpf, they already show all characteristics of maturation, meaning that cells are fully melanised and have mostly acquired their shape and positioning (Figure 1.09, (G)).

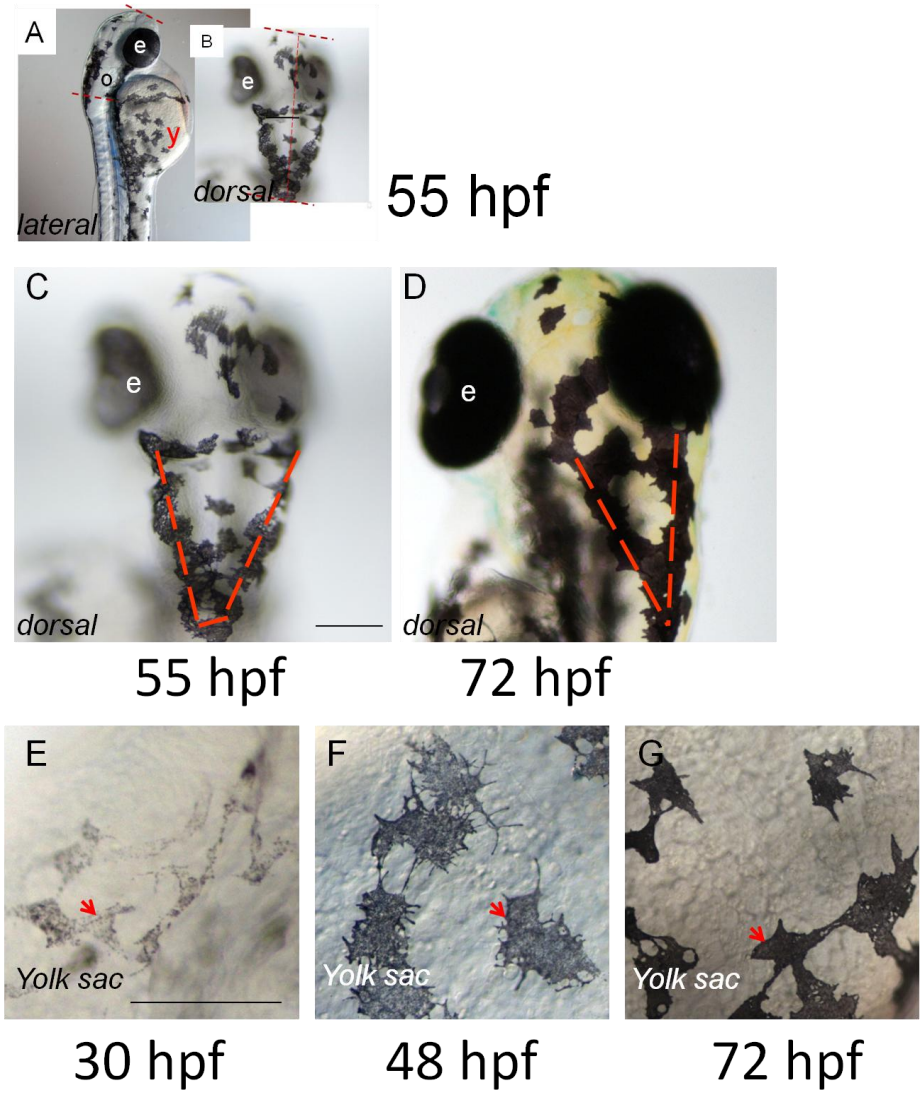

Figure 1.08: Observable aspects of melanocyte differentiation in zebrafish.

Cell positioning organisation is visible from around 55 hpf in zebrafish embryos, (A) lateral view, (B) dorsal view, (A-B, dotted lines show the section observed for determining the disruption of the cell pattern of organisation, from the anterior brain to the posterior part of the optic vesicle), (C) head dorsal view (the dotted lines show early "U" shape organisation of cells in dorsal head). At 72 hpf, the pattern is fully established ((D) head dorsal view, the red dotted line shows the "U" shape organisation). The cells of the yolk sac (E,F,G, red arrowheads show melanocytes), at 30 hpf cells are small, grey and elongated (E), at 48 hpf, cells are darker, bigger and more dendritic (F), and at 72 hpf cells are mostly mature, saturated in melanin and less dendritic (G). e: eye; y: yolk sac; o: otic vesicle. Scale bar: 100 µm.

1.15.4. Xanthophores are yellow pigmented cells present in zebrafish

Xanthophores are yellow pigmented cells found in the dermis in zebrafish (Figure 1.09). The pigments they contain are carotenoids and pteridine. Like melanocytes, xanthophores are dendritic cells. Several important markers for xanthophores are known, two of them are two enzymes of the pteridine synthesis cascade, the GTP cyclohydrolase (*gch*) and xanthine dehydrogenase/oxidase (*xdh/xod*) (Ziegler, 2003, Odenthal *et al.*, 1996). In zebrafish, the xanthophore precursors, xanthoblasts, appear around 18 hpf and requires *pax3* (Lister *et al.*, 2006, Minchin and Hughes, 2008). *pax3* morpholino knockdown triggers severe xanthophore reduction based on the diminution of *xdh* positive cells, as shown by *in situ* hybridisation analysis investigating *xdh* expression in injected zebrafish embryos (Minchin and Hughes, 2008). In zebrafish, the roles of *pax3/pax7* in xanthophores and in melanocytes still need to be clarified. Furthermore, secondary *pax3*-like and *pax7*-like genes, *pax3b* and *pax7b* respectively, exist in zebrafish and may well act in part redundantly on pigment cell development. Another factor, the receptor *colony stimulating factor 1 receptor* (*csf1r),* is involved in xanthophore development and marks differentiation starting around 25 hpf. First signs of yellow pigmentation can only be observed later, around 60 hpf (Lacosta *et al.*, 2007, Minchin and Hughes, 2008).

There has been suggestion that xanthoblasts and melanoblasts could share the same precursor. For instance, the loss of *pax3* and the loss of xanthophore pigment has been associated with an increase in melanocyte number in zebrafish induced by a developmental delay (Minchin and Hughes, 2008). However, the question of whether or not xanthoblasts and melanoblasts share the same precursor has not been fully investigated and if *pax3* could act in a cell autonomous manner to mediate xanthophore fate choice from a chromatoblast precursor remains to be tested.

1.15.5. Iridophores are light-reflective cells present in zebrafish

Iridophores are oval shaped shiny reflective cells containing light reflecting platelets of guanine which are strictly organised to increase light reflectance and from which depends the wavelength of light reflected (Figure 1.09) (Oshima, 2001). There are four types of iridophores; two motile types, the blue iridophores found in dark blue stripes, the light blue iridophores found in the dorsal skin; and two immotile types, the dark blue iridophores found in the dark blue stripes and the white iridophores found in white stripes (Hirata *et al.*, 2003). Iridophore specification has been suggested to occur around 20 hpf in zebrafish while differentiation is observed later around 42 hpf. The gene *ltk* has been found to be required for iridophore development (Lopes *et al.*, 2008). However, the genes involved in iridophore development downstream *ltk* are not yet completely described. Loss of *ltk* has recently been found to be responsible for *shady* mutant loss of iridophores (Lopes *et al.*, 2008). It has been suggested that *ltk* was expressed in two phases corresponding to promoting iridophore development at two different timepoints. *ltk* expression was observed early, and likely in a multipotent progenitor, where it could be required for iridophore fate choice and later it exclusively persisted in iridoblasts/iridophores (Lopes *et al.*, 2008).

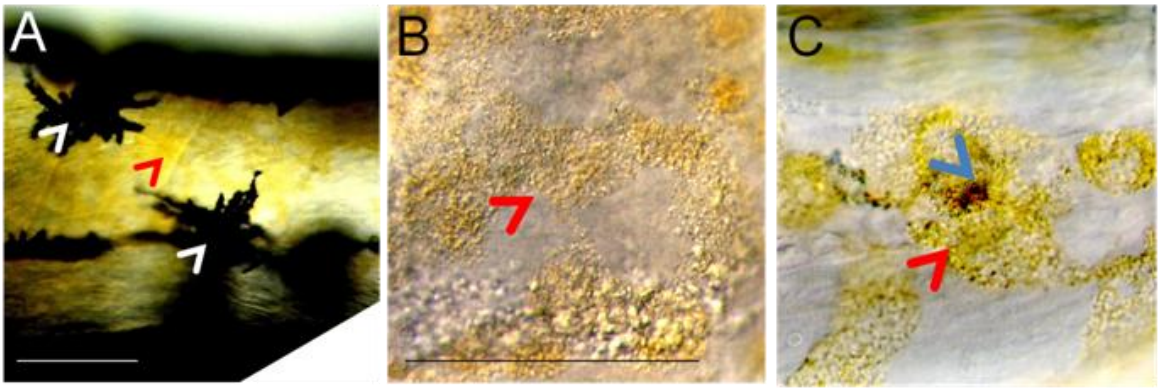

Figure 1.09: The three pigment cell types present in zebrafish and visible at 72 hpf

In the trunk of embryos, in lateral view (A), black melanocytes and yellow xanthophores can be observed (A, white arrowheads point at melanocytes, the red arrowheads point at xanthophores in 72 hpf embryo in bright field). A close up on xanthophores in the dorsal head (B, the red arrowheads show xanthophores) and in the dorsal trunk (C, the red arrowheads show xanthophores) in a 72 hpf embryo treated with PTU to avoid melanisation. In the trunk, iridophores can be observed (C, blue arrowhead shows an iridophore). Scale bar: 50 µm.

1.16 Building the melanocyte GRN model

1.16.1 Systems Biology as an approach to melanocyte development

Throughout this study, a systems biology approach has been adopted to improve the understanding of the GRN underlying melanocyte development. Systems Biology is a field which focuses on the integrated study of multiple components of a system simultaneously. It also allows integration of quantitative data of a system and utilises modelling to understand the system's dynamics. The use of mathematical and computational modelling has allowed the exploration of biological processes to gain insights which might not be possible through traditional lab based experimentation due to complex interactions and feedback between multiple components within a system. Consequently, systems biology is a growing tool for research into genetics and related fields. Significant examples of the use of mathematical modelling in biology include the Michaelis-Menten equations describing enzyme kinetics, Turing's studies in morphogenesis, the work of Hodgkins and Huxley, (1952) describing membrane potentials in neurophysiology (M.Sriram Iyengar, 2011).

Systems biology proceeds via iterative rounds of biological data collection and mathematical modelling as described in Figure 1.10. Where the system changes in time, the model is a dynamic one. Its variables are the components which vary with time, its parameters are numerical values which encode information about the system which is not included in the dynamic state, meaning that these parameters do not vary. The system may most simply be encoded by ordinary differential equations (ODE), by which the model gives the rates of change of the variables as functions of the state at a given time. In ODE, there is only one independent variable with ordinary derivatives. Another type of equations, partial differential equations (PDE), contains unknown multivariable functions and their derivatives are described as functions of several variables. PDE are often used to model multidimensional systems i.e. systems with more than one independent variable. Mathematical modelling is limited by the quality and the range of quantitative biological data.

In zebrafish, Chan *et al.*, (2009) modelled the GRN underlying embryonic development and more particularly the signalling responsible for dorsoanterior–ventroposterior patterning and endoderm formation. They used Pubmed and Zfin databases, combined with the Medscan software, to integrate the data available in the literature and to investigate the regulatory motifs and feedback loops responsible for ventral and dorsal patterning. This study allowed them to describe the intracellular role of *dharma* and *tailless 1* (*tll1)/chordin* in cross-inhibiting GRN motifs for dorso-ventral polarity and the role of maternally driven regulatory loops for determination of the dorso-ventral axis.

Further aspects essential in cell development can be integrated by the systems biology approach, for example, the determination of cell to cell heterogeneity and the stochasticity of gene expression. These two aspects can explain the differences of cells emerging from apparently homogeneous cell population in the same environment. As an important challenge, linking the systems biology and the developmental biology fields, it will be crucial to model cell to cell variability during development to understand

parameters which are important for cell specification and differentiation. As explained and tested in Mao and Resat, (2004), the role of stochasticity in gene expression and regulatory events is at the centre of this challenge and it these aspects will be detailed in the Chapter 4.

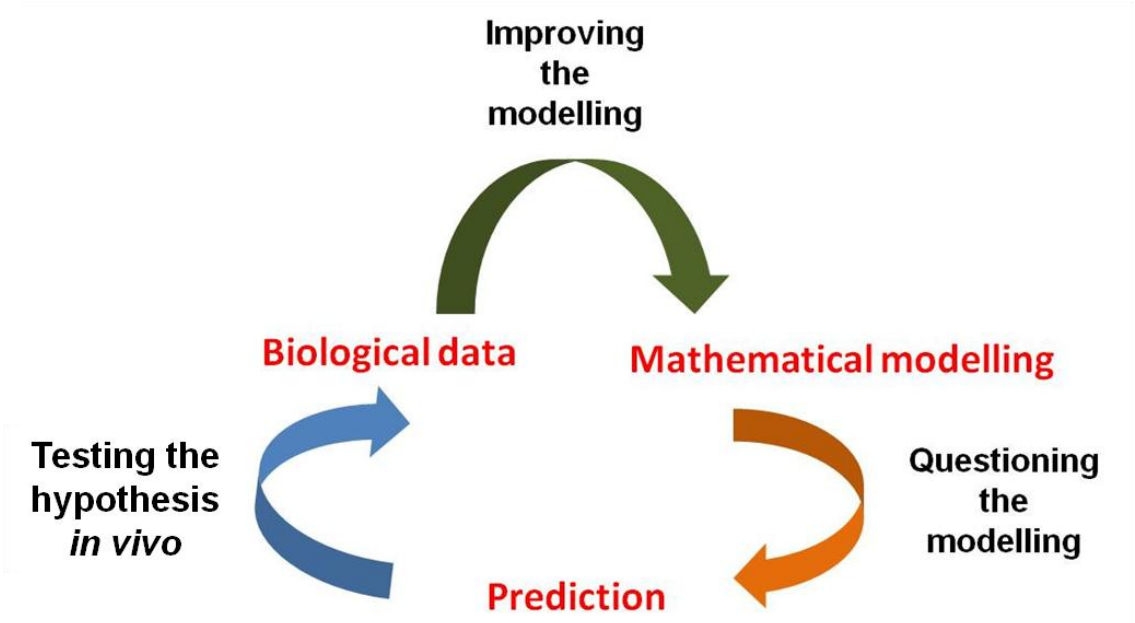

Figure 1.10: Simplified representation of an iterative systems biology approach.

The starting point of this systems biology study was biological data. Data collected were then used to build a mathematical model. The model was used with representative parameter values to run simulations. The new features of the biological system could be predicted from these simulations and, predictions were tested against the existing, or the new, experimental observations. This iterative process allowed the confirmation, or re-adjustment, of the mathematical model. The hypothesis derived from the modelling predictions could then be tested, *in vivo*, and used to improve the system and to better mimic the *in vivo* system. This powerful method allows insight into the biological system and better understanding of the key factors and their fluctuations.

1.16.2 *In vivo* study of melanocytic gene expression allowed the definition of the first melanocyte GRN

Building the melanocyte network in zebrafish, Greenhill *et al,* (2011) focused on the dynamic regulation of the two well described transcription factors *sox10* and *mitfa*. The mathematical model constructed from experimental results, collected *in vivo,* was the starting point of experiments carried out here (Figure 1.11). The study of melanocytic gene expression in WT and in *sox10*^{t3} and *mitfa*^{w2} mutants allowed, in combination with an iterative process of modelling, the assembly of a GRN for melanocyte development. *sox10* and *mitfa* show a very specific and complex inter-regulatory feedback loop during melanocyte development which allows the activation of melanocyte specification. This inter-regulation also permits the maintenance of the expression of the genes involved in melanocyte differentiation, as well as, the loss of early specification factors such as *sox10*. The GRN of melanocyte development allows the representation of the complex aspects of the regulatory mechanisms implicating *sox10* and *mitfa* in melanocytes in zebrafish.

1.16.3 The modelling predicted the existence of a factor involved in the maintenance of *mitfa* expression in melanocytes

The mathematical modelling made predictions of novel and potentially important relationships between genes in the melanocyte GRN (Greenhill *et al*., 2011)**.** A direct or indirect negative feedback loop causes *mitfa* dependent downregulation of *sox10*. Clearly, if Sox10 is lost, another process has to replace the role of Sox10 in maintaining *mitfa* expression in differentiated melanocytes. This factor was named Factor Y, and was predicted to show the following properties: 1) be activated during melanocyte differentiation, 2) be a direct or an indirect activator of *mitfa*, 3) be indirectly or directly activated by Mitfa, and 4) be required for maintenance of melanocyte differentiation (Figure 1.11). Given that Wnt signalling is a direct activator of *mitfa* during melanocyte specification, it is a plausible candidate regulatory factor for melanocyte differentiation and maintenance of *mitfa*. This hypothesis is the subject of Chapter 3, whereby Wnt signalling is tested as a possible candidate for the unknown Factor Y.

1.16.4 Mitfa can directly regulate *sox10* expression

In vivo data showed that *sox10* expression and Sox10 proteins were decreasing during melanocyte differentiation in zebrafish. Although, it was not tested in zebrafish if *mitfa* expression was maintained in melanocytes until late differentiation phase, it was shown that *mitfa* expression was maintained in melanocytes after *sox10* expression decreased. The simple melanocyte GRN predicted that the loss of *sox10* expression would result, either directly or indirectly, from the expression of *mitfa*. Greenhill *et al.,* (2011) suggested that Mitfa could directly repress ***s****ox10* expression by binding to one or more of the six M-boxes (Mitfa-binding sites) identified in the 7.2 kb *sox10* promoter region shown to reproduce the initial *sox10* expression pattern (Dutton *et al.*, 2001).

To assess if Mitfa could be directly repressing *sox10* expression, this study focused on the *Tg(-7.2sox10:GFP)* reporter line, in which a 7.2 kb fragment of the promoter proximal region of *sox10* genomic DNA drives GFP expression. Previous results showed that *mitfa* overexpression caused a clear GFP expression in transgenic fish at both an early time point (6 hpf), as well as later (10.5 hpf), consistent with possible direct regulation. In contrast, in the same experiment, very few (6 %) embryos injected with *sox10* RNA showed GFP expression at 6 hpf, whereas essentially all transgenic embryos showed GFP by 10.5 hpf (Greenhill *et al.*, 2011). This is consistent with the idea that s*ox10* did not directly regulate this reporter construct itself. The 7.2 kb of *sox10* regulatory sequences in the *Tg*(-7.2*sox10*:*GFP)* transgene contains six consensus M-boxes, making it plausible that Mitfa bound directly to this promoter. This began to narrow the search for the region of the *sox10* promoter which is likely to mediate this response to Mitfa. Greenhill *et al.,* (2011) repeated these experiments in the *Tg*(- 4.9s*ox10*:*EGFP)* line in which the 5' three M-boxes were absent (Carney *et al.*, 2006). Interestingly, this transgene showed no response to injected *mitfa* mRNA at 6 hpf. This result suggested that if Mitfa regulated *sox10* expression, it would be via one or more of the 3' M boxes. Importantly, these experiments, which examined the reporter in the context of zebrafish blastomeres, did not necessarily reflect the promoter's response in melanoblasts. Therefore, *sox10* expression was investigated in *mitfa*^{w2} mutants in order to better understand *mitfa*'s role on *sox10* repression in the melanocyte lineage. If Mitfa was necessary for repression of *sox10,* the prediction was that *mitfa* mutants should show persistent s*ox10* expression. In *mitfa* mutants, at 72 hpf, a stage when wild-type embryos show no detectable *sox10* expression in melanocytes, but rather show strong expression in the peripheral nervous system and ear, *sox10* expression could be detected in the position of the dorsal stripe (Greenhill *et al.*, 2011). Expression of GFP fluorescent protein, when driven by *sox10* promoter, responded to ectopic *mitfa* expression. There are no published reports of MITF (positively or negatively) regulating *Sox10* expression in mouse, but the correlation observed between an ectopic activation of *mitfa* and a strong transcriptional activation of *sox10* in early zebrafish embryos allowed Greenhill *et al.,* (2011) to suggest that a co-repressor would turn Mitfa into a negative regulator of *sox10* in melanocytes *in vivo* (Greenhill *et al.*, 2011). Consequently, the hypothesis was suggested that a *mitfa*-dependent repression of *sox10* could be the cause for the gradual diminution of *sox10* expression, which led to a loss of Sox10 protein and mRNA detection by 52 hpf in melanocytes in zebrafish. Mitfa and a negative co-repressor, were responsible for *sox10* downregulation, and it would be interesting to identify this co-repressor.

This hypothesis is plausible knowing that it has previously been shown that Mitfa, as a transcription factor, could recruit co-regulators, co-activators, or co-repressors, of gene expression, to the promoter of specific genes, to modulate their expression specifically in melanocytes. The chromatin deacetylase protein (Hdacs) responsible for epigenetic downregulation of gene expression, were tested as a candidate as Mitfa co-repressor of *sox10* in melanocytes as presented in Figure 1.11. Ignatius *et al.,* (2008) studied *hdac1/colgate* mutant zebrafish and described a persistent activation of *sox10* expression compared to WT, in the dorsal region of zebrafish embryos by 48 hpf. This phenotype could be the result of a loss of repression of the gene in absence of Hdac1. A decrease in *sox10* expression could be Mitfa and Hdac dependent with Hdac being a Mitfa dependent

co-repressor of *sox10* (Figure 1.11) and this hypothesis was presented and tested in Chapter 5.

1.16.5 Sox10 represses genes downstream of *mitfa* except *tyrp1b*

Greenhill *et al.*, (2011) also showed that *sox10* had a repressive effect on *dct, tyrosinase* and *silva* but interestingly not on *tyrp1b*. This repression was underlined by the observation of residual melanisation in *sox10* mutants and in *sox10/mitfa* double mutants as detailed in Chapter 5. Furthermore, when embryos were injected at one cell stage with *sox10* and *mitfa* sense RNA, *tyrp1b* expression was readily detected at 6 hpf, whereas *dct, silva* and *tyrosinase (tyr)* were not. These results suggested that *sox10* expression could repress the *mitfa*-mediated expression of most of the melanocyte differentiation genes tested, but that *tyrp1b* expression was not affected by this effect, and that the timing of *tyrp1b* expression was limited by *mitfa* expression. In Chapter 5, this aspect of *mitfa* and *sox10* regulatory interactions was re-evaluated using a different method. The repression of *dct* expression, but not of *tyrp1b* expression by Sox10, which had been studied in Greenhill *et al.*, (2011) by WISH and immunofluorescence techniques, was replicated using the technique of qPCR**.** Consequently, the levels of expression of *mitfa, sox10, dct* and *tyrp1b* were investigated in WT and $sox10^{t3}$ and $mitfa^{w2}$ mutants in order to quantitatively assess the Sox10 dependent repression of some genes downstream Mitfa.

Thus, it seems that, in melanocytes in zebrafish, *sox10* could have a pivotal role in enhancing specification through activation of *mitfa*, but also in maintaining an undifferentiated state by repressing melanocyte differentiation gene expression. It was then suggested that, once *mitfa* expression is activated, it would be maintained in melanocytes, turning down *sox10* expression and maintaining a differentiated state. Whether or not Mitfa could activate *mitfa* expression was also another hypothesis raised by the modelling. The preliminary experiment for testing if Mitfa could activate its own expression in zebrafish is described in Chapter 5.

Importantly, direct experimental testing demonstrated that *sox9b* was involved as a weak *sox10*-independent activator of melanocyte differentiation gene expression (Greenhill *et al*., 2011). However, whole-mount *in situ* hybridisation experiments have shown that neither *sox9a* and *sox9b* expression replaced *sox10* expression in zebrafish embryo melanocytes.

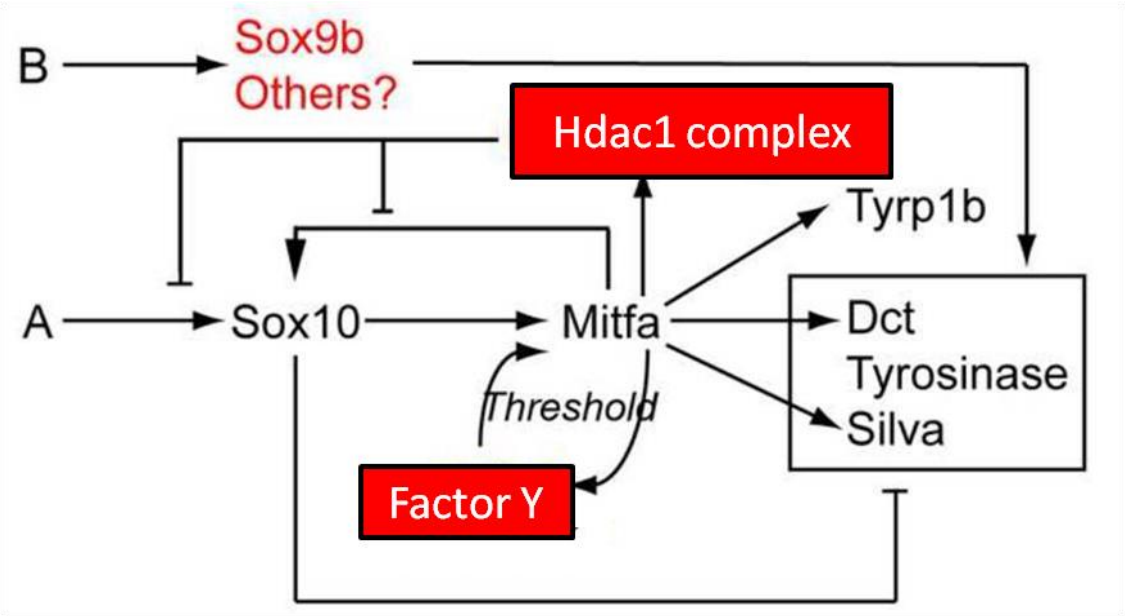

Figure 1.11: Model of the GRN underlying melanocyte development built from experimental data.

sox10 is activated by activators (A) early in NC cells. *sox10* activates *mitfa* expression but represses expression of several genes downstream of *mitfa* including *dct*, *tyrosinase* and *silva*, but not *trp1b*. The model predicted new features for the network and two aspects of the model were tested. Firstly, after *sox10* loss, the modelling predicted that an unknown factor, which was called Factor Y, was required to maintain *mitfa* expression. Wnt signalling was tested as a candidate for Factor Y. *mitfa* itself could be part of this regulation. Secondly, the role of Hdac1 as a Mitfa dependent co-repressor of *sox10* was investigated. (adapted from Greenhill *et al.*, (2011)).

1.17 Describing Wnt signalling

In Chapter 3, Wnt signalling was tested as a candidate for Factor Y. In order to introduce the general regulatory mechanisms of Wnt signalling, the basic pathway is presented here. This is further developed, in to the context of my experimental approaches, in Chapter 3.

Canonical Wnt signalling is a pathway used repeatedly in embryonic development (Barker, 2008). The canonical Wnt/β-catenin pathway is critically involved in the processes of patterning, organogenesis, proliferation, regeneration and cell–cell adhesion (Takada *et al.*, 1994, van de Wetering *et al.*, 1997, Ungar and Calvey, 2002, Barker, 2008). More particularly, it is a key factor for head induction, cardiac development and the formation of extremities (Deardorff *et al.*, 2001, Lewis *et al.*, 2004, Wu *et al.*, 2005). The canonical Wnt pathway involves the Wnt protein binding to its membrane receptor, Frizzled (Fzd) (Figure 1.12). In the absence of the Wnt protein, the glycogen synthase kinase-3β (GSK3β) sequestrates β-catenin in a complex in the cytoplasm preventing activation of the pathway. The binding of Wnt to its receptor Fzd allows the activation of β-catenin via repressing GSK3β, leading to the release of β-catenin from its cytoplasmic complex. β-catenin then translocates to the nucleus to activate gene expression with a co-activator, Lymphoid Enhancer-binding Factor-1 (Lef-1) which also functions as a transcription factor (Kofahl and Wolf, 2010). Free β-catenin can also bind to E-cadherin and α-catenin to modulate the conformation of the cytoskeleton (Figure 1.12). β-catenin degradation is strictly regulated. Indeed, β-catenin protein is constantly produced and the mechanisms causing its degradation require sequential phosphorylation via different components like casein kinase 1α (CK1α). CK1α phosphorylates β-catenin at Ser45 and then β-catenin is phosphorylated at three further N-terminal serine and threonine residues (Ser33, Ser37 and Thr41 in humans) by GSK3β. These phosphorylations occur within the destruction complex which also contains proteins such as phosphatases and the two scaffold proteins adenomatous polyposis coli (APC) and axin-1. *β*-transducing-repeat-containing protein (*β* –TrCP), a subunit of the ubiquitin ligase complex, can then recognize and mark the complex with ubiquitin, causing its proteasome-dependent degradation.

The non-canonical Wnt pathway is activated by the binding of the Wnt protein activators of Frizzled and its co-activators, ROR2, a member of the receptor tyrosine kinase-like orphan (ROR) family, and, the protein Related to Tyrosine Kinase (RYK). This signal is transduced in the cell via three pathways; the Dishevelled (Dsh)/c-Jun Kinase (JNK) dependent pathway, involved in planar cell polarity (PCP); the Dsh/ROCK dependent pathway, involved in actin cytoskeleton regulation; and the Ca^{2+}/Nuclear Factor of activated T cells (NFAT) dependent pathway (Figure 1.13) (Dorsky *et al.*, 1998).

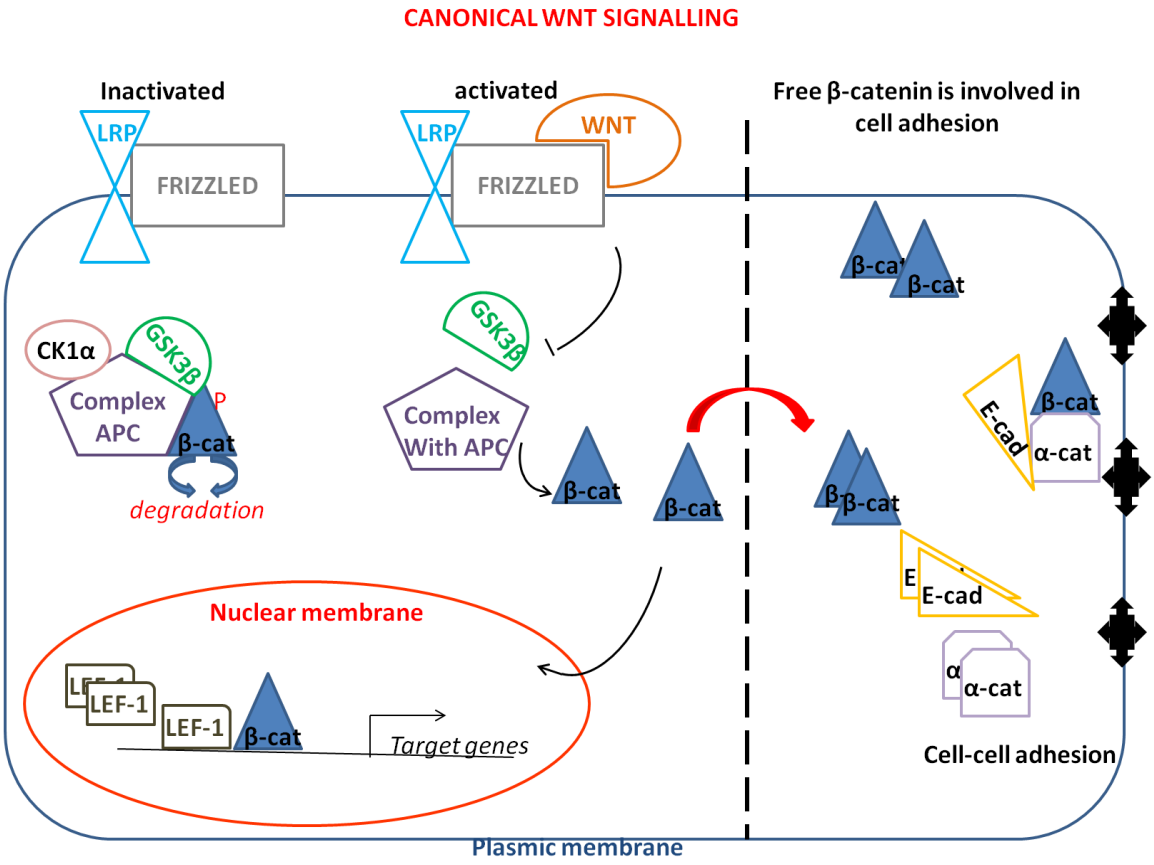

Figure 1.12: Description of the Wnt signalling canonical pathway and the roles of free β-catenin in cells.

In the presence of the Wnt signal, Wnt binds to its receptor Frizzled (with co-receptor LRP5/6) leading to inhibition of GSK3-β and release from the APC/CK1a complex in the cytoplasm. The liberation of β-catenin from the degradation complex which includes APC and Axin proteins, results in the translocation of β-catenin to the nucleus. This translocation to the nucleus permits the activation of the effectors of the Wnt pathway, β-catenin and its co-activator, Lef/Tcf, for the transcription of targeted genes. In the absence of Wnt signalling, part of the complex, β-catenin (β-cat) is phosphorylated and targeted for degradation. The activation of Wnt signalling leads to increase β-catenin in the cytoplasm. At the membrane, β-catenin can associate with α-catenin (α-cat) and E-cadherin (E-cad) to regulate cell polarity. The black structures represent tight junction proteins regulated by β-catenin/ α-catenin/ E-cadherin (Adapted from Gilbert, S. Developmental Biology, 9th Edition.)

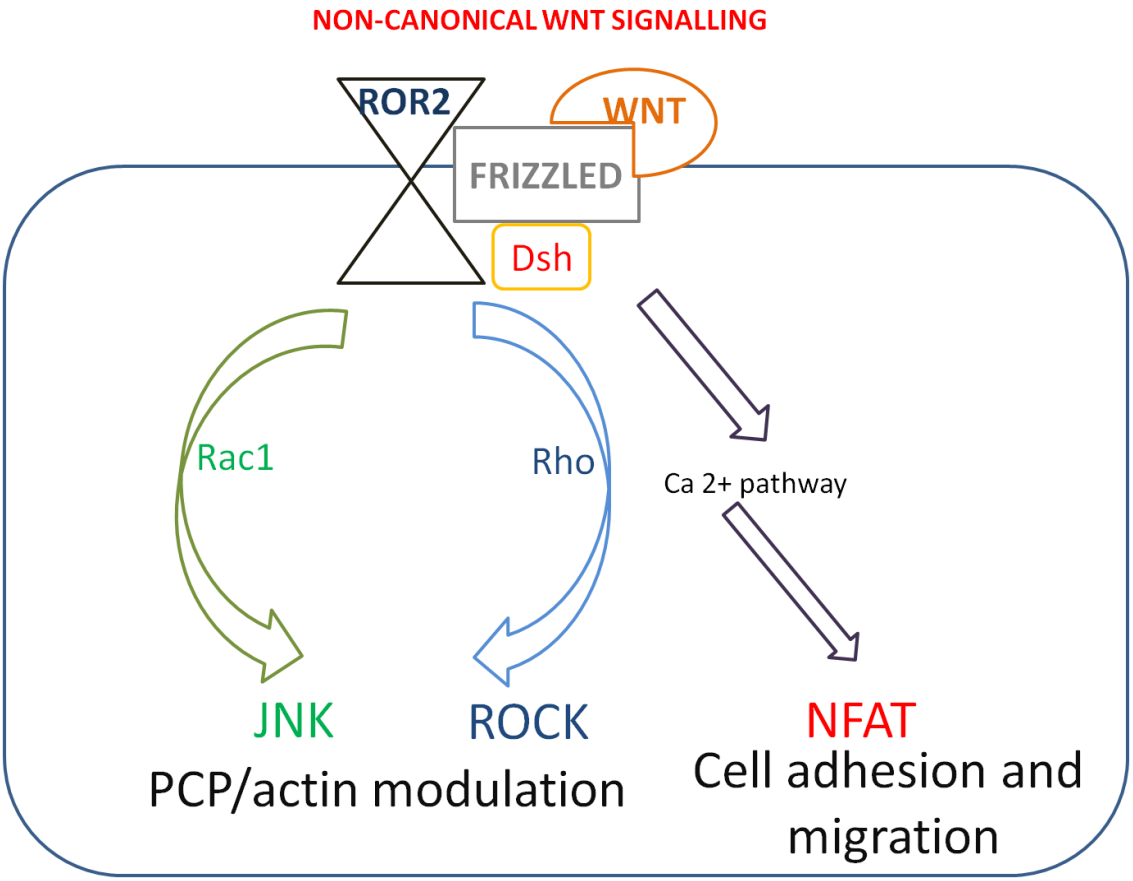

Figure 1.13: The role of the non-canonical Wnt signalling in cells.

Activation of the non-canonical Wnt signalling patway, by the Wnt protein, which binds to a receptor Frizzled, and the co-receptor ROR2, allows the activation of the dishevelled (Dsh) dependent pathways. This activation leads to regulation of the Planar Cell Polarity (PCP) and to the modulation of the actin cytoskeleton by activating the proteins ROCK and JNK. ROCK is activated by a cascade which involves the small G- protein Rho, and the activation of JNK involves the activation of the small G-protein Rac1. The non-canonical Wnt pathway also activates the Ca^{2+} dependent pathway which leads to activation of NFAT and which is involved in cell adhesion and cell migration.

1.18 Melanocyte development is affected by Wnt signalling

As further described in Chapter 3 and briefly described here, Wnt signalling has been shown to be required for melanocyte specification. Furthermore, it is a known activator of *mitfa* at early stages (Dorsky *et al.*, 1998). *In vitro* studies showed that *Mitf-M* promoter possesses TCF/LEF1 binding sites. It has been reported that Wnt signalling was capable of activating *Mitf* transcription through those TCF/Lef1 binding sites (Takeda *et al.*, 2000a, Dorsky *et al.*, 2000a). This result has suggested a direct activation of *Mitf* by TCF/LEF1 at their binding site. Studies in mouse, *Xenopus* and zebrafish converged to show the crucial role played by Wnt signalling in melanoblast specification (Aoki *et al.*, 2003, Dorsky *et al.*, 2000b). Additionally, an inhibitor of the canonical Wnt signalling pathway, Dickkopf-1 (DKK1), is secreted by fibroblasts in the dermis of human skin and suppresses melanocyte differentiation via the suppression of *β*-catenin and consequently decreases expression of MITF (Yamaguchi *et al.*, 2007).

The molecular details of the components underlying this process are less clear, although in zebrafish, *wnt1*, *wnt3a*, as well as, the receptors *frizzled 8* and *10*, were found to be expressed in the dorsal neural tube. This suggests that the pathway might be activated in this region (Nikaido *et al.*, 2013, Saint-Jeannet *et al.*, 1997b, Yanfeng *et al.*, 2003). This is consistent with the position of activation of *mitfa* expression. Furthermore, Wnt signals are widespread in the embryo and hence it is plausible that Wnt signalling could be an important factor in maintenance of *mitfa* expression at later stages, although its role during melanocyte differentiation has never been tested *in vivo*.

1.19 Heterogeneity of gene expression is important in melanocyte development

As previously explained, cell development consists of two crucial events, cell specification and cell differentiation. It is essential to understand the genetic mechanisms regulating these events. These mechanisms can be of two types: regulated or stochastic (Elowitz *et al.*, 2002, Fournier *et al.*, 2007, Garg *et al.*, 2009, Gillespie, 2009, Gupta *et al.*, 2011, McAdams and Arkin, 1997, Raj and van Oudenaarden, 2008). Both of these phenomena can cause heterogeneity and cell to cell variability, which can make each individual cell, from the same population, different to another one. In melanocytes, cell specification is marked by the expression of *mitfa*, a specification factor. During specification, cells show activation of specific factors which can influence cell fate choice. Cell commitment is defined by the transition from the phase of specification to a phase where cells are engaged in a fate and are no longer sensitive to other specification signals. Cell commitment is not clearly defined in melanocyte development, however, expression of *dct* can be understood as a marker for specification and differentiation, the phase when cells will acquire their specific phenotype (Kelsh, 2006a, Dutton *et al.*, 2001, Curran *et al.*, 2009). Cell to cell heterogeneity is probably a very important parameter for cell specification and cell commitment. Cell to cell heterogeneity combined with genetic stochasticity can trigger two

cells of the same population, in the same environment, to activate different genetic programs. Stochasticity is particularly important when key factors are present at low levels, creating probabilistic conditions for gene expression activation. Variations of expression, due to intrinsic noise create variability in cell populations from which cell diversity can emerge. For example, like that shown in a study by Elowitz *et al.,* (2002) on *E.coli*. In Chapter 4, *dct, trp1b, sox10* and *mitfa* expression levels were tested by reverse transcription quantitative real time polymerase chain reaction (RT-qPCR) at five different timepoints. The data was collected and analysed in accordance to previous studies by Quaranta and Garbett (2010) and Peixoto *et al.,* (2004) for the analysis if genetic variability.

1.20 Aims of the project

In this study, several approaches were combined to improve the modelling of the GRN involved in melanocyte development. A gene candidate approach, *in vivo*, as well as gene expression quantification approaches were applied in order to characterise the melanocyte population from early to late stages and to better observe mechanisms of gene regulation. The general aims of this study were to better understand the regulatory relationship between *sox10* and *mitfa* during melanocyte development and to test the role of other unknown and poorly described factors. Specifically we wanted to test the following hypotheses:

- **Did Wnt signalling fulfil the criteria to contributing to Factor Y?**

The first approach for testing the melanocyte GRN model was to identify a candidate for Factor Y (Chapter 3). Wnt pathway was tested as a limiting factor for maintenance of stable melanocyte differentiation. Wnt signalling has already been implicated in melanoblast specification because it is required for first *mitfa* expression. It has also been shown that the Wnt signalling effectors, Tcf /Lef1 and β-catenin, were able to bind *mitfa* promoter to enhance its expression (Dorsky *et al.*, 2000b). For these reasons, the Wnt pathway was a strong candidate for Factor Y and this hypothesis was tested using two small molecule activators of the Wnt signalling, BIO and LiCl. These experiments and results are described in Chapter 3.

- **Adapt quantitative techniques to analyse gene expression levels and their heterogeneity in the NC and melanocyte development during differentiation.**

A second objective was to better understand the development of pigment cells, from the multipotent precursors to the differentiated cells. One key issue which remained unanswered concerned the precise dynamics of expression for key melanocyte genes including *mitfa* and *sox10* in developing melanocytes. Although both were assumed to persist in mouse, it was not clearly demonstrated (Hou and Pavan, 2008). The modelling depends on the observation that *mitfa* expression was maintained in differentiated melanocyte in zebrafish, whereas *sox10* expression was lost. The levels of both *mitfa* and *sox10* expressions were tested by qPCR. The technique of RT-qPCR in pools of five cells allowed us to investigate gene expression in cell population at a fine resolution (Chapter

4). Analysis of the heterogeneity of key gene expressions, combined with analysis of the gene expression time-courses, allowed better description of gene expression in melanoblasts and melanocytes (Chapter 4).

- **- Quantify the level of melanocytic gene expression in WT and mutants to test the GRN model.**
  - Does Hdac activity have a role in repressing Sox10 expression?
  - Can Mitfa activate its own expression?

Finally, we analysed expressions of *dct, trp1b,* s*ox10* and *mitfa* in *mitfa*^{w2} and in *sox10*^{t3} mutants in order to test the predictions of the GRN *in vivo* using quantitative methods (Chapter 5). Furthermore, two potential key features of the *sox10* and *mitfa* regulatory mechanisms suggested by the modelling were tested (Chapter 5). Firstly, a potential feature tested was the role of Hdacs as a co-repressor for the Mitfa-dependent repression of *sox10* in melanocytes. Secondly, the hypothesis that *mitfa* could be positively self-regulating its own expression was investigated (Chapter 5).

Chapter 2. Material and Methods

2.1 Fish Husbandry

All zebrafish (*Danio rerio)* lines, Wild type (AB) zebrafish, transgenic lines *Tg(-7.2sox10:EGFP),* (Carney *et al.,* 2006) and *Tg(TOP;dGFP)* (Dorsky *et al.,* 2002) as well as mutant lines *mitfa*^{w2} (Lister *et al.,* 1999), *mitf*a^{b692} (Lister *et al.*, 2001), *sox10*^{t3} (Kelsh *et al.*, 1996b) zebrafish, were kept at University of Bath and handled as suggested by Home Office directives and as described in the referred Zebrafish book, (Westerfield, 2000). All the crosses were set up between fish overnight and the embryos were collected in the morning. Embryos were raised in embryo medium (EM) (0.5 µM sodium chloride 0.17 µM potassium chloride 0.33 µM calcium chloride 0.33 µM magnesium sulphate 0.1 % methylene blue in distilled water) at 28.5 °C and staged according to Kimmel *et al.*, (1995). Watchmakers'No5 forceps were used for the manipulation of embryos, to remove the chorion, between laying and hatching. Embryos older than 15 hpf, which were to be manipulated in any way, were anaesthetised with triccaine (Ethyl 3-aminobenzoate methanesulphonate, 4 g/L stock, final concentration approximately 0.2 % v/v). Where appropriate, melanisation was inhibited, using 1-phenyl-2-thiourea (PTU) (Sigma-Aldrich, England), before 24 hpf and at a final concentration of 0.003 % to 0.0015 % in EM. All experiments complied with institutional and national animal welfare laws, guidelines and policies.

2.2 Cell dissociation methods

This method has been adapted from The Zebrafish Book, (Westerfield, 2000). Dechorionated embryos were rinsed three times in 1X Holtfreter's solution (0.35 % (w/v) NaCl, 0.005 % (w/v) KCl, 0.01 % (w/v) $CaCl_2$, 0.02 % (w/v) $NaHCO_3$ in H2O), transferred to an 1.5 mL Eppendorf and disaggregated with a micropestle (Eppendorf, Hamburg, Germany) by firmly inserting the micropestle in the tube 5-6 times, being careful not to grind the cells. The disaggregate was then centrifuged in a cooled benchtop centrifuge (Spectrafuge 24D, Jencons-PLS) at 1100 rotation per minute (rpm) for 5 minutes and the supernatant was discarded. The pellet was re-suspended in 1 mL of 0.5 % Trypsin-EDTA (Gibco) using a P1000 pipette tip. Cells were incubated for 15 minutes at room temperature and pipetted every 5 minutes to help break down the large clumps of cells, to enable the small clumps to be broken down into single cells. Cells were then centrifuged for 5 minutes at 1100 rpm (Spectrafuge 24D, Jencons-PLS), the supernatant was discarded and cells were re-suspended in 1 mL of EM. Suspension was filtered using a 40 µm cell strainer into a 50 mL Falcon tube (BD Bioscience, NJ, USA). The cell trainer and the falcons were previously rinsed with 10 % FBS (Foetal Bovine Serum) /PBS (Phosphate

Buffered Saline, PBS: 2.7 mM KCl, 137 mM NaCl in sterile water) to prevent cells from sticking to plastic equipment. After filtering, the Eppendorf was rinsed with 500 µL of medium (10 % FBS/PBS) which was re-filtered. The filter was then washed with another 500 µL of medium (10 % FBS/PBS). The filtering process was performed to ensure that only single cells (not clusters) were processed.

2.3 Plasmid DNA preparation for cloning

All the molecular biology methods described here are referred to the "Molecular Cloning: A Laboratory Manual" book from Sambrook and Russell, (2001).

2.3.1 Transformation and bacterial growth conditions

The transformations of plasmid DNA into *E. coli* competent cells were performed by heat shock. DH-5αF' (Clontech Laboratories Inc., CA) strain was prepared by Dr Masataka Nikaido using chemically induced competency. 30 mL of competent *E. coli* cells at -80 ºC were defrosted on ice for 20 minutes with occasional mixing of the 1.5 mL microfuge tube. 1 µL of 1 $\mu g.mL^{-1}$ stock plasmid was added to the cells and the mixture was then kept on ice for 20 minutes with the occasional gentle mixing. The tubes were then incubated at 42 ºC water bath for 42 seconds and immediately placed on ice and left for 5 minutes.

After transformation, cells were incubated in 9 volume Luria Broth medium (Sigma-Aldrich, England, LB, (2.5 % (w/v) base in Milli-Q water)) for one hour. 100 µL of the cells/LB mixture was then spread on LB-agar plates containing the appropriate antibiotic at the appropriate concentration overnight at 37 ˚C. Antibiotics were ampicillin (Sigma-Aldrich, England) at 50 $\mu g.mL^{-1}$ or kanamycin (Sigma-Aldrich, England) at 25 $\mu g.mL^{-1}$. Prospective positive colonies on the LB-agar plates were then picked and grown in LB-medium with antibiotic. Cells were then incubated overnight at 37 ºC in a shaking incubator, the culture volume was chosen according to the specific extraction protocols.

2.3.2 Minipreperation of plasmids DNA

Colonies were selected from LB-agar plates and were grown overnight in 3 mL LB medium with appropriate antibiotic. The plasmid DNA was purified using Promega Wizard miniprep or QIAGEN DNA purification kits from which all solutions come from. 1.5 mL culture was harvested by centrifugation for 5 minutes at 14,000 rpm (Techne Genofuge 16M). The supernatant was discarded and the cells re-suspended in 250 µL Cell Resuspension Solution (Promega). 250 µl Cell Lysis Solution (Promega) were added and mixed, followed by 10 µL pf Alkaline Protease Solution (Promega). The lysate was incubated for 5 minutes at room temperature. 350 µL of Neutralisation Solution (Promega) were then added and mixed. The lysate was centrifuged for 10 minutes at 14,000 rpm (Spectrafuge 24D, Jencons-PLS). A spin column (Promega) was inserted into a collection tube and after centrifugation the cleared lysate was applied to the column. This was centrifuged for 1 minute at 14,000 rpm (Spectrafuge 24D, Jencons-PLS). The flow-through was discarded and the column was washed firstly, with 750 µL and then, with 250 µL, of

Wash Solution (Promega), by applying the solution to the column (Promega) and centrifuging for 1 minute. The column (Promega) was then centrifuged for a further 2 minutes (Spectrafuge 24D, Jencons-PLS) to ensure that all the Wash solution (Promega) had been cleared from the column (Promega). The DNA was then eluted from the column (Promega) by placing the column (Promega) in a clean microcentrifuge tube (Promega), applying 100 µL of nuclease-free water to the column (Promega) and centrifuging for 1 minute at 14,000 rpm (Spectrafuge 24D, Jencons-PLS). The DNA was checked on a 1 % agarose gel (1 % (w/v)) (UltraPure Agarose, Invitrogen) before storage at -20 ˚C.

2.3.3 DNA digestion

DNA was mixed with 2 µL of 10x buffer appropriate to the enzyme used (Promega or Invitrogen), 1 µL of restriction enzyme (Promega or Invitrogen) appropriate for the experiment, and 13 µL MilliQ water. The digests were then incubated for 2 hours at 37 ˚C. The digests were run on a 1 % agarose gel to look for the presence of the expected bands. If the plasmid was not fully digested a further 1-3 µL of enzyme (Promega or Invitrogen) were added and the incubation at 37 ˚C was extended for 2 hours, or was processed over-night at 4 ˚C. The digests were then run on a 1 % agarose gel to check for complete digestion.

2.3.4 Gel extractions

Where it was required to extract a band from a gel (agarose gels 0.8 – 2 % (w/v) (UltraPure Agarose, Invitrogen), to send for sequencing, the required band was excised from the gel and the DNA purified from this band, using a Qiaquick Gel Extraction Kit (Qiagen). When the band had been excised from the gel, the gel slice was weighed. Three volumes of Buffer QG (Qiagen were added to the gel slice in a 2 mL microcentrifuge tube (i.e. 300 µL Buffer (Qiagen) for every 100 mg of gel). The mixture gel slice/Buffer QG (Qiagen) was incubated at 50 ˚C for 10 minutes until the gel slice had dissolved. One gel volume of isopropanol was then added to the mixture and mixed. A Qiaquick spin column (Qiagen) was placed in a 2 mL microcentrifuge tube and the sample was applied to the column. The mixture was centrifuged for 1 minute at 14,000 rpm (Spectrafuge 24D, Jencons-PLS) and the flow-through was discarded. Where the volume of the sample exceeded 750 µL the column was spun once, and the remainder of the sample was added to the column to be spun again. The column was washed by applying 750 µL of Buffer PE (Qiagen) to the column and centrifuging for one minute at 14,000 rpm (Spectrafuge 24D, Jencons-PLS the flow-though was then discarded. The column was centrifuged again at 14,000 rpm (Spectrafuge 24D, Jencons-PLS) for 1 minute to remove all residual Buffer PE (Qiagen). The column was then placed in a clean microcentrifuge tube and the DNA was eluted by applying 30 µL or 50 µL of MilliQ water to the column. The column was then incubated at room temperature for 1 minute and was centrifuged for 1 minute at 14,000 rpm (Spectrafuge 24D, Jencons-PLS). The sample was then observed on a 1 % agarose gel (UltraPure Agarose, Invitrogen).

2.4 *In vitro* transcription of RNAs

All the molecular biology methods described here are referred to the "Molecular Cloning: A Laboratory Manual" book from Sambrook and Russell, (2001).

2.4.1 RNA preparation using mMessage mMachine (Ambion)

The transcription reaction was set up using mMessage mMachine kit (Ambion) as followed. First, the Nuclease free water (Ambion) was added to bring final volume to 20 µL. Then, 10 µL of 2x NTP/CAP (Ambion), 2 µL of the 10x reaction buffer (Ambion) and 1 µg of the template DNA, were added to the mixture. Finally, 2 µL of enzyme mix (SP6) (Ambion) were added and the reaction mixture was mixed and incubated at 37 ˚C for 2 hours. After that, 1 µL of the TURBO DNase (Ambion) was added to the sample which was mixed and incubated at 37 ˚C for 15 minutes. Finally, the RNA was recovered using a MEGAclear kit (Ambion).

2.4.2 Purification of *in vitro* transcribed RNA using a MEGAclear kit (Ambion)

An RNA transcription reaction was made up to 100 µL with Elution buffer (Ambion). First, 350 µL of the Binding solution (Ambion) and 250 µL of 100 % Ethanol were added. The mixture was mixed and pipetted to the filter in a collection tube. This was centrifuged for 1 minute at 14,000 rpm (Spectrafuge 24D, Jencons-PLS). The collection tube (Ambion) was discarded and the filter washed twice with 500 µL Washing Solution (Ambion). The filter was centrifuged once more, for 1 minute at 14,000 rpm (Spectrafuge 24D, Jencons-PLS) and the solution was discarded. To elute the RNA, 50 µL Elution Buffer (Ambion) was preheated to 95 ˚C and was applied to the filter. In a clean collection tube, the mixture was centrifuged for 1 minute at 14,000 rpm. This last step was repeated to increase the yield.

2.4.3 mRNA extraction from zebrafish embryos

Phenol/Chloroform purification and ethanol precipitation

In most cases 50 embryos were transferred into 2 mL tubes. 1 mL of TRI REAGENT (Sigma-Aldrich, England, T9424) was first added under the hood and the solution was well homogenized with syringes (25 mm). TRI reagent (Sigma-Aldrich, England) is a commercially available reagent for single step total RNA isolation (Chomczynski and Sacchi, 1987). The solution was then centrifuged at 12,000 rpm (Spectrafuge 24D, Jencons-PLS) for 10 minutes and the supernatant was transferred to new tubes. 0.2 mL of pure chloroform (per mL of reagent) was added and the solution was vortexed for 15 seconds and was then left standing at room temperature for 10 minutes. Then, the mixture was centrifuged 15 minutes at 12,000 rpm (Spectrafuge 24D, Jencons-PLS) at 4 °C and the upper aqueous phase was transferred to a fresh tube. 0.5 mL isopropanol per tube per mL of TRI reagent (Sigma Aldrich, England) was added and the solution was vortexed for 5-

10 seconds at room temperature. The solution was centrifuged for 10 minutes at 12,000 rpm (Spectrafuge 24D, Jencons-PLS) at 4 °C, and the supernatant was removed. The RNA pellet was washed in 1 mL 75 % ETOH by inverting the tube gently. The solution was finally spun for 5 minutes at 7500 rpm (Spectrafuge 24D, Jencons-PLS). Once the supernatant was taken off, the pellet was left to dry and 10 µL of DEPC-treated water was added. 1 µL of the solution was run on a 1 % agarose gel (UltraPure Agarose, Invitrogen) to attest of the purity and the concentration was measured with the spectrophotometer (Biomate 3, Thermo Scientific). If required, solutions were stored at -80 °C and were thawed and spun for 5 minutes at 12,000 rpm (Spectrafuge 24D, Jencons-PLS), before re-use.

2.5 Reverse Transcription of *in vitro* synthesised RNA or extracted from embryos.

The Invitrogen First strand cDNA synthesis kit with Superscript III (Invitrogen) was used for the reverse transcription according to the manufacturer's protocol. 0.5 µL of random primers (250 ng/µL) (Promega), 5 µL of dNTPs (2 mM) (Promega), 7.5 µL of RNA (1 µg of total RNA +DEPC-MQ) were first mixed and incubated for 5 minutes at 65 °C and then at least 1 minute at 4 °C. Then, 4 µL of 5X first strand Invitrogen buffer, 1 µL of 0.1 DTT, 1 µL of RNAse out (Invitrogen) and 1 µL of superscript III (Invitrogen) Reverse Transcriptase (Invitrogen) (RTase)/µL were added to the previous mix and left 5 minutes at 25 °C, 60 minutes at 50 °C, and 15 minutes at 70 °C. Finally, 80 µL of DEPC-treated water was added to the mixture, and the concentration was measured using the spectrophotometer (Biomate 3, Thermo Scientific). If required, solution could be kept at -20 °C.

2.6 Single cell Reverse Transcription

Embryos were first disaggregated by following the method previously described (see section 2.2). Cells were then selected using a very thin capillary glass (3 ½ Drummond glass capillaries (Drummond Scientific Co., Broomall, PA) set on a microinjector (Drummond Scientific Co., Broomall, PA) and by being pulled up by a puller (Sutter Instrument Co., Novat,CA) under an Eclipse E800 microscope (Nikon). Single cells were then immediately put in a small PCR tube to process to the reverse transcription protocol adapted from Bengtsson *et al.,* (2008) (Figure 2.01). The cells were kept in a 10 % FBS/PBS solution in a Petri dish (Sterilin). Cells targeted were of a round shape, in the bottom of the dish. The capillary was filled with oil and a bubble of air was created using the puller in order to separate the cell from the oil and also allowing the visualissation the cell and the solution once pulled. Cells picked were black when picking differentiated melanocytes or GFP positive when picking s*ox10*-EGFP neural crest cells. Importantly, iridophores could be "grey" looking under incident light but here melanocytes could be distinguished by their typical brown colour.

Reverse transcription master mixes were made according to Bengtsson *et al.*, (2008), (Figure 2.02). In a first time, cells were immersed in the lysis buffer, Guanidine Thiocyonate (GuSCN, Sigma-Aldrich), at a concentration of 0.5 M (diluted in water). Bengtsson *et al.*, (2008) showed that, at this concentration, GuSCN (Sigma-Aldrich) was one of the most efficient buffer for breaking cell membrane while preserving mRNA from the RNAses degradation. This lysis buffer was diluted to the optimal concentration of 40 mM prior reverse transcription, so that it did not interfere with the enzymatic reactions (Bengtsson *et al.*, 2008). Furthermore, in regard to enzyme activity, the ratio Reverse transcriptase (RT)/Taq polymerase was controlled to avoid inhibition of PCR reaction by RT (Bengtsson *et al.*, 2008). Therefore, the concentration of the Superscript III (Invitrogen) was decrease to a ratio < 2 (RT Unity/Taq polymerase Unity) to allow the optimal efficiency of the PCR.

The first Master Mix (MM1) for the reverse transcription was added on top of the cell/ 0.5 M lysis buffer solution in the 200 µL PCR tube. The MM1 contained 2.5 µM Oligo d(T) (Promega), 2.5 µM Random Primers (Promega), 0.5 µM dNTPs (Invitrogen) and 5 mM dTT (Invitrogen). The mix (cell/lysis buffer + MM1) was then incubated for 5 minutes at 65°C. The second Master Mix (MM2, (1x reaction buffer (Invitrogen), 40 Unity RNAse inhibitor (Invitrogen) and 20 Unity of Surperscript III (Invitrogen)) was then added, and samples were incubated 5 minutes at 25 °C, 80 minutes at 55 °C, and 15 minutes at 70 °C (Figure 2.02). Samples were then conserved in freezer at -20 °C.

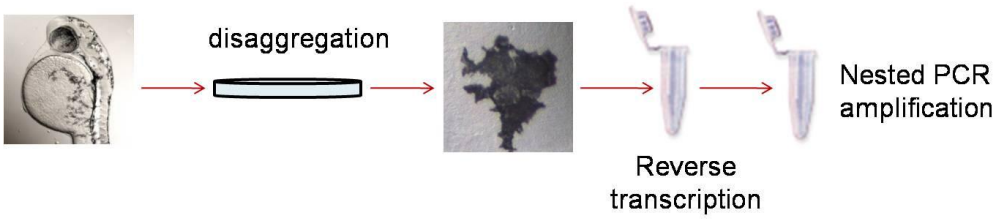

Figure 2.01: Single cell preparation for reverse transcription and nested or quantitative PCR.

Embryos were disaggregated and cells were isolated in 10 % FBS/PBS solution in 90 mm Petri dishes (Sterilin). Cells were then picked one by one and released in a PCR tube in about 1 nL 10 % FBS/PBS solution. The adjusted volume of lysis solution Guanidine Thiocyonate (GuSCN, Sigma-Aldrich) was then added and, cells were kept on ice until proceeding to the rest of the reverse transcription protocol. mRNA extraction and reverse transcription were processed in the same tube according to Bengtsson *et al.*, (2008) to avoid loss or contamination.

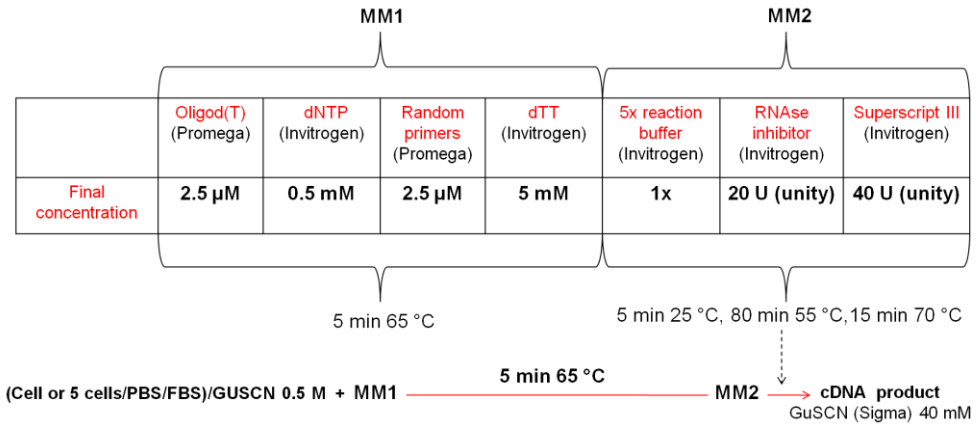

Figure 2.02: Table showing final concentrations for single cell or five cells reverse transcription Master Mix 1 and 2.

First, the cell is bathed in 4 µL of 0.5 M Guanidine Thiocyanate (GuSCN, Sigma-Aldrich, England) solution. Secondly, the first Master Mix (MM1) was added and samples were incubated at 65 °C for 5 minutes. Thirdly, Master Mix 2 (MM2) was added and samples were incubated (5 minutes at 25 °C, 80 minutes at 55 °C, and 15 minutes at 70 °C). Samples could be stored at -20 °C. The Superscript III (Invitrogen) was used from stock preparation concentrated at 200 U per µL.

2.7 PCR and Nested PCR

The GoTaq Green Maxter Mix (Promega) was always used for PCR reactions. PCR reactions were set according to the Promega's manufacture's protocol, in 25 µL final volume. A mixture of 0.1 µM of each right and left primers was used for each PCR reaction. Using a spectrophotometer (Biomate 3, Thermo Scientific), a volume of experimental DNA corresponding to 1 µg of material was added to the mixture, as well as, 12.5 µL of the GoTaq Green Master mix (Promega) and MilliQ water was added to a total volume of 25 µL. The PCR program used was: 2 minutes 95 °C, 35 cycles (1 minute at 95 °C, 1 minute at 60 °C, 1 minute at 95 °C) and 5 minutes at 72 °C, in PCR thermocycler machine (G-Storm, GS00001 or G-Storm, GF00482). Samples were stored at -20 °C when needed. Products were run on a 1 % agarose gel ((w/v) (UltraPure Agarose, Invitrogen).

For nested PCR, the two amplification rounds were processed as described for PCR reactions however, two different pair of primers were used, the "external" set in a first time for the first round of amplification and the "internal" set in a second time for the second round of amplification. For the first round of amplification, cDNA issued from embryos/cells was used as template, while for the second round of amplification, DNA from first round amplification was used as template (Figure 2.03).

Primers have been designed using Primer3 Plus software (http://www.bioinformatics.nL/cgi-bin/primer3plus/primer3plus.cgi.) software to all span an intron. These allowed to control and observe when genomic sequences were amplified (Table 2.01).

Table 2.01: The following primers were used and amplicon sizes are shown:

GENE	Amplicon length	Primer forward	Primer reverse
mitfa **external**	**287 bp**	AAACCCCCTCGAAGTACCAC	AAGTCCTGCATCCATGAACC
internal	**215 bp**	GCACTAGGAGCCAAGCTGAG	TTGGAATCAAGCTACAGTGATGA
β-actin **external**	**482 bp**	TACCCCATTGAGCACGGTAT	GTTCCCATCTCCTGCTCAAA
internal	**251 bp**	TACAATGAGCTCCGTGTTGC	CATGGGGAAGAGCGTAACC
ltk **external**	**172 bp**	ATGCTGCCAGTCAAATGGAT	ATGCGACCTCCACCAGTTAC
internal	**107 bp**	TGCCACCTGAAGCTTTCCTA	ACAGCAGTACCCCGAATGAC

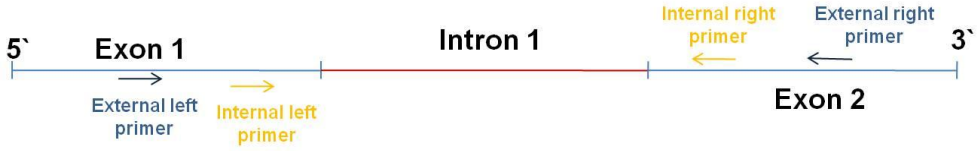

Figure 2.03: **Primer design for nested PCR**.

An external and an internal set of primers were designed spanning an intron to detect amplification of genomic sequence from amplification of cDNA.

2.8 qPCR

Real time quantitative PCR (RT-qPCR) was performed using SYBR Green I PCR Master Mix (Roche) and a Lightcycler II (Roche) machine according to the manufacturer's instructions (Roche). Absolute and relative quantification were performed from samples. For relative quantification, gene expression was normalized against zebrafish *gapdh* expression in wild-type embryos and, data were analysed using the (ΔΔCt) (Livak and Schmittgen, 2001) method and the Pfaffl method (Pfaffl, 2001).

2.8.1 The concept of Ct

The threshold cycle (Ct) is the most important measure in fluorescence based reverse transcription-PCR (RT-PCR) as it allows reproducible quantification (Higuchi *et al.*, 1993). The Ct defines the number of cycles required for the fluorescence signal to significantly rise above the background. The measure of the fluorescence represents the amount of product amplified during the amplification reaction. The more concentrated the sample initially was, the least number of cycles it took to reach the Ct. Therefore, the Ct value was not affected by the limiting phase of the amplification, the plateau, in which reactants become limiting and measurements uncertain. A first step of calibration of amplification reaction is always required when using specific primer sets. For this, the standardized procedure for building the standard curve was applied. Five reactions corresponding to for five diluted concentrations (1/10 dilutions from a prepared pure cDNA pool) were processed and Ct(s) could be determined for each reaction, as described below. The standard curves and melting curves were then analysed for these reactions in order to assess for proportionate amplification (PCR efficiency (E)) and specificity of amplification.

2.8.2 Standard of mRNA calibration for relative and absolute quantification

Calibration of qPCR reaction is essential for determining the reliability of qPCR amplification (Ct(s) reliable and well proportionate to relative or absolute amount in samples) using specific primer sets (Table 2.02). For assessing of qPCR reaction

calibration, it is required to build the standard curves for each primer set from high to low concentration. Standard curves also allow the association of a Ct to a relative (using a reference gene) or an absolute quantification.

Calibration is a standardized procedure consisting in measuring Ct(s) in five samples obtained by logarithmic dilutions (sample 1, sample 1/10, sample $1/10^2$, sample $1/10^3$, sample $1/10^4$, sample $1/10^5$) of a first concentrated yield (sample 1). Standard curves allow to determine PCR amplification efficiency (E) which is calculated as described in Livak and Schmittgen, (2001) and Liu *et al.*, (2009). The distance (number of cycles) between each Ct value is used to measure the reliability of amplification. Indeed, during PCR, the yield was theoretically doubled (E = 2 corresponding to PCR efficiency = 100 %), therefore, the slope, which corresponds to the theoretical distance between Ct(s) for a standard curve should be a value close to -3.32 [(dilution 1 in 10) is $E = 10^{(-1/slope)}-1$ when E = 2, slope = -3.32]. For individual standard curves, values of the slope of the different test sets ranged from −3.19 to −3.56 reflecting amplification efficiency of 90–110 %. For each primer set used in these experiments (tested genes and reference genes), a standard curve allowed to determine and to analyse Ct(s) and therefore relative and absolute quantification. Importantly, this calibration process is not a control for specific experiments. Once the primers were calibrated for qPCR reactions, they could be used for any experiments and each specific experiment required a specific control (untreated, WT condition prepared in the exact same condition as the treated or mutant to which it is compared to). Comparison of mRNA expression was commonly presented by relative fold changes for relative quantification.

Importantly, for preparing the standard curves, single species cDNA solutions were diluted in cDNA reverse transcribed from plant extracted mRNA (*Arabidopsis sp*., kindly given by Dr R. Scott lab, University of Bath) in order to replicate the cell/embryo cDNA solution background. Therefore, plant cDNA was diluted to low concentration in MiliQ water, and used to dilute the single specie cDNA solutions.

The choice of the reference gene as a stable and highly expressed gene was crucial for relative expression determination. Here *gapdh* was used as a reference gene for relative quantification. For absolute quantification of gene expression, the mRNA mass was converted to a gene copy number using an equation adapted from Staroscik, (2004). This calculation was based on the assumption that the average weight of a base pair (bp) is 650 Daltons. This meant that one mole of a bp weighs 650 grams and that the molecular weight of any double stranded DNA template could be estimated by knowing and multiplying the product's length (in bp) and 650. The number of molecules of template per gram could be calculated using the Avogadro's number, $6.022x10^{23}$ molecules/mole, and finally, the number of molecules or number of copies of template in the sample, could be estimated by multiplying by 10^9 to convert to ng and then multiplying by the amount of template (in ng) (Staroscik, 2004) as follows:

$$\textbf{Gene copy number} = [\text{mRNA(pg)} \times 6.022 \times 10^{20}] / [\text{Amplicon(bp)} \times 1 \times 10^9 \times 650]$$

For standard curve reactions built for absolute quantification, all mRNA were synthesized from plasmids, *in vitro* as described below (see section 2.4.1**)** using SP6 mMESSAGE mMACHINE® Kit (Ambion) according to manufacture protocol. Each mRNA species concentration and purity was measured using a spectrophotometer (Biomate 3, Thermo Scientific) and was then reverse transcribed as previously described **(**see section 2.4). Concentration for cDNA of each species was then assessed and copy numbers were calculated formulas in section 2.7.2.

Table 2.02: Primer pairs used for qPCR (5`-3`):

GENE	Primer forward	Primer reverse
gapdh	ACCAACTGCCTGGCTCCT	TTACTTTGCCTACAGCCTTGG
β-actin	TACCCCATTGAGCACGGTA	GTTCCCATCTCCTGCTCAAA
mitfa	CTGGACCATGTGGCAAGTTT	TGAGGTTGTGGTTGTCCTTCT
sox10	TTCTCGCTCTTCACACAACG	CGGACATCTGAGACTGCTGA
dct	TCTTCCCACCTGTGACCAAT	ACCAACACGATCAACAGCAG
trp1b	CGACAACCTGGGATACACCT	AACCAGCACCACTGCAACTA

2.8.3 Data and statistical analysis

In order to follow the fold change in gene expression over time using relative quantification, the Ct value was used in samples of the corresponding qRT-PCR amplification. Two methods were used to determine relative quantification, the method described in Livak *et al.,* (2001), also called the (ΔΔCt) method, and the method developed by Pfaffl *et al.,* (2001).

In the (ΔΔCt) method, the Ct value of the tested gene (WT or untreated conditions and mutant or treated conditions) were corrected for background variations using the Ct value of the reference gene in the corresponding sample for the same condition ($Ct_{(tested\ gene)}$-$Ct_{(reference\ gene)}$ = ΔCt). Then, the difference: $\Delta Ct_{(tested\ control\ condition)}$ - $\Delta Ct_{(tested\ gene\ mutant\ or\ treated)}$ = ΔΔCt, was used to determine the fold difference between WT/untreated (control or also called calibrator) and mutant/treated samples (gene expression differences). The fold difference between the calibrator and the tested condition is determined by $2^{-(\Delta\Delta Ct)}$ (Livak and Schmittgen, 2001).

In Chapter 4, REST 2009 software (Pfaffl, 2001, Pfaffl, 2009) and (ΔΔCt) method were used to analyse data. Both methods Pfaffl, 2001 and Livak *et al.,* (2001), used the comparison to a reference gene and to a calibrator situation. The Pfaffl method differed from the (ΔΔCt) method by the fact that it took account of qPCR efficiencies differences in determining quantification. The Pfaffl software also allowed randomization of tests which permitted to avoid false positive results. Statistic analysis could be realized to determine the significance of quantification differences. However, prior to this analysis, it had been ensured that qPCR efficiencies were comparable. For absolute quantification, transcript

copy numbers were assessed using a standard curve. Ct(s) associated to each sample were associated to copy numbers.

In Chapter 4, statistical analysis processed in R allowed to assess gene expression correlation using a linear regression test as well as significance of gene expression variations using Fisher test. Data collected were also used to mathematically describe and fit gene expression time-course in R (Crawley, 2007)

In Chapter 5 Student's t-test with the Bonferroni correction for multiple comparison (Dunn, 1961) were performed using GraphPadPrism 5.0 to test the null hypothesis (no significant difference in gene expression levels between *mitfa* and *sox10* mutants). In all the tests, differences were considered significant if p-value < 0.017.

2.9 Antibody staining

Embryos were fixed in 4 % Paraformaldehyde (PFA) in PBS (Phosphate buffered saline, Oxoid) overnight at 4 °C. They were washed three times for 5 minutes in PBSX (PBS with 0.1 % (v/v) Triton X-100) and three times for 1 hour in MilliQ water. Embryos were incubated in blocking solution (1 % DMSO, 5 % Goat/Sheep serum diluted in PBSX) for at least 2 hours. They were then incubated at room temperature overnight in polyclonal mouse serum primary antibody (Polyclonal IgG Mouse Anti-GFP Primary Antibody) diluted 1 in 200 in blocking solution (10 % (w/v) of Blocking Reagent (Roche, Manhein, Germany, in 1xMAB (100 mM Maleic Acid 90 mM NaCl In Milli-Q water, adjust pH to 7.5 and autoclave, this solution could be prepared and kept in the freezer). Embryos were washed in PBSx once briefly and three times for 1 hour. They were incubated overnight at room temperature in Alexa Fluor 488 fluorescent anti-mouse secondary antibody (Polyclonal IgG Alexa Fluor 488 goat anti-mouse) diluted 1 in 500 in blocking solution (1 % DMSO, 0.5 % Saponin, 1 % BSA 2 % Goat/Sheep serum in PBS). Embryos were then washed once briefly and three times for 30 minutes in PBSX. They were placed in 50 % glycerol for visualisation and storage.

2.10 Whole mount *in situ* hybridisation (WISH)

In situ hybridization was performed using the Kelsh lab protocol adapted from Henrique *et al.*, (1995). All amounts of liquid are 1 mL.

Preparation of zebrafish embryos

Embryos were fixed overnight in 4 % PFA/PBS at 4 ˚C. To dehydrate embryos they were washed once in PBT (PBS with 0.5 % Tween) for 5 minutes and twice for 10 minutes in 100 % methanol and then placed in methanol at -20 ˚C at least overnight.

Staining Day 1 - Probe hybridisation

Embryos were rehydrated by washing 5 minutes in 75 % methanol, in 50 % methanol, in 25 % methanol and finally twice for 5 minutes in PBT. Once rehydrated, embryos were fixed for 20 minutes in 4 % PFA/PBS. Embryos were then subjected to Proteinase K (10 mg/mL stock, Roche) digestion for varying times depending on age. 24 hpf embryos were incubated in a 1/10000 dilution (100 $\mu g.mL^{-1}$) of Proteinase K for 15 minutes. Older embryos were incubated in a 1/1000 dilution (10 $\mu g.mL^{-1}$) of Proteinase K for 20-45 minutes for 27-48 hpf embryos or 45-60 minutes for 50-60 hpf embryos. Digestion was followed by a brief wash in PBT and re-fixing for 20 minutes in 4 % PFA/PBS. Embryos were then washed twice in PBT for 5 minutes each. Embryos were pre-hybridised in hybridisation mix (HM: 50 % (v/v) Formamide 5X SSC 50 ng/mL Heparin 500 ng/mL tRNA 5) for 1-3 hours in a 68 ˚C water bath. Embryos were hybridised overnight at 68 ˚C in 200 µL hybridisation mix with 1/100 dilution of probe.

Staining Day 2 - Antibody binding

Hybridisation mix with probe was removed to be kept at -20 ˚C and recycled. The embryos were washed quickly in hybridisation mix at 68 ˚C and then washed as follows (2xSSC and 0.2xSSC were diluted in DEPC treated water from a stock solution 20xSSC : 3 M NaCl 300 mM sodium citrate Adjust the pH to 7.0 with a few drops of 1 M HCl In Milli-Q water):

- 10 minutes 75 % HM / 25 % 2xSSC at 68 °C.
- 10 minutes 50 % HM / 50 % 2xSSC at 68 °C.
- 10 minutes 25 % HM / 75 % 2xSSC at 68 °C.
- 10 minutes 2xSSC at 68 °C.
- 2x30 minutes 0.2xSSC / water at 68 °C.
- *5 minutes* *75 % 0.2xSSC/25 % PBT at RT* (room temperature)
- 5 minutes *50* % 0.2xSSC/50 % PBT at RT
- 5 minutes *25 % 0.2xSSC/75 % PBT at RT*
- 5 minutes *MABT at RT (Dilute MAB 5X with Milli-Q water and 0.1 % (v/v) Tween20)*

Embryos were then incubated for 2-4 hours at room temperature in blocking solution (PBT with 5 % sheep serum, 2 mg/mL BSA). They were incubated overnight at 4 ˚C with anti-DIG alkaline phosphatase (Roche) diluted 1/2000 with blocking solution.

Staining Day 3 – Colouration

The anti-serum was removed. Embryos were washed once quickly in PBT, then six times for 30 minutes in PBT and three times for 5 minutes in NBT/BCIP buffer (Roche). Embryos were then incubated in staining solution in the dark at room temperature. For blue staining, 200 µL NBT/BCIP solution (Roche) was diluted in 10 mL of NBT/BCIP buffer (Roche). Reactions were stopped by washing quickly in PBT and were stored in 4 % PFA/PBS at 4 ˚C. Before mounting for examination on a microscope embryos were transferred to 50 % glycerol for at least 30 minutes.

2.11 Morpholino Injection

Mc1r morpholino (25-bp of Danio mc1r ORF sequence based on the accessioned sequence NM_180970 (NCBI) , 5'-AGTGATGGCGCGAAGAGTCGTTCAT- 3`, (Gross *et al.*, 2009)) was injected in 1-2 cell staged embryos. This morpholino was previously designed and reported by Gross *et al.,* (2009). However, neither the efficiency of the morpholino nor the knockdown of Mc1r translation were assessed by Gross *et al.,* (2009) *in vivo*, therefore it was not clear whether this morpholino could be validated. Morpholino injections were carried out with 1 nL of 0.2 µM (= 12.7 pg) diluted in 1X Danieau solution (58 mM NaCl 0.7 mM KCl 0.4 mM MgSO4, 0.6 mM Ca(NO3)2 5 mM Hepes pH 7.6 in Milli-Q water).

2.12 DNA/RNA microinjection

Embryos were injected using a Nanoject II (Drummond Scientific Co., Broomall, PA) between 1 to 2 cell stages. Needles were pulled on a Micropipette puller (Sutter Instrument Co., Novat,CA) from 3 ½ Drummond glass capillaries (Drummond Scientific Co., Broomall, PA). DNA/RNAs were diluted in MilliQ water with 0.005 % phenol red (0.05 % (w/v) phenol red In Milli-Q water). Embryos to be processed for *in situ* were fixed in 4 % PFA (4 % (w/v) paraformaldehyde in PBS Autoclaved. PBS is firstly warmed to 60 ºC and then PFA is added, it is necessary to adjust pH to improve PFA solubilisation) overnight at 4 °C before being dechorionated, re-fixed at room temperature for approximately one hour and dehydrated according to the whole mount *in situ* protocol (see section 2.9).

2.13 Sequencing

The DNA sequencing was performed commercially by one of two external companies, Eurofins MWG Operon, London, UK or Geneservice, UK. Sequence data was analysed using the BLAST tool on the NCBI website (www.ncbi.nLm.nih.gov).

2.14 Microscopy

-Photography of live and stained embryos

Live embryos were anesthetized with tricaine (ethyl 3-aminobenzoate methanesulfate salt) (MS222 Sigma-Aldrich, England) to approximately 0.003 % mounted in methylcellulose or between bridged coverslips and photographed using a Nikon sight DS-U1 camera (Nikon) mounted on an Eclipse E800 microscope (Nikon).

Stained embryos were viewed in whole mount by placing them in a drop of 80 % glycerol between stacks of No 1 coverslips on a slide, with a coverslip placed over the top.

Embryos were then viewed using a Nikon Eclipse E800 using either DIC or fluorescence microscopy as appropriate and photographed using a SPOT camera (Image

Solutions) or Nikon sight DS-U1 camera (Nikon) together with NIS Elements F software or a dual mode cooled CCD camera (Hamamatsu). For rapid sorting/scoring embryos were viewed on an MZ12 dissecting microscope (Leica).

-*Observing single cells*

Melanised or fluorescent cells were observed by wide-field fluorescent microscopy on an Eclipse E800 (Nikon) using a DS-U1 camera (Nikon).

- *Confocal microscopy*

For confocal imaging, embryos were imaged under a Zeiss Confocal microscope (LSM510 Meta). Live embryos for confocal microscopy were mounted into 2 % agarose.

2.15 Image analysis

Pictures were formatted using Adobe Photoshop 7.0, cell dendricity and cell organisation were analysed using the free ImageJ software (Abramoff, 2004). For dendricity analysis, single cell pictures were isolated in a restricted area around the cell. The cell perimeter was next determined using the software function and the roundness parameter could be calculated. For analysis of cell organisation, pictures of 72 hpf dorsal head embryos showed dark cells on a bright background (zebrafish embryo). Colours were then inverted (software function) and edges were found (software function).

2.16 Small molecule treatments

BIO*, (2'Z,3'E)-6-Bromoindirubin-3'-oxime:* gsk3β inhibitor (purchased from Calbiochem, 361550-1MG) diluted in DMSO (Dimethyl sulfoxide, Sigma). BIO solution diluted at 10 mM was kept in dark at -80 °C and was used within maximum 3 months after receiving to avoid destabilisation of the molecule which could affect its activity. In treatment experiment, BIO was used at a concentration of 5 µM and controls were exposed in DMSO in same concentration as applied in BIO treatment.

LiCl*: 3M* Lithium chloride (Sigma-Aldrich, 203637 -powder, ≥99.99 %) was diluted in EM and used as 200 mM concentration. The solution was kept at RT and changed each month.

Trichostatin A (TSA): TSA (Sigma, T8552), hdac inhibitor (Vanhaecke *et al.*, 2004) was diluted in DMSO and kept at -20 °C. Controls were exposed to DMSO in same concentration as applied in TSA treatment (1 µM).

2.17 Statistics

All data treatments were processed in Excel or R (Crawley, 2007) and statistical tests in GraphPad Prism 5 (http://www.graphpad.com/prism/p5.htm), Analyse-it, XLSTAT (Excel associated softwares) or R (Crawley, 2007).

Chapter 3. Testing Wnt signalling as a candidate for Factor Y

3.1 Introducing the hypothesis that Wnt signalling is a good candidate factor for Factor Y

3.1.1 The existence of Factor Y is suggested by *in vivo* data

Features of the GRN responsible for the maintenance of melanocyte differentiation are not known. However, it has been suggested that melanocyte differentiation was established by maintaining *mitfa* expression in cells, although the exact mechanism has not been described. In this Chapter, the aim was to specifically test for the existence of, and test a candidate for, a factor involved in the maintenance of *mitfa* expression which would stabilise the GRN of differentiated embryonic melanocytes.

A GRN underlying melanocyte development was previously proposed, based upon the experiments presented in Greenhill *et al.*, (2011) introduced in the Introduction Chapter. One critical factor for melanocyte survival is Mitfa, the master gene for melanocyte development (Lister *et al.*, 1999). *In vivo* data have shown that *mitfa* is expressed in melanocytes until at least 48 hpf (Greenhill *et al.*, 2011). However, whether or not *mitfa* expression was highly maintained in all cells after 48 hpf remained unclear. According to the model, the decrease and the loss of *sox10* expression between 28 hpf and 52 hpf justifies the need for a factor, which we called Factor Y, to maintain *mitfa* expression in melanocytes and allow melanocyte differentiation.

Due to its role in the GRN, Factor Y would be defined by several characteristics: 1) it would be activated during melanocyte differentiation. 2) It would enable the activation of *mitfa* expression, probably from 28- 48 hpf, or to 72 hpf, depending on whether or not *mitfa* expression is maintained in melanocytes until 72 hpf. 3) The model predicted that the suppression of Factor Y would cause regression and/or death of melanocytes around 40 hpf as a result of the loss of *mitfa* expression (Johnson *et al.*, 2010), and finally, 4) in contrast, elevated Factor Y activity would, in turn, exaggerate melanocyte differentiation and *mitfa* expression in melanocytes.

By definition, both Mitfa and Factor Y are required for the persistence of this feedback loop activation. Consequently, blocking one of these two factors is predicted to cause a loss of this regulatory feature. Importantly, the level of *mitfa* activation would need to reach a certain threshold for the positive feedback loop activated by Factor Y to be stably maintained (Greenhill *et al.,* 2011). Without this condition, this regulatory feature would be in an unstable state, and melanocyte differentiation would be destabilised.

In the context of the model, Factor Y would either be one key factor, or an ensemble of factors, required for the maintenance of *mitfa* expression during melanocyte differentiation. In this Chapter, we investigated the possibility that Wnt signalling is a candidate for Factor Y.

3.1.2 The role of Wnt signalling in melanocyte differentiation is suggested by its role in specification

In zebrafish, the role of the Wnt signalling pathway in melanocyte specification has been well described. The two effectors of Wnt signalling, Lef1 and β-catenin, can activate *mitfa* transcription. β-catenin can rescue melanocyte specification in *sox10* mutants (Dorsky *et al.,* 1998). However, it remains unknown whether the same regulatory interaction could also have an ongoing role in melanocyte differentiation, for example, in the maintenance of *mitfa* expression after *sox10* expression loss. Here, the canonical Wnt signalling pathway was tested as a potential candidate factor involved in the maintenance of *mitfa* expression and of melanocyte differentiation after *sox10* loss in melanocytes.

Other studies in different biological models have also shown that Wnt signalling, via Lef-1 and β-catenin, was required for melanocyte specification. For example, mutant mice deficient in *Wnt-1* and *Wnt-3a* lack pigment cells (Ikeya *et al.,* 1997, Novak and Dedhar, 1999, Saint-Jeannet *et al.,* 1997a). The overactivation of *wnt-1* in zebrafish, as well as, overexpression of *Wnt-1* or *β-catenin* in mouse neural tube explants, promoted pigment cell formation and led to melanocyte expansion and differentiation (Dorsky *et al.,* 1998, Dunn *et al.,* 2000b). Furthermore, study of B16-F0 murine melanoma cells in culture *in vitro* and normal human melanocytes (NHM) have shown that β-catenin was not only involved in LEF-1 dependent regulation of *Mitf*, but also interacted with MITF to activate MITF-specific target genes (Schepsky *et al.,* 2006, Saito *et al.,* 2002). Consequently, the MITF-β-catenin interaction competitively redirected the β-catenin transcriptional activity away from the Wnt regulated genes, to the MITF target promoters (Dorsky *et al.,* 1998). However, the effective contribution of the canonical Wnt/β-catenin pathway in melanogenesis in adult human melanocytes has not been fully studied (Bellei *et al.,* 2010).

3.1.3 The TOP;dGFP reporter allows detection of Wnt signalling activation in zebrafish

To test the activation of Wnt signalling in melanocytes, it was important to define a reliable method to detect activation of effectors of the pathways. Dorsky *et al.,* (2002) built a useful tool, the TOP;dGFP zebrafish transgenic line, to describe and track the Wnt signalling/ β-catenin responsive cells. TOP;dGFP fish express a destabilised GFP variant

under the control of a promoter consisting of four consensus Lef1 responsive elements, and a minimal promoter (Korinek *et al.,* 1997, Dorsky *et al.,* 1998). Destabilized GFP (dGFP) is a variant of GFP with a fused degradation domain (Li *et al.,* 1998). Studies have shown that the half-life of the dGFP ranged between one and two hours which allows the monitoring of gene induction in living tissues (Li *et al.,* 1998). Consequently, the transient dGFP reporter can be detected by fluorescence microscopy in living tissues and it allows us to follow the Lef1 responsive cells in embryos throughout development (Dorsky *et al.,* 2002).

Dorsky *et al.,* (2002) described the expression of the TOP;dGFP reporter during zebrafish development and described the dynamic changes, from 12 hpf to 72 hpf, in the parts of the embryo where the cells expressed the reporter (see Dorsky *et al.,* (2002) for details). The study showed that the reporter could be detected from the gastrulation stage in the dorsal organizer, the ventrolateral mesoderm, the tailbud, and in the midbrain-hindbrain boundary (tectum), where Wnt signalling was known to be activated and required (Heasman *et al.,* 1994, Schneider *et al.,* 1996, Takada *et al.,* 1994, McMahon and Bradley, 1990). Expression of dGFP was also observed in the NC at 18 hpf by *in situ* hybridisation on sections (Dorsky *et al.,* 2002). However, the activation of the pathway in developing melanocytes was not investigated.

The expression of the dGFP in the TOP;dGFP was previously investigated using WISH in zebrafish during the phase corresponding to the late differentiation of embryonic melanocytes (at 55 hpf, 72 hpf and 96 hpf) (Figure 3.01) (Dr Masataka Nikaido, Dr Robert Kelsh Laboratory, University of Bath). At 55 hpf, WISH revealed expression of the GFP in the tectum, as well as, in cells of the trunk which correspond (localisation, and morphology) to melanocytes of the dorsal stripe (Figure 3.01, B and C). At 72 hpf, the expression of GFP in the tectum was still strong, however, the expression in the cells of the dorsal stripe in the trunk was faint (Figure 3.01, E and F). At 96 hpf, the signal remained detectable in the tectum but no expression was found in the trunk (Figure 3.01 (H)). Consequently, these results showed that until 55 hpf, the activation of Wnt signalling could still be detected in the melanocytes of the dorsal stripe. It remains possible that the Wnt signalling pathway was still activated in melanocytes at 72 hpf at a low level, below the threshold for detection by WISH. In this study, the detection of the activation of Wnt signalling was tested in single melanocytes during the time window corresponding to the cell differentiation phase.

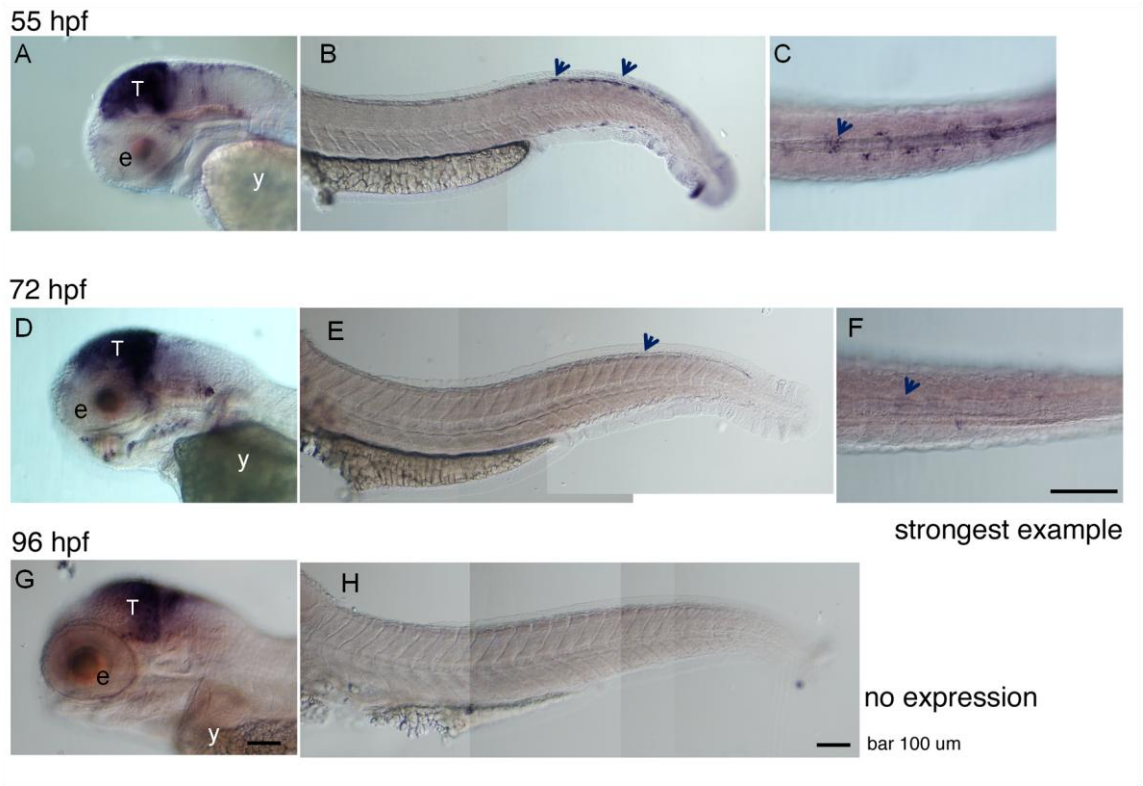

Figure 3.01: Detection of GFP in TOP;dGFP transgenic embryos by WISH.

A non-hydrolysed *egfp* probe was used to detect GFP in the transgenic TOP;dGFP embryos by whole-mount *in situ* hybridisation at 55 hpf (A-C), 72 hpf (D-F) and 96 hpf (G-H). At 55 hpf, the blue/purple signal is observed in the tectum as shown in lateral view (A) and in the trunk in the dorsal line of melanocytes as shown in (B) in lateral view and in (C) with the dorsal view (in both pictures, arrowheads show cells expressing the signal). At 72 hpf, the signal could still be observed in the tectum as shown in (D) in lateral view and it was also faintly detected in the dorsal line of the trunk (E, lateral view, F dorsal view, arrowheads show cells expressing the signal). At 96 hpf, the signal could still be detected in the tectum (G, lateral view of the head), but in the trunk (H, lateral view). Key: e: eyes, T: tectum, y: yolk sac. (Nikaido M, unpublished data)

3.1.4 GSK3β is a negative regulator of the canonical Wnt signalling pathway

Glycogen Synthase Kinase 3 beta (GSK3β) is a negative regulator of canonical Wnt signalling (see Introduction Chapter). Here, the role of GSK3β is further described in order to show that inhibition of this protein can activate the Wnt signalling pathway. In zebrafish, mouse, *Xenopus* and human, two isoforms of the serine/threonin protein kinase GSK3 are described, GSK3α and GSK3β. It is unclear if these two isoforms have a similar function *in vivo*. Lee *et al.,* (2007) demonstrated that GSK3α and GSK3β had different and non-redundant functions in cardiogenesis in zebrafish. Morpholino knockdown lead to the same morphological defect defined as pericardial edema. However, GSK3α was shown to be responsible for cardiomyocytes survival, whereas, GSK3β was shown to be implicated in valve formation and heart positioning through Wnt/ β-catenin signalling (Lee *et al.*, 2007). GSK3β is involved in the canonical Wnt signalling via regulating β-catenin translocation to the nucleus. In the canonical Wnt signalling pathway, GSK3β maintains the phosphorylation of its substrate, β-catenin, in the absence of a signal. The Wnt-induced dissociation of β-catenin from the complex allows the stabilization and the activation of the free β-catenin. GSK3β recruitment to the membrane is dependent on the activation of Frizzled, the Wnt receptor (Figure 3.02). The Wnt co-receptor for the canonical Wnt signalling is called the low-density-lipoprotein receptor-related protein 5/6 (LRP 5/6). LRP 5/6 associates with GSK3β and inhibits its negative regulation of β-catenin (Barker, 2008, Chen *et al.*, 2000, Hur and Zhou, 2010, Lee *et al.*, 2004). The Figure 3.02 summarises the Wnt signalling pathway and GSK3β activity in *Mitf* regulation in melanocytes.

Besides being crucial for the canonical Wnt pathway, GSK3β is a central regulatory node which influences an extensive range of cellular processes regulated by multiple signalling factors (Hur and Zhou, 2010, Yost *et al.*, 1996, Sineva and Pospelov, 2010). Interestingly, GSK3β is involved at different levels of *mitfa* regulation. Firstly, GSK3β negatively regulates *mitfa* at a transcriptional level through inhibition of Wnt signalling. Secondly, at the protein level, GSK3β has the capacity to phosphorylate MITF protein enhancing its capacity to bind the promoter and to activate *Tyrosinase* expression (Figure 3.02) (Takeda *et al.*, 2000b). Consequently, GSK3β is a regulator of MITF activity turning these two antagonist functions “on” and “off” at different time points and under different conditions. However, the dynamics of these effects is still poorly understood and a direct role of GSK3β in melanocyte development has never been described.

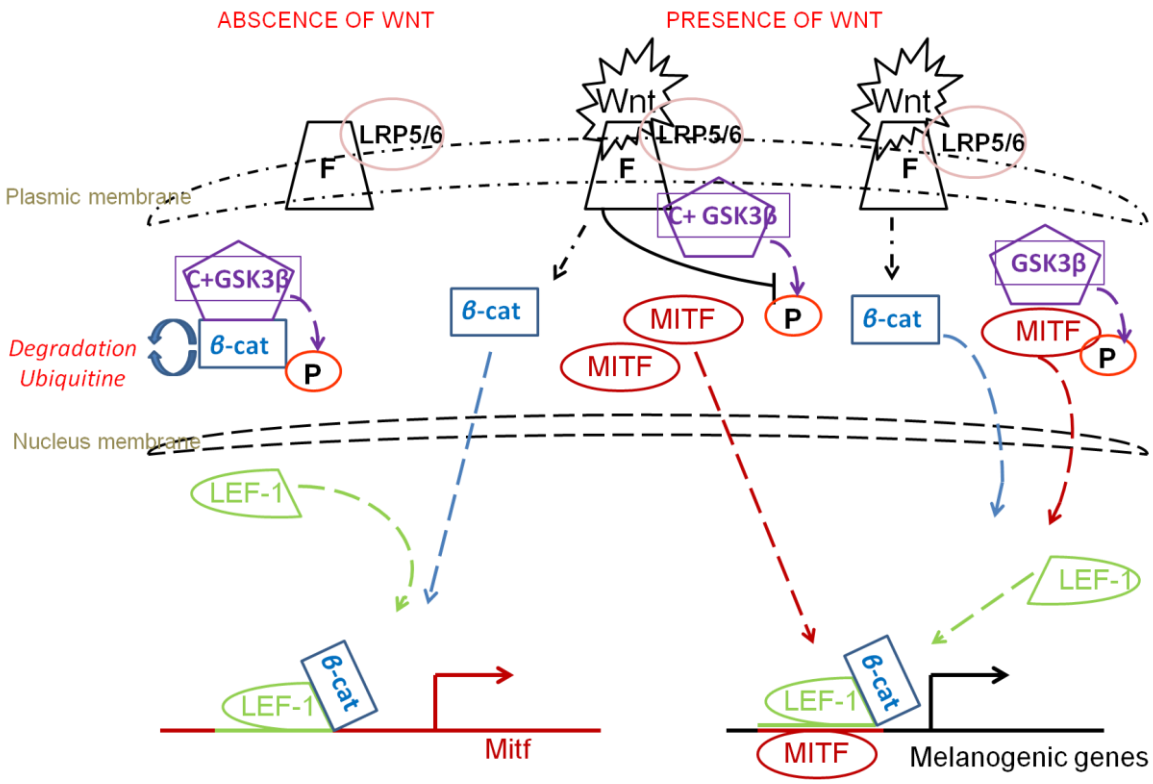

Figure 3.02: The activation of the canonical Wnt signalling pathway activates free β-catenin and allows the phosphorylation of MITF by GSK3β in melanocytes.

In the absence of Wnt signalling, GSK3β phosphorylates (P) β-catenin (β-cat) in a complex (C+ GSK3β). This phosphorylation prevents β-catenin from translocating to the nucleus and causes β-catenin degradation by the ubiquitine/proteasome complex. The canonical Wnt signalling pathway is activated when the Wnt protein binds its receptor, Frizzled (F), in the membrane and its co-receptor LRP5/6. This activation results in the segregation of GSK3β to the plasma membrane and prevents the phosphorylation and the degradation of β-catenin (β-cat). In the nucleus, β-catenin can interact with LEF1 for binding gene target promoters such as the *Mitf* promoter. As MITF accumulates it can act together with β-catenin and LEF-1 to activate melanogenic targets. Furthermore, GSK3β can phosphorylate MITF to enhance MITF activity. (Adapted from Saito *et al.*, (2002)).

3.1.5 Inhibiting GSK3β can result in boosting Wnt signalling

In zebrafish, experimental blocking of canonical Wnt signalling remains a challenge. No small molecules have been developed to repress Wnt or to inhibit activity of its receptor and co-receptor, Frizzled/LRP5/6. Experiments to block Frizzled activity using morpholinos in zebrafish have not shown clear effects on melanocyte development, probably because of the redundancy of the Frizzled receptors (Nikaido *et al.*, 2013). The *ichabod/ β-catenin* zebrafish mutant carries the maternally expressed mutation *ichabod* which inactivates β-catenin. This mutation is homozygous lethal in 99 % of the progeny. Thus, only 1 % of embryos, called escapers, can survive. However, these escaper embryos show strong disruption of formation of the anterior axis, which does not permit their use for the study of the melanocyte GRN (Kelly *et al.*, 2000). Consequently, in these experiments we used the chemical inhibition of GSK3β to manipulate Wnt signalling and test effects of activation of the pathway in melanocyte differentiation. The effects of the treatments with two small molecules, which are known inhibitors of GSK3β, were assessed in melanocyte development. These molecules, the 6-bromoindirubin-3'-oxime (BIO) and the Lithium Chloride (LiCl), were used to activate the Wnt pathway during different phases of melanocyte development.

BIO is a well-characterised GSK-3α/β inhibitor. It has been used to investigate Wnt signalling in many model systems, including mammalian cardiomyocytes in cell culture, melanoma cells (B16-F0) in normal human melanocyte (NHM) cells, in mouse embryonic stem cells, and in zebrafish (Tseng *et al.*, 2006, Bellei *et al.*, 2010, Bellei *et al.*, 2008, Sineva and Pospelov, 2010, Kim *et al.*, 2008). BIO is a cell permeable indiburin compound which acts as a highly potent, selective and reversible adenosine tripohosphate (ATP)-competitive inhibitor of GSK-3α/β. Its specificity has been tested against various kinases, such as, Cdk's (cyclin-dependent kinase), as well as many other commonly studied kinases like MAP kinases, PKA (protein kinase A), PKC isoforms (protein kinase C, involved in non-canonical Wnt pathway), PKG (protein kinase G), CK (creatin kinase), and IRTK (receptor tyrosine kinase) (Calbiochem, 361550 GSK-3 Inhibitor IX, Merck Chemicals Ltd., UK). Importantly, the inhibition of GSK3β using BIO has been shown to activate *Mitf* expression and activity via increased levels of free, stabilised, β-catenin (Bellei *et al.*, 2008). In human and mouse embryonic stem cells (ESCs), treatment with BIO resulted in increased β-catenin activity and promoted self-renewal and pluripotency which both contribute to the maintenance of stem cell properties (Sineva and Pospelov, 2010). Studies have also shown that BIO could specifically promote proliferation of mammalian cardiomyocytes (Tseng *et al.*, 2006). p38-MAPK activity has also been associated with increased mammalian cardiomyocyte proliferation, therefore, it has been suggested that BIO may interact with, and inhibit, the p38-MAPK pathway (Tseng *et al.*, 2006). However, this hypothesis remains to be tested.

Lithium Chloride (LiCl) is another small molecule traditionally used to activate Wnt signalling. LiCl is a stimulator of β-catenin as well as an inhibitor of GSK3β (Klein and Melton, 1996). In *Xenopus*, experiments using lithium trigger a posteriorisation of the embryos, observed by the duplication of the dorsal axis and the loss of ventral tissues (Kao

and Elinson, 1988). Incubation of fasted rat hepatocytes with LiCl could activate the glycogen synthase and the glycogen phosphorylase, mimicking the effects of insulin (Bosch *et al.*, 1986). LiCl is also one of the best treatments for bipolar disorder in humans, however, the mechanisms involved in these effects remain poorly understood (Price and Heninger, 1994, Avissar *et al.*, 1988). Several hypotheses have been suggested for this mechanism. The accepted and previously dominant hypothesis was that LiCl would cause inositol depletion (Berridge *et al.*, 1989, Avissar *et al.*, 1988). This was suggested after experiments had shown that LiCl could inhibit the inositol monophosphate (IMPase), and could decrease the levels of inositol (inositol 1,4,5 trisphosphate, (InsP3)) in cells, by blocking the cell Insp3-dependent response to extracellular signals (Berridge *et al.*, 1989, Avissar *et al.*, 1988). Furthermore, in *Xenopus*, injections of inositol could prevent teratogenic effects caused by LiCl treatment (Busa and Gimlich, 1989). However, this hypothesis did not explain the effect of LiCl on glycogen synthase enzyme. Several studies have described and used LiCl for its role as an Inositol Phosphate 3 (IP3) inhibitor (Stachel *et al.*, 1993, Jin and Thibaudeau, 1999, Klein and Melton, 1996, Van Lookeren Campagne *et al.*, 1988). However, when Klein *et al.*, (1996) used more specific IMPase inhibitors when they became available (1000 fold more potent as IMPase inhibitors, than LiCl (Atack *et al.*, 1994)), the study intended to reproduce the effects of LiCl in *Xenopus.* Unexpectedly, the phenotype, described as embryo dorsalisation, observed with LiCl could not be reproduced with these inhibitors (Klein and Melton, 1996). Because LiCl could affect embryo dorsalisation and because it had been suggested to be a glycogen synthase inhibitor, its effects on GSK3β inhibition were investigated. The results showed that the lithium ion could inhibit 50 % of the GSK3β phosphorylating activity (Klein and Melton, 1996). It was then shown that LiCl could inhibit GSK3β mediated phosphorylation of protein substrates, such as the protein phosphatase inhibitor-2, without affecting the activity of other kinases (such as ERK-1/MAP kinase-mediated phosphorylation or CKII phosphorylation of casein). This suggested a relatively good specificity of the effects on GSK3β (Klein and Melton, 1996). LiCl was suggested to be a specific GSK3β inhibitor when the LiCl treatment phenotype was found to be similar to the "dorsalisation" phenotype observed in GSK3β dominant negative mutant in *Xenopus* (Dominguez *et al.*, 1995, Kao and Elinson, 1988).

Consequently, LiCl has been utilised as a Wnt activator and as a GSK3β inhibitor in several model systems including *Xenopus*, zebrafish and mammalian cell culture (Kim *et al.*, 2008, Klein and Melton, 1996, Florczyk, 2007). Importantly, effects of LiCl observed in *gsk3β Xenopus* mutant, and in LiCl treated *Xenopus* embryos, were also observed in zebrafish embryos. Stachel *et al.*, (1993), showed that treating zebrafish embryos at an early stage with LiCl could disrupt the pattern of formation and the axis of specification of embryos. Furthermore, it could cause hyper-dorsalisation of embryos by perturbing dorsal signals. Zhang *et al.*, (2003) showed that lithium could directly cause the increase of the level of the inhibitory N-terminal phosphorylation of GSK3β and of the level of the inhibitory phosphorylation at serine 9 *in vitro* in cell culture. Consequently, LiCl has been considered as a GSK3β inhibitor, however, the molecular effects of LiCl in cells remains to be fully defined.

In this study, BIO and LiCl were used as inhibitors of Gsk3β to activate Wnt signalling at different time points of melanocyte development *in vivo* in zebrafish from 7 hpf to 72 hpf. The results revealed that the levels of specificity and efficiencies as inhibitors of Gsk3β, were different for BIO and LiCl. Consequently, the interpretation of these experiments was not trivial and will also be discussed in regard to the complex activity of Gsk3.

3.1.6 Approach and aims

Using the systems biology approach we investigated a prediction from the GRN model that a factor was needed to maintain melanocyte differentiation and *mitfa* expression in melanocytes. Because of the leading role of Wnt signalling during melanocyte specification, we tested the hypothesis that a single candidate factor, Wnt signalling, could be limiting for melanocyte differentiation.

- To test the hypothesis, a transgenic reporter strain was first used to verify that Wnt signalling remained detectable in differentiated melanocytes until at least 72 hpf.
- The effects of activating Wnt signalling in melanocytes with BIO and LiCl were assessed in embryos and in melanocytes.
- The treatments with inhibitors of GSK3β were utilised to test the role of Wnt signalling on melanocyte development in zebrafish embryos and more particularly on melanocyte differentiation.

3.2 Results

3.2.1 TOP;dGFP reporter revealed the time-course of Wnt signalling activity in melanocytes

The activation of Wnt signalling was investigated during the melanocyte differentiation time-window to validate the pathway as a candidate for the suggested Factor Y. Wnt signalling activity was traced in melanocytes from 30 hpf to 72 hpf using fish of the transgenic line TOP;dGFP (van de Wetering *et al.,* 1997, Dorsky *et al.,* 2002, Korinek *et al.,* 1997). To study the activation of the dGFP reporter in these cells, fish were treated with 1-phenyl-2-thiourea (PTU, but only ¾ of the dose required for inhibiting 100 % melanin synthesis in order to observe light melanisation and to be able to distinguish melanocytes) to avoid the dark cells absorbing the fluorescence. Observing GFP auto-fluorescence in living tissue could lead to the detection of false positives or false negatives samples which was difficult to assess. Therefore, instead of investigating the activation of dGFP in living embryos, we used the technique of immunofluorescence which allowed staining for GFP in embryos at different stages of cell differentiation.

Figure 3.03 shows to the detection of the activation of Wnt signalling in TOP;dGFP in control embryos at 40 hpf. This Figure shows the activation of the dGFP in the tectum and in melanocytes in TOP;dGFP embryos. In order to determine whether or not Wnt signalling remained activated during melanocyte differentiation, melanocytes were scored for expression of dGFP during the differentiation phase. The detection of dGFP was tested at 30 hpf, 36 hpf, 48 hpf, 51 hpf and 72 hpf in thirty melanocytes in fifteen zebrafish individuals (n= (15 x 30) in total, n= 450). The quantification of the proportion of GFP positive melanocytes at each timepoint is shown in Figure 3.04. At early stages, the majority (78.5 %) of melanocytes had readily detectable GFP expression (Figures 3.04, (A)), indicating that most cells at this stage, were responsive to Wnt signalling. However, a decrease of GFP positive melanocyte number was observed through differentiation (Figure 3.04, (C-D)). At later stages, only a low proportion of cells still showed detectable GFP expression (9 %; Figures 3.04 (E)). Importantly, at this stage melanisation was more intense than at early stages. This might be partly reflecting the difficulties of the detection of weak fluorescence in even partially-melanised melanocytes which are very light absorbent. However, it is possible that Wnt signalling was not activated in most melanocytes at 72 hpf and that its activation decreased through cell differentiation. The fact that Wnt signalling was highly activated in melanocytes from 30 hpf to 48 hpf led us to consider that Wnt signalling could be a potentially important factor in melanocyte differentiation during this period. However, its role at later stages was more difficult to assess due to potential decreased activity in cells.

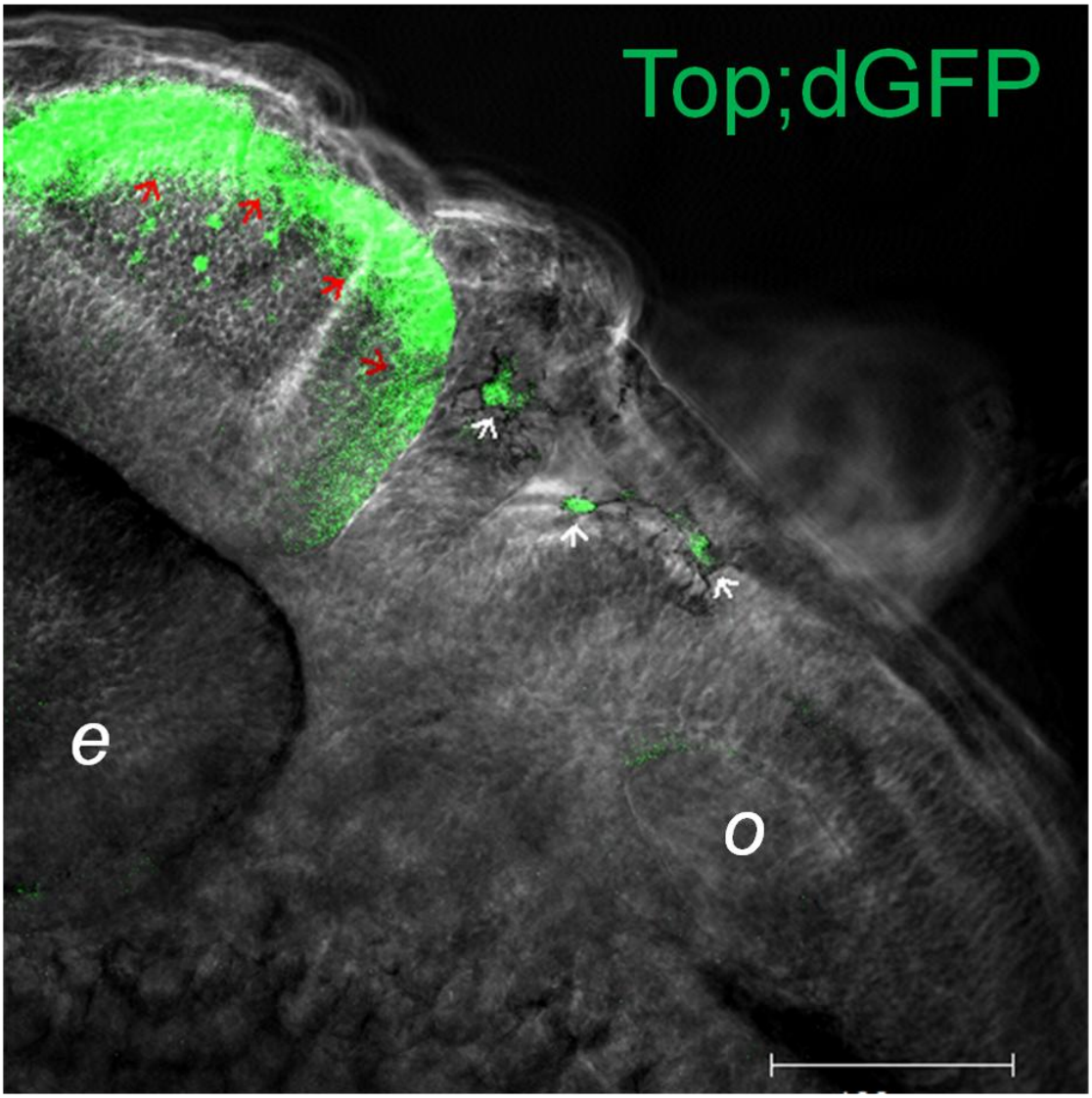

Figure 3.03: Control TOP;dGFP embryos express GFP in the tectum and in melanocytes at 40 hpf.

Expression of GFP was investigated by immunofluorescence in TOP;dGFP embryos treated with PTU (3/4 dose to observe expression in lightly melanised cells) at 40 hpf and documented using a confocal microscope. 60 embryos were investigated and the head of a representative embryo is shown in lateral view, with fluorescence and bright field merged to observe co-localisation of melanisation and GFP. The red arrowheads point at GFP expression in the tectum and the white arrowheads point at melanocytes expressing GFP. Key: e: eyes; o: otic vesicle. Bar: 100 µm.

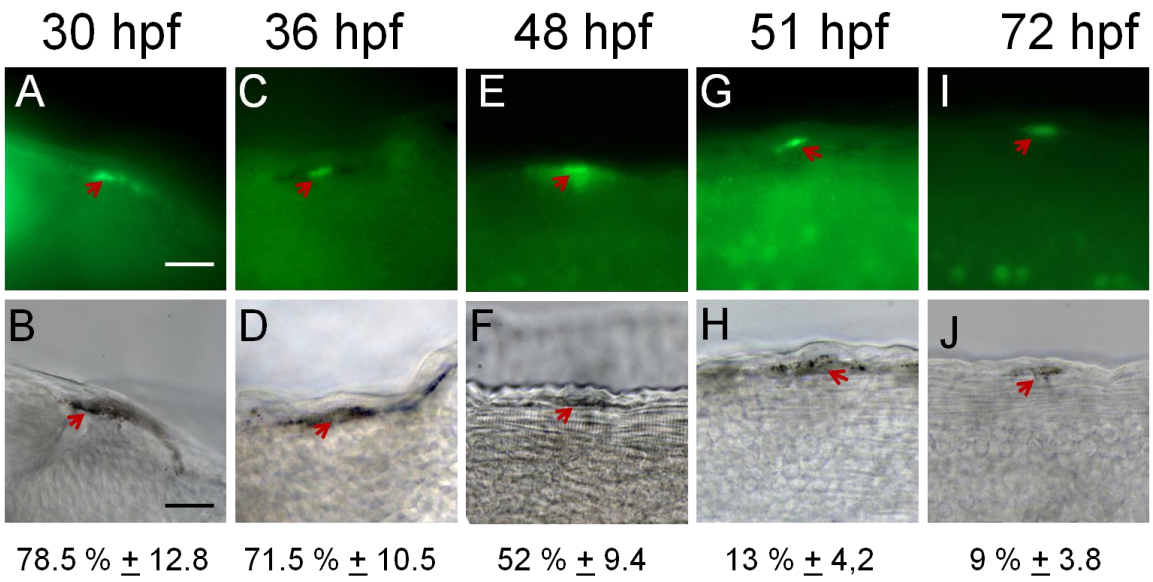

Figure 3.04: Detection of the Wnt signalling in melanocytes during differentiation in TOP;dGFP transgenic zebrafish.

Detection of dGFP by immunofluorescence staining in TOP;dGFP transgenic embryos in melanocytes from 30 hpf to 72 hpf. Single melanocytes are presented in fluorescence optic (A,C,E,G,I) and bright field (B,D,F,H,J) respectively. In the top panels, arrowheads show dGFP expression in melanocytes; in bottom panels, arrowheads show the cell corresponding to the cell presented on the panel on top. At 30 hpf (A-B), (percentage of cells expressing GFP ± s.d. of percentages of cells expressing GFP in each embryo) 78.5 % ± 12.8 of melanocytes showed GFP activation , at 36 hpf, (C-D), 71.5 % ± 10.5, at 48 hpf (E-F), 52 % ± 9.4, at 51 hpf (G-H), 13 % ± 4.2, and at 72 hpf (I-J), 9 % ± 3.8. At each stage, 30 melanocytes were assessed for GFP expression in 15 embryos, in the dorsal head, and trunk, and lateral trunk, throughout the anterior posterior axis (n = 450). Scale bar: 10 µm.

3.2.2 BIO and LiCl treatments resulted in characteristic Wnt signalling defects

Wnt signalling is responsible for the posteriorisation/dorsalisation of the embryos during development (Schneider *et al.*, 1996, Klymkowsky *et al.*, 2010, Takada *et al.*, 1994, Saint-Jeannet *et al.*, 1997a, Kim *et al.*, 2000a, Lee *et al.*, 2007). Experiments of overactivation of the Wnt pathway during early embryonic development in zebrafish resulted in the posteriorisation of embryos, as observed in zebrafish *headless*/*tcf3* mutants, or in *Xenopus* embryos (Kim *et al.*, 2000a, Roose *et al.*, 1998, Klymkowsky *et al.*, 2010). Here, the reproducibility of the phenotype of posteriorisation was tested in embryos after long treatments with BIO and LiCl.

Embryos were treated from the early stage of 7 hpf to late differentiation stage at 72 hpf to test whether Gsk3β inhibition, with LiCl and BIO, could reproduce the posteriorising/dorsalising effect of the activation of the Wnt signalling (Figure 3.05, (A-I)). The results showed that the activation of Wnt signalling resulted in a loss of anterior structures, such as, the eyes, the forebrain and part of the midbrain causing a shift in the midbrain/forebrain boundary (not shown on picture) (also described in Kim *et al.*, (2000) in *headless/ tcf3* zebrafish mutant). A reduction in the size of the embryo's head was also observed (Figure 3.05 (D,G)) as well as, a pericardial edema in BIO (5 µM) treated embryos, also described in Lee *et al.*, (2007), (Figure 3.05, (G)). In this long-term treatment, both BIO and LiCl, induced a significant elevation of the number of melanocytes, (mean ± s.d, p-value at unpaired, one-tailed t-test, n= 20, $p < 0.001$), control, (31 ± 3.2), LiCl (55 ± 5.1, p=0.000075), BIO (60 ± 3.5, p=0.00026). This could be consistent with the known role of Wnt signalling in activation of melanocyte specification (Dorsky *et al.*, 1998).

These results showed that both, LiCl and BIO treatments could reproduce the Wnt specific overactivation phenotype. However, other hypotheses for explaining the increase in cell number were not tested. An abnormal melanocyte shape (not quantified), as well as, an enhanced xanthophore pigmentation were also observed (Figure 3.05, (D,E,G,H) compared to the control (A,B)).

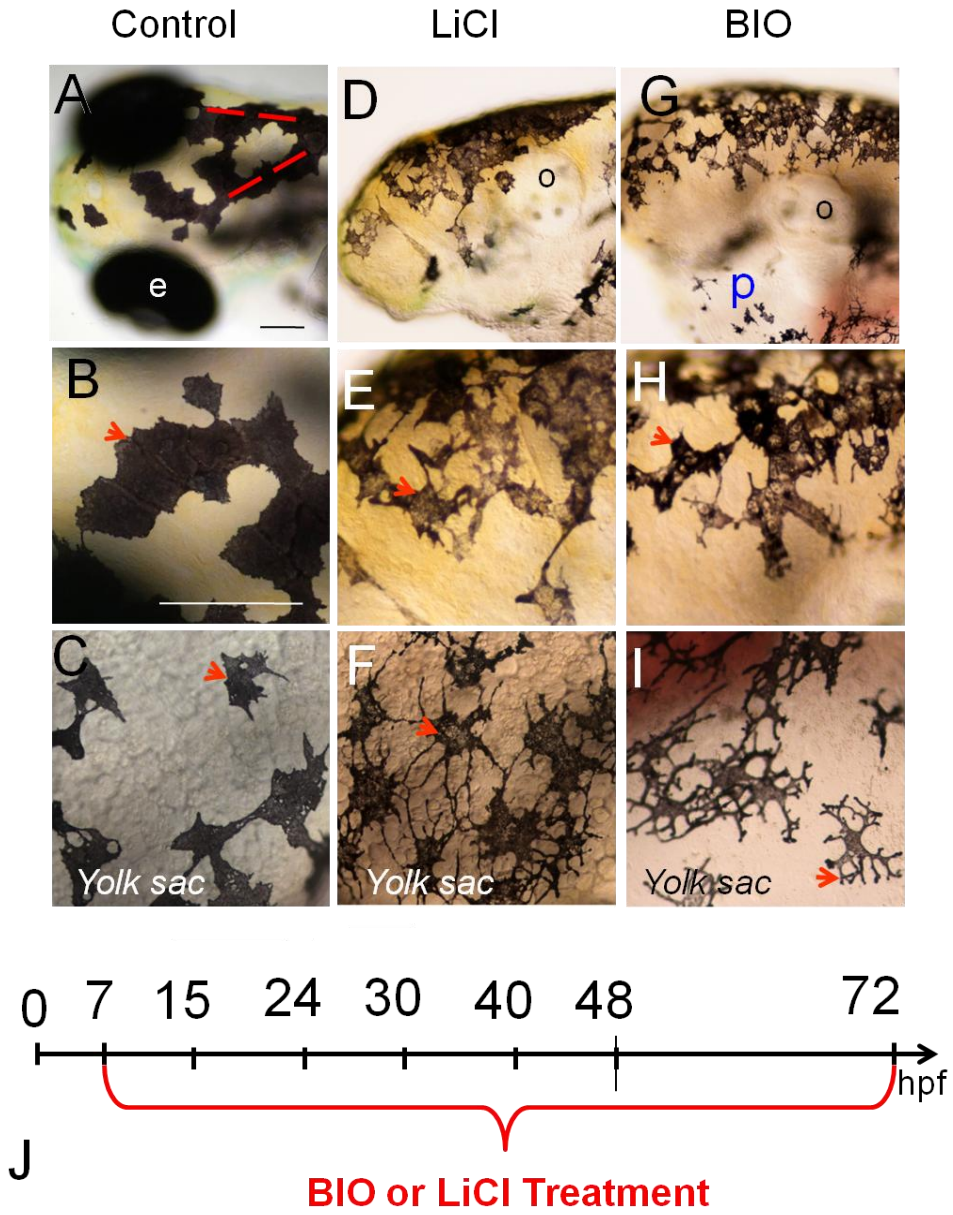

Figure 3.05: Embryos treated with LiCl and BIO from 7 hpf to 72 hpf show over-posteriorisation/dorsalisation.

Control DMSO treated embryos (A,B,C), LiCl (200 mM) treated embryos (D,E,F), and BIO (5 µM) treated embryos (G,H,I) were documented. LiCl and BIO treated embryos show a loss of most anterior structures including eyes (comparing dorsal head pictures, (D, G) to (A)). Close-ups on cells of the dorsal head show differences in cell shape and cell organisation pattern (B,E,H) (arrowheads show melanocyte in (B), (E) and (H)). A pericardial edema (G) can be observed as the pericardiac envelop is swollen. These embryos show a clear increase in melanocyte dendricity as shown in cells of the yolk sac (arrowheads show the cells in (C), (F) and (I)). In total, 120 embryos were observed for each condition and representative embryos are shown here. e: eye; y: yolk sac; o: otic vesicle; p: pericardial edema. Scale bar: 100 µm. (J) shows a diagram of window period for this treatment, from 7 hpf to 72 hpf.

3.2.3 BIO and LiCl activated dGFP expression in TOP;dGFP fish

To verify if LiCl and BIO were suitable reagents to activate the Wnt pathway in melanocytes, we tested their capacity to elevate the expression of the dGFP reporter in TOP;dGFP fish, in both whole embryos and melanocytes.

Embryos were treated from 15 hpf to 40 hpf to cover the specification phase as well as the early differentiation phase (Figure 3.06). At this stage, control TOP;dGFP DMSO treated fish showed typical and weak GFP expression in the tectum and in the trunk (Figure 3.06) (Dorsky *et al.,* 2002). The results show that in the same conditions, both LiCl and BIO could elevate the dGFP expression in the tectum of embryos (Figure 3.06). It was even more dramatically-increased in the BIO-treated embryos. Figure 3.06 also revealed that LiCl treatments caused an increase of GFP expression in cells that were likely to be xanthoblasts. These cells could be distinguished by their positioning and their typical dendritic shape at this stage. Whether activation of the GFP in xanthophores resulted from an off target (non-specific) effect of lithium was unclear. Further study of the basis for this xanthophore phenotype, and for its specificity to LiCl, would be of interest, but have not been assessed here.

We then assessed whether activation of GFP was detectable directly in melanocytes of LiCl or BIO-treated TOP;dGFP embryos. Analysis of the GFP activation revealed that GFP expression was always colocalised within melanocytes in embryos treated with BIO from 15 hpf to 40 hpf (Figure 3.07). Furthermore, in BIO treated embryos, more GFP+ melanocytes could be observed compared to the control. This effect is studied further in section 3.2.4 where we tested activation of cell specification after BIO treatments. In BIO treated embryos, the intensity of the GFP signal seemed to be boosted in melanised cells compared to the signal observed in control melanocytes. However, we did not quantify the amount of GFP expression within individual melanocytes as the resolution of one cell within one image taken was not sufficient for reliably assessing GFP fluorescence within each cell. To overcome this limitation, the experiment should be repeated at a higher magnification focusing on individual cells. In contrast, activation of the signal in embryos treated with LiCl mostly did not co-localise with the melanised cells but instead seemed to be boosted in other cells of the skin which could be xanthoblasts. Figure 3.08 presents stacks of three pictures corresponding to three focal planes. The stacks are shown as the series of the three pictures taken on each focal plane for each condition. The results confirmed that on each focal plane, the GFP was fully co-localised with melanised cells in control and BIO treated embryos but not in LiCl treated embryos. We speculate that non-specific effects of LiCl action may help boost Wnt signalling in the development of cells like xanthoblasts.

Altogether, this data suggested that Wnt signalling could be activated in embryos with BIO and LiCl, although, only BIO seemed to be efficiently boosting the signal in melanocytes during the differentiation phase. The intensity of the signal could not be quantified due to the resolution in melanocytes however, activation of the dGFP was clear in the tectum specifically with BIO. Based on this experiment, only BIO was suggested to be relevant for further tests on the role of Wnt signalling in melanocyte differentiation.

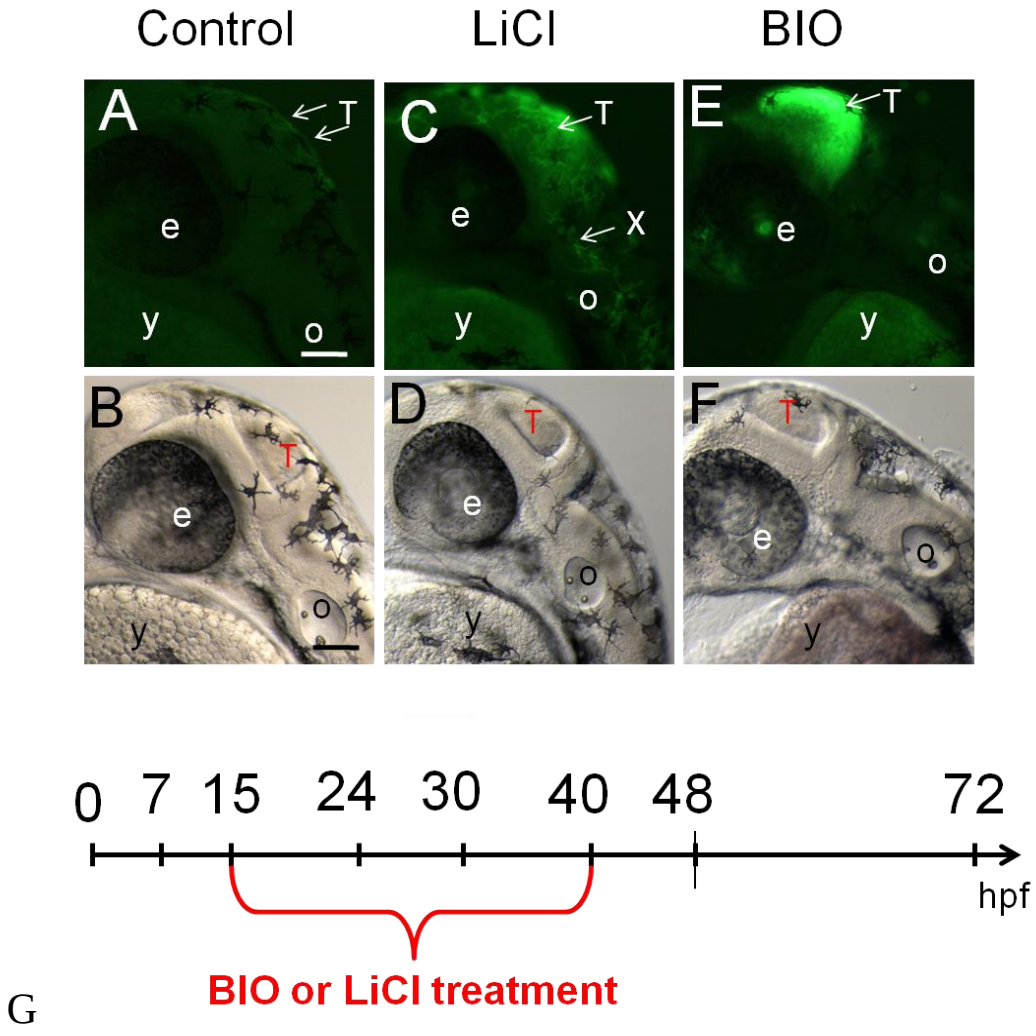

Figure 3.06: BIO and LiCl treatment (15 - 40 hpf) elevates Wnt signalling in the transgenic TOP;dGFP zebrafish embryos.

Lateral view of embryo heads with confocal imaging showing GFP expression after immunostaining in fluorescence (top panels, (A-C-E)) and their corresponding bright field images (bottom panels (B-D-F). Treatment lasted from 15 hpf to 40 hpf when embryos were fixed with 4 % paraformaldehyde for immunostaining. 40 hpf TOP;dGFP DMSO treated embryos, (A-B) (arrowheads indicate the tectum), 40 hpf LiCl (200 mM) treated embryo (C-D) (both the arrowheads in (C) indicate xanthoblast), 40 hpf BIO (5 µM) treated embryo (E-F), (in (E) arrowheads indicate the tectum). Pictures were taken and processed using the same parameters in order to compare intensity of fluorescence of the GFP. For each condition, 160 fish were assessed through two experimental repeats (fish were assessed by fluorescence microscopy and for each condition, 10 fish were chosen for confocal imaging). Phenotypes presented here were representative of fish observed for each condition. e: eye; y: yolk sac; o: otic vesicle; X: xanthoblast. Scale bar: 100 µm. (G) The diagram shows the start (15 hpf), the end (40 hpf) and the length of treatments.

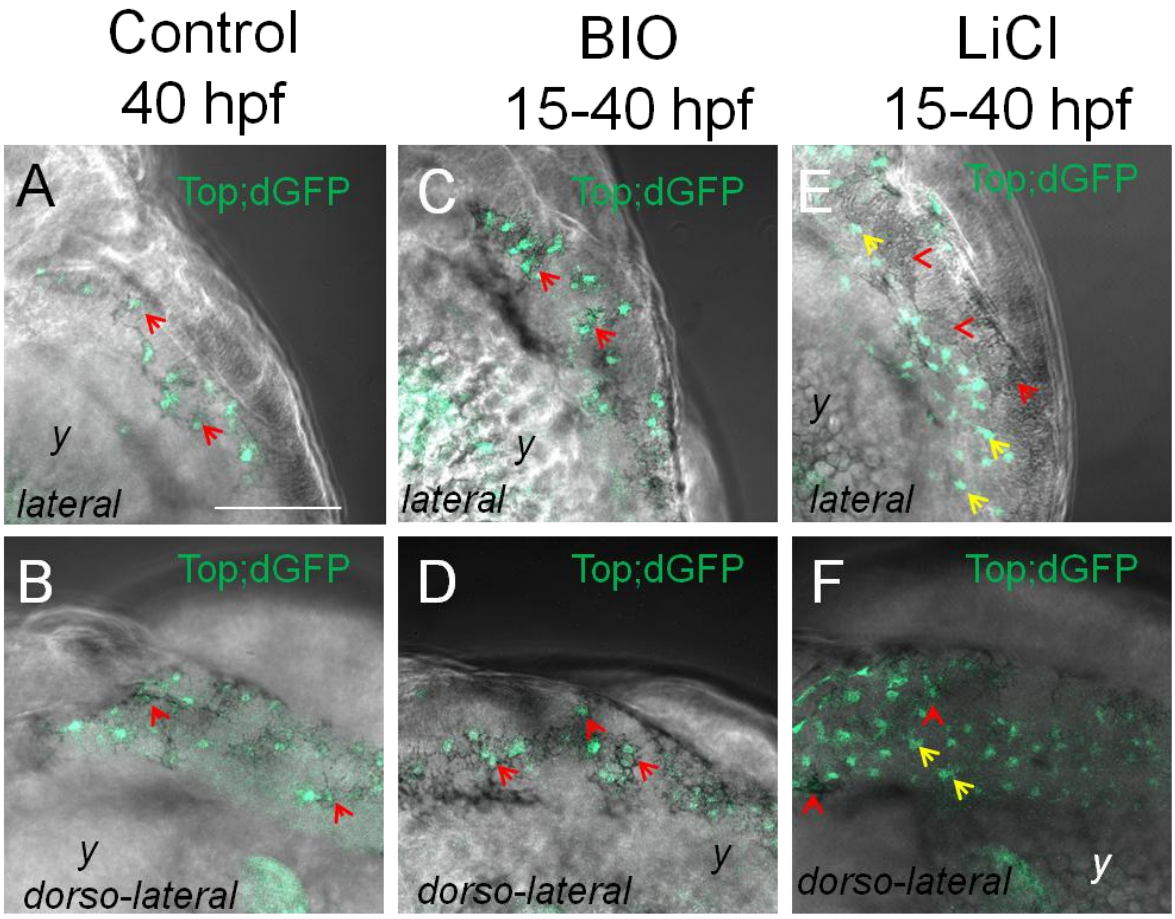

Figure 3.07: The TOP;dGFP reporter reveals activation of Wnt signalling in melanocytes of BIO treated embryos.

GFP expression was investigated by immunostaining in TOP;dGFP embryos treated from 15 hpf to 40 hpf and embryos were imaged using a confocal microscope. The fluorescence and the bright field images were merged to observe the expression of GFP in cells. Control embryos showed expression of GFP in most melanocytes (A,B) (red arrowheads points at some melanocytes expressing GFP). BIO treated embryos also showed expression of GFP in most melanocytes (C,D) (red arrowheads points at some melanocytes expressing GFP). In LiCl treated embryos the results showed that melanocytes did not show activation of GFP (E,F) (red arrowheads point at melanocytes, in E, most melanocytes did not show activation of GFP and in F, GFP expression could be detected in melanocytes pointed by the red arrowheads) but also mainly in other cells (yellow arrowheads point at non-melanocyte cells/potential xanthoblasts expressing GFP). Key: y: yolk sac. Bar: 100 µm.

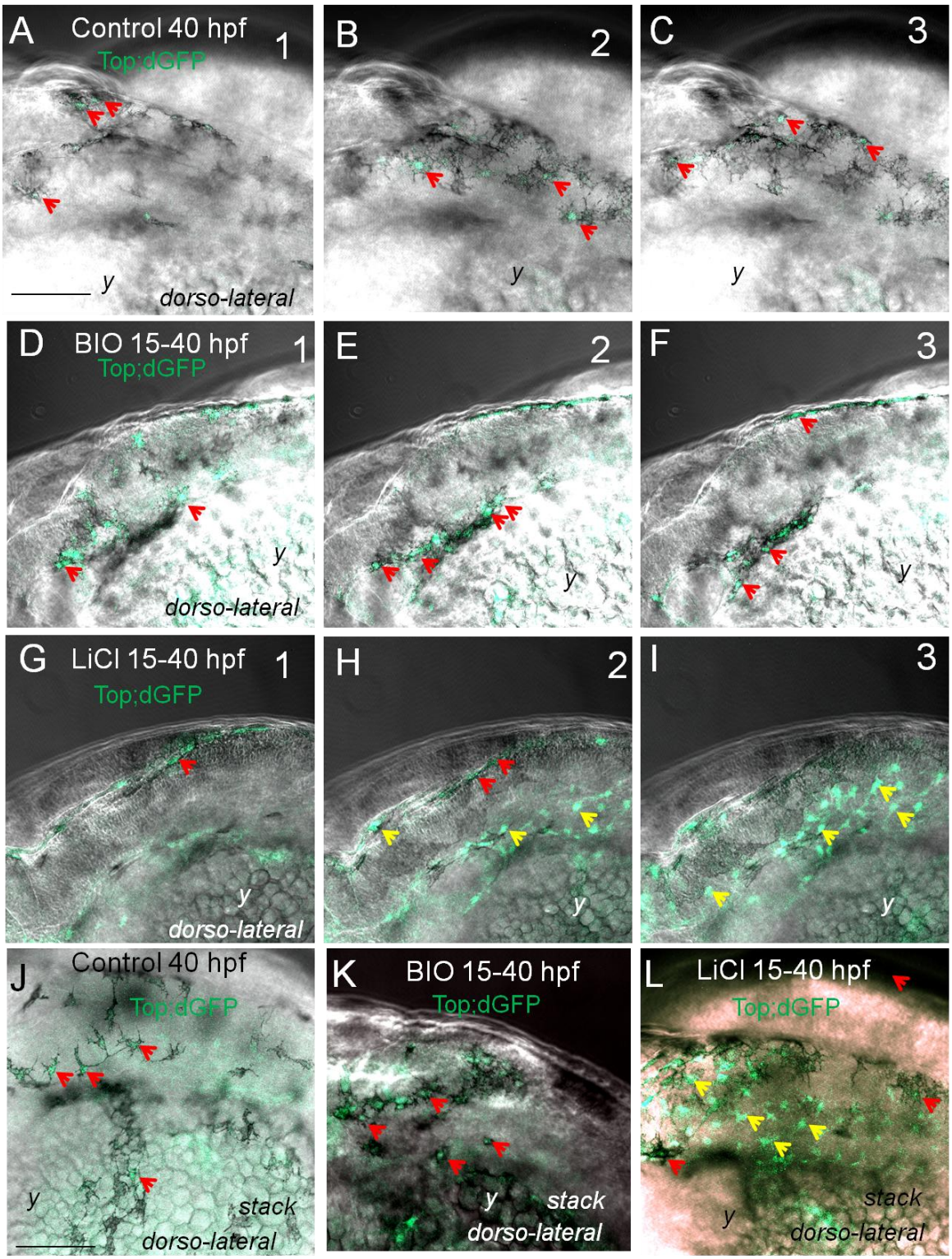

Figure 3.08: BIO activates GFP expression in melanocytes. See legend on the next page.

Figure 3.08: BIO activates GFP expression in melanocytes. See legend on the next page.

GFP expression was investigated by immunofluorescence of TOP;dGFP embryos; images show different focal planes with GFP expression. In each picture, red arrowheads point at melanised cells expressing GFP and yellow arrowheads point at non-melanised cells expressing GFP. The three focal planes (1,2,3) of the same embryo show GFP expression in the control embryo (A,B,C), in the BIO treated embryo (B,C,D) and in the LiCl treated embryo (G,H,I). Three images were combined as a stack and are shown as one image for the control (J), the BIO treated embryo (K) and the LiCl treated embryos (L). All BIO treated embryos expressed GFP with in melanised cells compared to controls and LiCl treated embryos only showed a few melanocytes expressing GFP through the focal planes. This result suggests that Wnt signalling was activated in melanocytes of BIO treated embryos only Key: y: yolk sac. The imaging conditions were the same throughout embryos of all conditions.

3.2.4 BIO treatment during the melanocyte specification phase resulted in increased melanocyte numbers

The Wnt signalling pathway has been shown to be involved in melanocyte specification and *mitfa* regulation at early stages (Hari *et al.*, 2012, Dunn *et al.*, 2000b, Schepsky *et al.*, 2006). Boosting the Wnt signalling activity during this period was expected to result in an increase of the number of melanocytes and a boost in *mitfa* expression. Here, the effects of both molecules were examined to control for the efficacy of the treatments to activate a Wnt signalling dependent process such as melanocyte specification. A short treatment phase (15-30 hpf) was defined to focus on the time when melanocyte specification occurs. The objective was to test whether LiCl and BIO treatments would cause an increase in both melanocyte number and *mitfa* expression, as a result of boosting cell specification (Figure 3.09).

Figure 3.09 shows that an elevation in melanocyte number was observed in heads and trunks of BIO treated embryos with BIO, (mean ± s.d, p-value at unpaired, one-tailed t-test, n= 20, $p< 0.001$), (control, 13 ± 2.1), BIO (32 ± 5.3, $p=0.00000059$), but not with LiCl (Figure 3.09). In contrast, melanocyte numbers in LiCl treatment were significantly decreased compared to the control (8 ± 2.3, $p=0.000006$) (Figure 3.09). Other mechanisms, or effects, could have caused an increase cell number in BIO treated embryos, such as an increased proliferation of cells. However, given the previous data showing a role for Wnt signalling in melanocyte specification from NC, the most parsimonious explanation is that BIO increases Wnt signalling and increases the number of melanocytes specified.

mitfa expression was investigated using the semi-quantitative technique of wholemount *in situ* hybridisation (WISH) to test whether the treatments caused an activation of *mitfa* expression (Figure 3.10). Fish treated with BIO showed a clear increase in *mitfa* expression, as shown by the number of *mitfa* expressing cells (Figure 3.10, (E-F)). In contrast, the experiment in LiCl treated embryos did not phenocopy this result as no increase of *mitfa* expression was observed (Figure 3.10, (C-D)). It could be suggested that the increase of *mitfa* expression in BIO treated embryos could be the cause of the increase of melanocyte number at 30 hpf, meaning that the number of cells expressing *mitfa* (corresponding to specified melanocyte number) had been increased by the 15 hpf-30 hpf BIO treatments. However, from this experiment it was difficult to assess whether this elevation could also be due to increase *mitfa* expression in cells at this stage.

Why LiCl treatments failed to phenocopy this result is not clear, but suggests that there are differences in the signalling effects of these molecules. Given our previous results (section 3.3.3) showing that LiCl treatments did not activate Wnt signalling in melanocytes, we interpret our data as showing consistently that LiCl is unable to activate Wnt signalling in the melanocyte lineage. In this context, direct testing of whether or not Gsk3β was significantly inhibited in cells after each treatment should also be assessed *in vivo* in melanocytes.

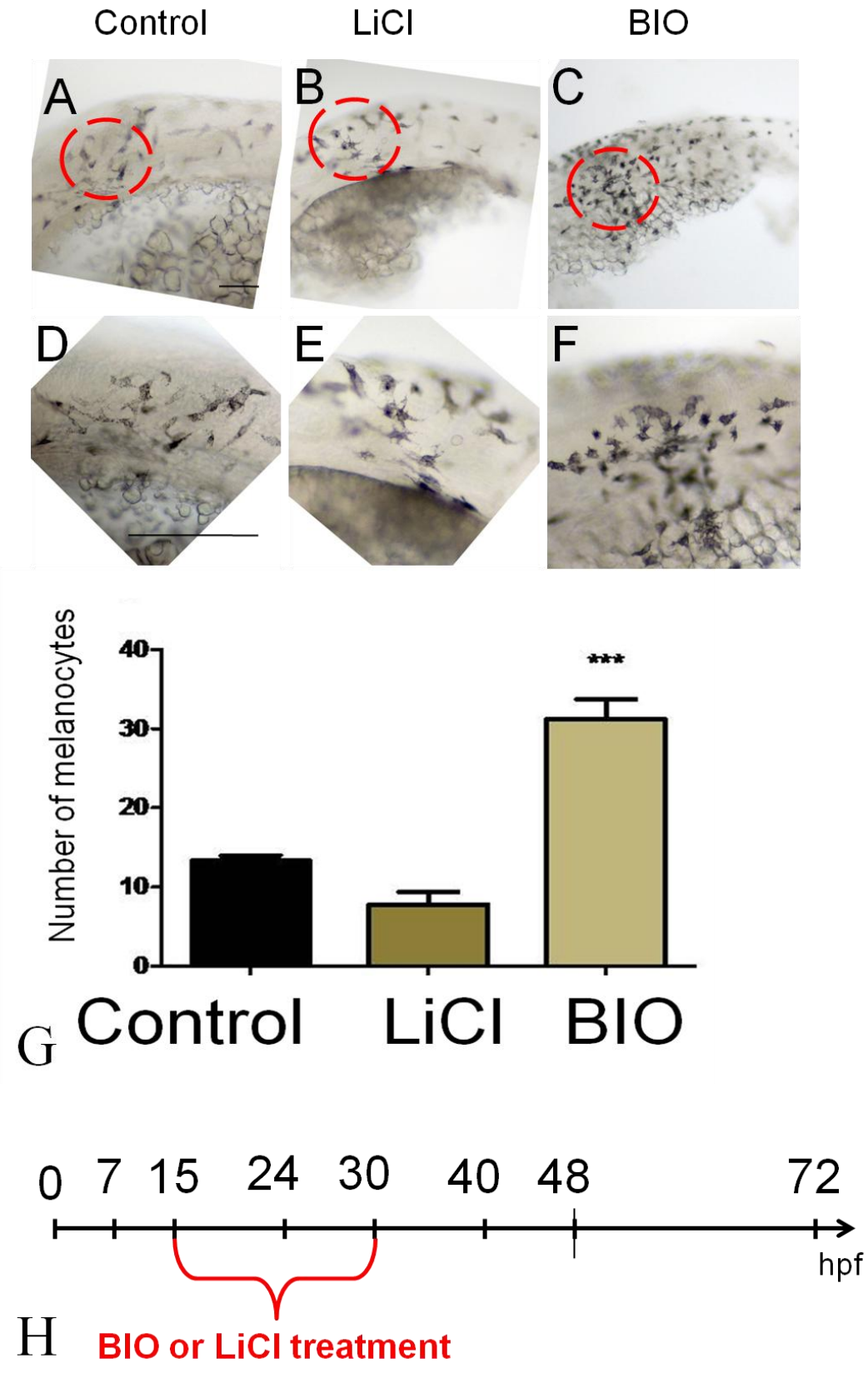

Figure 3.09: BIO treatment, but not LiCl treatment, (15-30 hpf) results in increased melanocyte number. See legend on the next page.

Figure 3.09: BIO treatment, but not LiCl treatment, (15-30 hpf) results in increased melanocyte number.

The trunk of live zebrafish control DMSO treated embryos (A-D), LiCl (200 mM) treated embryos (B-E), and BIO (5 µM) treated embryos (C-F), are shown in lateral view. The red circles in (A-C) are presented respectively in close up in (D-F). An increase in melanocyte number can be observed in treated embryos by comparing treated embryos (C-F) to the control (A-C). Scale bar: 100 µm**.** (G) Graph showing the average of melanocyte number counted in the dorsal head, from the anterior brain to the posterior boundary of otic vesicle, in 20 embryos for each condition. (***) indicates significant t-test result for cell number increase compared to the control (unpaired, one tailed, $P<0.001$. n=20 in each treatment (see text for details)). (H) Diagram of the timing and the length of the time window targeted for treating melanocytes during the specification phase (15 hpf to 30 hpf).

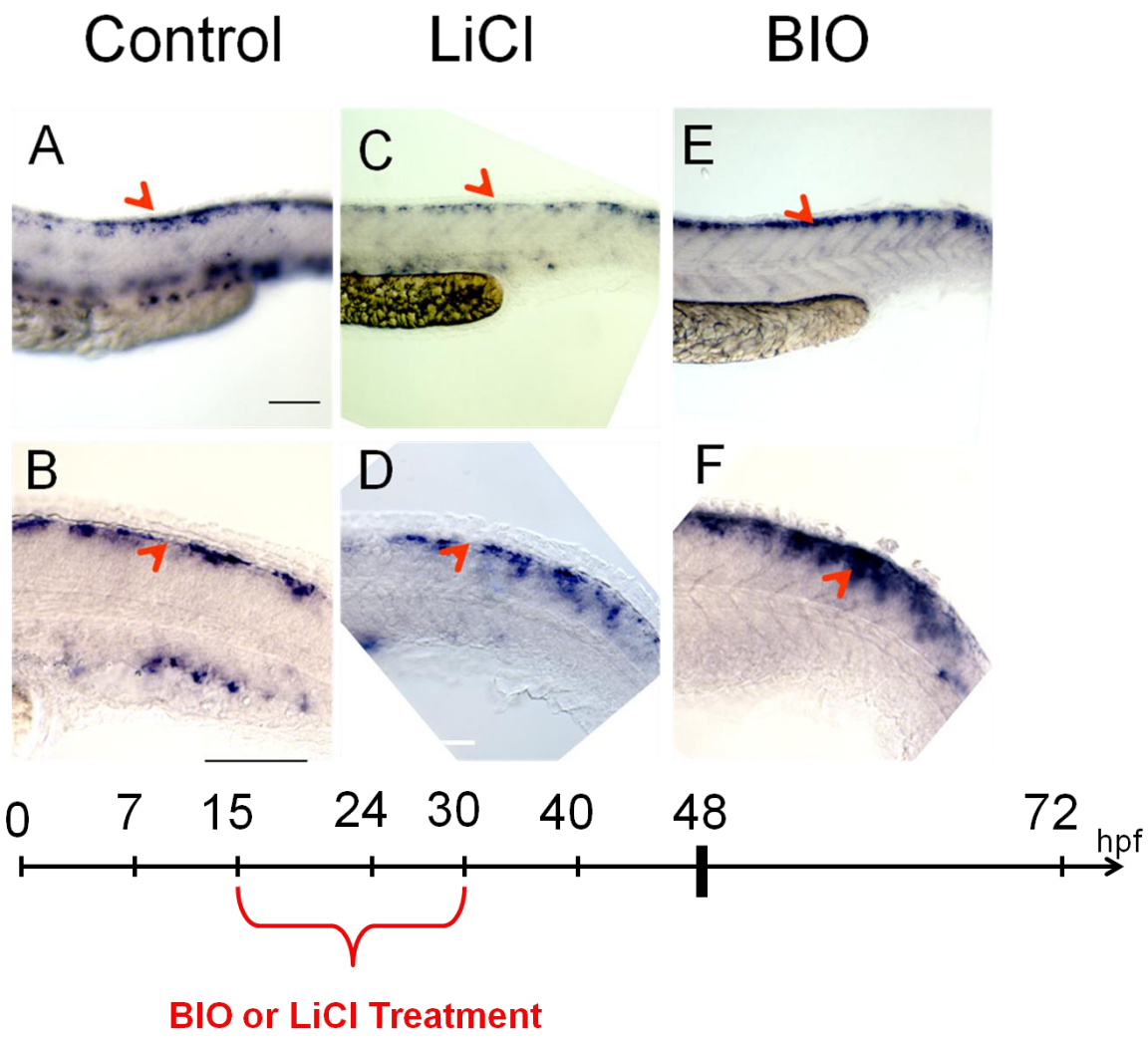

G

Figure 3.10: Effects of BIO and LiCl treatments (15-30 hpf) on expression of *mitfa* at 30 hpf.

Lateral views of posterior trunk (A,C,E) and anterior tail (B,D,F) of 30 hpf zebrafish embryos, after 15 hpf-30 hpf treatments showing WISH investigating *mitfa* expression. In the DMSO treated embryos (A-B), and in the LiCl treatment embryos (C-D), discontinuous *mitfa* expression can be observed in the dorsal region (arrowheads shows discontinuity of the signal), whereas, in the BIO treated embryos (E-F), *mitfa* expression is continuous in the dorsal region (arrowheads shows continuity of the signal), suggesting over-expression of *mitfa* compared to DMSO control. 80 embryos were analysed for each condition and pictures shows representative phenotype in each case. Scale bar: 100 µm. (G) Schematic shows the timing of treatment, during melanocyte specification time window.

3.2.5 BIO, but not LiCl, could be used as an activator of Wnt signalling in melanocytes

Taken together, these data show that BIO treatment, but not LiCl treatments, could effectively activate Wnt signalling in the melanocyte lineage, elevating melanocyte number when used during the melanocyte specification phase, most likely via elevated *mitfa* expression. These results were fully consistent with the expectation that the elevated melanocyte number at 30 hpf results from increased fate specification. An alternative method could be used to test for an increase of Wnt signalling in melanocytes, such as investigating β-catenin translocation to the nucleus. However, due to the lack of specificity of the newly release anti-β-catenin anti-body in zebrafish, we could not address this ourselves.

3.2.6 Supernumerary melanocytes survived until 72 hpf

Prior to addressing the main hypothesis relating to the ongoing role of the Wnt signalling for melanocyte differentiation, we investigated what happened to the supernumerary melanocytes observed at 30 hpf, following the 15-30 hpf BIO treatment. If the BIO treatment could activate cell specification and allow extra-specified cells to specify, commit, differentiate and survive until three days post fertilisation (dpf), this would support the hypothesis that their specification was *mitfa* dependent. Hence, it was investigated here by boosting Wnt signalling from 15-30 hpf and determining the melanocyte number at 48 hpf and 72 hpf.

The 15-30 hpf BIO treatments and the DMSO control treatments were repeated and, at 30 hpf, the embryos of both conditions were divided into two equal batches. One batch of BIO treated batch was rinsed and kept in embryo medium/DMSO only (“medium”) whereas the other was maintained in BIO treatments (“treatment”) (Figure 3.11). The DMSO treated embryos were also separated, one was maintained in DMSO, the other was rinsed and kept in medium/DMSO. In both batches of the DMSO treated embryos (rinsed or not), embryos were exactly similar (WT DMSO fish) and for more clarity, we call these controls. All embryo batches were then examined at 48 and 72 hpf (Figure 3.11, (A-E)). Melanocytes were then counted in the head/trunk regions of embryos to determine whether melanocyte numbers were increased at 48 and 72 hpf in both conditions (“medium” and “treatment”) compared with DMSO controls. In both groups (“medium” and “treatment”), embryos treated with BIO showed a significant increase in melanocyte number (Figure 3.11, (A-B)) (mean ± s.d, p-value in unpaired, one-tailed t-test, n=20) (for each condition, 20 of 160 observed embryos were randomly chosen for analysis), control 48 hpf (32.6 ± 1.99), 72 hpf (47.5 ± 1.96) “medium” 48 hpf, (44.2 ± 1.8) p= 0.00007, “medium” 72 hpf, (57.5 ± 1.29) p= 0.00003, “treated” 48 hpf, (43.8 ± 2.2) p= 0.00007, “treated” 72 hpf (58.09 ± 1.7) p= 0.000012). Additionally, the dendricity of these melanocytes was investigated at 48 hpf. The dendricity was significantly increased at 48 hpf after BIO treatments, for both “medium” and “treated” batches, compared to DMSO treated embryos (Figure 3.14, (C) (mean ± s.d, p-value) (BIO, “medium”, 3.07 ± 1.02,

p=0.00082. and "treatment" 3.3 ± 1.26, p=0.0059), (Control, 2.44 ± 0.43). However, the dendricity of cells at 72 hpf was not different from the control (data not shown).

These results suggested that Wnt signalling dependent increased specification of melanocytes led to an increase of cell commitment, so that neither mechanisms of compensation, nor mechanisms of inhibition, were preventing cell development until 3 dpf at least. In the dorsal and lateral head and in the dorsal trunk, melanocytes were not organised as in WT at 3 dpf, which suggests that either increasing Wnt or *mitfa* signalling, or both, was preventing the cells from adopting the WT patterning (Figure 3.11, head (C,E and I,K) and trunk (D,F and J,L)). Another explanation for this mis-organisation phenotype could be that the cell number was an important parameter for cells to organise themselves into the patterning on the dorsal stripe, as in WT. Furthermore, this organisation mechanism was either disturbed or prevented by an increase in cell number. Observing that supernumerary cells could survive until 3 dpf suggested that BIO treatments boosted the program of melanocyte specification but also commitment to the lineage.

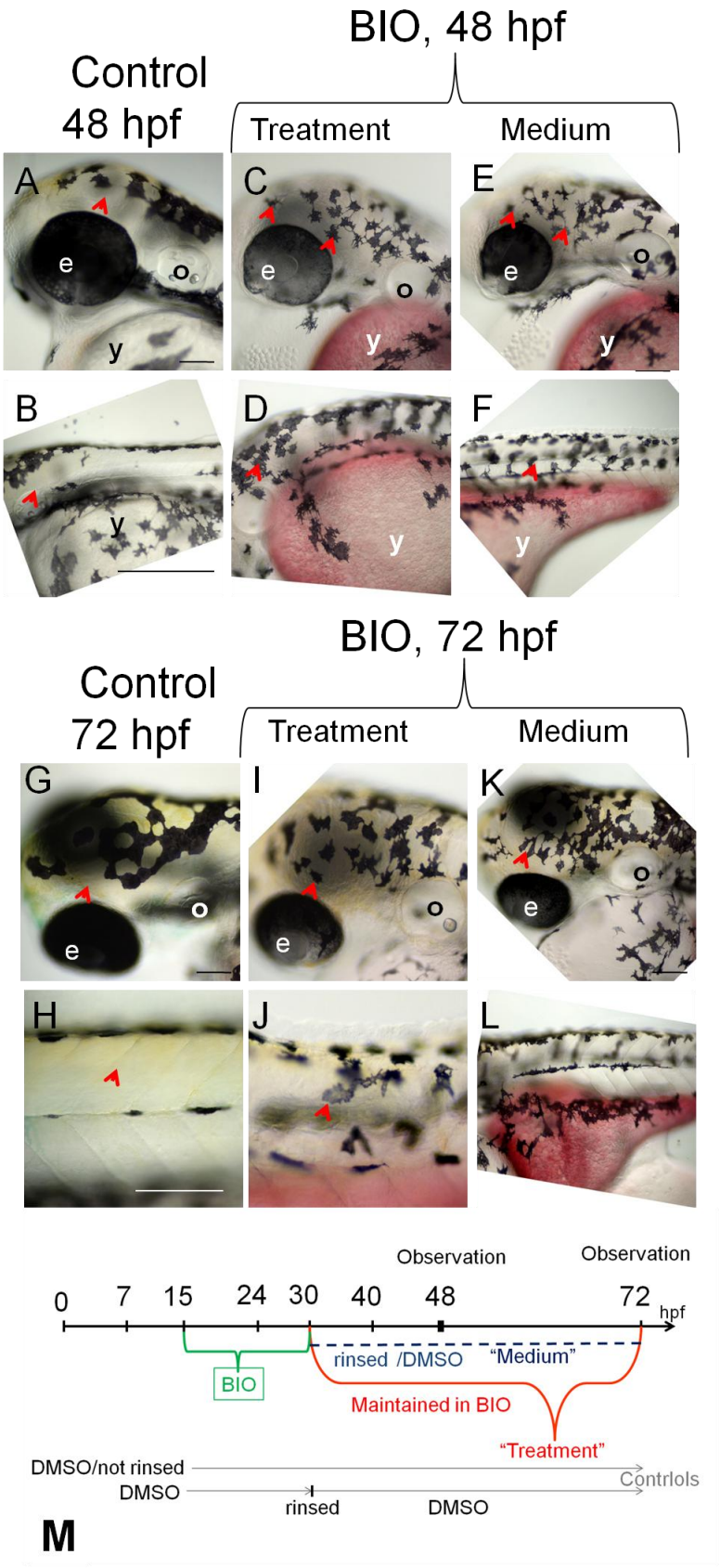

Figure 3.11: Extra melanocytes specified from 15 hpf to 30 hpf survive until at least 72 hpf. See legend on the next page.

Figure 3.11: Extra melanocytes specified from 15 hpf to 30 hpf survive until at least 72 hpf.

80 live zebrafish embryos were observed at 72 hpf for each condition. Live zebrafish embryos (A-I) at 48 hpf (A-F) and 72 hpf (G-I), in dorsolateral view of head (top panels) and lateral view of the trunk (bottom panels). Fish were treated from 15-30 hpf and for each of the "medium" and "treated" condition, they were observed at 48 hpf (C-D), and at 72 hpf (E-F). In both treatments, an increase of the melanocyte number could be observed compare to the DMSO treated control fish (A-B). In (A-G) no melanocytes could be seen around eyes (the red arrowhead shows that no melanocytes are found around eyes) whereas in treated fish, (C-E-I-K) cells could be observed close to the eye structure (red arrowheads show presence of cells around eyes). In control, (B-H) no melanocytes could be observed on the lateral trunk (red arrowhead), whereas, in BIO treated embryos (D-I), melanocytes were observed in the lateral trunk, outside of normal patterning (red arrowheads show the presence of cells in between lateral and dorsal stripes). e: eye; y: yolk sac; o: otic vesicle. Scale bar: 100 µm except (H,J) scale bar: 50 µm**.** (M) diagram showing the differences between "treatment" and "medium" batches. "medium" batch was only treated with BIO from 15 to 30 hpf and then rinsed and placed in DMSO/embryo medium and observed at 48 hpf and 72 hpf, whereas, the "treatment" batch was always maintained in BIO treatment until observation. DMSO treated controls were also divided into two batches. One was rinsed and placed in new DMSO/medium solution. The other was left in the same DMSO/medium solution, however, only one control fish is presented here as no differences could be seen between these DMSO controls.

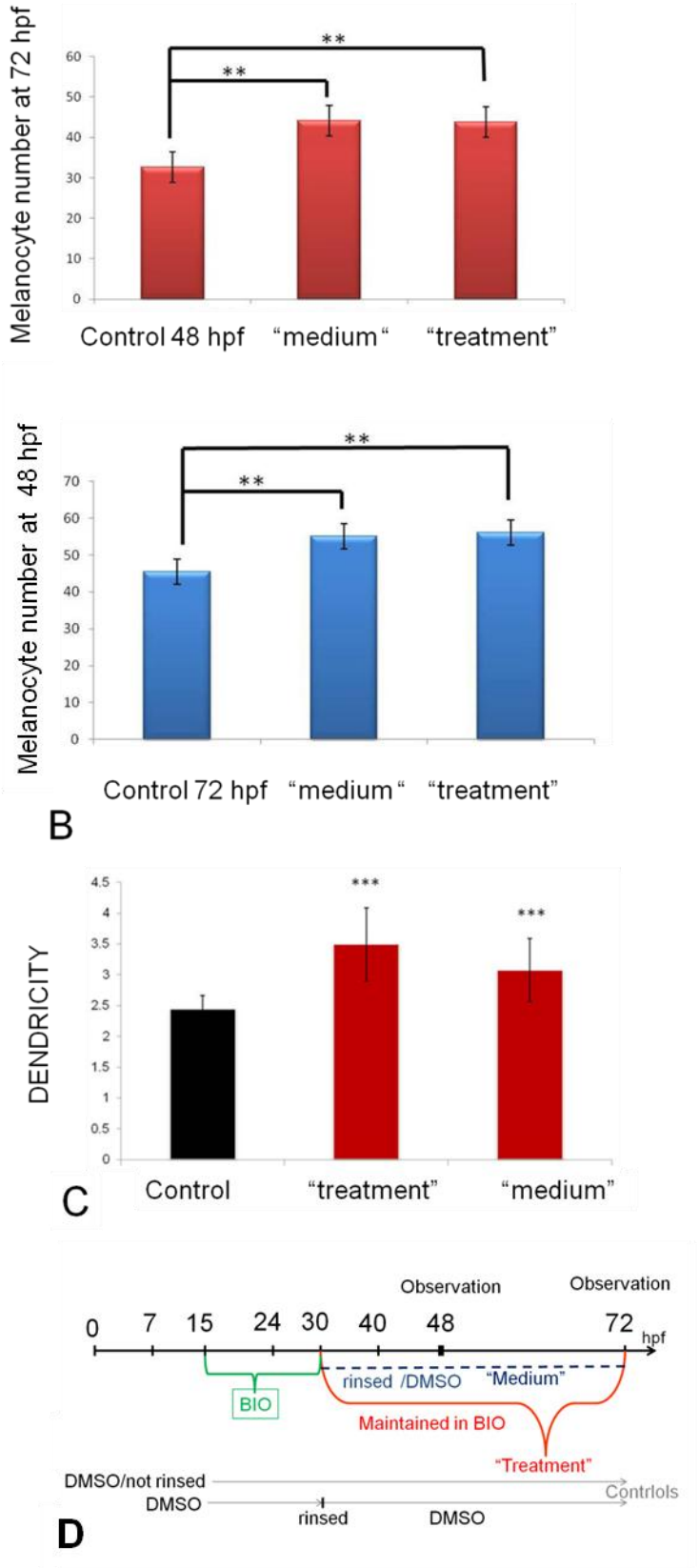

Figure 3.12: Melanocyte dendricity is boosted at 48 hpf and cell number is increased at 48 hpf and 72 hpf in both conditions ("treatment" and "medium"). See legend on the next page.

Figure 3.12: Melanocyte dendricity is boosted at 48 hpf and cell number is increased at 48 hpf and 72 hpf in both conditions ("treatment" and "medium

Melanocyte number was significantly increased in zebrafish treated embryos (A-B) at 48 hpf (A) (p-value<0.001), and 72 hpf (B), (p-value<0.001), in both "treatment" and "medium" batches. Melanocytes were counted in the head from the anterior brain to the otic vesicle in 20 embryos for each condition, n = 20 (see text for details). The cell dendricity R *(R = P2 /4pA, where A is the cell area and P the cell perimeter)* was significantly increased in both "treatment" (p=0.0059) and "medium" (p=0.00082) conditions, n= 20 cells on 10 different embryos were analysed for each condition (see text for details) at 48 hpf (C). (D) Diagram showing the differences between "treatment" and "medium" batches. "medium" batch was only treated with BIO from 15 to 30 hpf and then rinsed and placed in DMSO/embryo medium and observed at 48 hpf and 72 hpf, whereas, the "treatment" batch was always maintained in BIO treatment until observation. DMSO treated controls were also divided into two batches. One was rinsed and placed in new DMSO/medium solution. The other was let in same DMSO/medium solution, however, only one control fish is presented here as no differences could be seen between these DMSO controls.

3.2.7 Treating embryos during the melanocyte differentiation phase affected two aspects of cell differentiation

Later, cells enter in a phase of differentiation which involves the maturation of the cell phenotype. In zebrafish melanocytes, cells start showing the first signs of melanisation around 27 hpf and embryonic melanocytes would be mature by 3 dpf when many cells (in dorsal embryo at least) are in a postmigratory position, and that the level of melanin is high (and not obviously increasing at later stages). To test the role of Wnt signalling on melanocyte differentiation, the differentiation phase was divided into three time windows as described in Figure 3.13. Firstly, treatment A covered the whole differentiation period, from 24-72 hpf. Secondly, embryos were treated during the late differentiation phase (treatment B), from 48-72 hpf, when *sox10* expression becomes undetectable by WISH as demonstrated by Greenhill *et al.,* (2011). Thirdly, in treatment C, embryos were treated during early differentiation phase, from 24-48 hpf, when *sox10* expression is detectable by *in situ* hybridisation and immunofluorescence techniques, (Greenhill *et al.,* 2011). By dividing the differentiation phase in three time window, we could assess the changing effects of activation of Wnt signalling throughout melanocyte differentiation.

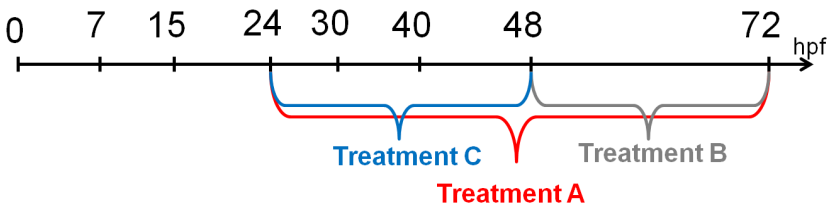

Figure 3.13: Time windows designed to target the melanocyte differentiation phase with BIO treatment.

Three time windows were targeted during the melanocyte differentiation phase. The treatment A covers all of the differentiation phase, from 24-72 hpf. In the treatment B, fish were treated from 48-72 hpf, during the late differentiation phase and treatment C covered the early differentiation phase, from 24-48 hpf.

3.2.7.a Embryos treated from 24 to 72 hpf show disrupted melanocyte pattern

To cover the early and late differentiation phases, embryos were first treated with BIO from 24-72 hpf (Figures 3.14-3.15). Cells in the head, and in the trunk, were dispersed and seemed to have lost the ability to organise and reproduce the typical pattern "U" of melanocytes (Figure 3.16, (G-J), Figure 3.17, (C-D)). The melanocytes in WT DMSO treated embryos dorsal head showed a characteristic circular or open U pattern at the anterior part of the dorsal stripe (Figure 3.14, (A-F)). In contrast, in the BIO-treated embryos these cells were less organised, more scattered, and lacked the clearly "U" shaped arrangement of cells was disrupted.

3.2.7.b Embryos treated from 48 to 72 hpf show disrupted melanocyte pattern

Treatment during the late differentiation phase also resulted in cell disorganisation (Figure 3.14, (K-N), Figure 3.15, (E-F)). As observed in the previous treatment, cells did not reproduce the typical "U" pattern observed in controls at 72 hpf, while cell shape was unaffected.

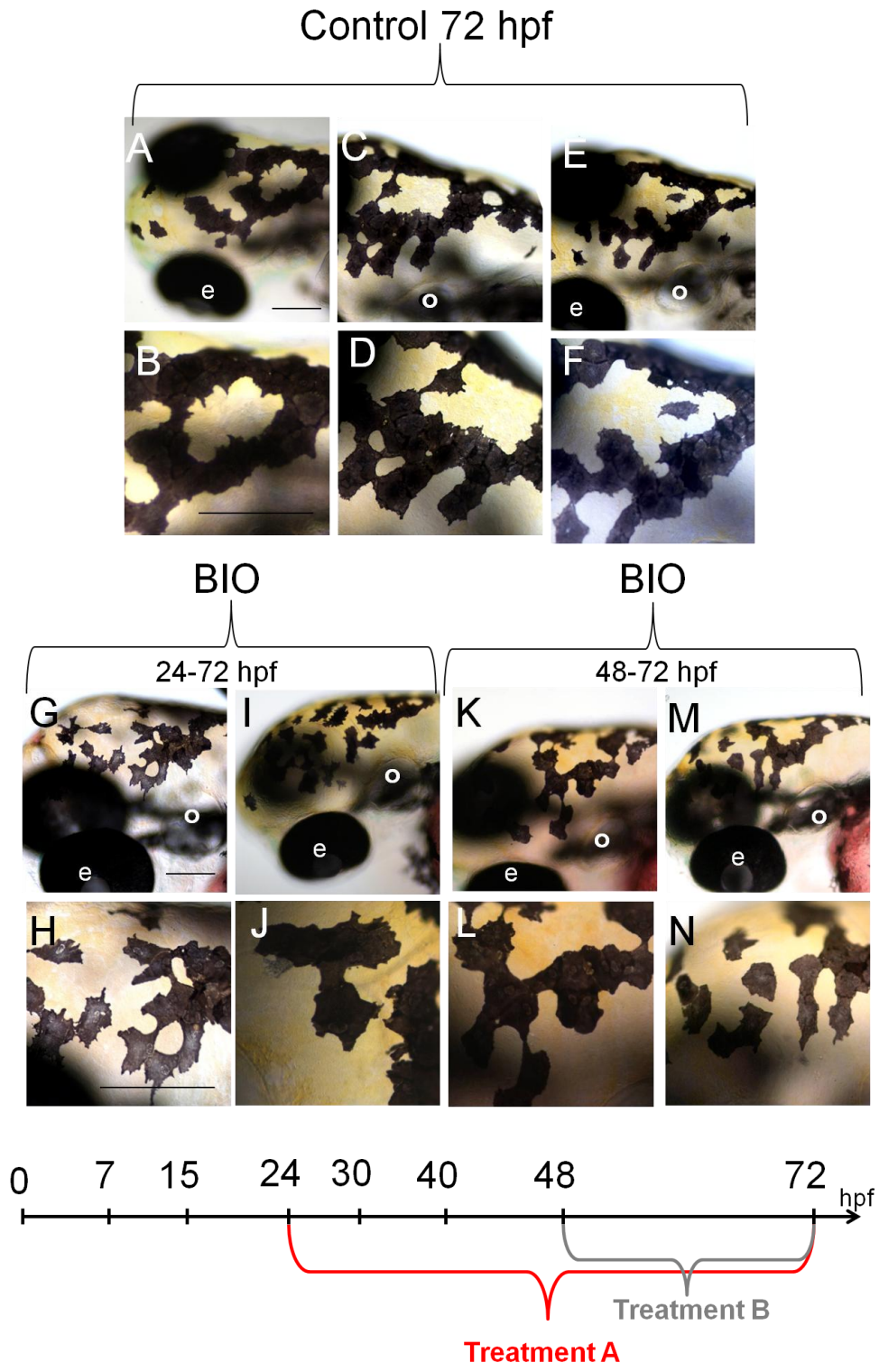

P

Figure 3.14: The BIO treatment (24-72 hpf and 48-72 hpf) affects cell organisation. See legend on the next page.

Figure 3.14: The BIO treatment (24-72 hpf and 48-72 hpf) affects cell organisation.

Dorsal view of heads of live embryos at 72 hpf, (A-N). Control DMSO treated embryo, (A-F) (lower panels always show close ups of the top panels), BIO treated embryo (G-N) show the loss of cell arrangement compared to the repeated conserved pattern observed at 72 hpf in control fish. 24-72 hpf BIO treated fish (G-J), 48-72 hpf BIO treated fish (K-N). 160 live zebrafish embryos were observed at 72 hpf for each condition and here we show two representative individuals for each treatment. e: eye; o: otic vesicle. Scale bar: 100 µm. (O) Diagram of BIO treatment period.

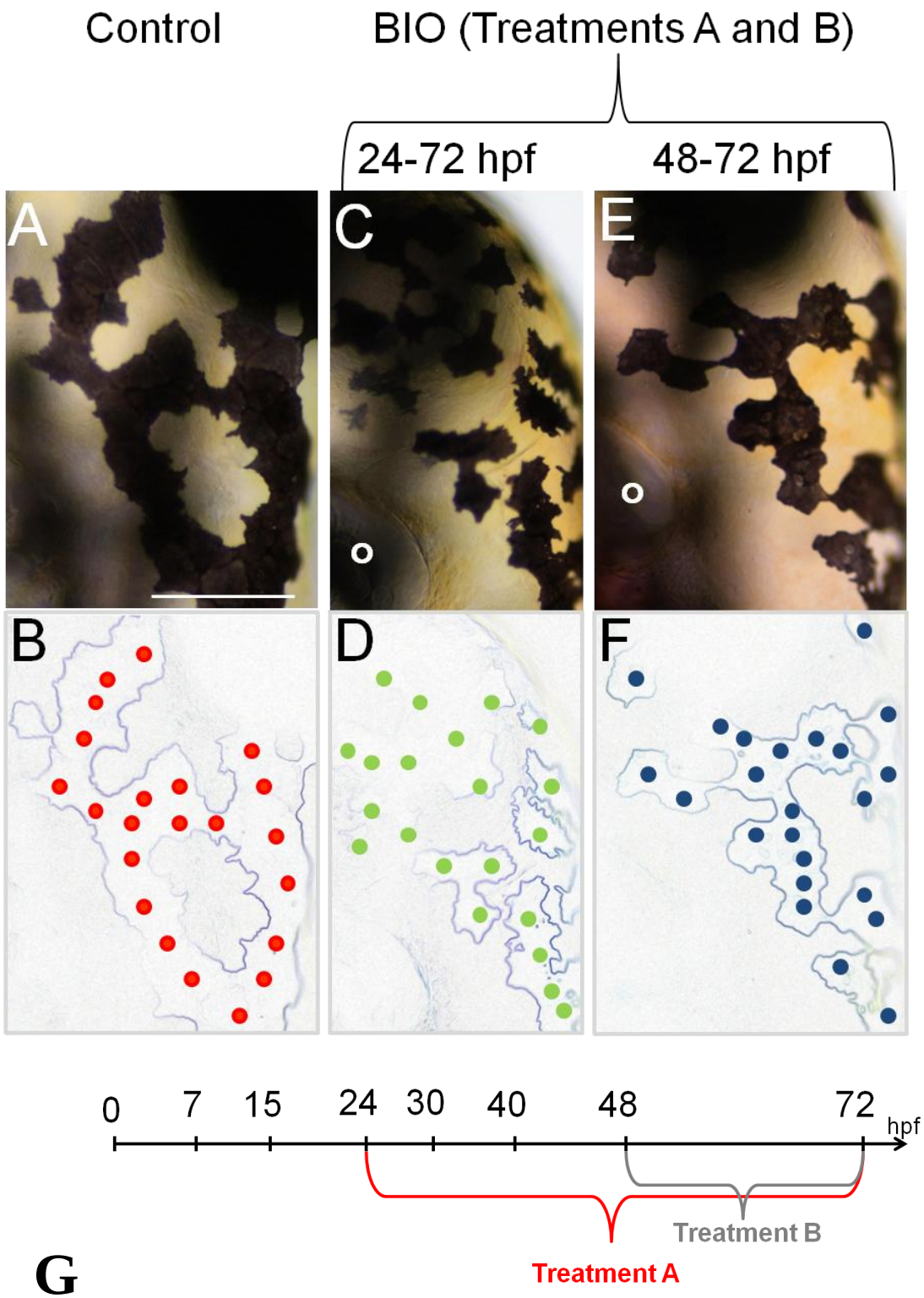

Figure 3.15: Melanocyte organisation is disrupted at 72 hpf, after 24-72 hpf and 48-72 hpf BIO treatments. See legend on the next page.

Figure 3.15: Melanocyte organisation is disrupted at 72 hpf, after 24-72 hpf and 48-72 hpf BIO treatments

Embryo heads in dorsal view at 72 hpf (A-C-E). DMSO control (A), BIO treated embryo from 24 -72 hpf, (C), 48-72 hpf BIO treated embryo (E). Images were processed in ImageJ (B-D-E) to find cell edges and to invert tones. Each point represents a cell and dispersion of cells could be observed but was not measured in treated embryos (D and F) compared to control (B). 160 live zebrafish embryos were observed for each condition. The phenotype shown here was consistently observed through treated embryos. Key: o: otic vesicle. Scale bar: 100 µm. (G) Diagram of BIO treatment period.

3.2.7.c Treating embryos from 24 hpf to 48 hpf leads to changes in melanocyte shape

Embryos were treated during the early differentiation phase, 24 - 48 hpf. Treatment with BIO during this phase resulted in changes in cell shape and more precisely, in an increase in cell dendricity (Figure 3.16). The roundness parameter, dendricity, was calculated as $R = P2 / 4pA$, where A is the cell area, and P, the cell perimeter. A and P were measured using ImageJ software. A significant increase in the cell dendricity was found with BIO treatments (Figure 3.16, (G-M), Figure 3.17, (B)) (mean ± s.d, p-value at t-test, unpaired, one-tailed test) (control, 2.44 ± 0.43) (BIO, 4.25 ± 1.68, p = 0.004). This result suggested that cell shape was an aspect of cell differentiation which was sensitive to BIO only from 24 - 48 hpf. In contrast to the results observed after the 15-30 hpf treatment, no increase in melanocyte number was observed after the 24-48 hpf treatment (mean+ s.d, p-value) (control, 23.9 ± 2.01, BIO, 23.1 ± 4.03, p=0.443). A probable explanation for this is that Wnt signalling was not limiting anymore for melanocyte specification at this stage or, more likely, that fate specification in the head region at least was complete.

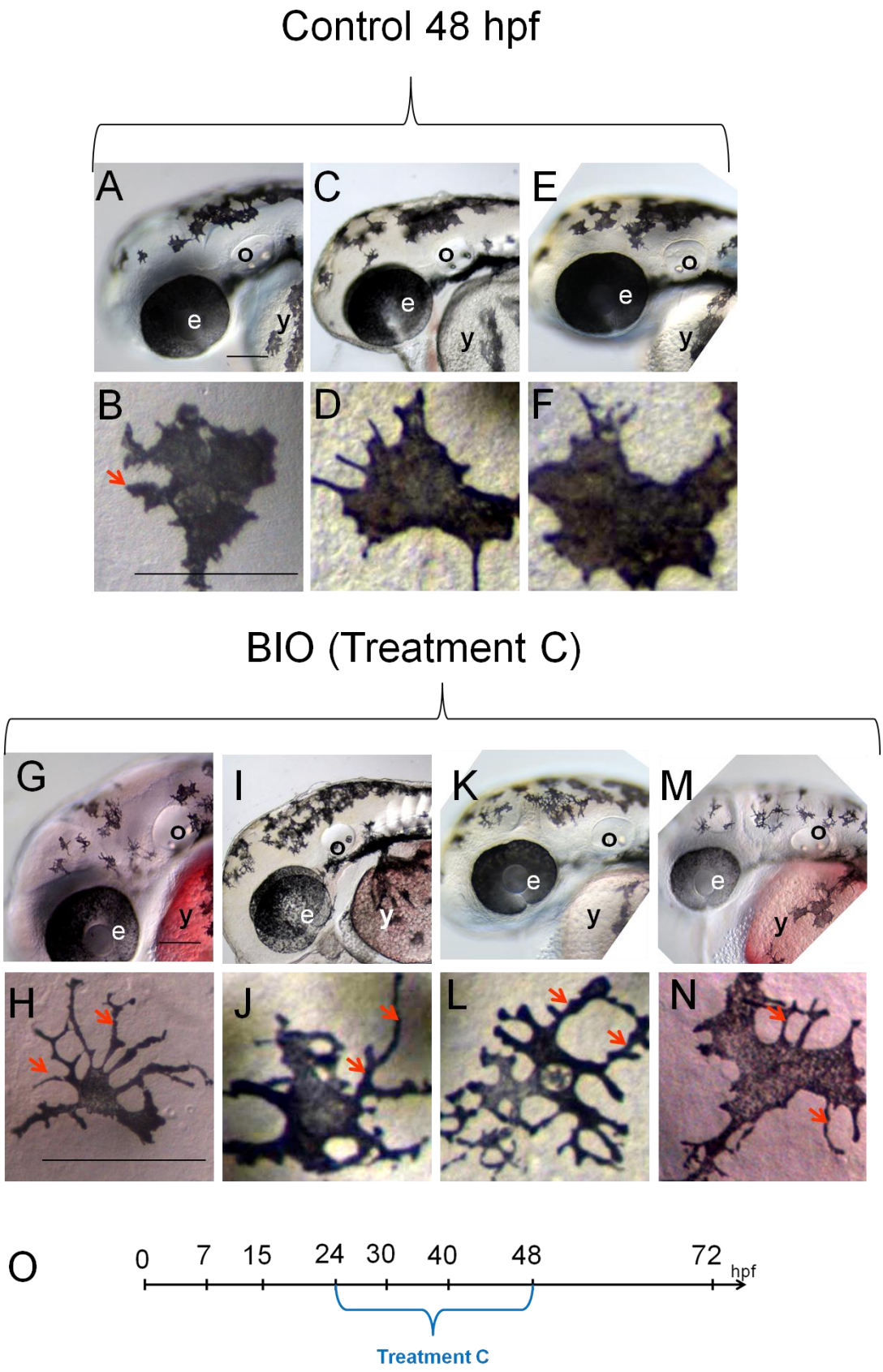

Figure 3.16: BIO treatment (24-48 hpf) increases melanocyte dendricity. See legend on the next page.

Figure 3.16: BIO treatment (24-48 hpf) increases melanocyte dendricity.

Live embryos at 48 hpf, (A-N). The heads of embryos are shown in a dorsolateral view for each condition, control DMSO treated embryos (A,C,E), BIO treated embryos (G,I,K,M) (arrowhead in (B) points at a dendrite). Representative single cells are also presented for each condition, control DMSO treated, (B,D,F), and BIO treated, (H,J,L,N, arrowheads points at dendrites). Scale bar: 100 µm except single cell panels, scale bar: 30 µm). 160 zebrafish embryos were observed for each condition, the phenotype shown here was consistently observed through treated embryos. e: eye; y: yolk sac; o: otic vesicle (O) Diagram showing BIO treatment time window.

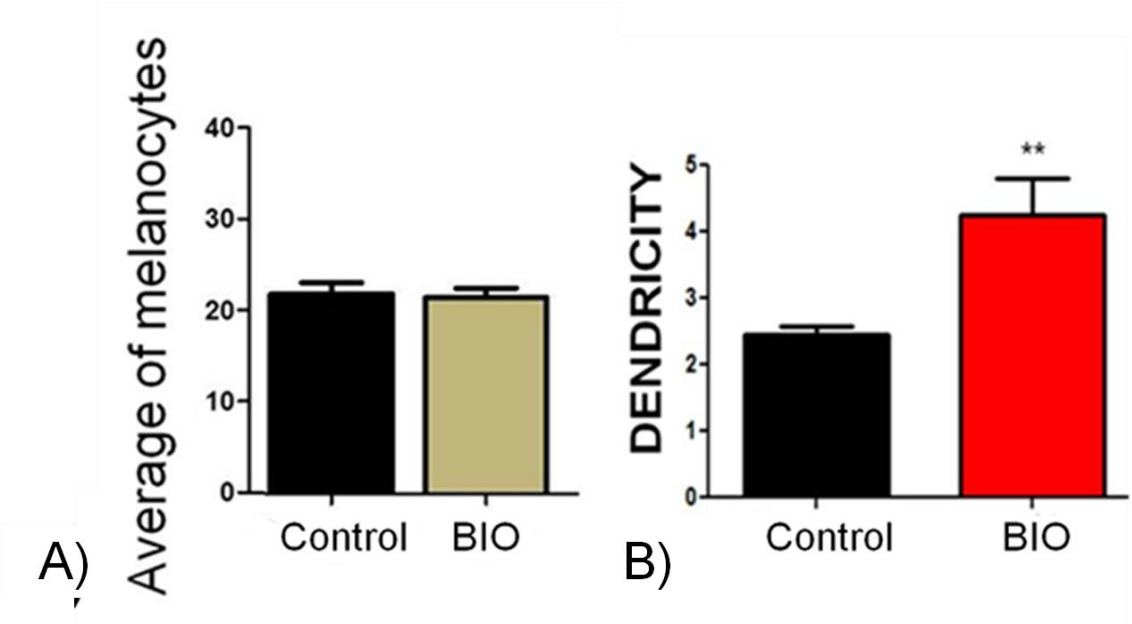

Figure 3.17: BIO treatment from 24-48 hpf caused an increase in melanocyte dendricity but did not increase cell number at 48 hpf.

The average melanocyte number was not changed in treated embryos compared to the number of melanocytes in the controls (160 embryos were observed for each condition and cells were counted from the anterior brain to the otic vesicle, in 20 embryos for each condition (n=20), control (mean ± s.d, p-value) 23.9 ± 2.01 and BIO, 23.1 ± 4.03, p=0.443, p-value>0.1 (A). Embryos treated with BIO showed a significant increase R *(R = P2/4pA, where A is the cell area and P the cell perimeter)* which corresponds to increased cell dendricity (for circle, R=1). 20 cells were investigated (n=20) in 10 different embryos for each condition. Control, R=2.44 ± 0.43, BIO R= 4.25 ± 1.68, p = 0.004, t-test result, p-value<0.01 (**) (B).

3.2.8 Treating embryos with BIO during melanocyte differentiation led to increased *mitfa* expression

In the context of our main hypothesis, boosting Factor Y activity should cause an increase in *mitfa* transcription. To test this, *mitfa* expression level was measured after BIO treatments using quantitative RT-PCR (Figure 3.18). The t-test was performed (mean relative expression level ± s.d, p-value), and showed that after 24-48 hpf BIO treatments, *mitfa* expression level was significantly increased from 100 to 535 ± 7.1, ($p = 0.00087$). The BIO treatment lasting from 48-72 hpf, and from 24-72 hpf, also caused a significant increase of the *mitfa* expression, 496 ± 9.8, $p= 0.0085$ and 872 ± 32.1, $p = 0.000092$, respectively. Consequently, *mitfa* expression was found to be increased by around five fold in embryos treated from both 24-48 hpf and 48-72 hpf, whereas, a nine fold increase was observed in embryos treated from 24-72 hpf.

The results of the RT-qPCR experiments showed a significant increase in *mitfa* expression in BIO treated embryos. At 48 and 72 hpf, *mitfa* expression was strictly restricted to melanocytes (Kelsh *et al.*, 2000). This showed that boosting Wnt signalling during melanocyte differentiation triggered an increase in *mitfa* expression. Interestingly, a correlation could be noted between the increase of *mitfa* and the time of exposure to the small molecule. Treatments lasting 24 hours (24-48 hpf, 48-72 hpf) seemed to increase *mitfa* expression about five fold while treatments lasting 48 hours (24-72 hpf) seemed to increase expression of *mitfa* about eight fold. This could suggest a positive feedback loop of Mitfa on *mitfa* expression itself explaining the greater increase observed in long term treatment.

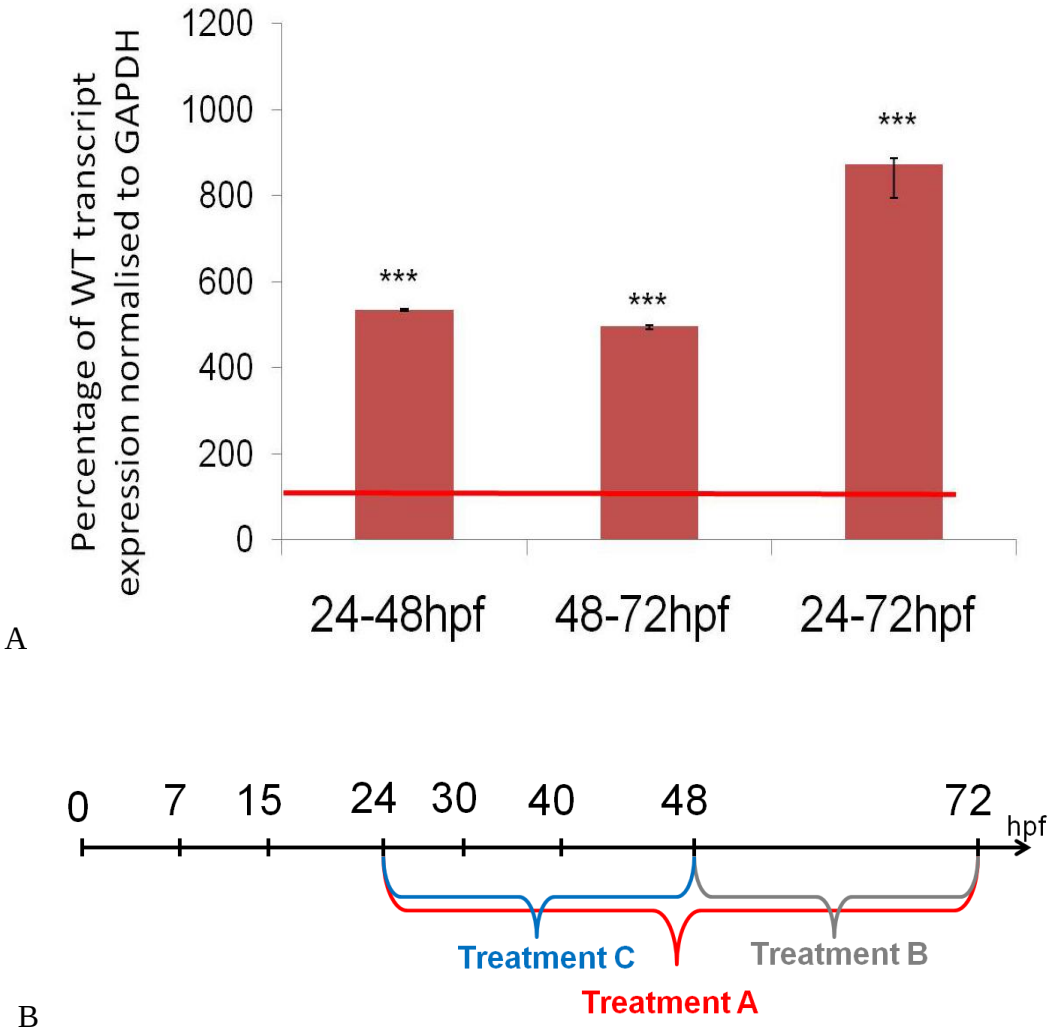

Figure 3.18: BIO treatments result in a significant increase in *mitfa* expression in zebrafish embryos.

Experiments of RT-qPCR comparing *mitfa* expression levels in WT and BIO treated embryos (WT *mitfa* level = 100 % transcripts (red line on graph)) (A). Gene expression was investigated in 10 samples of 50 pooled embryos for each condition, in triplicate. Expression levels were normalised to the stable expression of a reference gene, *gapdh*. All treatments caused significant increase of *mitfa* expression (t-test, two- tailed, 24-48 hpf, p= 0.00087, 48 72 hpf, p= 0.0085, 24-72 hpf, p = 0.000092). Key: p-value<0.001 on graph denoted as: (***). (B) Diagram showing time period of the three treatments (Treatment A, 24-72 hpf), (Treatment B, 48-72 hpf), (Treatment C, 24-48 hpf).

3.2.9 BIO treatments did not affect *mitfa* expression in *mitfa*^{w2} mutants

Wnt signalling has previously been shown to be required during cell specification as an activator of *mitfa*, independently of *mitfa*. Therefore, activating Wnt signalling with BIO treatments during melanocyte specification, in *mitfa*^{w2} mutant embryos, would result in activating *mitfa* expression. In contrast, during cell differentiation, the modelling suggested that activation of *mitfa* expression by Factor Y would be *mitfa* dependent, due to the feedback-loop. Consequently, in the context of this hypothesis, in the absence of *mitfa* expression (as in *mitfa*^{w2} mutant), activation of Factor Y would not be expected to lead to activation of *mitfa* expression. This hypothesis that boosting Wnt signalling would activate *mitfa* expression in the *mitfa*^{w2} mutant only when targeting the specification phase and not the differentiation phase, was tested here and the results are shown in Figure 3.20, (A-B)).

mitfa expression was investigated by WISH and the results showed that expression of *mitfa* was neither boosted nor changed when embryos were treated during melanocyte differentiation phase (Figure 3.20, (C-L). At 48 hpf, *mitfa* was detected in the dorsal and the lateral region of the trunk. At 72 hpf, *mitfa* was detected in cells of the dorsal stripe and the lateral stripe. This suggested that, in the absence of *mitfa*, Wnt signalling could not activate *mitfa* expression after 24 hpf. In contrast, *mitfa* expression was boosted in *mitfa*^{w2} mutant embryos treated from 15-30 hpf as shown by the increase of the signal detected in the trunk (Figure 3.20, (A-B)). Using a quantitative technique such as RT-qPCR could be interesting to quantitatively assess the changes of *mitfa* expression level with treatments.

According to these results, Wnt signalling dependent activation of *mitfa* during melanocyte differentiation is likely to be *mitfa* dependent. This feedback regulation is consistent with the hypothesis of Factor Y predicted by the modelling. However, one aspect of this loop which was not tested is the activation of Factor Y by Mitfa. For investigating this aspect of Factor Y, we would need to analyse activating factors binding *mitfa* regulatory sequences by ChIP for instance.

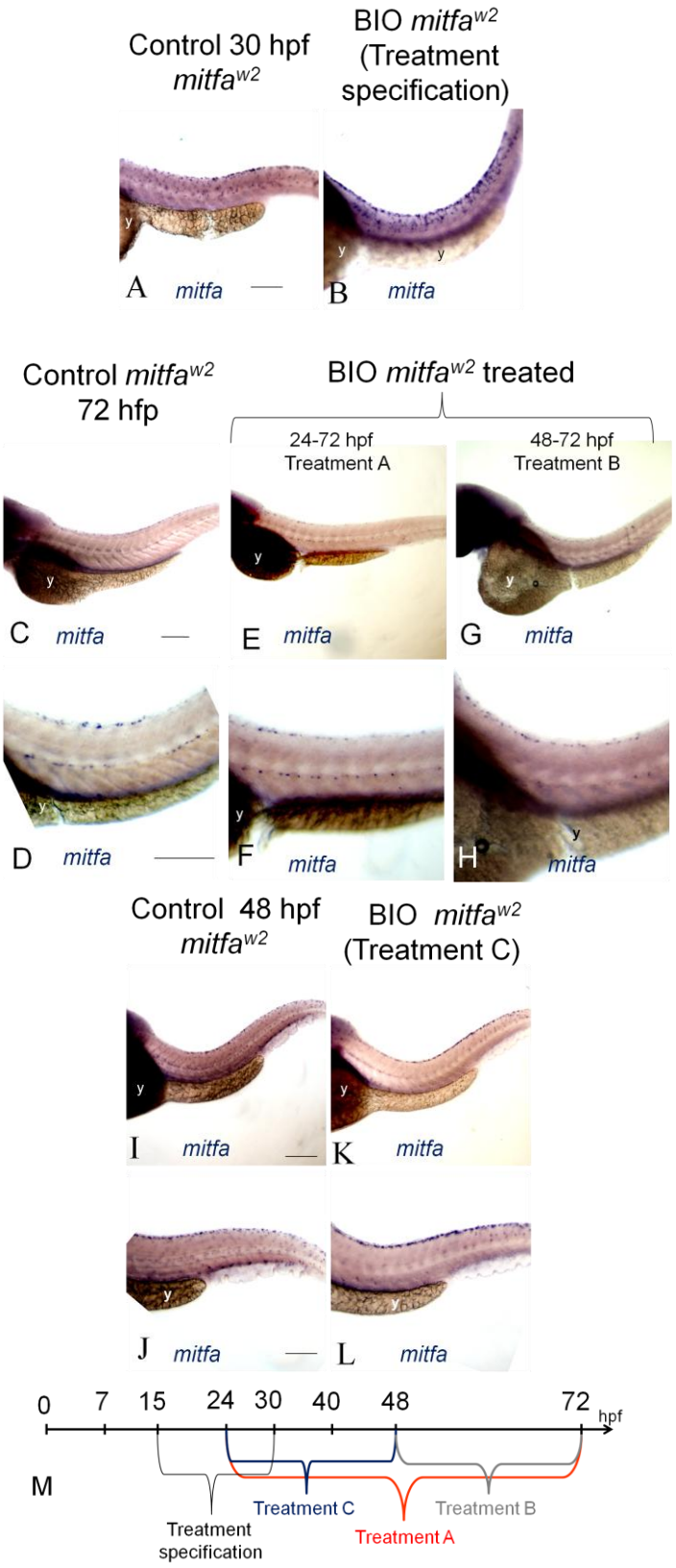

Figure 3.19: *mitfa* expression is not changed in *mitfa*^{w2} mutant embryos treated with BIO treated during melanocyte differentiation. See legend on the next page.

Figure 3.19: *mitfa* expression is not changed in BIO treated *mitfa*^{w2} mutant embryos during melanocyte differentiation.

WISH testing *mitfa* expression in *mitfa*^{w2} mutant fish showing. Lateral views of the trunk for the representative phenotype, for each condition (A-L), at 30 hpf (A,B), 72 hpf (C-H) and 48 hpf (I-L). 15-30 hpf *mitfa*^{w2} mutant BIO treated embryo (B) showed an increased *mitfa* expression compared to *mitfa*^{w2} mutant DMSO treated embryo (A). 24-72 hpf (E,F) and 48-72 hpf (G,H) *mitfa*^{w2} mutant BIO treated embryo did not show difference of *mitfa* expression compared to control *mitfa*^{w2} mutant DMSO treated embryos (C,D). 24-48 hpf *mitfa*^{w2} mutant BIO treated embryo (K, L) did not show difference with *mitfa*^{w2} mutant control DMSO treated embryo (I,J). 40 zebrafish embryos were investigated for each condition. y: yolk sac. Scale bar: 100 µm. (M) Diagram showing the time period for each treatment.

3.2.10 BIO treatments could activate *mitfa* expression in WT embryos but did not influence *sox10* expression

In the modelling, the hypothesis of the activation of *mitfa* expression by Factor Y, was mathematically defined as a *sox10* independent process. Consequently, the activation of Factor Y should not cause activation of *sox10* expression. This is important to verify that the activation of *mitfa* expression, observed when treating embryos with BIO, was not an indirect effect of increased *sox10* expression. Therefore, the next experiment aimed at investigating whether BIO treatment caused increased *sox10* expression.

sox10 expression was investigated by WISH in both control and BIO treated embryos after treatments A,B and C (Figure 3.20), to test the effects of Wnt signalling on activating *sox10* expression (Figure 3.20). The results showed that *sox10* expression was not affected by BIO treatments as no differences were observed between the treated and the control embryos. At 30 hpf, *sox10* was expressed in the otic vesicle, in the cranial ganglia (Figure 3.20, A,D) and dorsally and laterally in NC pre-migratory cells of the trunk (Figure 3.20, B,E,C.F). At 48 hpf and at 72 hpf, *sox10* expression was observed in the otic vesicle and dorsally and laterally in Dorsal Root Ganglia (DRG)s and glial cells (Figure 3.20). No differences were observed for the expression of *sox10* between the control and the treated conditions. This suggested that the Wnt signalling dependent increase of *mitfa* expression was independent of Sox10 and therefore, could play a role in *in vivo* melanocyte differentiation.

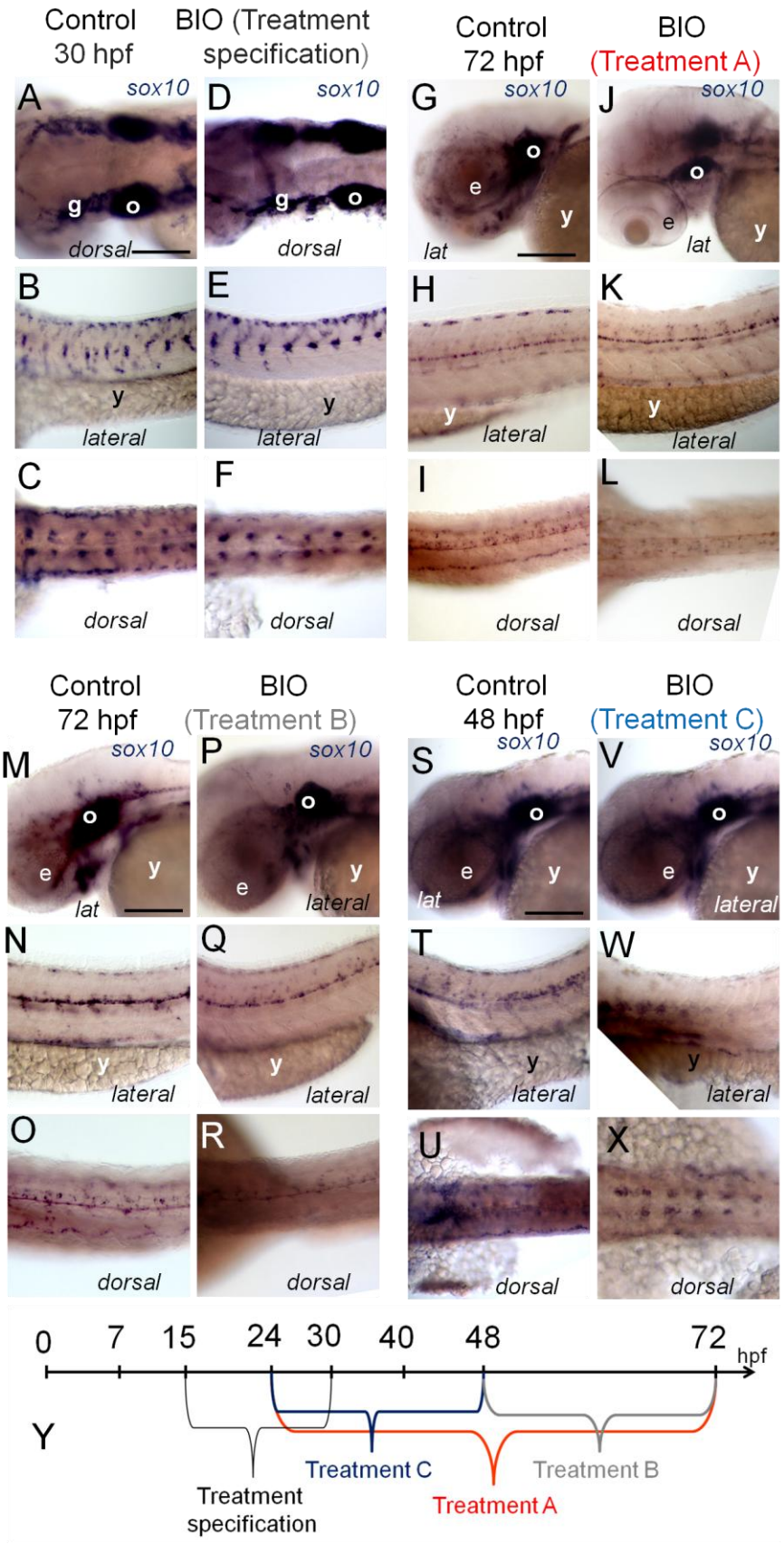

Figure 3.20: BIO treatments have no effects on *sox10* expression. See legend on the next page.

Figure 3.20: BIO treatments have no effect on *sox10* expression.

sox10 expression was investigated by WISH after treatments with BIO. The results showed no difference in the *sox10* expression between the control DMSO treated embryos and the BIO treated embryos. *sox10* expression is shown in the head of the embryos, (A,D,G,J,M,P,S,V) in dorsal view, but also in the trunk of embryos, (B,E,H,K,N,Q,T,W) in lateral view *(lat*), as well as, in the anterior trunk (C,F,I,L,O,R,U,V). The DMSO treated embryos treated for different periods are shown as following: 15-30 hpf (A-B) , 24-72 hpf (G-I), 48-72 hpf (M-O), 24-48 hpf (S-U), and BIO (5 µM) treated embryos are shown as following: 15-30 hpf treatment (D-F), 24-72 hpf treatment (J-L), 48-72 hpf treatment (P-R), 24-48 hpf treatment (V-X). e: eye; y: yolk sac; o: otic vesicle; g:cranial ganglia. 40 zebrafish embryos were investigated for each condition, a representative phenotype for each batch is presented here. Scale bar: 100 µm. (Y) treatment corresponding to 24-72 hpf (treatment A), 48-72 hpf (treatment B), treatment 24-48 hpf (treatment C).

3.2.11 Treating embryos with LiCl during melanocyte differentiation had contrasting effects

When testing LiCl treatment effects during melanocyte specification, we found that in contrast to the effects observed with the BIO treatments, LiCl treatments did not affect melanocyte development. Specifically, the treatments did not boost Wnt signalling nor *mitfa* expression (at 30 hpf) in melanocytes and there was no increase of the melanocyte number during melanocyte specification. Instead, GFP expression in the TOP;dGFP reporter was boosted in other cell types which could be xanthoblasts. Xanthophore pigmentation was also increased. Here we present the contrasting effects of LiCl in melanocyte differentiation.

Treating embryos from 48-72 hpf and 24-72 hpf triggered a disruption of cell organisation (Figure 3.21). The causes of disruption to cell organisation with LiCl were not directly investigated and it was not tested if it could be related to the loss of organisation observed with BIO treatments. Melanocyte number was increased when treating embryos from 24 to 48 hpf (Figure 3.22, (B-C)), (control, 21.5 ± 2.01, LiCl 28.5 ± 5.09, p = 0.0014), however, the cell dendricity at 48 hpf was not changed (data not shown).

mitfa expression was investigated using RT-qPCR in embryos treated with LiCl during melanocyte specification (Figure 3.23). The t-test was used to test for a difference in the mean relative expression levels of each condition (mean relative expression level ± s.d). After the 24-72 hpf LiCl treatment, *mitfa* expression increased to 260 ± 65.4, (p= 0.0076), whereas the 48-72 hpf LiCl treatment did not cause a significant change in *mitfa* expression level, 157 ± 80.7, (p=0.162). Finally after the 24-72 hpf treatments, *mitfa* expression was increased to 987 ± 308, (p=0.00035). This experiment showed a two and a half times increase of *mitfa* expression from 24 hpf to 48 hpf, and approximately a nine times increase from 24 hpf to 72 hpf treatments. However, treatment from 48 hpf to 72 hpf did not result in a significant increase of *mitfa* expression (Figure 3.23). In general, the effects with LiCl and BIO were difficult to compare and therefore must be interpreted with caution and in the context of understanding the activity of molecules within cells, as discussed later.

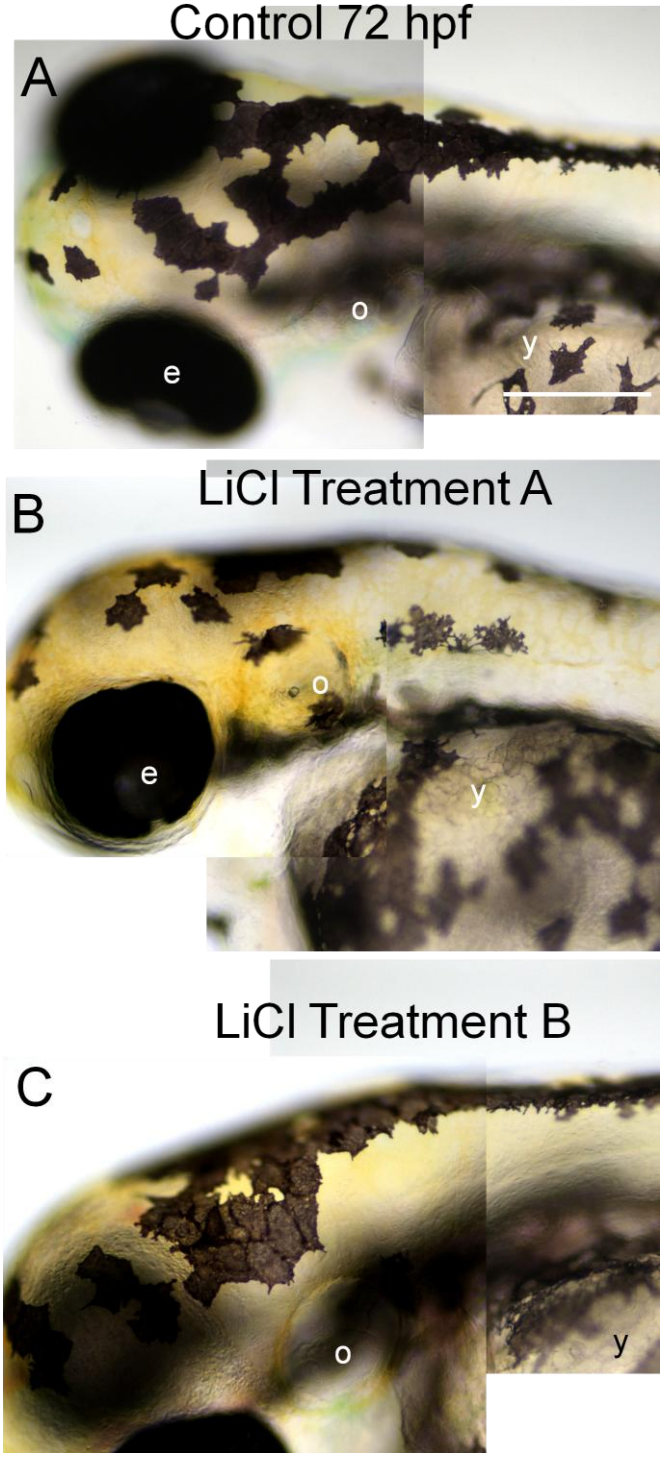

Figure 3.21: LiCl treatments (24-72 hpf) (48-72 hpf) disrupt cell organisation pattern. See legend on the next page.

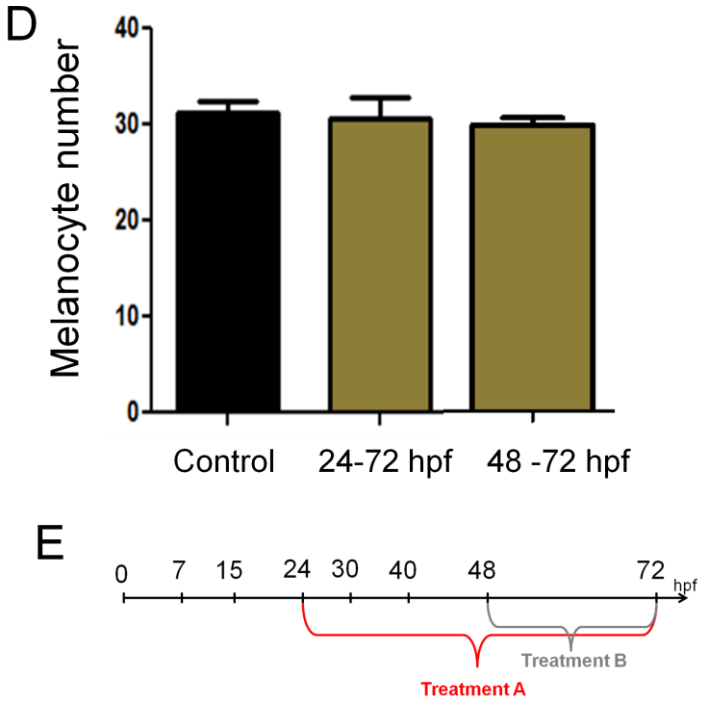

Figure 3.21: LiCl treatments (24-72 hpf) (48-72 hpf) disrupt cell organisation pattern

The head of a representative live embryo is shown in dorsolateral view (A-C). Melanocyte numbers were counted from the anterior brain to the optic vesicle in 20 embryos for each condition, and the t-test showed that no significant changes could be observed after the treatments. Compared to the DMSO control embryo (A), embryos treated with LiCl from 24-72 hpf, or from 48-72 hpf, show no significant increase in the melanocyte number ($p=0.08$) (B), (C) ($p=0.41$) in (D). In (B) and (C) cell organisation was disrupted. 160 zebrafish embryos were observed for each condition at 72 hpf. (E) Diagram of treatment periods. Scale bar: 100 µm. e: eye; y: yolk sac; o: otic vesicle.

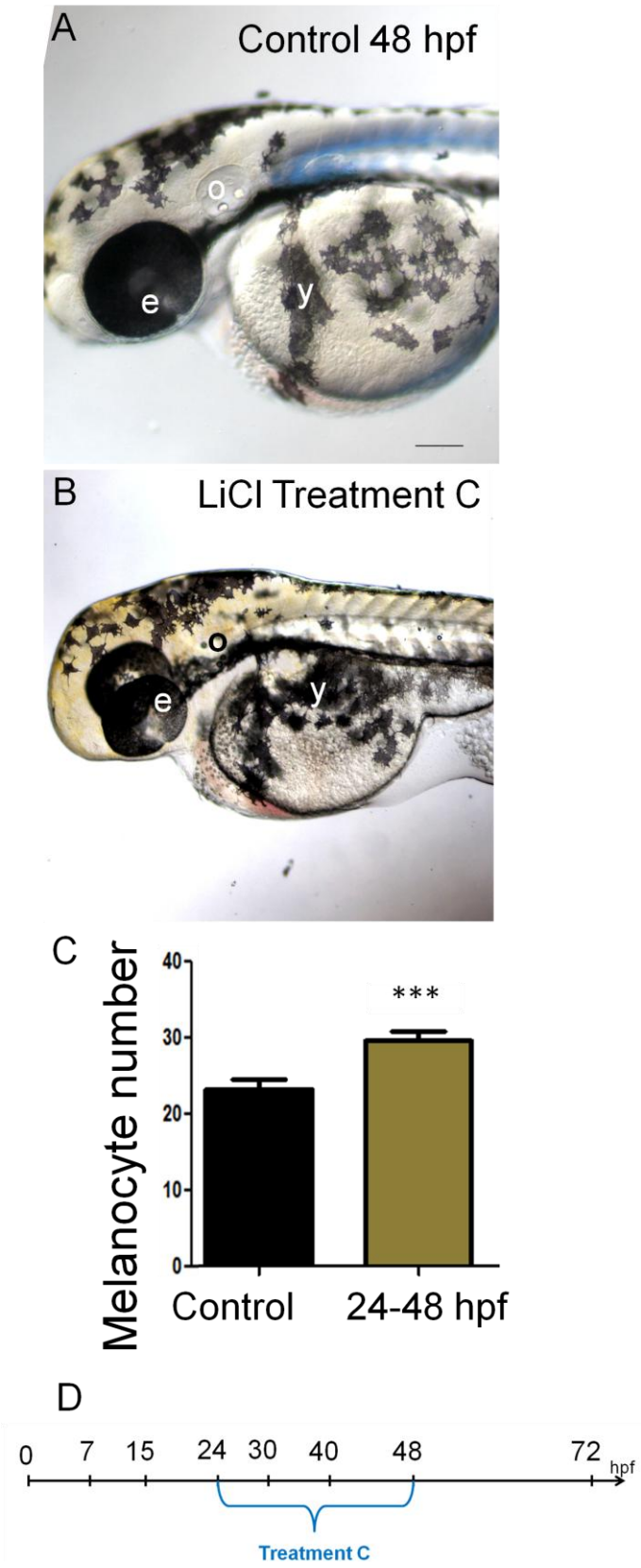

Figure 3.22: LiCl treatment (24-48 hpf) causes increased melanocyte number. See legend on the next page

Figure 3.22: **LiCl treatment (24-48 hpf) causes increased melanocyte number**

Embryos are shown in a dorsolateral view (A-B). DMSO treated control embryos (A), embryo treated with LiCl from 24-48 hpf (B) show significant increase in melanocyte number (p=0.0014) (t-test, 20 embryos were analysed for each condition, n=20), 160 live zebrafish embryos were observed at 48 hpf for each condition and 20 embryos were randomly chosen for counts. e: eye; y: yolk sac; o: otic vesicle. (C). Scale bar: 100 µm. (D) Diagram of treatment period.

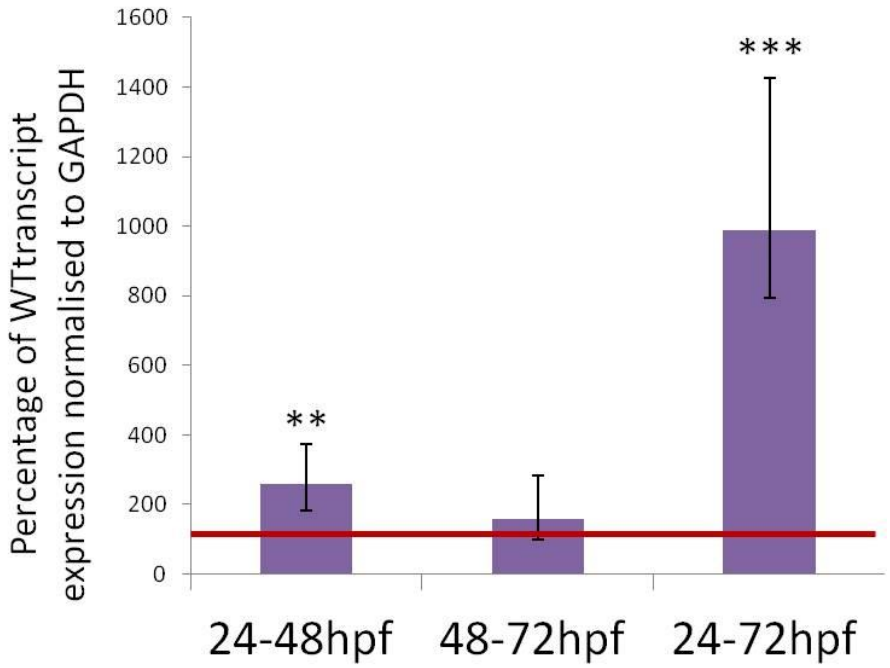

Figure 3.23: LiCl (200 mM) treatments (24-48 hpf and 24-72 hpf) result in a significant increase in *mitfa* expression in zebrafish embryos.

Experiments of RT-qPCR testing *mitfa* expression level in WT and LiCl treated embryos (WT *mitfa* level = 100 % transcripts (red line on graph)). *mitfa* expression was investigated in 10 samples of 50 pooled embryos for each condition, in triplicates. Expression levels were normalised to *gapdh* expression. A t-test was performed: after 24-72 hpf LiCl treatment, *mitfa* expression was significantly increased p= 0.0076, whereas 48-72 hpf LiCl treatment did not cause significant change in *mitfa* expression level, p=0.162. Finally after 24-72 hpf treatments, *mitfa* expression was significantly increased p=0.00035. p-value <0.01 (**) and p-value <0.001 (***).

3.2.12 Xanthophore pigmentation is increased in embryos treated with LiCl

While having contrasting effects in melanocytes compared to BIO, LiCl treatments showed consistent activation of xanthophore pigmentation. Furthermore, increased GFP expression was observed in xanthoblasts in TOP;dGFP embryos treated with LiCl from 15 to 40 hpf (see Figure 3.08, (C)). Here, we show that yellow pigmentation at 48 hpf and 72 hpf was dramatically boosted after LiCl treatments (Figure 3.24). Figure 3.24 shows embryos treated with PTU and LiCl from 24-48 hpf. The increased yellow pigmentation is clearly observable in the dorsal head and the lateral and dorsal trunk when compared to control embryos.

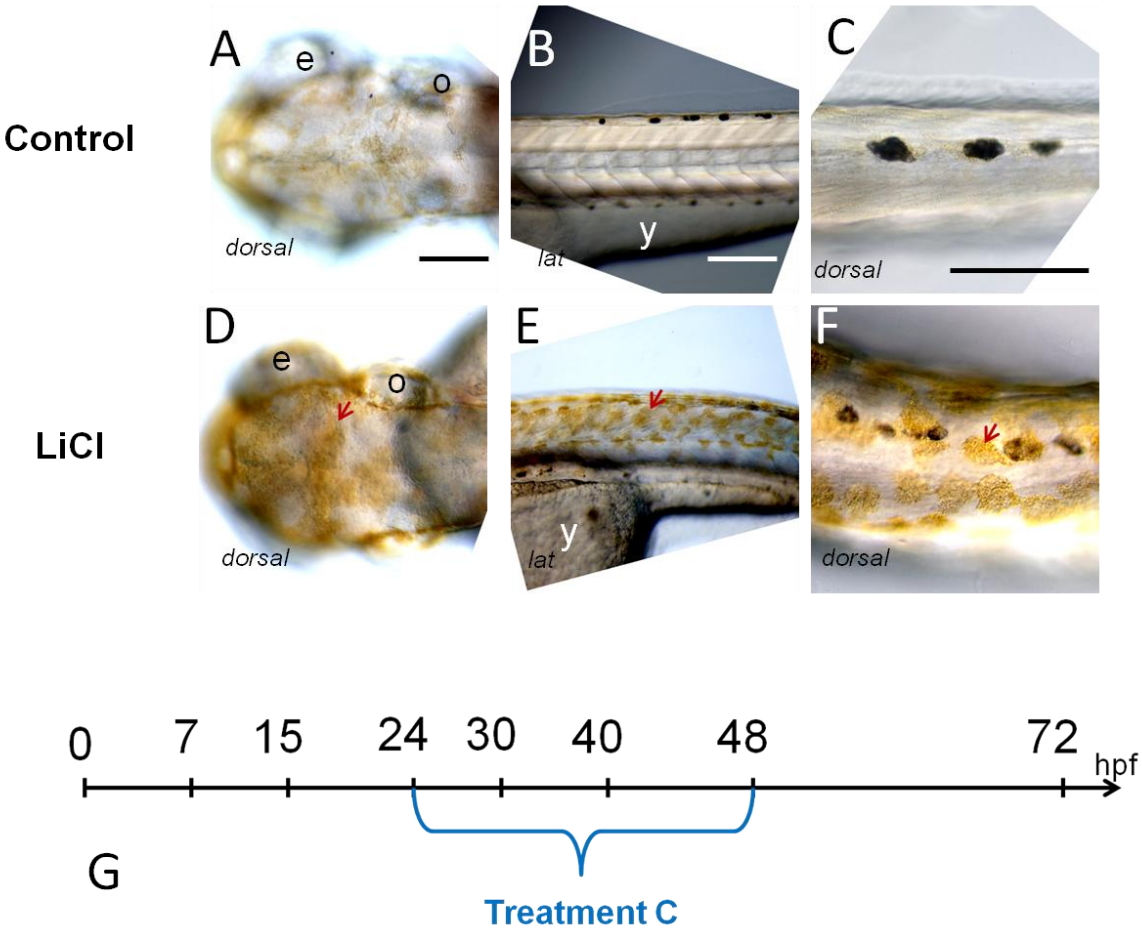

Figure 3.24: LiCl treatment (24-48 hpf) leads to increased xanthophore pigmentation.

48 hpf control DMSO treated zebrafish (A-C), and 48 hpf BIO treated zebrafish fish (D-F), after 24-48 hpf treament. All embryos were treated with PTU to block melanin synthesis. In (D-F), the red arrowheads show the increased xanthophore pigmentation. (A-D) show embryo heads in dorsal view (*dorsal*), (B-E) show embryo trunks in lateral view (*lat*) and (C-F) show a close up on embryo trunks in dorsal view (dark cells are iridophores). 160 embryos were observed for each condition and the representative embryos are shown here. e: eye; y: yolk sac; o: otic vesicle. Scale bar: 100 µm. (G) Diagram showing the time period for the treatment.

3.2.13 LiCl treatments might trigger increased xanthophore differentiation

The embryos were treated with LiCl during two time periods to determine whether the boost of xanthophore pigmentation resulted from either increased cell specification or increased cell differentiation. From15-30 hpf, the treatment covered the specification phase as xanthophore specification was suggested to occur between 18-25 hpf, and from 24-48 hpf it covered cell differentiation phase (Figures 3.25-3.26) (Parichy *et al.*, 2000b). After treatments, embryos were examined for the expression of an early xanthoblast/xanthophore marker, *xdh*. The 15-30 hpf treatment did not trigger an unequivocal increase of *xdh* expression (Figure 3.25). Comparing *xdh* expression in the lateral trunk, it seemed that cell migration could be affected by the treatments (Figure 3.25, B-E). Only the 24-48 hpf treated fish showed a clear increase in *xdh* expression in the tail (Figure 3.26). However, as it was not investigated whether the expression level was activated in each cell in the tail compared to control, or if the number of developing cells in the tail was increased, we could not distinguish between differentiation or specification defect.

This experiment was repeated with BIO in order to test whether BIO could activate xanthophore specification and differentiation. The results of the WISH showed no differences between DMSO treated embryos and BIO treated embryos for *xdh* expression after treatments (data not shown).

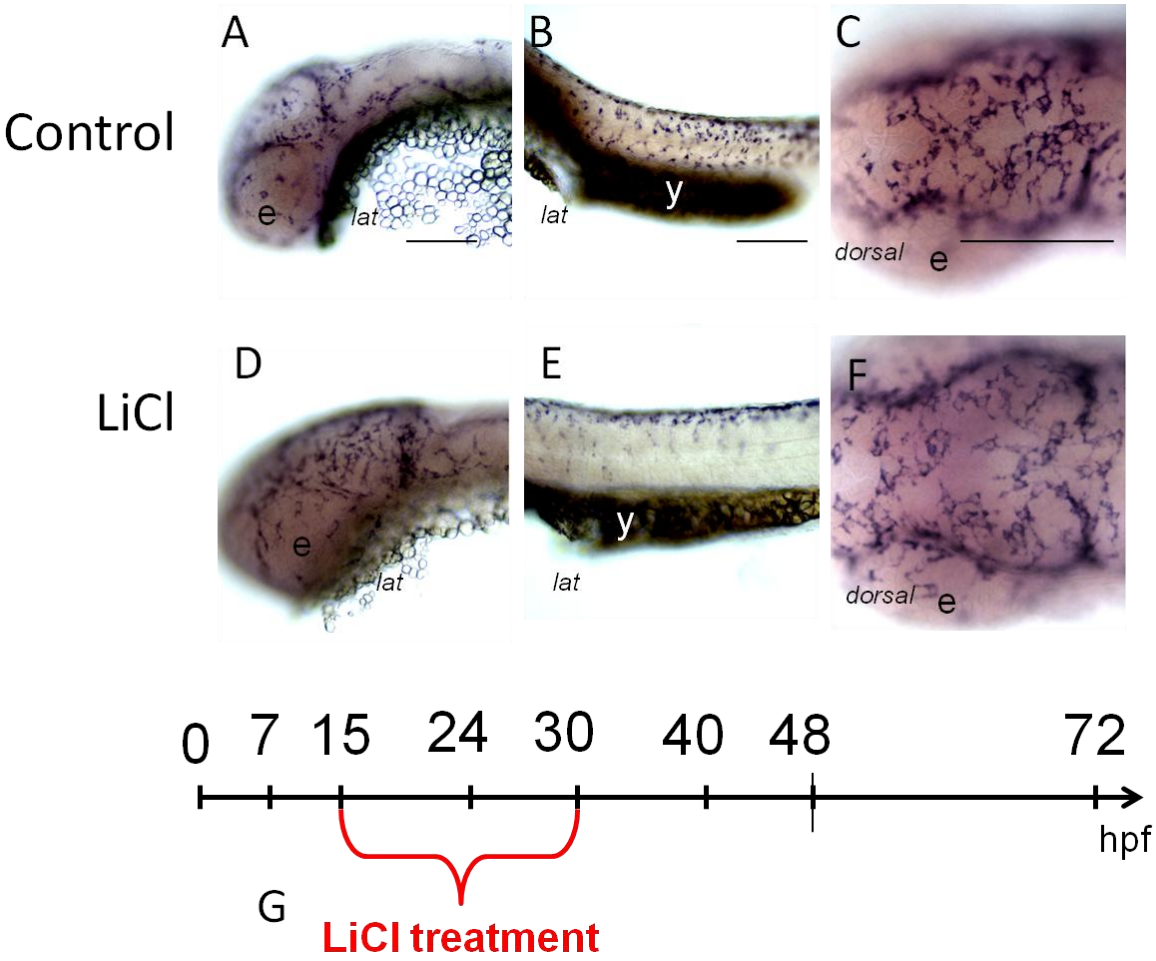

Figure 3.25: LiCl treatment (15-30 hpf) did not boost *xdh* expression.

80 zebrafish embryos were investigated by WISH and observed for expression of *xdh*. Representative embryos are shown, DMSO control embryo at 30 hpf (A-C) and embryo treated with LiCl, from 15 to 30 hpf, which covered the xanthophore specification phase (18-25 hpf) (D-F). (A,D) lateral view of head, (B,E) lateral view (*lat*) of trunk, (C,F) dorsal view (*dorsal*) of head. e: eye; y: yolk sac. Scale bar: 100 µm. (G) Diagram showing the time period for the treatment.

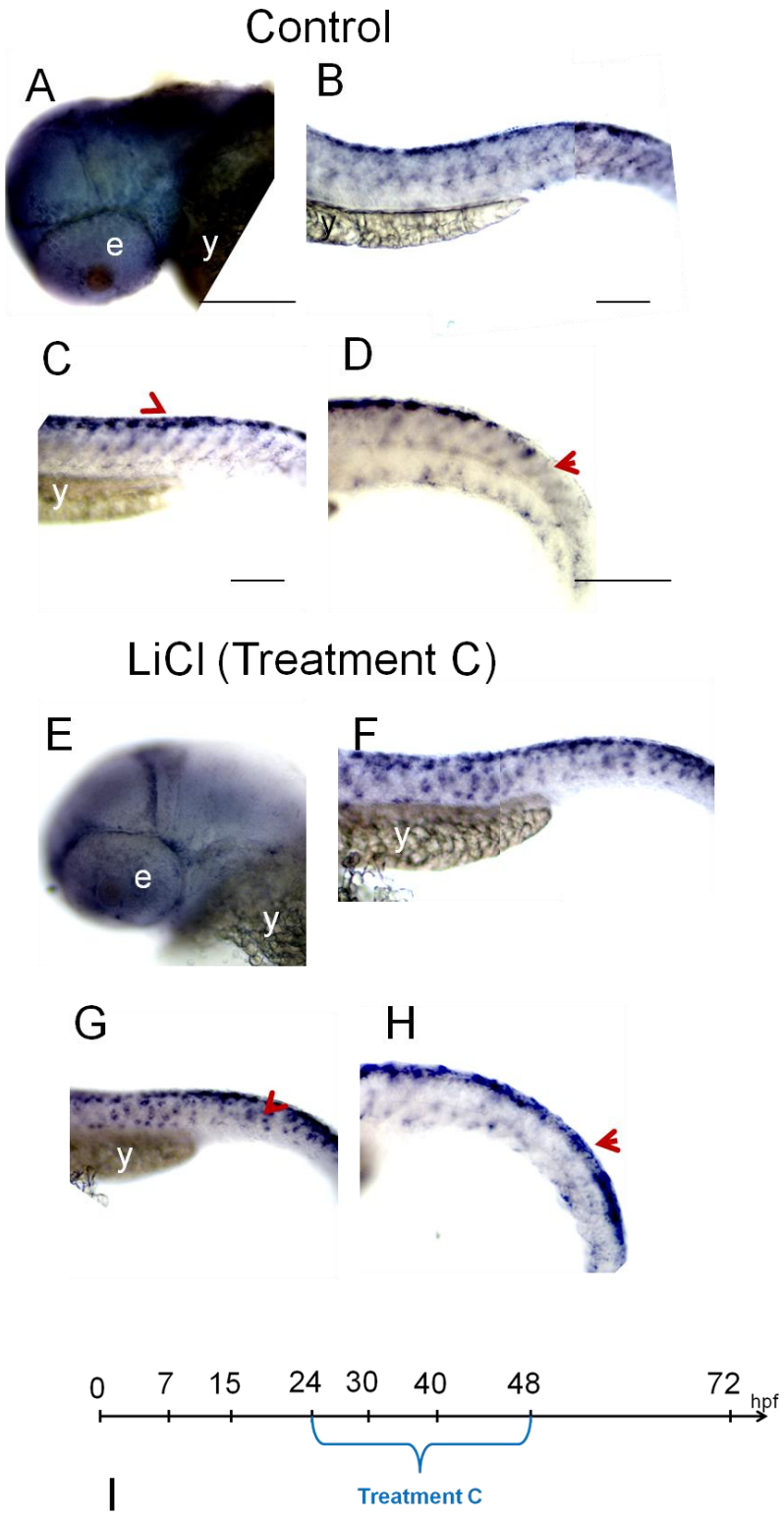

Figure 3.26: LiCl treatment (24-48 hpf) lead to increase *xdh* expression in tail. See legend on the next page.

Figure 3.26: LiCl treatment (24-48 hpf) lead to increase *xdh* expression in tail.

80 zebrafish embryos were investigated by WISH and observed for expression of *xdh* for each condition. Representative embryos are shown here. Control DMSO treated fish (A,-D), LiCl treated embryo (E-H). Lateral trunks are shown in (B, C, F, G, red arrows show blue signal). Lateral view of the tails are shown in (D-H, red arrowhead in (H) shows continuity of expression in tail compare to (D) where red arrowhead shows faint expression in tail). Heads in dorsolateral view are shown in (A-E). Scale bar: 100 µm. (I) Diagram showing the time period for the treatment.

3.2.14 Xanthophore development is affected by LiCl at late stages

To determine whether LiCl treatments covering the xanthophore specification phase from 15-30 hpf could cause an increase in xanthophore pigmentation at 48 hpf and 72 hpf, the same experimental set up ("medium" and "treatment" batches) was used as described for the BIO treatments in section 3.2.5 (see diagram in Figure 3.27,(P)). In short, TOP;dGFP embryos were treated from 15-30 hpf and were divided into "medium" and "treatment" batches at 30 hpf. In the "medium" batch, embryos were rinsed, whereas, in the "treatment" batch, embryos were maintained in LiCl treatment until 48 hpf and 72 hpf. Embryos were then incubated at 27 °C until 48 hpf and 72 hpf, the results are presented in Figure 3.27.

The boost of pigmentation in xanthophores was not observed at 48 hpf nor at 72 hpf in the "medium" batches (Figure 3.27). In contrast, a clear increase of yellow xanthophore pigmentation as well as an increase of dGFP was observed in these cells both after 15-48 hpf and 15-72 hpf in the "treatment" batches (Figure 3.27). This phenotype corresponded to the phenotype observed previously when treating embryos from 24-48 hpf (section 3.2.13). This suggested that LiCl treatment throughout a minimal period between 24-30 hpf was crucial for elevated xanthophore pigmentation (Figure 3.27).

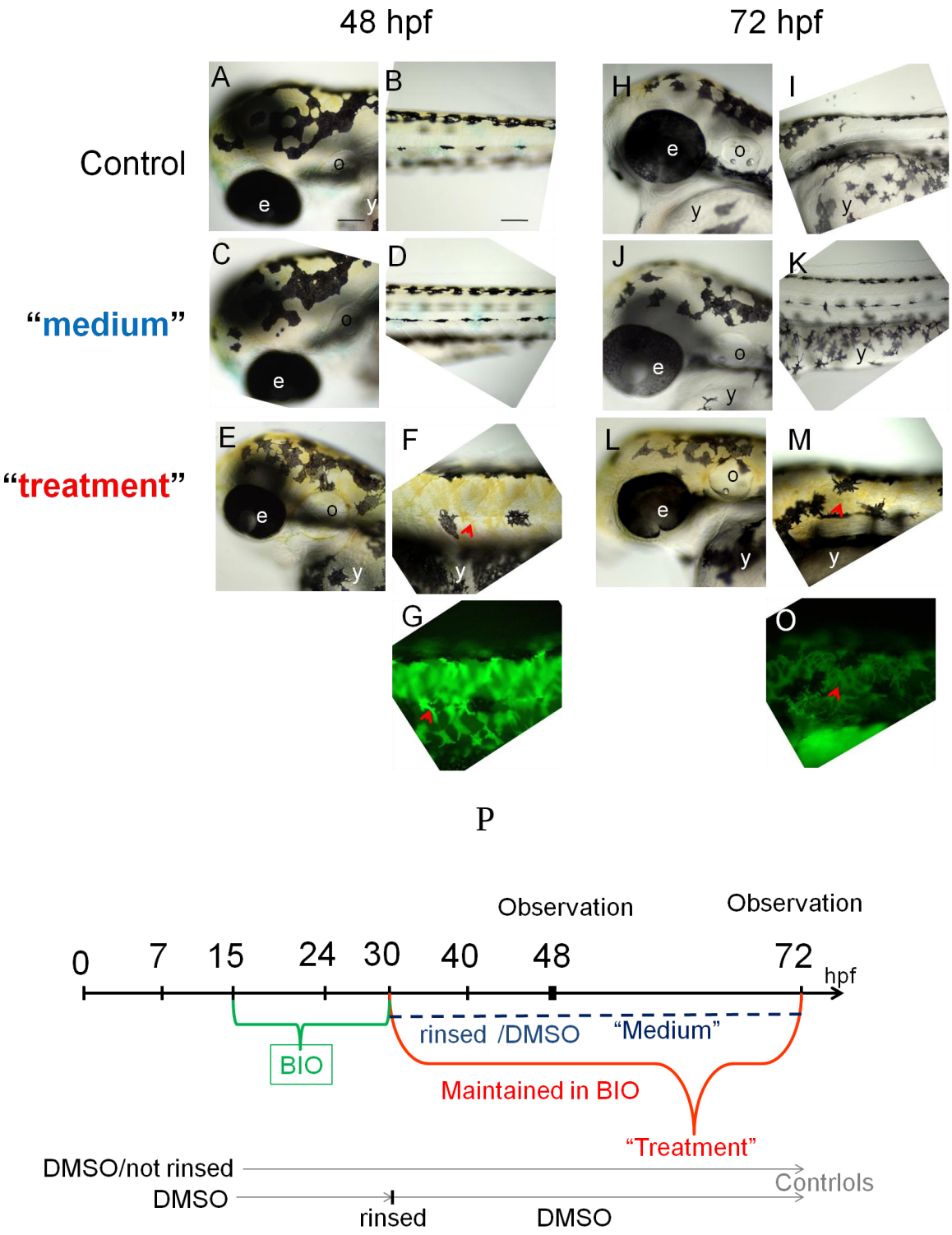

Figure 3.27: LiCl treatment in TOP;dGFP fish. See legend on the next page.

Figure 3.27: LiCl treatment in TOP;dGFP fish.

Embryos were treated from 15-30 hpf, half were rinsed ("medium") (C,D,J,K) and then observed at 48 hpf (C,D) and 72 hpf (J,K). The rest were maintained in LiCl treatment "treatment") (E,F,L,M,G,O) and observed at 48 hpf (E,F,G) and 72 hpf (L,M,O). Heads are shown in a dorsolateral view in (A,C,E,H,J,L) and trunks are shown in lateral view in (B,D,F,G,I,K,M,O). Both at 48 hpf and 72 hpf, the "medium" batches did not show changes of xanthophore pigmentation compared to control at 48 hpf (A,B), and 72 hpf (H,I) respectively. However, both "treatment" batches showed increased xanthophore pigmentation compare to control embryos. Arrowheads in (F-M) point at increased xanthophores, as do arrowheads shown in the trunk, where these cells also showed increased dGFP (arrows in (G-O) respectively). 80 TOP;dGFP transgenic zebrafish embryos were observed for each condition and the phenotype was consistenly observed in treated embryos. e: eye; y: yolk sac; o: otic vesicle. Scale bar: 100um. (P) Diagram showing the differences between "treatment" and "medium" batches. The "medium" batch was only treated with BIO from 15 to 30 hpf and then rinsed and placed in DMSO/embryo medium and observed at 48 hpf and 72 hpf, whereas, the "treatment" batch was always maintained in BIO treatment until observation. DMSO treated controls were also divided into two batches. One was rinsed and placed in new DMSO/medium solution. The other was left in the same DMSO/medium solution, however, only one control fish is presented here as no differences could be seen between these DMSO controls.

3.2.15 Summarising the effects of LiCl and BIO treatments on melanocytes and xanthophore development

Figure 3.28 and Table 3.01 summarise the effects of BIO and LiCl in embryos. BIO treatment during the times of melanocyte differentiation led to increased *mitfa* expression in embryos. *mitfa* was strictly expressed in melanocytes after 30 hpf, therefore, this result suggested that *mitfa* was increased in melanocytes. Knowing that BIO treatment could activate Wnt signalling in melanocytes, this result was consistent with the model predictions. No boost of *mitfa* expression was observed in *mitfa*^{w2} mutant treated embryos suggesting that activation of *mitfa* by BIO was *mitfa* dependent. The BIO treatment did not cause elevation of *sox10* expression, therefore, inhibition of Gsk3β seemed to activate *mitfa* expression in a *sox10*-independent manner, as predicted for Factor Y. It remains to be tested if the activation of Wnt signalling, or another effect depending on Gsk3β inhibition, was the cause of this phenotype.

To summarise the effects of LiCl on melanocyte differentiation, elevated cell numbers were observed in the 24-48 hpf treatments. Interestingly, this could be correlated with melanocyte number increase after the 24-48 hpf treatment. This result is unlikely to be the consequence of increased melanocyte specification as the experiments testing the activation of Wnt signalling in melanocyte with LiCl showed that the molecule failed to activate the pathway. However, it was possible that due to the differences of molecule activities, LiCl could be boosting cell proliferation from 24-30 hpf.

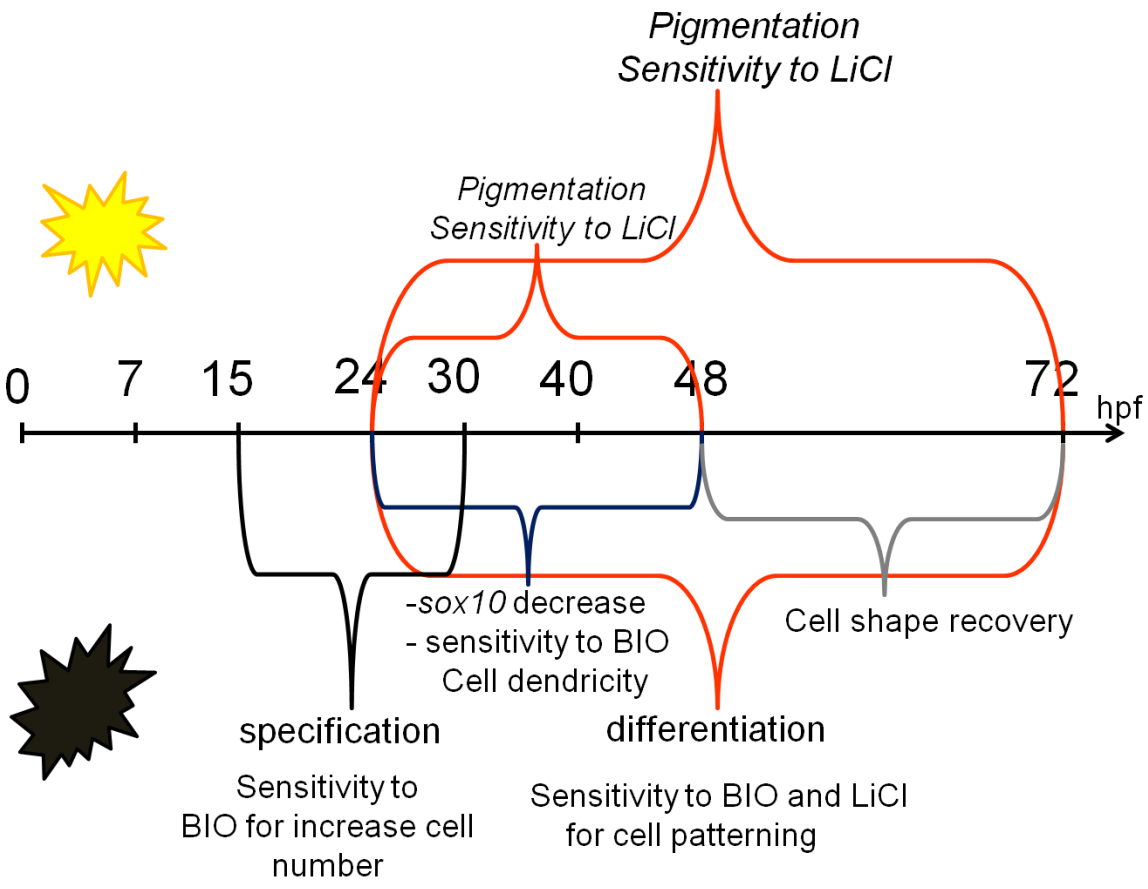

Figure 3.28: Scheme summarising the effects of BIO and LiCl treatments on melanocytes and xanthophores.

Treating zebrafish embryos from 15-30 hpf leads to increased melanocyte specification. Treatment from 24-48 hpf affects melanocyte shape and treatments from 24-72 hpf and 48-72 hpf lead to disorganisation of cells in head. LiCl specifically boosts xanthophore pigmentation from 24/30-48 hpf and increase pigmentation was also observed after 24-72 hpf treatment.

Table 3.01: Summarising the effects of LiCl on melanocyte and xanthophore, and the effects of BIO on melanocytes.

	LiCl	BIO
7 – 72 hpf LONG TERM	Loss of eyes Shift of the midbrain/hindbrain boundary Reduced head size Increase melanocyte number	Loss of eyes Shift midbrain/hindbrain boundary Reduced head size Increase melanocyte number
15 – 30 hpf SPECIFICATION	NO increase of the melanocyte number NO boost of the *mitfa* expression (WISH) NO boost of the *xdh* expression (WISH)	Increase melanocyte number Boost of the *mitfa* expression (WISH) NO boost of the *xdh* expression (WISH)
15 – 40 hpf	No colocalisation and no activation of Wnt signalling in melanocytes Boost of Wnt signalling in other cells (xanthoblasts) Slight increase of Wnt signalling in the tectum of embryos	Colocalisation and potential activation of Wnt signalling in melanocytes (not quantified) No boost of Wnt signalling in other cells Dramatic increase of Wnt signalling in the tectum
24 – 72 hpf DIFFERENTIATION	Loss of the melanocyte organisation pattern Boost of the *mitfa* expression (RT-qPCR) NO boost of the *xdh* expression (WISH) Boost of xanthophore pigmentation	Loss of the melanocyte organisation pattern Boost of the *mitfa* expression (RT-qPCR) NO boost of the *xdh* expression (WISH) No boost of xanthophore pigmentation
24 – 48 hpf EARLY DIFFERENTIATION	Increase melanocyte number Increase xanthophore pigmentation Boost *mitfa* expression (RT-qPCR) Boost of the *xdh* expression (WISH)	Increase melanocyte dendricity No increase xanthophore pigmentation Boost of the *mitfa* expression (RT-qPCR) No boost of the *xdh* expression (WISH)
48 – 72 hpf LATE DIFFERENTIATION	Loss of the melanocyte organisation pattern NO Boost of the *mitfa* expression (RT-qPCR) NO boost of the *xdh* expression (WISH)	Loss of the melanocyte organisation pattern Boost of the *mitfa* expression (RT-qPCR)

3.3 Discussion

Our results showed that with BIO, but not LiCl, we could: 1) dramatically activate Wnt signalling in the tectum of embryos; 2) observe colocalisation of Wnt signalling activation in melanocytes; 3) measure increase number of melanocytes at early stages. In contrast, treatment with LiCl showed: 1) light activation of Wnt signalling in the tectum; 2) activation of Wnt signalling in cells that are likely to be xanthoblast (shape, position), 3) increase xanthophore pigmentation. Furthermore, activation of *mitfa* expression was consistently oobserved with BIO treatments using WISH and qPCR whereas, it could only be observed once with LiCl treatments. BIO is a well described inhibitor a GSK3β. Even if we could not measure Wnt signalling activation in single melanocytes after BIO treatments, our data suggest that we could activate Wnt signalling in the tectum and that Wnt signalling was activated in melanocytes, suggesting or bringing a new arguments for suggesting that Wnt signalling was activated in melanocytes after BIO treatments. However, activation of the Wnt pathway in BIO treated melanocytes should be quantified. Our results suggest that boosting β-catenin in melanocytes caused changes in cell shape. It still needs to be determined whether this was due to the role of β-catenin in cell adhesion or indirectly to its transcriptional role which has allowed activation of *mitfa* which in turn can regulate cell shape. The cell organisation disruption could also be related to the role of β-catenin in cell adhesion. Our results suggest that the increase xanthophore pigmentation observed with LiCl treatments is unlikely to be Wnt signalling dependent as it was not observed with BIO. Consequently, an off target effect of LiCl, which remains to be determined, could be responsible for this phenotype.

3.3.1 Discussing the efficacy of the experimental set up to improve the targeting of the canonical Wnt signalling pathway in the future

It is important to ask to what extent Wnt signalling was crucial *in vivo* in melanocytes and to what extent ours results support or reject the hypothesis of the existence of Factor Y. To confirm that the effects of cell organisational and shape changes were dependent on Wnt signalling, it would be necessary to address four potential limitations of the experimental methods. These four fundamental points could be investigated to clarify the effects of the small molecule treatments and the role of Wnt signalling in melanocyte development. These points are summarised here and in the Figure 3.29. The following should be investigated:

1- The inactivation of GSK3β caused by BIO and perhaps LiCl in cells in zebrafish.

2- Activation of the p38-MAPK pathway by the treatment.

3- The increase of free β-catenin in the cytoplasm as a result of the treatments and its consequences on the cell adhesion complex.

4- The increase translocation of β-catenin to the nucleus in melanocytes.

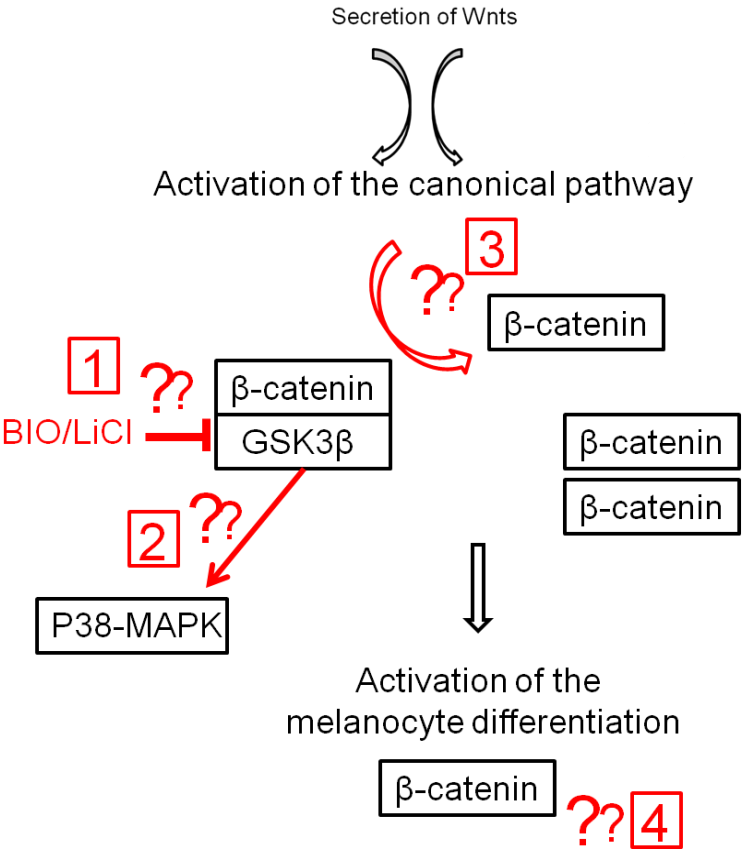

Figure 3.29: Four points need to be investigated to validate the method used in these experiments to activate Wnt signalling in melanocytes in zebrafish.

Controlling the validity of these experiments will first require the assessment of whether or not the small molecules (BIO and LiCl) were significantly inhibiting GSK3β activity (1). Secondly, we should test whether the p38-MAPK pathway was also activated by the treatments (2). Thirdly, whether the level of free β-catenin was significantly increased after treatments (3) and finally whether this also triggered increased translocation of β-catenin to the nucleus (4).

3.3.2 The efficacy of GSK3β inhibition triggered by BIO and LiCl was not assessed in cells.

In these experiments we investigated the activation of the TOP;dGFP reporter in melanocytes of embryos treated with the small molecules. The intensity of the GFP in single melanocytes seemed increased but this could not be quantified at our resolution. This would have to be further quantified in single cells by investigating dGFP expression, in cells or in fish, with more resolution than here. However, the boost of GFP in the tectum of BIO treated fish was clearly observable. Consequently, both the colocalisation of the Wnt signalling and the boost of the signal in fish after BIO treatments suggested that, in contrast with LiCl, BIO could efficiently inactivate GSK3β in cells. BIO stabilized all forms of β-catenin (phosphorylated or not) and indirectly increased the level of the Ser 675- β-catenin form causing the activation of both the canonical Wnt pathway and the β-catenin/Cadherin pathway involved in cell-cell adhesion (Sineva and Pospelov, 2010, Tseng *et al.*, 2006). The increase of free β-catenin levels in cells has been observed in studies using BIO suggesting that BIO treatments could activate Wnt signalling, consistent with our results (Sineva and Pospelov, 2010, Sato *et al.*, 2001, Tseng *et al.*, 2006).

LiCl is described as a direct and an indirect inhibitor, of GSK3α/β. In direct inhibition, lithium impedes enzymatic activation of GSK3β by competing with another ion, Mg^{2+}, which is required at the cation binding site of the GSK3β enzyme. The indirect inhibition of GSK3β by LiCl could be due to the activation of the protein kinase B (AKT/PKB) which would allow the phosphorylation of the single serine residues (serine-21 for GSK3α; serine-9 for GSK3β) of the regulatory aminoterminal domain. However, LiCl is also described as an inhibitor of other pathways. Interestingly, Jin and Thibaudeau (1999) used LiCl in zebrafish as an inhibitor of the IP-signalling pathway. Jin and Thibaudeau (1999) treated zebrafish embryos from 24 hpf to 6 dpf at a concentration of 50 mM LiCl and they did not note any increase in melanocyte number. However, a weak increase in melanin production could be measured after the 5 days treatment. In our study, we did not observe increased melanisation, however, we treated embryos for shorter periods which might not have been sufficient to trigger this change. The embryos shown in Jin and Thibaudeau (1999) after treatments seemed to show a melanocyte organisation defect as observed in our experiments, however, they did not discuss the significance of it. No xanthophore phenotype was discussed nor described. In their study, the five days long LiCl treatments led to accumulation of IP3 (inositol triphosphate). This inositol phosphate accumulation then caused stimulation of pigmentation in zebrafish embryos through the synthesis and the deposition of melanin within the melanocytes. Increased melanisation could be due to several changes, such as, stimulation of cell proliferation, stimulation of cell differentiation or dispersion of melanosomes throughout the cell, as well as, an activation of the synthesis and the deposition of melanin into melanosomes. The Jin and Thibaudeau (1999) study suggested that various signalling pathways were potentially affected directly or indirectly by lithium, including the IP3 pathway and/or GSK3s. An increase of melanin content and of Tyrosinase activity in LiCl treated embryos was also observed when embryos were treated in combination with a protein-kinase A (PKA) and C (PKC) inhibitor (forskolin). This suggested that the PKA/PKC pathway, the GSK3

pathway, and/or the IP3 pathway, could all work together for the regulation of melanin production. The Jin and Thibaudeau (1999) study showed that LiCl can interact with other pathways than the GSK3 pathway. Together with our results, it suggests that the LiCl dependent effects observed in our study were probably caused by the stimulation of a different factor/pathway other than the Wnt signalling pathway.

It would be interesting to assess the inhibition of GSK3β in cells. An *in vitro* GSK3β kinase assay could allow the quantification of the level of GSK3β activity (Zhang *et al.*, 2003). Testing the levels of substrate phosphorylation by Gsk3β would allow quantifying the ratio of activated /unactivated protein with or without treatment. Lastly, testing GSK3β phosporylation at the N-terminal, and at the serine 9, could also allow measuring GSK3β inhibition.

3.3.3 The role of the cAMP pathway activation as a side effect of GSK3β inhibition

GSK3β is a serine/threonine kinase which can target different factors of different pathways such as, Adenosine-Monophosphate (AMP) Response Element-Binding protein (CREB), the nuclear factor of activated T cells (Nfat) family in neurons, Mothers against decapentaplegic homolog 1 (SMAD1), and c-Jun13 and β-catenin, in different cell types (Sineva and Pospelov, 2010, Hur and Zhou, 2010). Previous studies have described the effects of inhibiting GSK3β with BIO in cardiomyocyte development. Because inhibition of p38-MAPK activity has been shown to promote mammalian cardiomyocyte proliferation, it was suggested that BIO could interact with it to regulate cardiomyocyte proliferation in culture (Tseng *et al.*, 2006). However, no direct inactivation of the p38-MAPK was detected after BIO treatments in cardiomyoctes in the study and the role of p38-MAPK is not clear.

Bellei *et al.*, (2010) described the effects of inhibition of the GSK3β by the cAMP pathway. Bellei *et al.*, (2010) used BIO (up to 24 hrs treatment, 1µM) and transient transfection to activate β-catenin activity in B-16 melanoma cells. They observed activation of most Wnt targets following inhibition of GSK3β activity, including Mitf. They also show that cAMP pathway dependent inhibition of GSK3β allowed free β-catenin to activate gene expression in the nucleus. They conclude that the cAMP pathway and β-catenin could work together to activate targets such as melanocytic genes. Whether or not the experiments presented in our study mimicked the effects of GSK3β inhibition by cAMP and/or activation of β-catenin by Wnt signalling has not been investigated. It will be important to test which of these pathways dominated the regulation of β-catenin for melanocyte development and if they could interact and compensate their effects. If the effects observed in our study were cAMP dependent or more widely GSK3β inhibition dependent, the mechanism and the hypothesis would have to be redefined to suggest that the cAMP pathway, or GSK3β, can influence certain aspects of melanocyte development. It will be important to determine if the canonical Wnt signalling pathway or the cAMP pathway (or both) were responsible for the phenotypes observed. If inhibition of Gsk3 had impacted on the cAMP pathway leading to either increased cell dendricity, loss of cell organisation or to activation of *mitfa* during melanocyte differentiation, then this study

would have to be re-interpreted as the investigation of the role of cAMP activation on melanocyte differentiation. Alternatively, if both the Wnt pathway and the cAMP pathway were activated, then this study would also need re-interpretation as the role of Gsk3 in regulating melanocyte differentiation.

3.3.4 Increase in free β-catenin in the cytoplasm could be responsible for the cell shape and the cell organisation phenotype

β-catenin is a major protein for the maintenance of the architectural structure of the cell. It regulates the activity of Cadherins by binding and linking Cadherins to the actin cytoskeleton through α-catenin (Figure 3.31) (Nelson and Nusse, 2004). The mis-regulation of the β-catenin/ Cadherins regulatory control could lead to impaired cell adhesion and migration resulting in changes in cell shape/cell organisation. The study of normal human epidermal melanocytes *in vitro* reported that active β-catenin could regulate both the increase and the decrease of the melanocyte dendricity by adjusting the levels of two downstream modulators, PKCf and PKCd (Kim *et al.*, 2010). Kim *et al.*, (2010) showed that overexpression of PKCf resulted in the decrease of the levels of the proteins Rac1 and Cdc42, known for their potential role in organising the actin cytoskeleton. Consequently, this led to a reduction of dendrite formation in melanocytes. In contrast, overexpression of PKCd led to an increase of Rac1 and Cdc42 levels and to an increase of melanocyte dendrite numbers. Whether this mechanism was activated by the BIO treatments was not tested here.

Increased Mitfa could appear as an alternative mechanism for the changes observed in cell shape and organisation. Studies in *Xenopus* reported that increased X-*mitfα* expression could result in increased melanocyte dendricity and cell dispersal (Kumasaka *et al.*, 2005, Kawasaki *et al.*, 2008). Kumasaka *et al.*, (2005) used *Xenopus laevi* to test the effects of constitutive activation of *mitfα* (*Xlmitfα* -M) as well as the effects of dominant negative *mitf (dnmitfα*) expression in melanocytes. The study showed that overactivation of *Xlmitfα* led to increased melanocyte number, increased cell dendricity and increased *dct* expression. In contrast, *dnmitfα* expression caused decreased melanocyte number, decreased cell dendricity and decreased *dct* expression. Kawasaki *et al.*, (2008) used the same system to better investigate the effects of *mitfα* on dendricity and on melanosome dispersion. The results suggested that *mitf* could control the melanocyte morphology aspects such as dendricity, maybe via the protease Rab27 (Carreira *et al.*, 2005, Carreira *et al.*, 2006, Tachibana *et al.*, 1996)

It would be important to assess whether the changes in cell shape, and cell organisation, observed with the BIO treatments were caused by either the activation of the β-catenin/E-cadherins complex (Figure 3.30); by the β-catenin dependent regulation of PKCf and PKCd; or finally by a β-catenin dependent activation of *mitfa* which could have resulted in changes in the regulation of a protease involved in cell dendricity, such as Rab27a.

3.3.5 The role of β-catenin as an effector of Factor Y

In these experiments we observed an apparent decrease of dGFP expression in melanocyte after 48 hpf. This observation could be an artefact of the detection technique in which increasing melanin levels in differentiating melanocytes may interfere with GFP detection. However, the GFP could be detected in melanocytes suggesting that in normal situation, the cells were certainly responsive to the Wnt signalling and did experience some level of Wnt signalling. An alternative approach to test whether or not Wnt signalling was maintained in melanocytes after 48 hpf would be to test the levels of nuclear β-catenin in melanocytes in embryos throughout their differentiation. This same approach used on treated embryos could also confirm the efficiency of BIO treatments and could assess whether LiCl could cause activation of β-catenin. If both molecules can cause this effect, then the differences in the phenotype could be explained by the different efficacies of the molecules, or perhaps, the side effects they cause. For this, the double marking of melanocytes using GFP reporter in *mitfa*-GFP transgenic line, and another antibody staining for β-catenin, could allow the observation of co-localised signals in cells in PTU treated embryos.

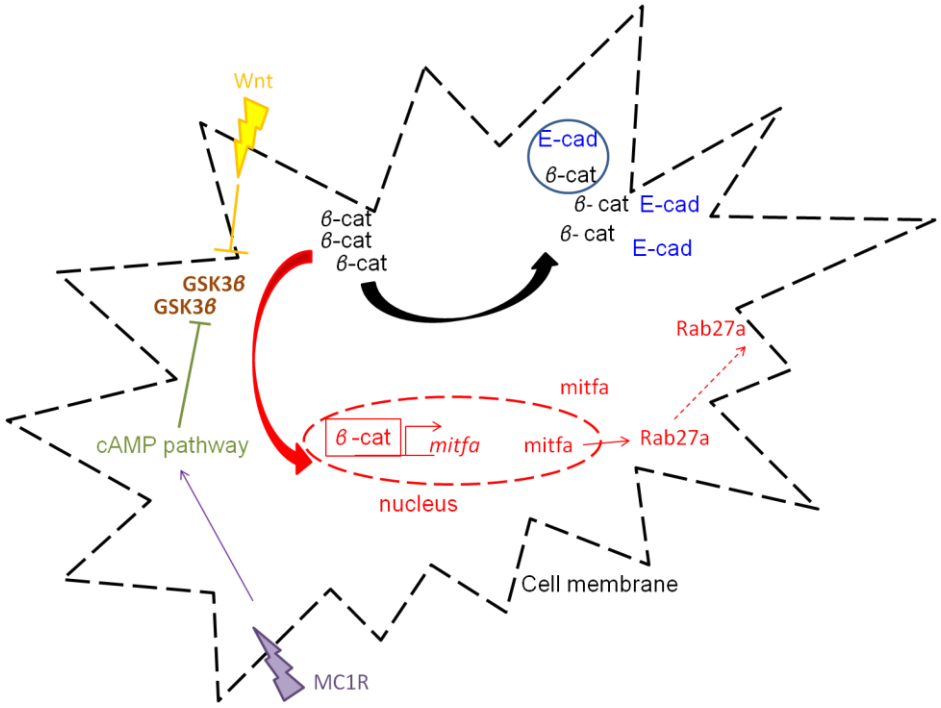

Figure 3.30: GSK3β inhibition increases free β-catenin levels in cells

Increased free β-catenin (β-cat) causes a boost of the canonical Wnt pathway (red arrow). The levels of free β-catenin are increased, consequently, the translocation of β-catenin to the nucleus is increased. This can lead to the activation of *mitfa* expression, and it could cause the potential increase of expression of the GTProtease Rab27a, which could in turn, be the cause of changes in cell shape. The free β-catenin (β-cat) can also accumulate at the membrane, to associate with E-cadherins (E-cad) in a complex to regulate the cytoskeleton (black arrow). The cAMP pathway, via MC1R signalling, is also a negative regulator of GSK3β. Therefore if the cAMP pathway was boosted in by the treatments, it could have enhanced the inhibition of GSK3β.

3.3.6 The results suggest that Wnt signalling can affect melanocyte differentiation but it is not a limiting factor in the process

In these experiments, the hypothesis of the role of Wnt signalling as a single limiting factor for melanocyte differentiation was tested. In the light of the results described here, it seems that Wnt signalling is not limiting for melanocyte differentiation. The definition of Factor Y was re-assessed as an ensemble of factors which contribute to the maintenance of the differentiated state in melanocytes.

In regard to the data, the changes observed in melanocytes, such as cell shape and organisation, were suggested to be indirect effects of elevated *mitfa* expression which is supported by the study of *X-mitfα* effects in melanocyte dendricity in Kawasaki *et al.*, (2008) in *Xenopus*. Melanisation is also an important but not a major aspect of melanocyte differentiation. In our experiments the melanin content was investigated looking at the absorbance at 490 nm, as used in the study of melanisation in zebrafish by Jin and Thibaudeau (1999). It was found never to be increased however, our treatments were significantly shorter compared to Jin and Thibaudeau (1999). Consequently, the weak increased melanisation observed in Jin and Thibaudeau (1999) might have been due to the cumulative effect of continuous treatment over a longer period of time compared to ours. To assess if Wnt signalling was essential for the melanocyte differentiation process, and more particularly, for *mitfa* expression activation at this stage, it would be fundamental to test the inhibition of Wnt signalling. According to the model, loss of Factor Y should cause melanocyte dedifferentiation after 36 hpf via a decrease, or a total loss, of *mitfa* expression. Therefore, if the inhibition of Wnt signalling in melanocytes resulted in a sudden decrease of *mitfa* after about 36 hpf, then it would be plausible that Wnt signalling could be directly required for *mitfa* maintenance.

In 2010, a screening study aimed to investigate small molecules targeting to inhibit Wnt signalling's activity in colon cancer (Chen *et al.*, 2010). However, this was unsuccessful and more work is needed to indentify an inhibitor. In zebrafish, no small molecules have been successfully developed or tested for this purpose. Consequently, other methods should be developed in order to test Wnt inhibition in melanocyte development.

Lowering β-catenin activity specifically in melanocytes will be crucial, and thus, a new mutant or transgenic tool could be created to reach this objective *in vivo*. Dorsky *et al.,* (2002) used injection of Lef1 morpholino at one cell stage to assess the gene expression changes ectopically. The experiments resulted in a loss of posterior tail structures however, the 36 hpf injected embryos did not seem to show a decrease in melanocyte pigmentation compared to the control embryos (Dorsky *et al.*, 2002). In the study, Dorsky *et al.,* (2002) tested the efficacy of the morpholino in blocking the translation of injected targeted plasmids in reticulocyte lysates. However, it is surprising that no failure of cell melanocyte specification was caused by the injections. In a previous study, Dorsky *et al.,* (1998) had used injection of the mRNA of the truncated versions of the negative regulator, Tcf-3, and of a dominant negative version of Wnt-1 in premigratory NC in *Xenopus* and in zebrafish (Dorsky *et al.,* 1998). The conclusion was that β-catenin

injection could rescue the Tcf-3 phenotype. In contrast, the β-catenin injection did not rescue the phenotype when blocking Wnt1, the mechanism of these interactions still needs to be investigated.

Two different experiments could be performed to test the effects of inhibition of Wnt signalling on melanocyte differentiation:

- Creating a new conditional, temperature dependent, β-catenin mutant using *mitfa* heat-shock promoter *(mitfa*^{fh53} from Johnson *et al.,* (2010)), could allow the inactivation of Wnt signalling in melanocytes at specific timepoints. Therefore, using temperature induction (25°C) of a dominant negative mutated, or truncated, version of β-catenin, fused to GFP (IRES), in melanocytes would allow the testing of the role of β-catenin at different timepoints. This method would also permit the control of the activation of the construct with the GFP reporter. Inactivation of β-catenin, from 15-30 hpf, should lead to decreased melanocyte specification and should trigger a reduction of the number of melanised cells at 30 hpf. Inactivation of β-catenin, from 24-48 hpf, and from 48-72 hpf, could cause severe changes in melanocytes, such as, a regression of the cell differentiation or a decrease of cell dendricity and even a decrease of melanisation. Finally, loss of Wnt signalling in melanocytes would trigger a decrease or even a loss of *mitfa* expression. However for these experiments, a new temperature sensitive β-catenin allele would need to be identified.

- In Hari *et al.,* (2002), a Cre/LoxP system was used with tamoxifen to induce a constitutive version of β-catenin (*Ctnnb1*$^{\Delta ex3}$*)* in *sox10* expressing melanoblasts (*sox10*-Cre) in mouse. In zebrafish, the Cre/LoxP system was not thought to be efficient, however, a recent study published from Hans *et al,* (2009) showed that the Cre/LoxP system was perfectly suitable in this model. Rodrigues *et al.,* (2012) developed a new transgenic tool in zebrafish, a *sox10*-Cre line *Tg(-4725sox10:Cre)(ba74)* which marked all NC derived pigment cells. This tool could be used, in combination with a LoxP tamoxifen inducible truncated version of β-catenin, to test for the effects of impaired Wnt signalling activity in melanocytes between 36 and 48 hpf.

3.3.7 Complex aspects of Factor Y

The activation of Wnt signalling during melanocyte differentiation caused increased *mitfa* transcription. Interestingly, the *Mitf* regulatory network in melanocytes contains numerous connections with the signalling pathways and genes involved in the full range of different functions for the maintenance of the melanocyte. *mitfa* has also been described as an oncogenic factor and its roles in the survival of melanocytes, the cell cycle and the proliferation of cells, have been described in several studies (Bertolotto and Ballotti, 2009, Bondurand *et al.*, 2000, Carreira *et al.*, 2005, Carreira *et al.*, 2006, Cheli *et al.*, 2012, Cronin *et al.*, 2009, Garraway *et al.*, 2005, Goding, 2000, Hou *et al.*, 2000, Johnson *et al.*, 2010, Kido *et al.*, 2009, McGill *et al.*, 2002, Mellgren and Johnson, 2004, Phung *et al.*,

2011). Consequently, it could be suggested that the activation of a direct or an indirect activator of *mitfa*, such as Factor Y in the context of the modelling, might be expected to cause dramatic effects in differentiated melanocytes.

Firstly, Factor Y is likely to correspond to multiple components. As in a progression process, or in a process of several steps, misregulation of melanocyte differentiation, via *mitfa* increase or decrease could require the disruption of several key factors which remain to be defined.

Secondly, if *mitfa* expression was not key after 48 hpf, then activating *mitfa* after 48 hpf would have no effect, or an indirect effect, on melanocyte differentiation. However, we show in Chapter 4, that *mitfa* expression is maintained at low levels until at least 72 hpf in melanocytes, consequently it is plausible to suggest that it could be a key factor to maintain for melanocyte differentiation.

Thirdly, epigenetic mechanisms should be taken into account for investigating Factor Y. It is plausible that epigenetic regulation would be responsible for the changes of *mitfa* expression level, from melanocyte specification to melanocyte late differentiation phase. Consequently, if epigenetic mechanisms were responsible for maintaining *mitfa* expression silent or low during melanocyte differentiation, then a misregulation of these mechanisms could cause important misregulation of melanocyte differentiation.

3.3.8 Identifying other candidates for Factor Y

Given the limited effects of overactivation of Wnt signalling, we propose that Factor Y may consist of an ensemble of factors which together maintain *mitfa* expression. Factor Y, if it exists, was redefined as an ensemble of factors, which could maintain the equilibrium in melanocyte state when differentiated. Therefore, other candidate factors could be at play in this role such as Mitfa itself, Tyro3, cAMP via p38 and the Mc1r pathways (Phung *et al.*, 2011, Maresca *et al.*, 2010, Zhu *et al.*, 2009, Gross *et al.*, 2009).

3.3.8.a Mitfa itself as a potential candidate for Factor Y

It has been shown *in vitro* that MITF could be an auto-regulator of its expression (Saito *et al.*, 2002). However, it remains unclear *in vivo*, if, and when, Mitfa could be responsible for its own activation. In Chapter 5, the response of activation of *mitfa* expression to ectopic *mitfa* induction was tested in zebrafish to explore the possibility of Mitfa as a candidate for regulation of *mitfa.* Interestingly, there is currently no evidence in melanocytes for a factor which would antagonise *mitfa* effects and prevent melanocytes from expending or overexpressing *mitfa* after 24 hpf. This could suggest that the network did not need such a factor to maintain a balanced *mitfa* level in melanocyte but rather another mechanism, perhaps involving dynamic transcription or epigenetic regulation, could regulate its level.

3.3.8.b *tyro3* as a candidate for Factor Y

The receptor tyrosine kinase 3 (Tyro3) could positively regulate *Mitf* expression in melanoma cells in culture (Zhu *et al.*, 2009). Furthermore, Tyro3 knockdown triggered the reduction of the tumourous potential of aggressive melanoma cells *in vivo* in xenograft in nude mice (Zhu *et al.*, 2009). It would be interesting to test the role of Tyro3 in normal melanocytes and particularly in *mitfa* regulation during cell differentiation.

3.3.8.c The cAMP pathway as a candidate for Factor Y

Other candidate factors for Factor Y are the cyclic AMP (cAMP) and the MAPK pathways. cAMP is an intracellular signalling pathway which is modulated by extracellular signals such as α-msh/MC1R, p38, MEK and PKA (Mansky *et al.*, 2002, Price *et al.*, 1998, Phung *et al.*, 2011, Saha *et al.*, 2006). Interestingly, Liang *et al.*, 2011 showed a link between the regulation of CtBP2, the cAMP/PKA pathway and activation of *Mitf* in melanocyte differentiation in NC culture. CtBP2 is a co-repressor of Wnt signalling. The study showed that the degradation of CtBP2 caused the activation of *Mitf* expression and triggered melanocyte differentiation via the activation of the cAMP/PKA pathway (Liang *et al.*, 2011). In zebrafish, the PKA/cAMP pathway has also been shown to induce *mitfa* expression by activating the degradation of the antagonist factor, CtBP2 (Liang *et al.*, 2011). CtBP2 has also been shown to be physically interacting with β-catenin to inhibit β-catenin in absence of cAMP pathway activation (Figure 3.31) (Liang *et al.*, 2011). GSK3β can also be inactivated by the p38-MAPK pathway to activate both β-catenin transcriptional and non-transcriptional functions in cells (Bellei *et al.*, 2008). If the cAMP and Wnt signalling pathways both regulate *mitfa* via β-catenin would have to be determined in further experiments. Bertolotto *et al.*, (1998) have demonstrated that forskolin treatment stimulating the cAMP pathway led to increased *tyrosine-related proteins 1* and *2* (*Trp1* and *Trp2/Dct*) expression in B16 melanoma cells (Bertolotto *et al.*, 1998). The study described the effect of cAMP stimulation on increased binding of MITF on M-box of *Trp1* and *Trp2/Dct* promoters (Bertolotto *et al.*, 1998). The results showed the plausible role of cAMP in cell melanisation, via MITF. Therefore, it would be interesting to study the role of cAMP by blocking its activation specifically in melanocyte at a certain stage. Interestingly, (Ishizaki *et al.*, 2010) showed that two specific inhibitor of the MEK signalling had no effects in pigmentation in zebrafish. Whether another component of the pathway could be responsible for activation of melanocytic genes could be tested.

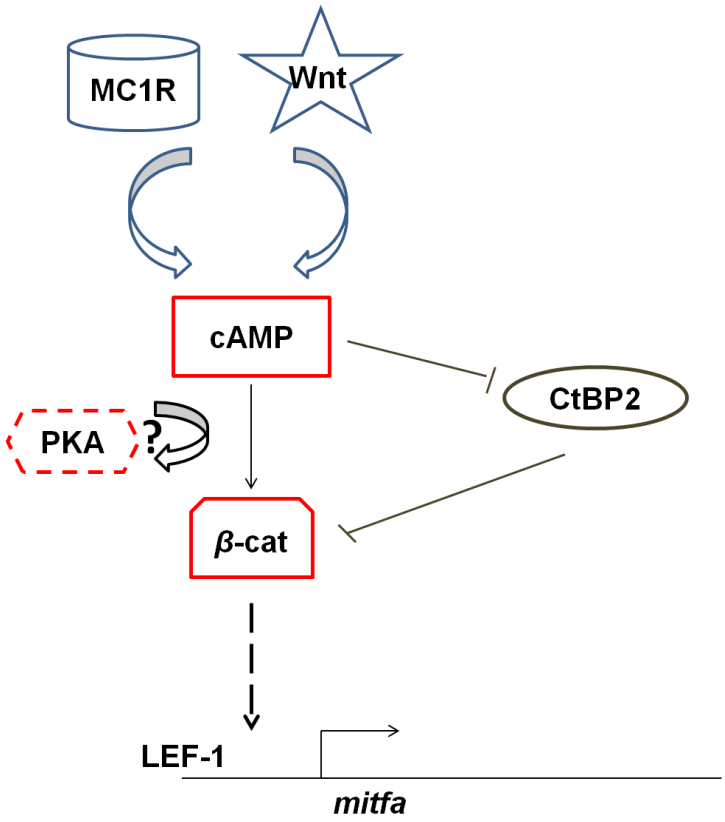

Figure 3.31: Activation of the cAMP pathway in melanocytes.

In melanocytes, Mc1r and Wnt signalling could both activate the cAMP/PKA signalling by boosting β-catenin (β-cat) activity, and by inhibiting an inhibitor of β-catenin, CtBP2. This would lead to increased β-catenin in the nucleus and cause *mitfa* activation. The mechanism by which PKA co-regulates the β-catenin activity is not well understood so far.

3.3.8.d Mc1r pathway as a candidate for Factor Y

Mc1r is a transmembrane receptor and member of the GPCR (G protein couple receptor) superfamily of genes. It is comprised of an N-terminal domain, seven hydrophobic transmembrane domains, and a carboxy terminal domain (Vassilatis *et al.*, 2003). Mc1r is activated by the binding of its ligand, α-Msh, which triggers the activation of the cAMP signalling and results in an intracellular increase in the cAMP levels (Li *et al.*, 2010, Maresca *et al.*, 2010). The activation of Mc1r can lead to the activation of downstream effectors in the pigmentation pathway, including the target gene *Mitf*, which transcription was up-regulated by cAMP signalling in melanocytes (Figure 3.32) (Widlund and Fisher, 2003). cAMP signalling, via the PKA and the CREB pathways, can trigger expression of MITF in melanocyte in mammals (Kabbarah and Chin, 2006). Consequently, Mc1r is a good candidate for Factor Y (Appendix 2).

3.3.8.e Disc1 as a candidate for Factor Y

Recent findings suggested that Disrupted in schizophrenia 1 (DISC1) could prevent GSK3β from phosphorylating β-catenin via physical interaction (Hur and Zhou, 2010). DiscI could then positively affect β-catenin transcriptional activity by preventing GSK3β inhibition. Mitf is a target of β-catenin, therefore, Disc1 could be an indirect activator of Mitf, by the activation of Wnt signalling. No melanocyte phenotype has been described in *disc1* zebrafish mutant. However, Drerup *et al.*, (2009) showed an abnormal increase of *sox10* expression in these mutants. The role of Disc1 could then be important for *mitfa* expression by activating β-catenin and inhibiting *sox10* in melanocytes, although, this remains to be tested.

3.3.9 Xanthophore pigmentation was boosted after LiCl treatments

Using LiCl for analysis of GSK3β inhibition in melanocytes showed inconsistent effects compared to BIO. The lack of reliability with the use of the molecule throughout the different tests has resulted in the need for careful interpretation of the results obtained for the melanocyte development. In contrast, activation of xanthophore development was very consistent with LiCl.

dGFP expression was observed in LiCl treated embryos, localised to cells that could be identified as xanthoblasts by their position and morphology. This correlated strikingly with the elevated xanthophore pigmentation seen in LiCl-treated embryos. In contrast, we were not able to detect an increase in xanthophore pigmentation in BIO-treated embryos; if there was an increase, it was never as strong as when treating with LiCl. One hypothesis could be that in these cells, a pathway targeted by LiCl might limit pigmentation. It remains unclear if the xanthophore pigmentation boost was triggered by the LiCl dependent activation of Wnt signalling or by the stimulation of another pathway as a side effect of LiCl treatment. The lack of effect from the more specific inhibitor, BIO, argues for the off-target mechanism being key.

After the 24 hpf to 48 hpf treatment, the increase in xanthophore pigmentation correlated with a boost of *xdh* expression in the tail. However, it is not clear whether this

expression activation could be the cause of increased pigmentation. Other factors could probably be affected by the treatment. Consequently, these experiments did not show a dramatic increase of *xdh* expression and another marker should be tested to understand the cause of increased yellow pigmentation at 48 hpf. It seemed that expression of *xdh* was not activated after treatment during cell specification (15-30 hpf), therefore, it could be suggested that cell differentiation aspects, such as cell pigmentation, were increased by the treatments. Increased cell number could result in cell pigmentation increase however we did not investigated it. Only embryos treated during the 30 hpf to 48 hpf period showed increased xanthophore pigmentation at 48 hpf and 72 hpf. Altogether, these experiments showed that LiCl treatment, from 30 hpf to 48 hpf, could activate a limiting factor in xanthophore pigmentation development and cause an increase of the *xdh* expression. Furthermore, because *xdh* expression was not boosted after the 15-30 hpf treatments, it can be suggested that cell specification was not activated.

Another family of factors crucial for xanthophore specification and development is the *pax3/7* family (Minchin and Hughes, 2008). *pax3* is expressed in pigment precursor early in NC development, before 30 hpf. In zebrafish, the morpholino knockdown of *pax3* triggered the reduction of *sox10* expression at 25 hpf. *pax7a* and *pax7b*, are expressed only in xanthophore after their specification (Lacosta *et al.*, 2007, Lacosta *et al.*, 2005, Minchin and Hughes, 2008). It is unlikely that *pax7a* and *pax7b* could be the targets of LiCl in treated embryos as they are. LiCl could also be boosting any enzymatic reaction responsible for pteridin synthesis like that described in Ziegler, (2003).

These results are difficult to interpret and further experiments are needed to fully understand the activities of LiCl in cells. It is plausible that LiCl stimulated signalling pathways other than the Wnt signalling pathway. The LiCl induced effects on xanthophore pigmentation could be the consequence of the activation of another target of LiCl, resulting in the activation of Wnt signalling. An explanation for this could be that Wnt signalling activation in xanthoblasts was the result of a factor that was activated by LiCl, but not by BIO.

Knowing the lack of effect of BIO in xanthophores, it is unlikely that xanthophore response to LiCl would be Wnt signalling dependent. However, to study xanthophore development and specifically to investigate this possibility from 24 to 48 hpf, a new transgenic fish could be created. This fish line could, for instance, carry a truncated version of β-catenin-fused GFP protein under the control of *pax7* or *xdh* promoter. This would allow us to observe of the effects of a lack of Wnt signalling in xanthophore and to assess a potential lack of yellow pigment.

3.3.10 Conclusion

To conclude, we showed that Wnt signalling remained activated during melanocyte differentiation, however, we did not find that it was a limiting factor in the melanocyte GRN differentiation. Therefore, it is acceptable to reject its role as a single factor for Factor Y. Thus, pointing to the possibility that Factor Y could be an ensemble of factors which remain to be identified.

Chapter 4. Characterisation of Genetic Heterogeneity in Melanocytes

4.1 Introducing the concept of heterogeneity as an essential aspect of cell derivation from a multipotent pool

4.1.1 Genetic heterogeneity is a crucial aspect of both Neural Crest and melanocyte development

Variations of gene expression levels in individual cells within the same cell population may drive two apparently similar cells towards different fates (Baroffio *et al.*, 1991, Bronner-Fraser and Fraser, 1988, Quaranta and Garbett, 2010, Levsky and Singer, 2003). Bulk population studies determine the average gene expression level in cell populations, but fail to evaluate gene expression variations in individual cells (Peixoto *et al.*, 2004, Quaranta and Garbett, 2010, Kamme and Erlander, 2003, Klein *et al.*, 2003, Levsky and Singer, 2003). These variations in expression at an individual cell level are not only likely to be of importance for cell fate, but also evolutionarily important. Consequently, it is key to measure and understand the extent of the influence of these variations at the individual cell level.

The aim of this Chapter is to develop a specific approach to better understand individual cell activity and to better characterise the melanocyte population. Melanocytes are derived from the multipotent NC cell pool via the process of specification and differentiation. Previous genetic analyses have identified two crucial transcription factors for melanocyte development, *Sox10* and *Mitf* (Johnson *et al.*, 2010, Sommer, 2011, Kelsh, 2004, Kelsh and Eisen, 2000, Dutton *et al.*, 2001, Lister *et al.*, 1999). The understanding of the fine scale regulation and the activity of these factors in melanocyte populations through development is at the centre of this study. To reach this aim, we developed a method to detect and measure gene expressions in five cell pools. This technique could now be used to go further in the testing of models for understanding of the NC and of pigment cell development.

4.1.2 Heterogeneity within cell populations is the result of genetic variability and stochasticity

Gene expression heterogeneity can be a determining parameter for fate choice. Measuring the heterogeneity of gene expression of a cell population can also inform on the genetic state of the population. Cell heterogeneity could then be modelled through time and could inform on the genetic stability of a cell population. The genetic heterogeneity of cell population is associated with the gene expression variability in individual cells of this population. Genetic variability can be caused by both pre-programmed and/or stochastic variations from one cell to another (Stahlberg and Bengtsson, 2010, Elowitz *et al.*, 2002, Garg *et al.*, 2009, Gillespie, 2009, Janes *et al.*, 2010, Kaern *et al.*, 2005, Lipniacki *et al.*, 2006, Lei, 2009, Roberts *et al.*, 2011, Stolovicki and Braun, 2011). Consequently, the variability of gene expression is linked to regulated cell-to-cell heterogeneities as well as to stochasticity of gene expression.

Pre-programmed regulation can cause variability when certain factors are activated in a subset of cells due to the different characteristics of their regulatory network and to the conditions. Stochastic variability is caused by random transcriptional events. Stochastic activation of gene expression is observed when transcription factors are present in low numbers which are the condition for a probabilistic system. The stochasticity of gene expression can have no functional consequences but it can also provide the flexibility needed by cells to adapt to fluctuating environments, or to respond to sudden stresses. It is also a mechanism by which population heterogeneity can be established during cellular differentiation and development (Raj and van Oudenaarden, 2008, Janes *et al.*, 2010). Because of the difficultly of separating meaningful variations from irrelevant background variation of gene expression at a multi-cell level in all types of cells, it is necessary to investigate gene expression as close as possible to the single cell level.

4.1.3 Understanding genetic variability in melanoblast/melanocyte populations

In this Chapter, one objective was to measure the genetic variability of the melanoblasts and the melanocyte population. Comparing heterogeneity of cells in these cell populations through time could provide information on the genetic state of cells and consequently on the stability of the GRN driving their development at each time point. Previous genetic analyses of melanocyte derivation have suggested the existence of several potential precursors and here we present a preliminary view on the deciphering of the heterogeneity of gene expression in cells of the melanocyte lineage.

The variability of melanocytic gene expression in the melanoblast population has been suggested but has never been explicitly studied as an aspect of the development of the cell population. Figure 4.01 summarises melanocyte derivation from the NC pool and shows the potential precursors (melanoglioblasts, chromatoblasts, chromatoglioblasts, glioblasts, melanoblasts) which may well be present, albeit in unknown proportions, at

each stage. The presence of such precursors in the NC cell population would be expected to result in a certain cell to cell heterogeneity of gene expression in this population.

According to previous analyses, some variability could be expected in the expression of melanocytic genes within in the NC cell population (Curran *et al.*, 2010, Dutton *et al.*, 2001). Analysis of the regulatory interactions at play in melanocytes permitted us to build a mathematical model which indicated that *dct* expression was activated by Mitfa and repressed by Sox10, while *tyrp1b* expression was not repressed by Sox10 (Greenhill *et al.*, 2011). From 11 hpf to 18 hpf, s*ox10* was expressed in all NC cell precursors. At 18 hpf, *mitfa* expression was activated and marked a large proportion of *sox10* (+) cells which consists of a poorly-defined mixture of multiple precursors including neuroglioblasts, chromatoglioblasts and melanoblasts. This was deduced by the study of a *mitfa*:GFP transgenic fish line which showed that *mitfa* expression was initially detected in a broad population of *sox10* positive (+) cells from 18 hpf to 26 hpf knowing that at 24 hpf, GFP expression in this fish accurately reflected *mitfa* expression (Curran *et al.*, 2009). However, no single cell expression studies have been carried out to investigate the exact proportion of *sox10 (*+) cells activating *mitfa* transcription at early stages. Around 20 hpf, the genes coding for enzymes responsible for melanin synthesis, *dct, tyrosinase related protein 1* (*tyrp1b/trp1b), tyrosinase (tyr),* and *silver (si),* were activated by Mitfa in an unknown proportion of *mitfa* (+) cells. Interestingly, Curran *et al.*, (2009) showed that at 24 hpf, only 55 % of the *mitfa*:GFP cells were *dct* positive. From 23 hpf to 36 hpf, *mitfa* was broadly expressed in NC cells and neither the type nor the proportion of precursors in the pool of cells were determined (Curran *et al.*, 2009). The first sign of pigmentation can be observed around 27-29 hpf, but it is not clear yet when or how *mitfa* expression becomes restricted to the melanocyte lineage (Kelsh *et al.*, 1996b). After 30 hpf, *dct* and *tyrp1b* expression were strictly restricted to melanocytes as shown by experiments investigating colocalisation of melanin and *dct* expression by WISH (Kelsh *et al.*, 2000, Kelsh and Eisen, 2000, Thisse and Thisse, 2008).

After 36 hpf, expression of *mitfa* is restricted to melanoblasts/melanocytes until at least 48 hpf and melanisation increases until at least 72 hpf in melanocytes. In contrast, s*ox10* expression is decreased in these cells. Investigating gene expression in the population of melanocytes (after 36 hpf), will reveal the variability of gene expression in these cells during the process of cell differentiation. It is would be interesting to assess whether melanocytic genes are expressed homogeneously in this cell population or whether their expression shows strong variation, and, if it ever reaches homogeneity in the fully differentiated cells at 72 hpf.

In this study, we began to investigate melanocyte-related gene expression in both the NC cell population and the melanocyte population in order to test the genetic variability of their expression in these different cell populations through time. As described in Figure 4.02, two timepoints were analysed during the specification phase (23 hpf and 30 hpf) in isolated GFP+ NC cells (of mixed fate) from *sox10*:GFP(+) transgenic embryos and three timepoints were investigated throughout early to late differentiation (36 hpf, 48 hpf and 72 hpf) in melanised cells.

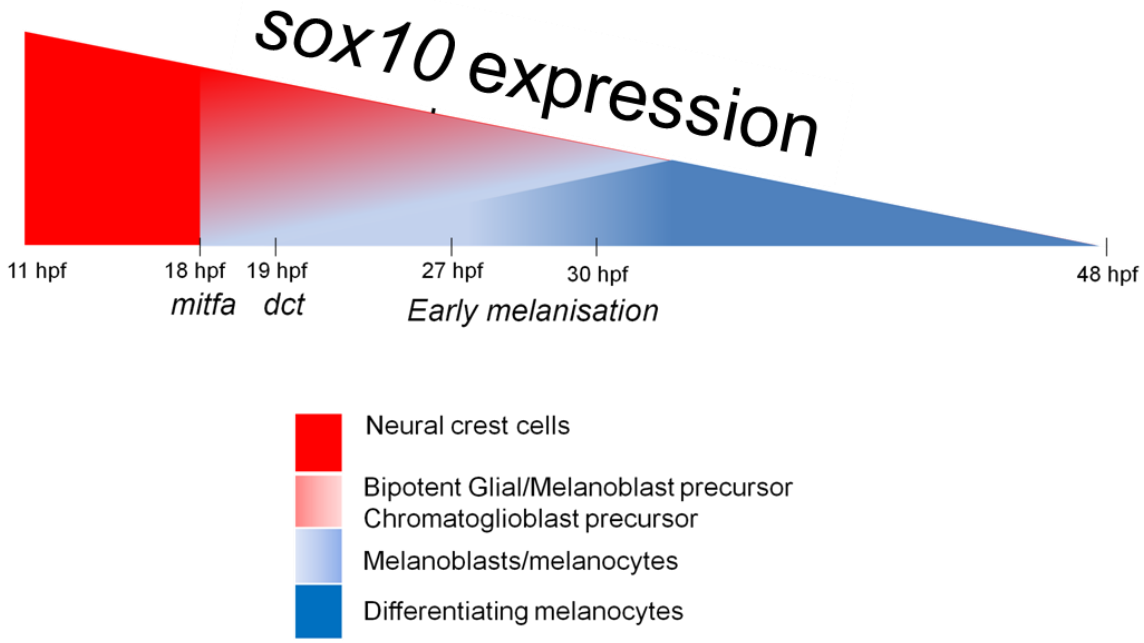

Figure 4.01: Time course of the derivation of melanocytes from a heterogeneous population of precursors.

From 11 hpf to 18 hpf, *sox10* is expressed in most NC cells (red cells). At 18 hpf, Sox10 activates *mitfa* expression in a majority of cells including cartilage and peripheral ganglia precursors. An unknown proportion of these cells could then be bipotent melanoglioblasts, or chromatoglioblasts, in zebrafish (mixture light blue/red/light red). Around 19 hpf, Mitfa targets such as *dct*, are activated in about 50 % of cells according to Curran *et al.*, (2006). Cells expressing *dct* could be defined as melanoblasts (blue). *sox10* expression decreases in melanoblasts and in differentiating melanocytes as cells are committing to the melanocyte fate. At 30 hpf, it is unclear whether some cells remain bipotent. At 48 hpf, *sox10* expression is difficult to detect, melanocyte specification phase is terminated and committed melanocytes undergo continuing differentiation (light blue and dark blue).

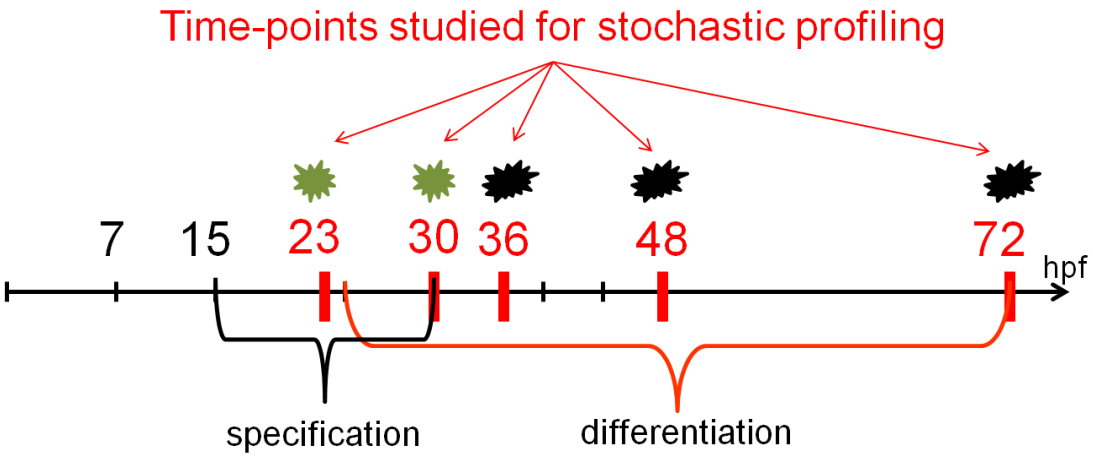

Figure 4.02: Time course for the stochastic profiling study of gene expression.

The five time points studied for the analysis of gene expression during melanocyte development are presented here. *sox10*-GFP cells were selected at 23 hpf and 30 hpf during cell specification (green cells) and melanised cells (black cells) were selected at 36 hpf, 48 hpf and 72 hpf during cell differentiation.

4.1.4 Melanocyte heterogeneity can be described by using quantitative methods within the approach of stochastic profiling

In this study, we used a stochastic profiling approach to quantitatively measure heterogeneity of gene expression in melanocyte populations. Stochastic profiling is a method which consists of measuring gene expression levels in multiple small pools of cells which have been randomly sampled from a population (Figure 4.03). The key elements for this method stem from repeated random sampling and comparison to a reference gene which is homogeneously expressed in the cell population.

This method was successfully used in several studies to quantify the variability of gene expression, such as in Janes *et al.*, (2010) and in Quaranta *et al.*, (2010). Low variability of gene expression is associated with homogeneity of gene expression in the population, while high variability of expression is associated with heterogeneity of gene expression in the cell population studied (Janes *et al.*, 2010, Quaranta and Garbett, 2010, Peixoto *et al.*, 2004). Figure 4.03 describes the stochastic profiling method. In brief, simply using a mean to describe expression does not inform us of the variation that occurs between cells, and similarly, sampling single cells is unreliable because of poor detection resolution. Instead, empirical studies show that repeat random samples of five cell pools are more informative about the degree of variation of gene expression within the population. As the number of samples of five cell pools increases, we can see the frequency of occurrence of different expression levels. When plotted as a histogram of the expression level, populations with low variation will have a narrow distribution with a well defined peak (left histogram), whereas, a population with high variation will have a wider and flatter histogram (middle graph).

In this study we characterised the cell to cell variability of expression of *mitfa*, *sox10, dct* and *tyrp1b* in two different cell populations; the early NC cell mixture of precursors; and differentiating melanocytes. Gene expression was measured by quantitative RT-qPCR in ten repeated pools of five cells for each gene. Gene expression heterogeneity was estimated by calculating the variances for each gene at each time point and was statistically compared to the house-keeping reference gene series using the Fisher test (analysed in Program R).

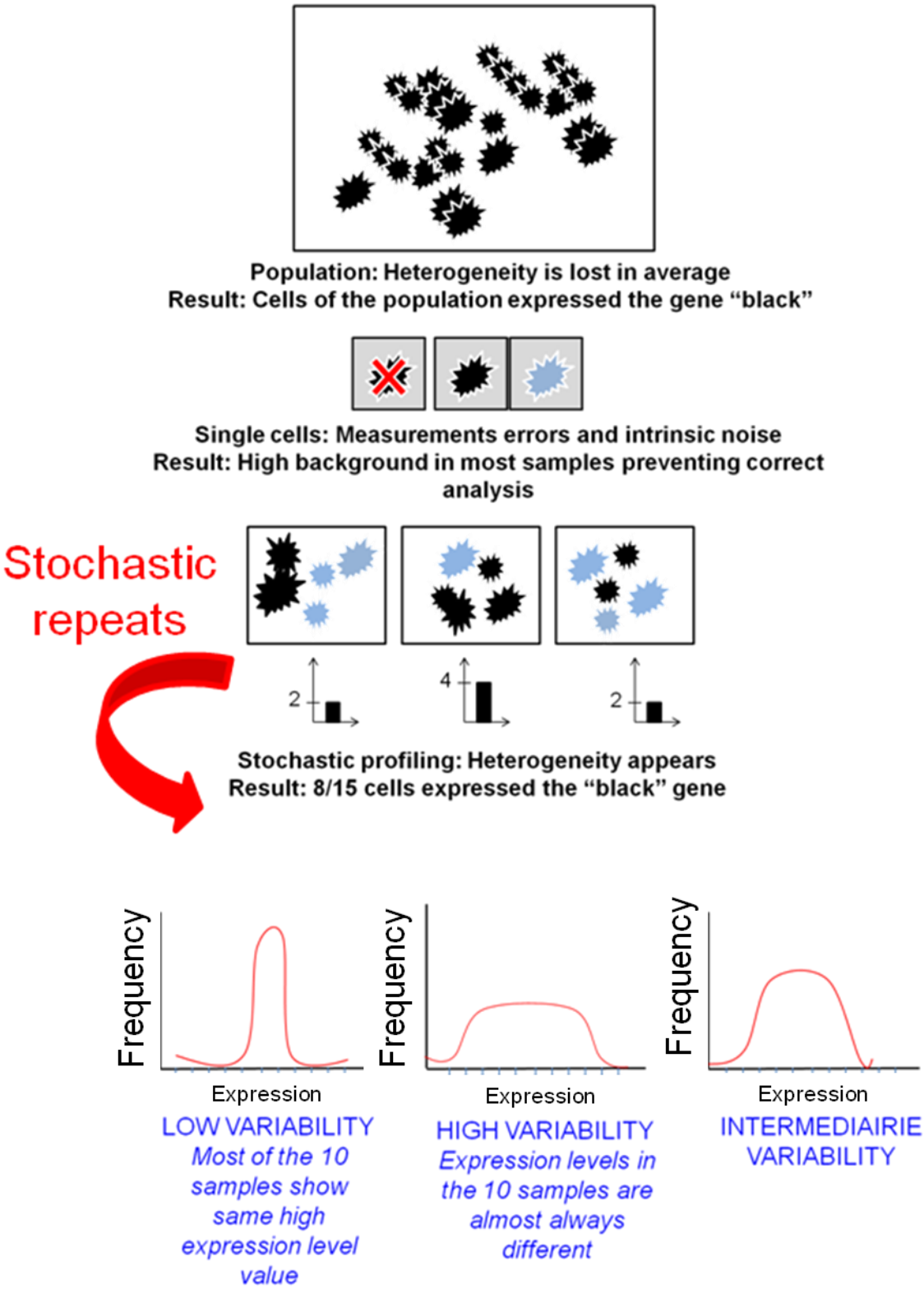

Figure 4.03: Method of stochastic profiling allows identification of heterogeneity in a cell population. See legend on the next page.

Figure 4.03: Method of stochastic profiling allows identification of heterogeneity in a cell population.

In the top panel, gene expression was measured in the whole cell population as an average; by definition, it is assumed that all the cells of the population expressed the gene of interest, "black". In this case, the background was not a problem (white background), but the heterogeneity could not be determined. In the middle panel, gene expression was measured in individual cells of a population. Gene expression heterogeneity could be observed (not all cells expressed the gene "black") however, with a very low amount of starting material, the measurements were subjected to important intrinsic background noise (grey background). This caused errors which could mislead the interpretation of the results. In the lower panel, gene expression was measured in repeated samples of five cells from the population, i.e. by stochastic profiling. Under these conditions, heterogeneity between cells can still be observed, and measuring gene expression level in each sample (the lower graphs show the "proportion" of cells expression gene "black" in each sample (one cell =1)) allowed the description of this heterogeneity. The intrinsic background variation is also greatly reduced compared to single cell experiment (white background). Whether the peak of the curve representing the frequency of samples at each level will be narrow or broad will indicate whether there was homogeneity or heterogeneity of 'black' expression in the cells. (adapted from Quaranta and Garbett (2010)).

4.1.5 Setting gene expression quantification using RT-qPCR

qPCR reactions have several advantages, one of which is that it has been shown to be significantly less variable than any conventional RT-PCR procedure (Wittwer *et al.*, 1997). Several studies measured the coefficient of variation for data from qPCR and RT-PCR and showed it to be very low with qPCR, 0·4 % **(**Lightcycler) which was significantly better than the 14 % reported in the same experiment for conventional RT-PCR (Zhang and Byrne, 1997, Wittwer *et al.*, 1997). The RT-qPCR method is very robust, however, data are less reproducible when working with very low copy numbers because of stochastic effects (also called "the Monte Carlo effect") (Peccoud and Jacob, 1996). Statistics of particle distribution predict that it should require a much greater number of replicates to differentiate 5 from 10 copies of RNA than for the differentiation of 5,000 from 10,000 copies (Dixon *et al.*, 2000, Klein *et al.*, 2003, Nygaard *et al.*, 2005, Taniguchi *et al.*, 2009, Yuan *et al.*, 2006). Importantly, the sequence and the structure of the target sequence, as well as the reverse transcription efficiency, allow only a proportion of the RNA to be reversed transcribed. In conjunction with small quantities of target molecules, several other variables, such as the efficiency of reverse transcription and qPCR, as well as, the exponential nature of PCR amplification, can cause many minor variations which can greatly influence the final yield of the amplified product (Wu *et al.*, 1991). Therefore, controlling each step, including the reverse transcription (RT) efficiency, is crucial. For these experiments, the RNA yields before RT, and the cDNA yield after RT, were controlled using agarose gels, and spectophotometric quantification when possible.

The analysis of the qPCR results is complex and has been discussed by several authors (Rutledge and Cote, 2003, Nygaard *et al.*, 2005, Yuan *et al.*, 2006). Particularly, there has been much debate regarding the assumption that all reactions would have the same efficiency rate resulting in a perfect doubling of the material at each cycle. Thus, in the field of "qPCR analysis", there has been a focus on better understanding and improving the methodology for analysis of qPCR data (Bar *et al.*, 2011, Larionov *et al.*, 2005, Livak and Schmittgen, 2001, Pfaffl, 2001). The major focus of the research in qPCR, are to optimise the detection of expression through a reliable method, and to improve the knowledge of the important parameters involved in amplification.

The validity of qPCR relies on the design and the optimisation of the primer pairs which allow the amplification of a specific DNA sequence with a good PCR efficiency. Quantification of gene expression by qPCR can be of two types: relative and absolute. In relative quantification analysis, the use of a reference gene is essential to subtract the background fluctuation of gene expression such as variations related to the cell cycle state. Therefore, the reference gene is often a housekeeping gene whose expression is unvarying in the system. In contrast, no corrections are applied in the absolute gene expression quantification method. In this case, the gene expression can be compared to the absolute expression quantification of a reference gene, shown to be homogeneous in the cell population. In both absolute and relative quantitative analysis, expression level is first determined by the raw (Ct). The Ct corresponds to the number of cycles necessary for the signal to exponentially rise above the background level when running the qPCR (Wong

and Medrano, 2005). However, for a reliable analysis of the Ct, it is crucial to first follow a strictly defined process of calibration. This calibration process allows the detection and the measurement of the fluorescence related to the concentration of the specific gene sequence target.

Both analysis methods require that the genes under investigation are calibrated for qPCR reaction by building a standard curve (Figure 4.04). The standard curve is not a control for a specific experiment, and once calibrated, the standard curve for a gene can be used to determine expression level for this gene in different experiments. However, it is important to derive a standard curve which covers the range of concentrations to be encountered experimentally, and to produce specific controls for each experiment.

4.1.5.a. Description of the method for the analysis of qPCR data used for relative quantification expression

Relative quantification is an accurate method to evaluate the changes in expression of a gene between experimental conditions but also through time when several timepoints are studied. It consists of utilising a reference gene (housekeeping gene) to normalise, and compare, raw expression levels of genes of interest. Therefore, it is of utmost importance to control and test for several reference genes in order to ensure that their expression level is stable within the system studied (Figure 4.04) (Ling and Salvaterra, 2011, Pei *et al.*, 2007)

Normalised expression can then be compared using different methods. A widespread method is the delta-Ct (ΔCt) method (Livak and Schmittgen, 2001, Bustin, 2000). This method consists of determining firstly, the difference in the Ct of the targeted gene and the reference gene [ΔCt = Ct target – Ct reference gene]. And secondly, the difference between the ΔCt of the calibrator (Wild Type (WT), or control/untreated condition) and the ΔCt of the sample (treated/mutant condition), [Δ(ΔCt) = ΔCt calibrator – ΔCt treated/mutant]. The processes of RNA extraction, and of reverse transcription of the cDNA, for the calibrator, need to have been performed in the exact same conditions as the mutant and the treated samples. The fold difference in gene expression level, between the calibrator, and the tested sample, is then determined by ($2^{-\Delta(\Delta Ct)}$). This value can be used to compare expression levels in samples. Figures 4.04, 4.05, and Table 1, detail and summarise this method.

This method has to be utilised with caution as it is based on a simplification which assumes that qPCR efficiencies for the genes compared are comparable. It is possible to compare expression level of several target genes by using relative qPCR analysis, if the slopes, and the PCR efficiencies (E), are less than 10 % different. This can be verified by determining the gradient of the slope of the line found when plotting the difference in Ct for the two genes, against the logarithm of the concentration. If the slope of this line is less than 0.1 (10 %), then efficiencies are deemed comparable. If it is not the case, another method which corrects for differences of qPCR efficiencies can be used for relative quantification, such as the Pfaffl method (Pfaffl, 2001). Because it takes efficiency parameters into account, the Pfaffl method has been thought to be more robust than the

Δ(ΔCt) method. It is key to determine efficiencies of qPCR amplification to use the appropriate method of analysis. In our study, the qPCR efficiencies were comparable, therefore, the Δ(ΔCt) method, as described in Figures 4.04 and 4.05, was chosen to analyse the data.

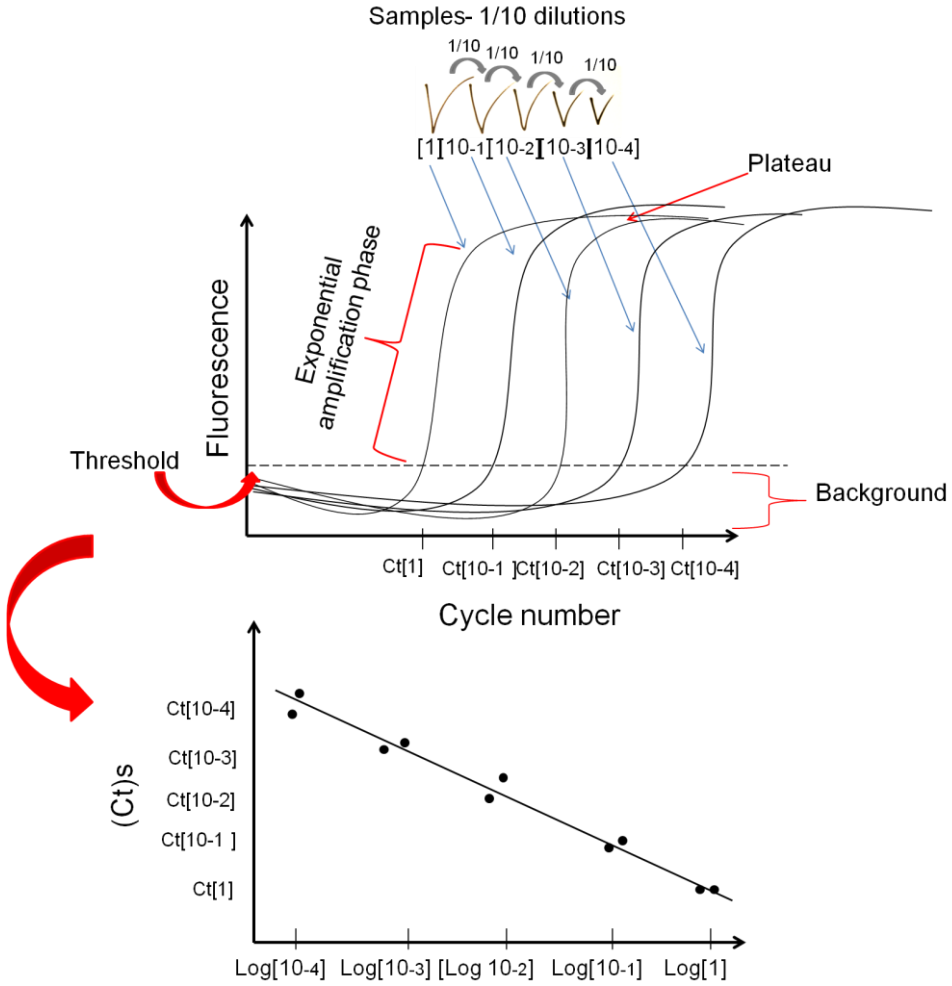

Figure 4.04: Construction of the standard curve to assess qPCR efficiency (E) for each primer set.

The standardised procedure for building the standard curve for each experimental and reference genes, starts with building a scale of five logarithmic dilutions ([1], [10^{-1}], [10^{-2}], [10^{-3}], [10^{-4}], [10^{-5}]). To span a large range of concentrations, sample [1], the most concentrated sample consists of a pool of a highly concentrated cDNA extracted from pooled embryos. The qPCR reaction is observed by plotting the fluorescence against the cycle number (top panel). It is defined by two phases, a phase of exponential amplification and a plateau which corresponds to the end of the reaction when reagents are limiting (as indicated on top panel). This reaction allows the determination of (Ct) for each concentration, from high to low, in each sample (in duplicate or triplicate, not shown here for clarity). The (Ct) corresponds to the cycle number required for the signal to rise above the background level which is set by the "Threshold". The (Ct) and the Logarithm of the concentration (Log[concentration]) for each sample are used to build the standard curve (lower panel). The gradient (slope) and the PCR efficiency (E) are then determined for each primer set [$E=10^{(-1/slope)}-1$].

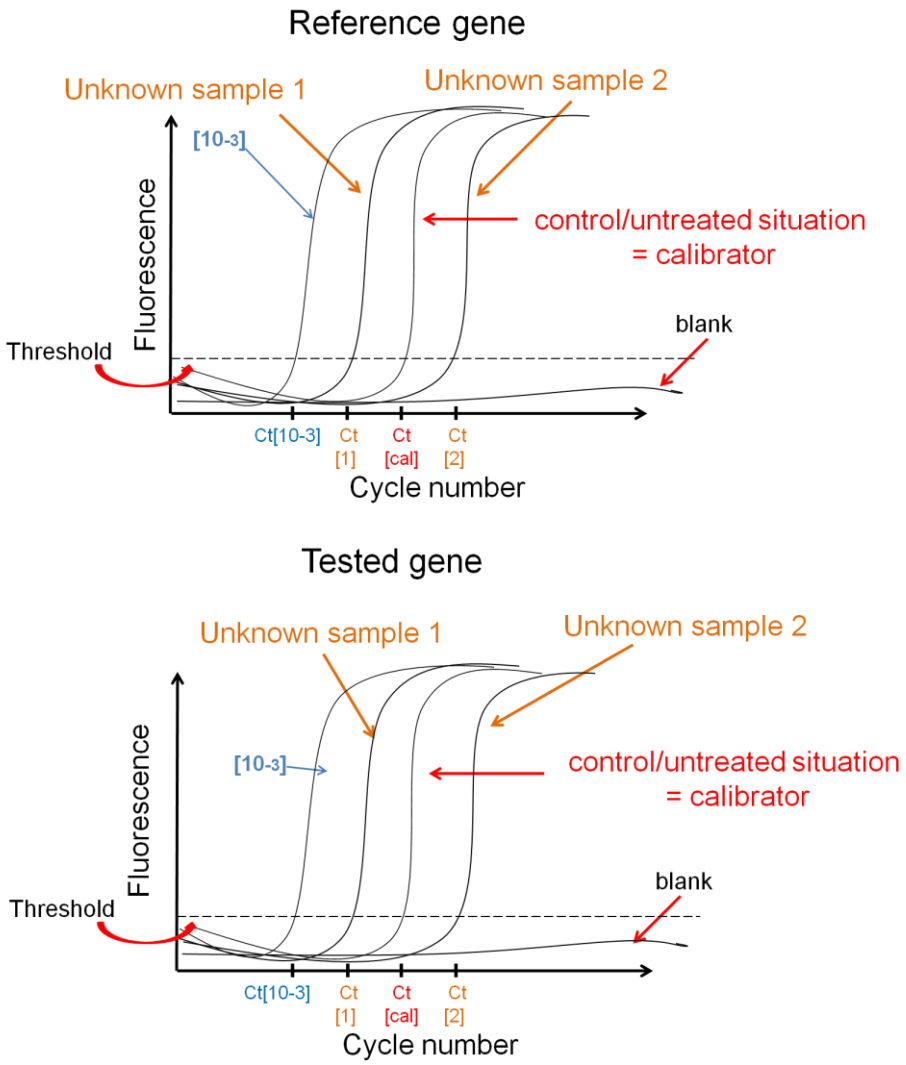

Figure 4.05: Schematic for the experimental set up and analysis for absolute and relative quantification of gene expression using the delta-delta Ct method.

For analysis of relative quantification of gene expression, four types of samples were run for both reference and tested genes. A sample of known concentration ($[10^{-3}]$) was run and used by the software to recall the standard curve and to associate Ct(s) to concentrations. The "calibrator/cal" sample which corresponds to the "control" or "untreated" condition was run. This sample represents the control for the experiment, it was processed exactly as the experimental samples corresponding to treated or mutant conditions called "unknown sample 1 and 2". Finally a negative control, "blank" which contains no cDNA was always run. The determination of quantification takes two steps. **1)** $Ct_{(\text{tested gene sample})} - Ct_{(\text{reference gene sample})} = \Delta(Ct)$, **2)** $\Delta(Ct)_{\text{calibrator}} - \Delta(Ct)_{\text{unknown sample}} = \Delta\Delta(Ct)$. The $\Delta\Delta(Ct)$ is then converted into fold change $2^{-\Delta\Delta(Ct)}$. For absolute quantification analysis, the concentration, or the copy number, was associated to the (Ct) by the software thanks to the previously built standard curve.

Table 4.1: Determination of relative expression using the ΔΔCt method

The determination of relative expression using the ΔΔCt method is a two step process. Firstly, the ΔCt(s) are determined by comparing the Ct of the reference gene to the Ct of the tested genes in both the calibrator sample (control) and the tested/unknown sample (mutant or treated). For this, the difference between the $Ct_{\text{tested gene}}$ and the $Ct_{\text{reference gene}}$ ($\Delta Ct_{\text{calibrator}}$) is calculated for the reference gene as well as, the difference of the $Ct_{\text{tested gene}}$ and the $Ct_{\text{reference gene}}$, ($\Delta Ct_{\text{unknown sample}}$), for the tested gene. Secondly, the difference between the $\Delta Ct_{\text{(calibrator)}}$ and the $\Delta Ct_{\text{(unknown sample)}}$ determines the $\Delta\Delta Ct_{\text{(unknown sample)}}$. This value is then used to define the fold changes in expression level between the unknown sample and the calibrator control condition ($2^{-\Delta\Delta Ct\,(\text{unknown sample})}$).

	Calibrator (untreated/WT situation)	**Unknown sample (treated/mutant)**	
Tested gene	Ct	Ct	
Reference gene	Ct	Ct	
Subtraction Ct	**$\Delta Ct_{\text{(calibrator)}}$ -**	**$\Delta Ct_{\text{(unknown sample)}}$**	**= $\Delta\Delta Ct_{\text{(unknown sample)}}$**

4.1.5.b Determination of a reference gene in the study system

One of the fundamental parameters to select for qPCR analysis is a correct reference gene. The reference gene needs to be expressed homogeneously in the system studied. Numerous reports showed that the choice of a reference gene depends on the model studied (Ling and Salvaterra, 2011). In theory, housekeeping genes are expressed in most types of cells as they are required to maintain the basic metabolic activities of cells. However, studies have shown that many so-called 'housekeeping genes' are expressed in a tissue-specific manner and that in some cases their level of expression within a cell population can vary significantly (Larionov *et al.*, 2005, Ling and Salvaterra, 2011). Several reference genes are commonly used, including principally *glyceraldehyde- 3-phosphate-dehydrogenase* (*gapdh*), *β-actin* and *ribosomal RNAs* (rRNA). Other mRNAs are also utilised occasionally, for example *histone H3* and *cyclophilin*. *β-actin* was one of the first RNAs to be used as an internal standard, and it is still advocated as a quantitative reference for RT-qPCR assays. The analysis of *β-actin* mRNA in *Drosophila melanogaster* showed that this housekeeping gene was expressed at moderately abundant levels in most cell types and encodes a ubiquitous cytoskeleton protein (Ling and Salvaterra, 2011). The RNA encoding GAPDH is ubiquitously expressed and moderately abundant in zebrafish. It is frequently used as an endogenous control for quantitative RT-PCR analysis because, in certain experimental systems, its expression seemed constant through time (Pei *et al.*, 2007, Winer *et al.*, 1999).

For my experiments, two genes, *β-actin* and *gapdh*, were tested for consistency through time to be validated as reference genes (section 4.2.2). In agreement with the findings of Pei *et al.*, (2007), good consistency was found with *gapdh* but not with *β-actin* for detection in qPCR in zebrafish.

4.1.6 Further investigating gene expression in single cells

To study the cell to cell variability in melanocyte population, a method to investigate gene expression in single cells was tested. For this study, the objective was to characterise the cell to cell variability of expression of four melanocytic genes, *mitfa, sox10, dct* and *tyrp1b.* At a single cell level the low quantity of starting material is always a major difficulty, therefore, the first technique developed was the single cell nested PCR which allowed us to use two rounds of amplification. Expression of both *mitfa*, a melanocyte marker, and *ltk*, an iridophore marker, was investigated at two time points, an early timepoint, 23 hpf (melanoblasts cells), and a late timepoint, 72 hpf (melanocyte cells). The efficacy of reverse transcription was investigated by using newly made cDNA from single cells and gene expression was amplified successfully. In this Chapter, the results of studying forty single cells, at 23 hpf and 72 hpf, by RT-nested PCR are described. The objective of this experiment was simply to ask whether gene expression was detectable or not and coexpressed, or not, in cells at these timepoints. Unfortunately, it was not possible to extend these experiments to single cell RT-qPCR. After performing qPCR on cDNA isolated from single cells as previously experimented for nested PCR, the gene expression

amplification failed. The single cell qPCR technique was not validated. In this Chapter, we detail the intent of testing single cell RT-qPCR investigating *dct* at 48 hpf.

4.1.7 Aims and approach

In this Chapter, data have been collected and analysed to pave the way to future quantitative modelling of the melanocyte GRN. The objective was to collect quantitative data to improve the understanding of the genetic variability of melanocytic genes via establishing a method of quantifying gene expression in five cell pools *ex-vivo*. The relationship between *sox10* and *mitfa* expression during melanocyte development was always a key focus of interest.

Firstly, quantitative data were investigated by analysing mean expression level of *mitfa*, *dct* and *tyrp1b* in the bulk melanocyte population. cDNA from pooled embryos were collected at 23 hpf, 30 hpf, 36 hpf, 48 hpf and 72 hpf and were analysed. Secondly, the heterogeneity of *mitfa*, *dct*, *tyrp1b* and *sox10* expression was statistically assessed at these time points. Thirdly, both the relative and the absolute expression levels of *mitfa*, *dct*, *tyrp1b*, and *sox10,* were presented and analysed in ten samples of five cells by qRT-PCR. Fourthly, the existence of a potential chromatoblast precursor was tested by investigating the expression profile of *mitfa* and *ltk* in forty single cells at 23 hpf and 72 hpf, by nested RT-PCR. These results could hint at the potential existence of pluripotent, or bipotent, precursor marked by *mitfa* expression at early stages. By developing a technique of quantification of gene expression in small pools of cells, we could define an approach which allowed us to go further in the characterisation of the melanocytic gene expression through time.

4.2 Results

4.2.1 Calibrating the parameters for gene expression detection

In our experiments, we used the SYBR Green I kit (Wittwer *et al.*, 1997). The reliability of the qPCR rests upon the quality of the standard curve and the analysis of the melting curve. Both of these processes are standardised procedures which describe the reliability and the efficacy of the primer sets to target and amplify the wanted cDNA sequence. This section's objective is to document the standardised calibration of the primer sets which was undertaken to specifically target each of the DNA sequences with optimal qPCR efficiency (E). The melting curve analysis is also described here.

Each mRNA sequence was synthesised and reverse transcribed *in vitro* to produce a highly concentrated pure sample of each cDNA sequence. The protocol used for reverse transcription was the same protocol as described for reverse transcribing similarly concentrated mRNA samples extracted from whole embryos. The cDNA pool was then diluted five times on a logarithmic scale. Importantly, each single species cDNA solution was diluted in cDNA reverse transcribed from plant extracted RNA (*Arabidopsis sp.*, kindly given by Dr R. Scott lab, University of Bath) to replicate the cell/embryo cDNA solution biological diversity in proportion for each cDNA concentration. The plant cDNA was diluted to low concentration in MiliQ water, and used to dilute the single species cDNA solutions.

The standard curve is a standard measure of efficiency of detection with specific primers. Consequently, it was not a control for a certain experiment, it was a standardised procedure to assess the efficiency (E) of the qPCR reaction (not of the reverse transcription), meaning to assess the reproducibility of the proportionate relationship between amplifications and concentrations in diluted samples. All the reactions preceding the amplification, such as the RT, had to be homogeneous to preserve the proportionality of concentration in the five samples. This is why it was not possible to first dilute the mRNA pool (logarithmic dilution) nor subsequently the use of different RT protocol (RT for whole embryo for highly concentrated samples and single cell/five cell pool RT protocol for lowly concentrated samples) for building the standard curves. A control for each specific experimental test was then required to assess expression levels using the specific experimental conditions.

SYBR Green I did not allow specific amplification of a sequence (which is the reason why it is very difficult to realise multiplex analysis with this kit). The specificity of the cDNA sequences amplified was assessed by the melting curves issued from standard amplifications. The melting curve of each amplified sequence was specific to the sequence as it depends on nucleotide content to determine the specific melting temperature (*Tm*). For each transcript targeted, the melting curve, showing the specific *Tm*, was presented to assess the specificity of the yield.

4.2.1.a Standard curve analysis

The efficiencies of the amplification reactions are a crucial parameter to assess for quantifying gene expression by qPCR. A variation of more than 10 % in PCR efficiencies for the target gene would not allow accurate quantification.

With a 100 % PCR efficiency (E), a logarithmic dilution (10x dilution) should give a difference between Ct(s) of 3.32 (every 3.32 cycles the amount of DNA amplified is 10 fold higher). qPCR efficiency (E) is related to the slope of the reaction by the following equation: [$E = 10^{(-1/slope)} - 1$]. If the slope of the standard curve is -3.32 then PCR efficiency is 100 %. PCR efficiency (E) between 90 - 110 % was acceptable (corresponding to a slope between -3.58 and -3.1) (Wong and Medrano, 2005). PCR efficiency (E) can be affected mainly by primer design, annealing temperature and Mg^{2+} concentration which can be optimised for maximising activity of the *Taq* polymerase.

Figures 4.06 to 4.11 show both the qPCR amplification of the five logarithmic dilutions and the standard curve built from the result of this amplification, *gapdh* (Fig. 4.06), *β-actin* (Fig. 4.07), *mitfa* (Fig. 4.08), *sox10* (Fig. 4.09), *dct* (Fig. 4.10), and *tyrp1b* (Fig. 4.11). For each figure, the amplification reactions showed an exponential amplification phase and reached a plateau. (Ct)s for amplification reactions were proportionate to sample concentration. The standard curve describes the PCR efficiency (E) and slope for each calibration. Slopes were comprised of between -3.56 and -3.18 which corresponded to PCR efficiency within the acceptable range (90 % and 110 %).

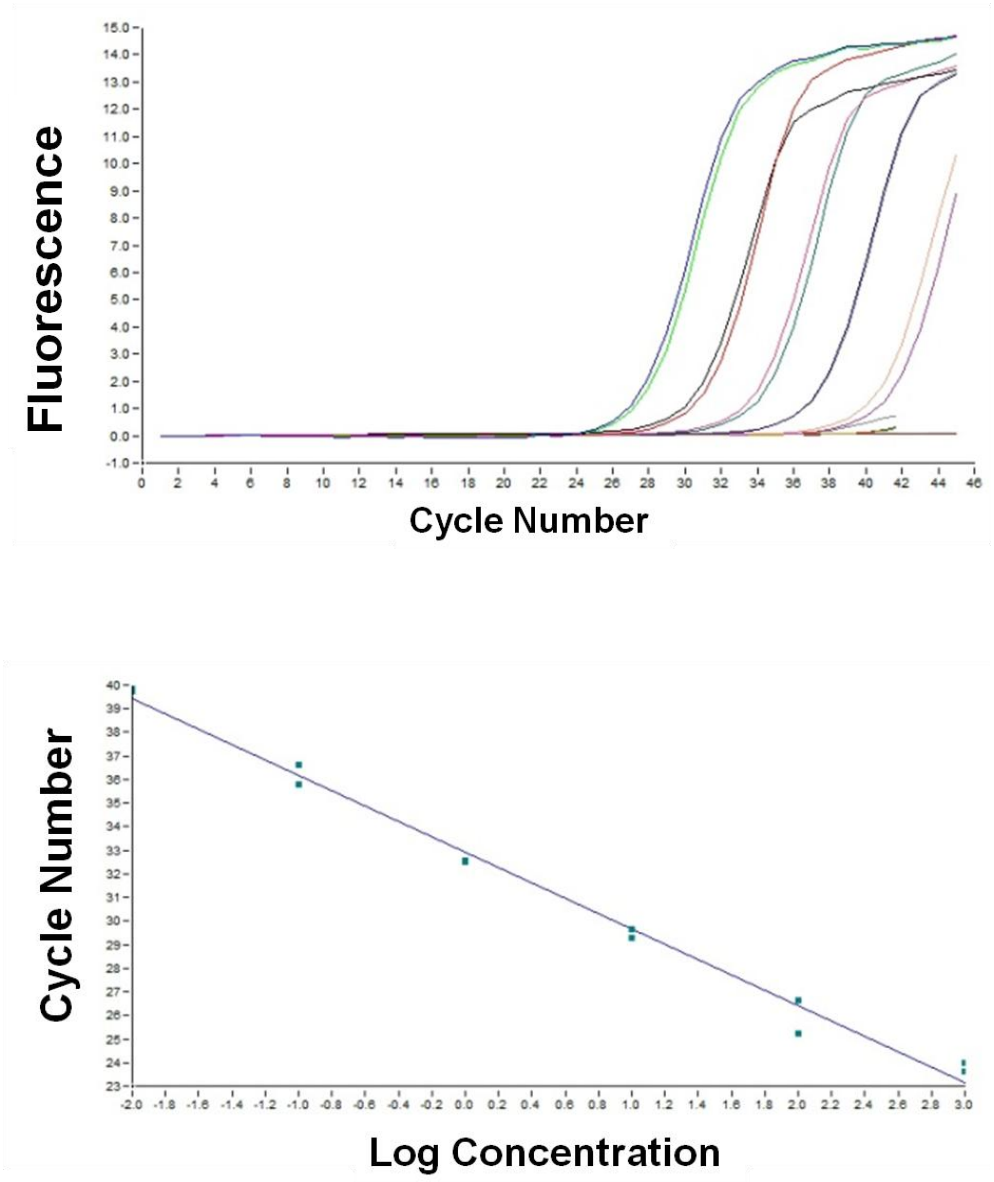

Figure 4.06: Standard amplification and standard curve for *gapdh*.

On the top panel, standard amplification; samples (duplicates are shown for each concentration) of five dilutions (1/10) of known concentration have been amplified in duplicates in order to build the standard curve shown on the lower panel. The qPCR efficiency was then calculated as well as the slope. slope = -3.257, E= 102.8 %

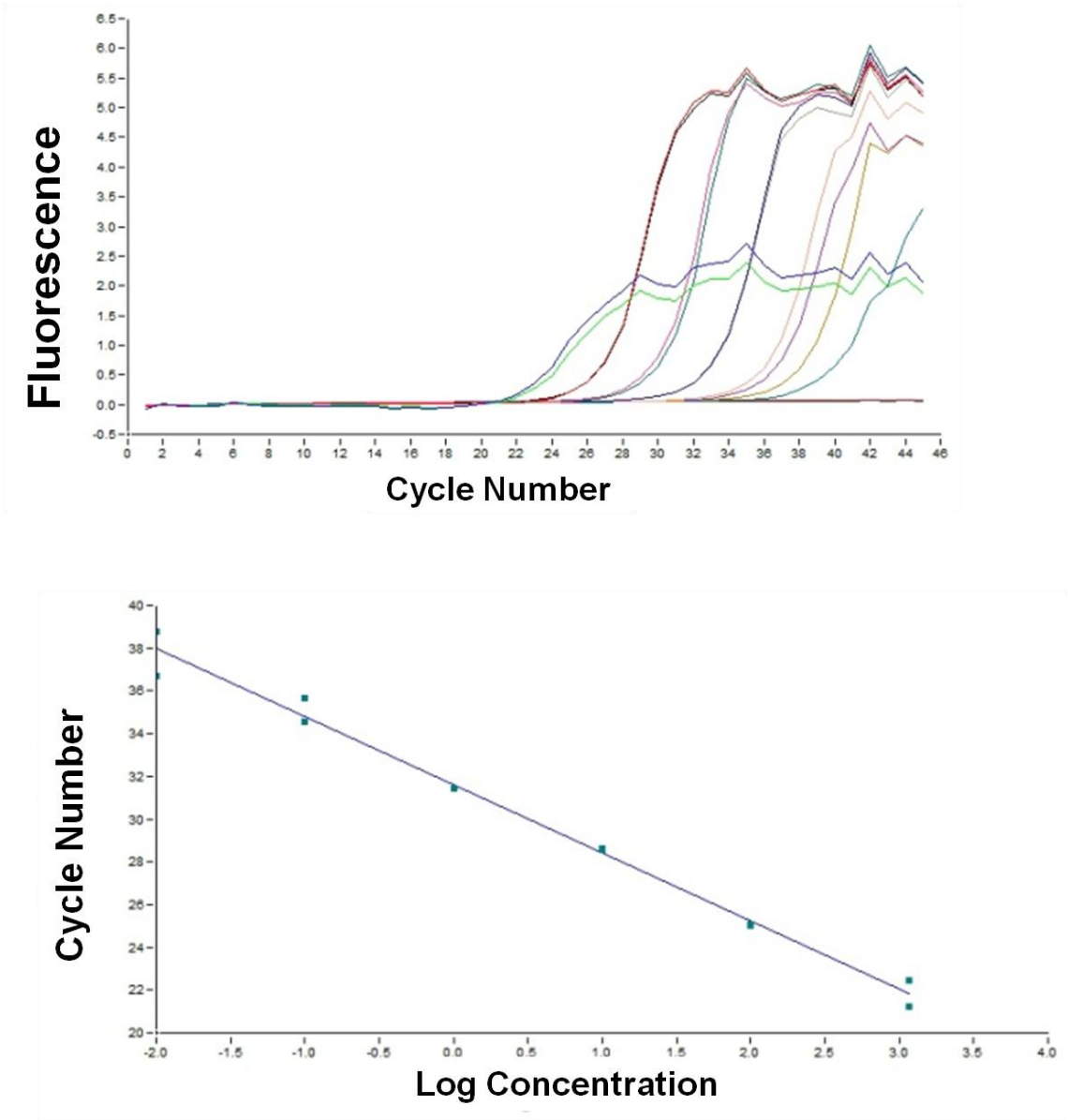

Figure 4.07: Standard amplification and standard curve for *β-actin*.

On the top panel, standard amplification; samples (duplicates are shown for each concentration) of five dilutions (1/10) of known concentration have been amplified in duplicates in order to build the standard curve shown on the lower panel. The qPCR efficiency was then calculated as well as the slope. slope = -3.185, E= 106.5 %

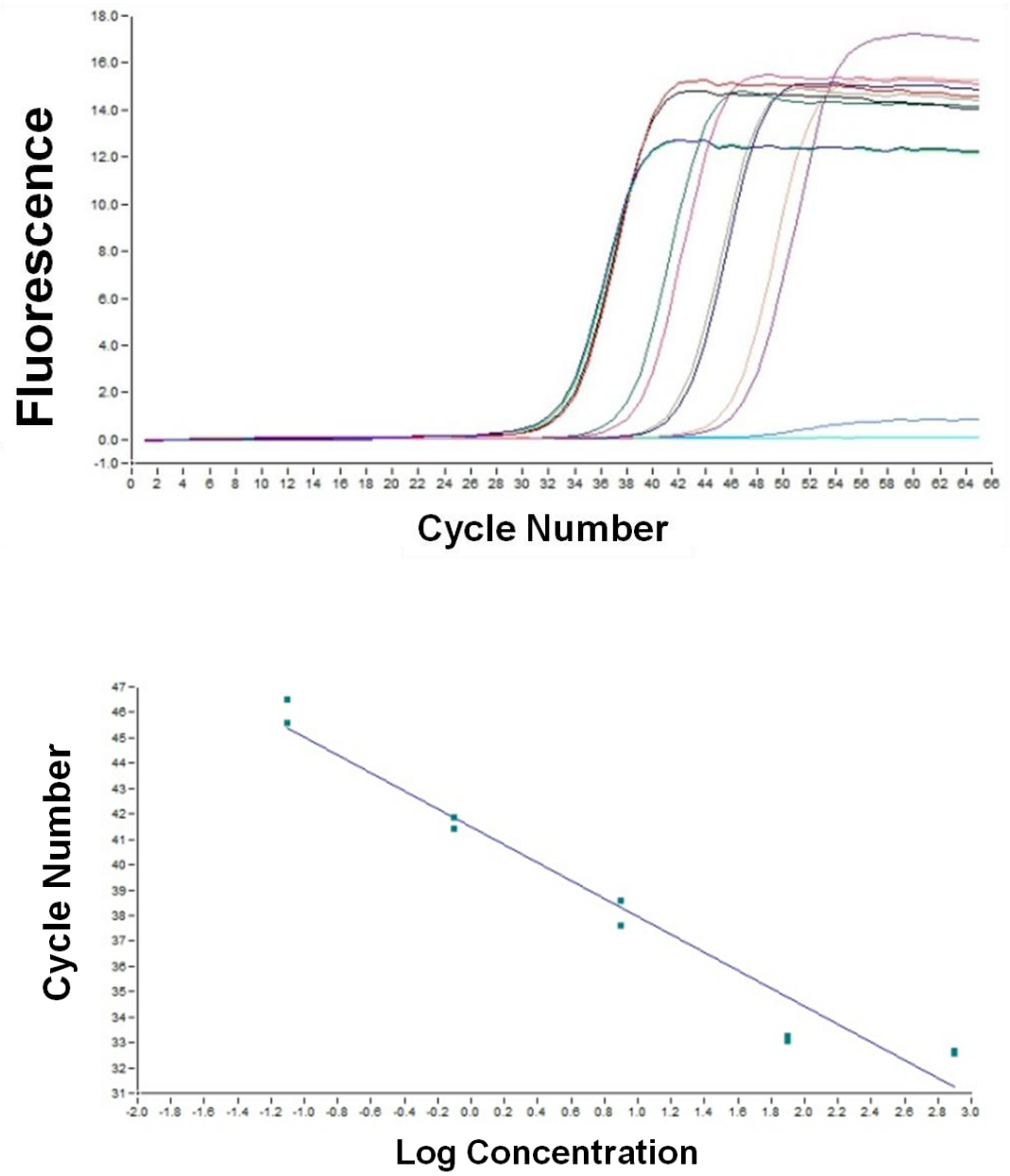

Figure 4.08: Standard amplification and standard curve for *mitfa*.

On the top panel, standard amplification; samples (duplicates are shown for each concentration) of five dilutions (1/10) of known concentration have been amplified in duplicates in order to build the standard curve shown on the lower panel. The qPCR efficiency was then calculated as well as the slope. slope = -3.553, E= 91.184 %

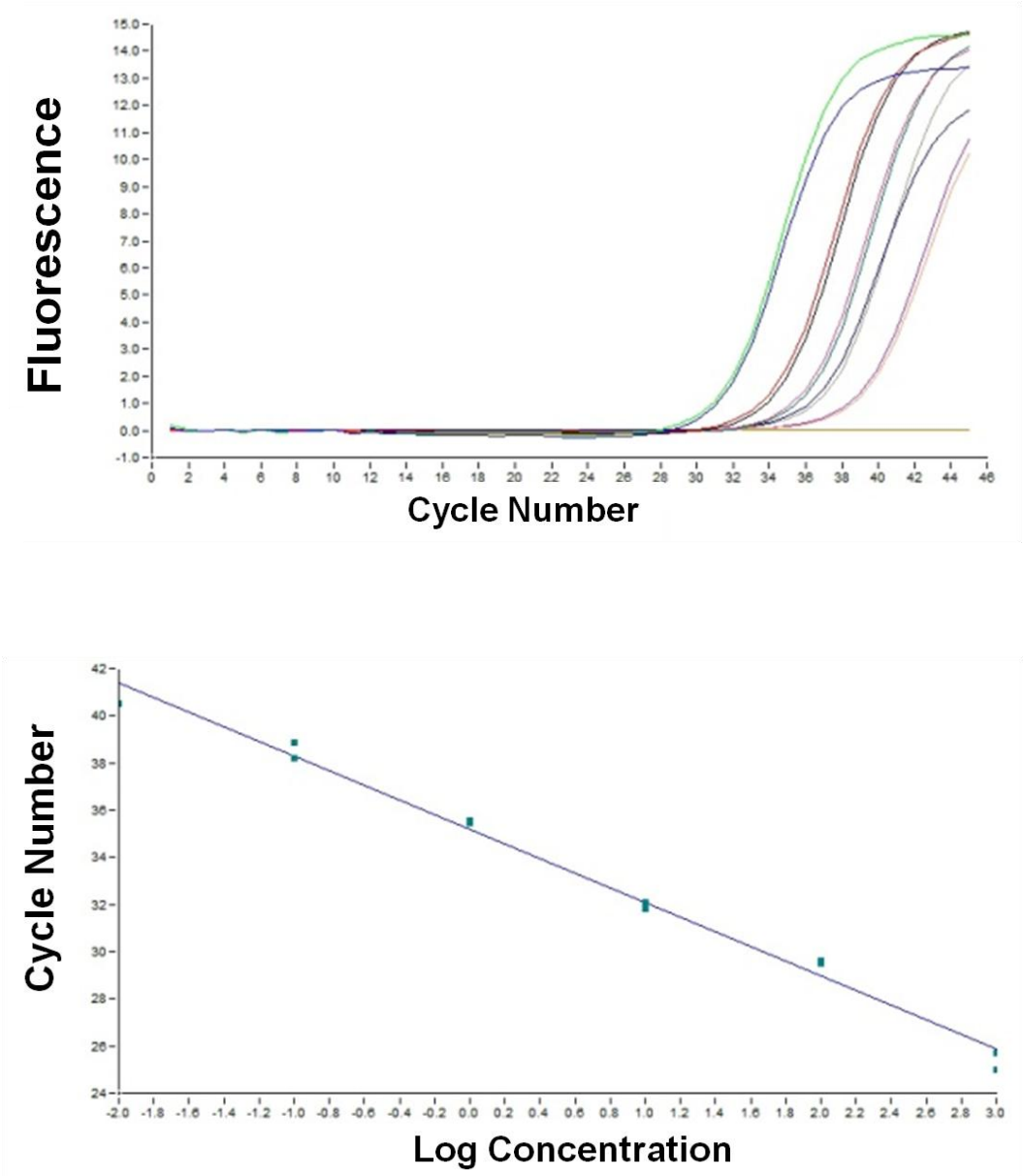

Figure 4.09: Standard amplification and standard curve for *sox10*.

On the top panel, standard amplification; samples (duplicates are shown for each concentration) of five dilutions (1/10) of known concentration have been amplified in duplicates in order to build the standard curve shown on the lower panel. The qPCR efficiency was then calculated as well as the slope. slope = -3.18, E= 106.3 %

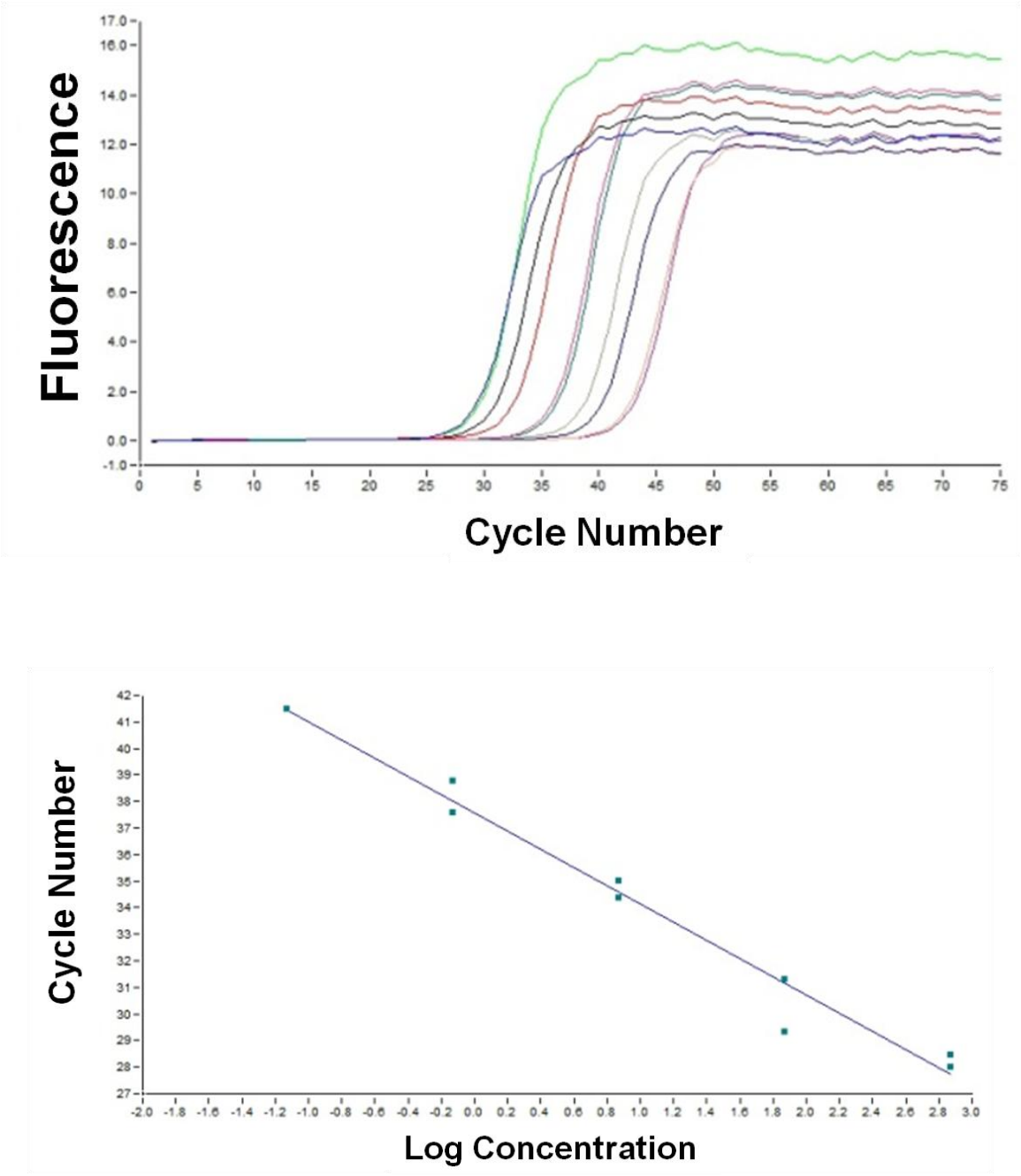

Figure 4.10: Standard amplification and standard curve for *dct.*

On the top panel, standard amplification; samples (duplicates are shown for each concentration) of five dilutions (1/10) of known concentration have been amplified in duplicates in order to build the standard curve shown on the lower panel. The qPCR efficiency was then calculated as well as the slope. slope = -3.438, E= 95.3 %

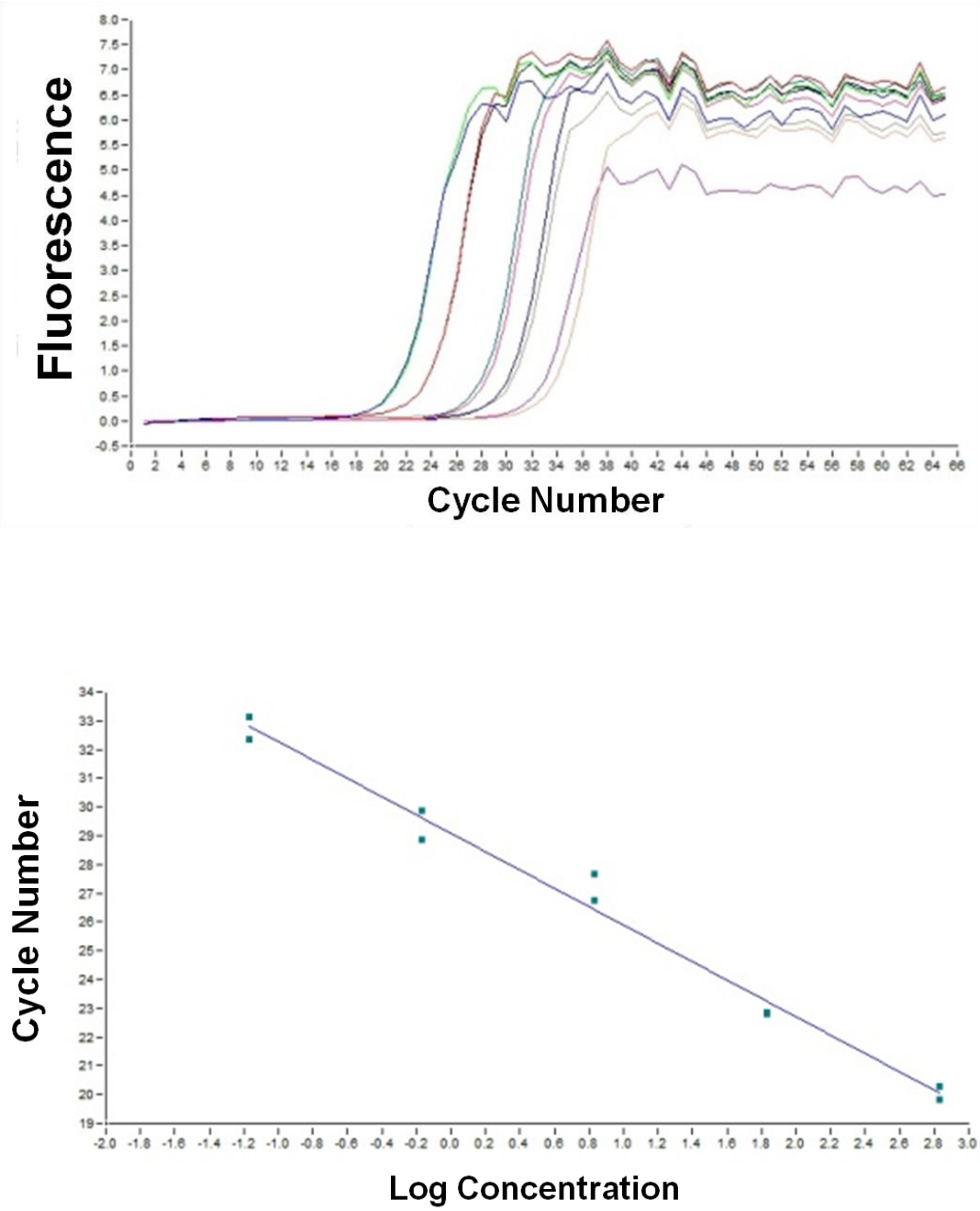

Figure 4.11: Standard amplification and standard curve for *trp1b*.

On the top panel, standard amplification; samples (duplicates are shown for each concentration) of five dilutions (1/10) of known concentration have been amplified in duplicates in order to build the standard curve shown on the lower panel. The qPCR efficiency was then calculated as well as the slope. slope = -3.192, E= 105.7 %

4.2.1.b Melting curve analysis

The melting curves were built by slowly increasing the temperature above the melting temperature (*T*m) of the amplicon and measuring the fluorescence. The *Tm* is defined by the temperature at which half of the DNA strands of the sequence are denatured (Breslauer *et al.*, 1986, von Ahsen *et al.*, 2001). The *T*m of the amplicon depends markedly on its nucleotide composition, thus, it is specific to each sequence and it allowed us to identify the specific signal obtained from the correct product. A characteristic melting peak at the melting temperature (*T*m) of the amplicon distinguished it from amplification of artifacts which would be expected melt at lower temperatures in broader peaks (Breslauer *et al.*, 1986). Comparing the melting temperature peak of each standard amplification reaction to the expected calculated peak for the sequence allowed detection of contamination, mispairing or any artifacts.

The specific melting curve temperature was calculated using the online Promega tool (http://www.promega.com/techserv/tools/biomath/calc11.htm#stacking). Estimation of the calculated value was adjusted to the Mg^{2+} (2 mM) and to the salt concentrations to prevent underestimation of this value in the context of these measurements in the reaction solution (von Ahsen *et al.*, 2001). Values for the *Tm* are presented in Table 4.2. Melting curves are presented in Figures 4.12-4.17 for all the primers used in the experiments (Fig.4.12, *gapdh*), (Fig.4.13, *β-actin*), (Fig.4.14, *mitfa)*, (Fig.4.15, *sox10*), (Fig.4.16, *dct*), (Fig.4.17, *trp1b*). This showed that the qPCR reaction specifically amplified the targeted sequences.

Table 4.2: Amplicon length and calculated melting temperature for each amplified sequence.

Gene	Amplicon length	Melting Temperature (*Tm*) in °C
gapdh	202 bp	89
β-actin	251 bp	89
mitfa	90 bp	84
sox10	428 bp	89
dct	166 bp	86
trp1b	98 bp	83

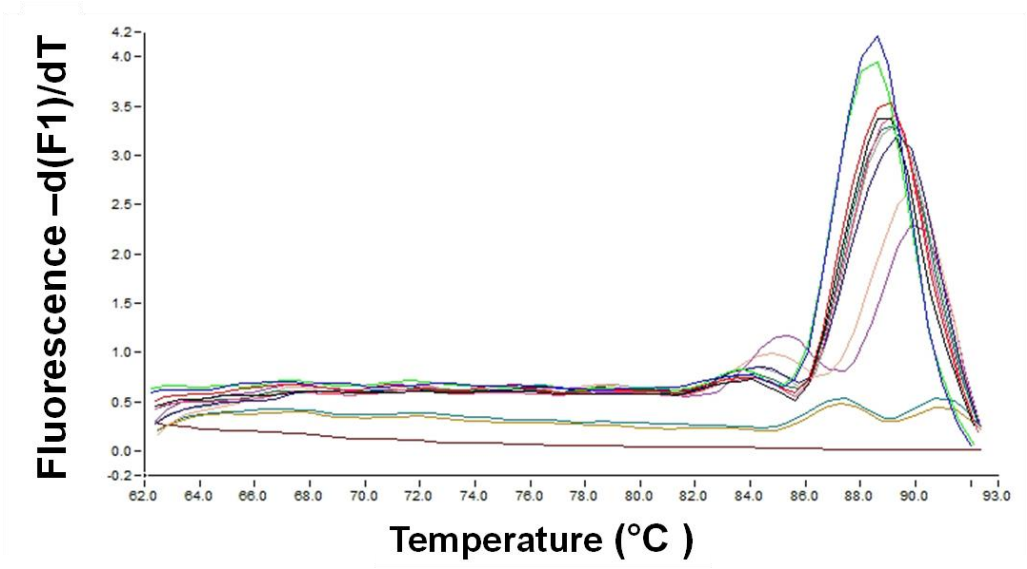

Figure 4.12: *gapdh* melting curve.

cDNA amplified with *gapdh* primers show a peak at 89 °C as predicted, showing the specificity of qPCR.

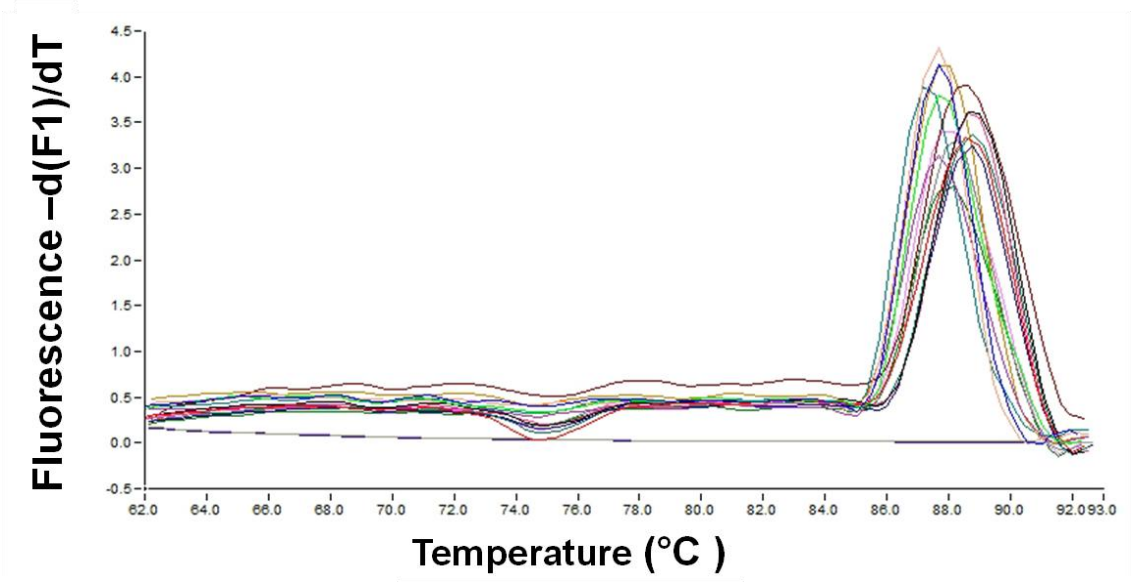

Figure 4.13: *β-actin* melting curve.

cDNA amplified with *β-actin* primers show a peak at 89 °C as predicted, showing the specificity of qPCR

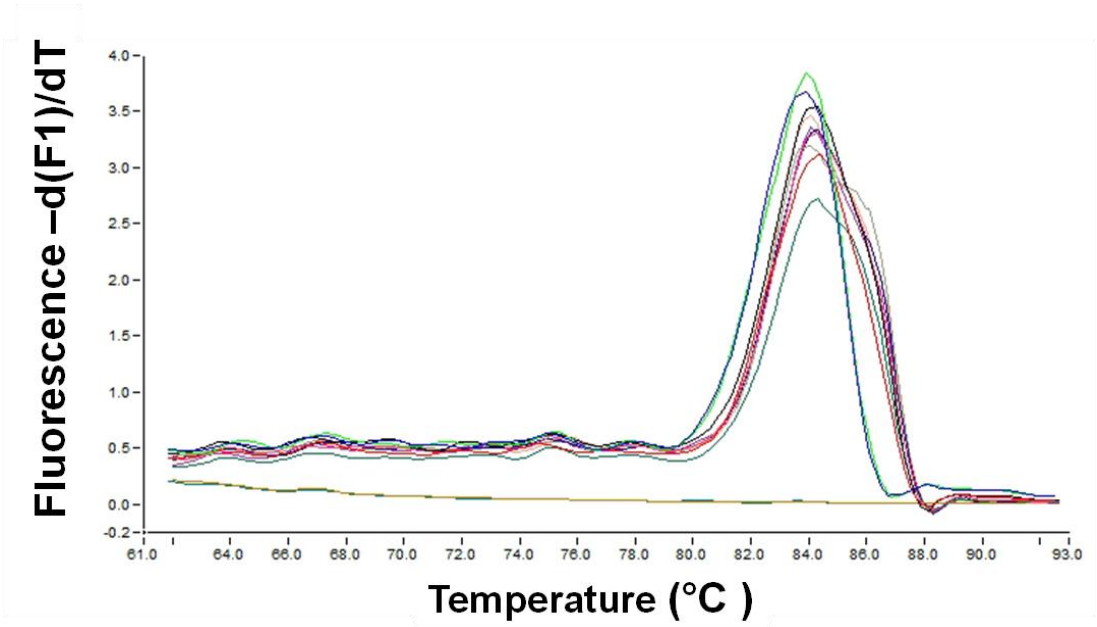

Figure 4.14: *mitfa* melting curve.

cDNA amplified with *mitfa* primers show a peak at 84 °C as predicted, showing the specificity of qPCR.

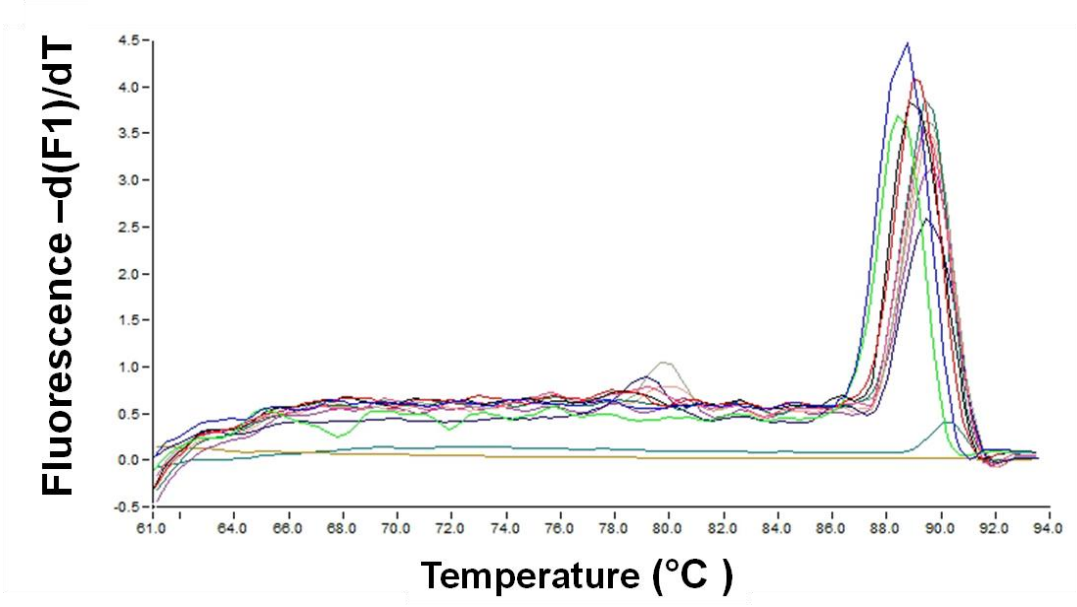

Figure 4.15: *sox10* melting curve.

cDNA amplified with *sox10* primers show a peak at 89 °C as predicted, showing the specificity of qPCR.

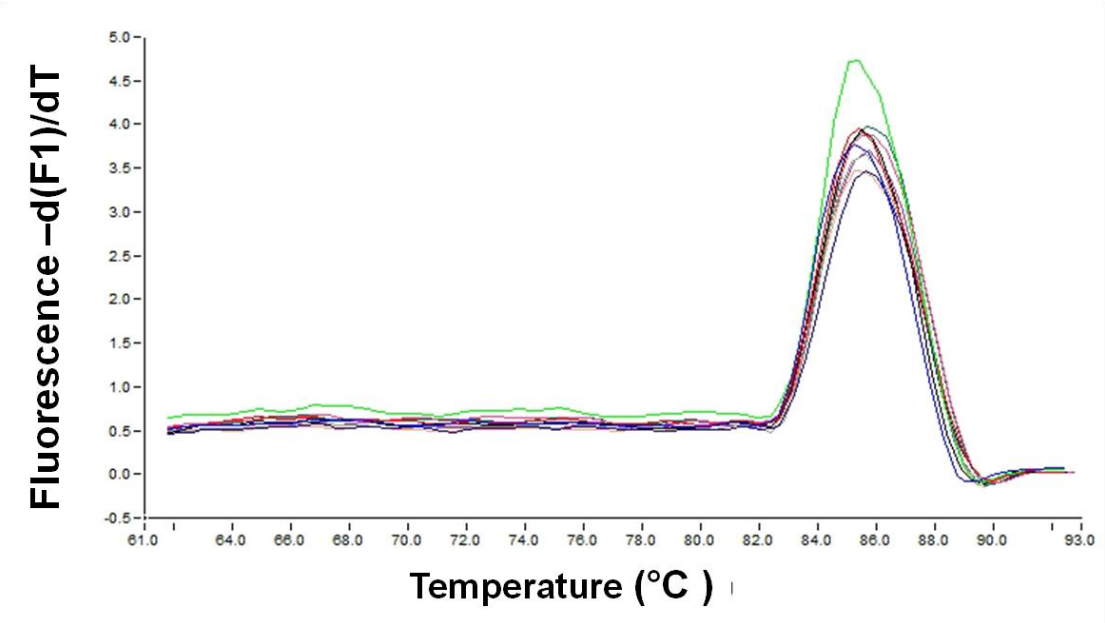

Figure 4.16: *dct* melting curve.

cDNA amplified with *dct* primers show a peak at 86 °C as predicted, showing the specificity of qPCR.

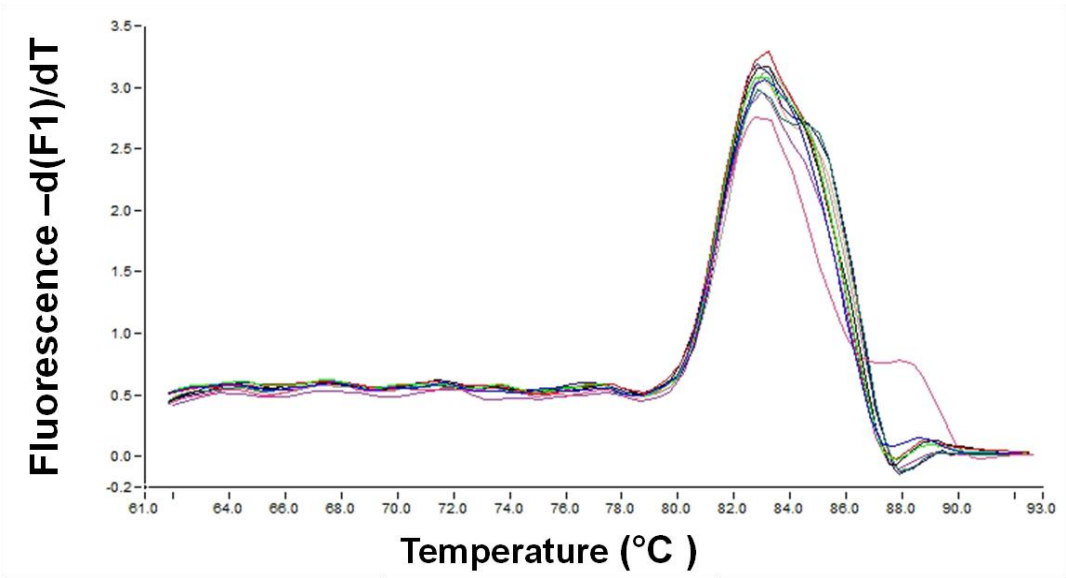

Figure 4.17: *trp1b* melting curve.

cDNA amplified with *trp1b* primers show a peak at 83 °C as predicted, showing the specificity of qPCR.

4.2.2 Establishing *gapdh* as a reference gene

4.2.2. a. Testing *gapdh* and *β-actin* as reference genes

Relative quantification analysis is based on the use of a reference gene to compare gene expression. Expression of the reference gene is characterized by the fact that it does not significantly vary between systems. For this experiment, two reference genes were tested, *gapdh* and *β-actin*. The variability of *gapdh* and *β-actin* expression level was determined through time, both in whole embryos and in random sampling of melanoblasts and melanocytes. The variance of expression levels was statistically tested through repeated samples using one-way ANOVA, two-tailed test.

β-actin and *gapdh* were tested in fifty pooled embryos at different timepoints, in triplicate samples. *β-actin* expression was tested at 30 hpf, 36 hpf, 48 hpf and 72 hpf, and was found to be significantly variable ($p = 0.0001$) (Figure 4.18). In contrast, *gapdh* expression was tested at 23 hpf, 30, hpf, 36 hpf, 48 hpf and 72 hpf, and its variance was not significantly changing ($p = 0.11$) (Figure 4.19). Therefore, *gapdh*, but not *β-actin*, was found to be homogeneously expressed in the system. Furthermore, *gapdh* expression variability was tested in ten repeated samples of five cells at five different time points and no significant variation was found between samples (in *sox10*-GFP (+) cells at 23 hpf, Fig 4.20, $p = 0.5212$, at 30 hpf, Fig 4.21, $p = 0.3934$, in melanised cells at 36 hpf, Fig 4.22, $p = 0.189$, at 48 hpf, Fig 4.23, $p = 0.8825$, at 72 hpf, Fig 4.24, $p = 0.883$).

These tests showed that *gapdh* expression was homogeneous in NC cells, melanoblasts and melanocytes through time in zebrafish. Thus, it was suitable for use as an external reference gene for qPCR experiments. In contrast, *β-actin* showed significantly variation in the system

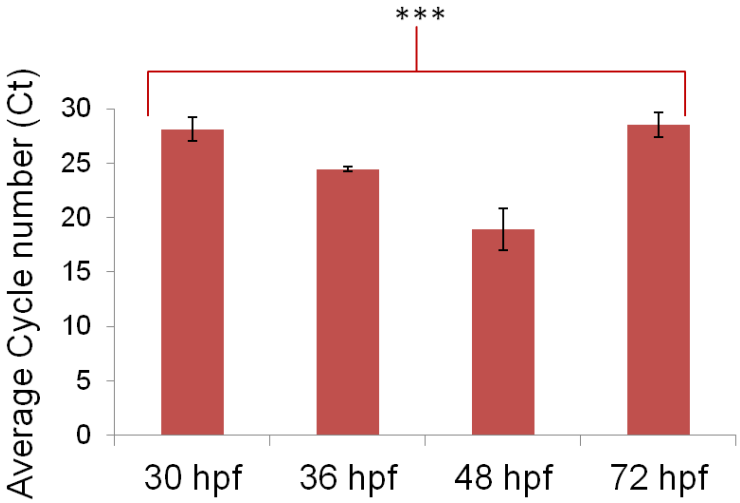

Figure 4.18: ***β-actin*** **expression level in pooled embryos varied significantly through time.**

Bars represent standard deviation of triplicates; one way ANOVA test, two-tailed, p = 0.0001, p<0.005, there is a significant difference in values between samples (***).

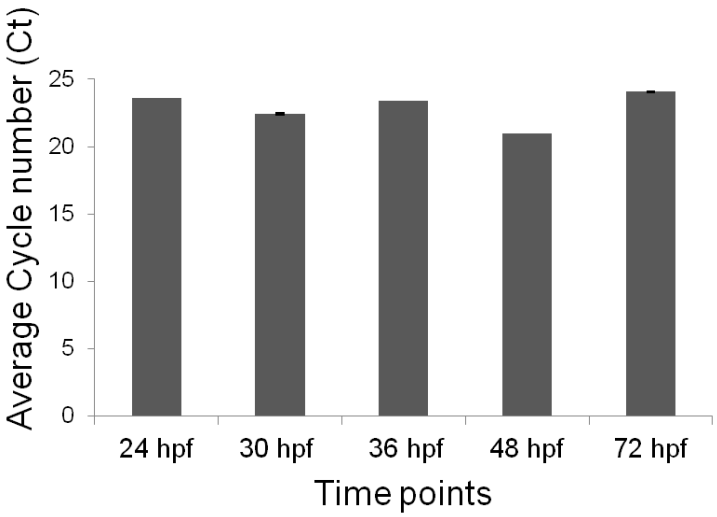

Figure 4.19: ***gapdh*** **expression level did not significantly vary through time, in pooled embryos.**

Bars represent standard deviation of triplicates, one way ANOVA test, two-tailed, p = 0.11. p>0.01.

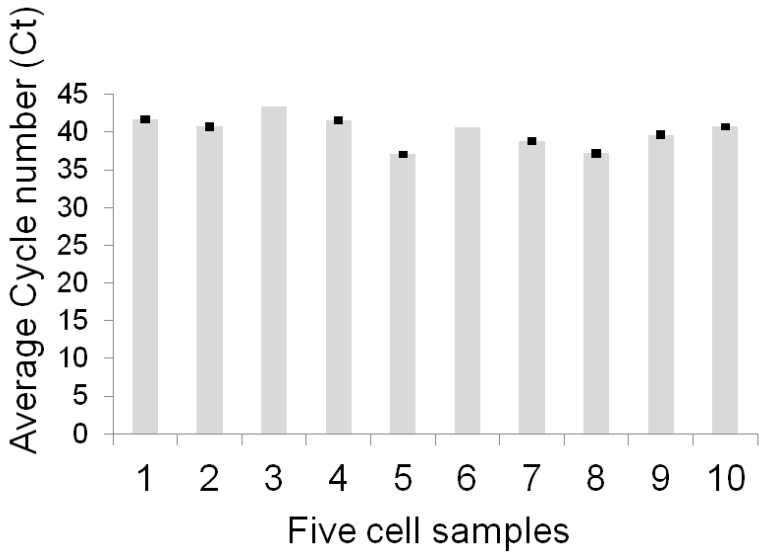

Figure 4.20: ***gapdh*** **expression level was homogeneous though ten repeated 5 cell samples at 23 hpf** ***(sox10*****-GFP cells).**

Bars represent standard deviation of triplicates, one way ANOVA test, two tailed, p =0.5212, p>0.005, there is no significant difference values through samples.

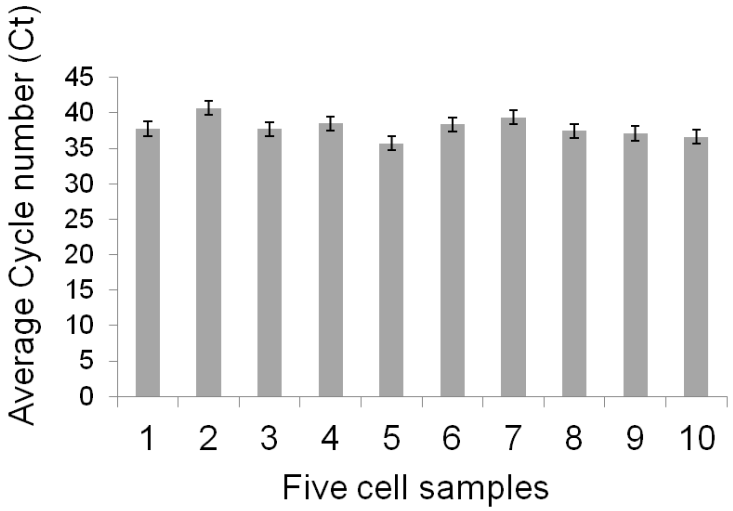

Figure 4.21: ***gapdh*** **expression level was homogeneous though ten repeated 5 cells samples at 30 hpf** ***(sox10*****-GFP cells).**

Bars represent standard deviation of triplicates, one way ANOVA test, two tailed, p =0.3934, p>0.005, there is no significant difference values through samples.

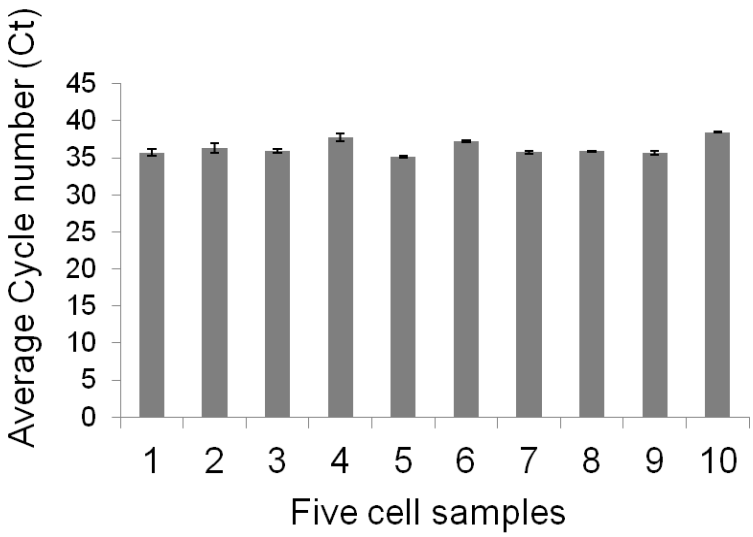

Figure 4.22: ***gapdh*** **expression level was homogeneous though ten repeated 5 cell samples at 36 hpf *(*melanised cells).**

Bars represent standard deviation of triplicates, one way ANOVA test, two tailed, p =0.189, p>0.005, there is no significant difference values through samples

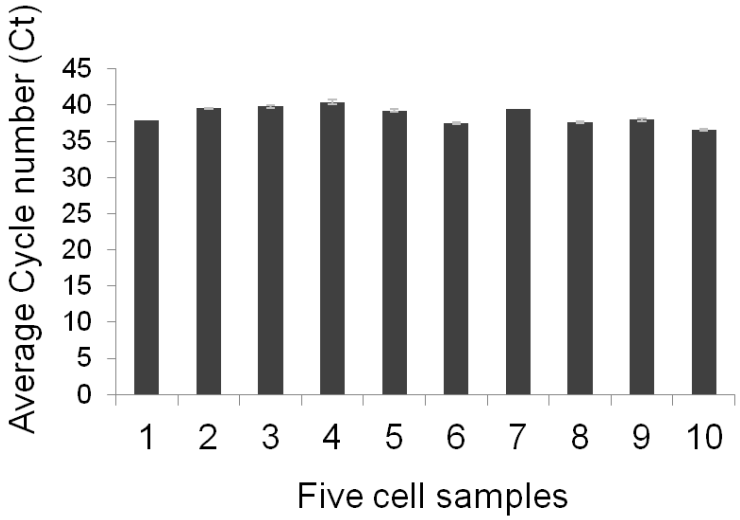

Figure 4.23: ***gapdh*** **expression level is homogeneous though ten repeated 5 cell samples at 48 hpf *(*melanised cells).**

Bars represent standard deviation of triplicates, one way ANOVA test, two tailed, p =0.8825, p>0.005, there is no significant difference values through samples.

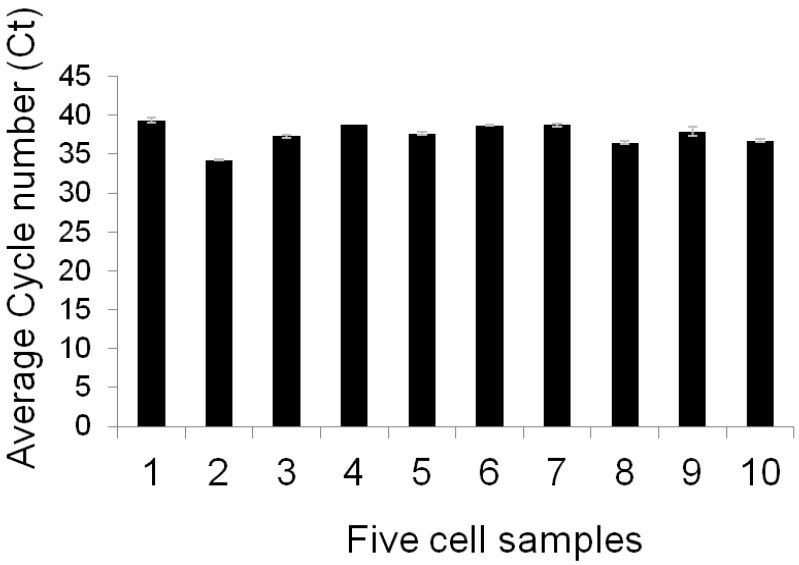

Figure 4.24: ***gapdh*** **expression level is homogeneous though ten repeated 5 cell samples at 72 hpf (melansied cells).**

Bars represent standard deviation of triplicates, one way ANOVA test, two tailed, p =0.8830, p>0.005, there is no significant difference values through samples.

4.2.3 Relative quantification of melanocyte specific gene expressions in pooled embryos

Having validated primer sets, protocols and a control reference gene, we next investigated the quantitation of gene expression in the embryo. First, gene expression was analysed in whole embryos, to obtain an average measure of transcript abundance at each stage. In this experiment, expression levels of *mitfa,* and of the two melanocytic genes *dct* and *tyrp1b*, were investigated in fifty pooled embryos (minus head which were omitted to exclude expression of genes such as *dct* in the RPE). *sox10* expression was not investigated here as its expression at 23 hpf stage marks all NC cells (Dutton *et al.*, 2001, Carney *et al.*, 2006). Gene expression was investigated at 23 hpf, 30 hpf, 36 hpf, 48 hpf and 72 hpf to observe changes in the developing melanocyte lineage at a population level.

In order to compare expression through time, the 23 hpf time point was established as the "calibrator" sample. All expression levels were expressed compared to the 23 hpf expression level for each specific gene (23 hpf = 100). The Livack method (delta-Ct) was applied to the data and statistics were calculated using the REST 2009 software which takes qPCR efficiencies into account. This allows randomisation which increases the robustness of the test. Data are presented in Figures 4.25 and the statistical results are shown in Table 4.3.

The Livack analysis method showed that *mitfa* expression level was lower at 30 hpf compared to 23 hpf. After 36 hpf, *mitfa* expression seemed to decrease in embryos and it was found to be significantly decreased at 72 hpf compared to the expression at 23 hpf. However, an increase is observed at 48 hpf. These results could suggest that *mitfa* was expressed more broadly at 23 hpf than at 30 hpf in NC cells. Consequently, if we relate these measurements to WISH investigating melanocytic genes in embryos at 72 hpf and showing exclusive expression in melanocytes, this *mitfa* expression decrease could be related to the restriction of *mitfa* expression to the melanocyte lineage through time. In contrast, *dct* expression significantly increased at 36 hpf, and then decreased until 72 hpf. *tyrp1b* expression seemed to increase and to be stabilised after 36 hpf when analysed with the Livack method. The increase of *dct* and *tyrp1b* expressions after 23 hpf suggests that these genes could have been expressed exclusively in melanoblasts since 23 hpf, and that their expression had increased while cells had gone through the differentiation process. The decrease of *dct* expression could be related to the reaching of a stable level of expression around 72 hpf. These speculative interpretations of the results are limited by the fact that many cells were pooled together and that expression level was averaged. Measuring gene expression in five cell pools could give more insight to the description of gene expression in the two cell populations.

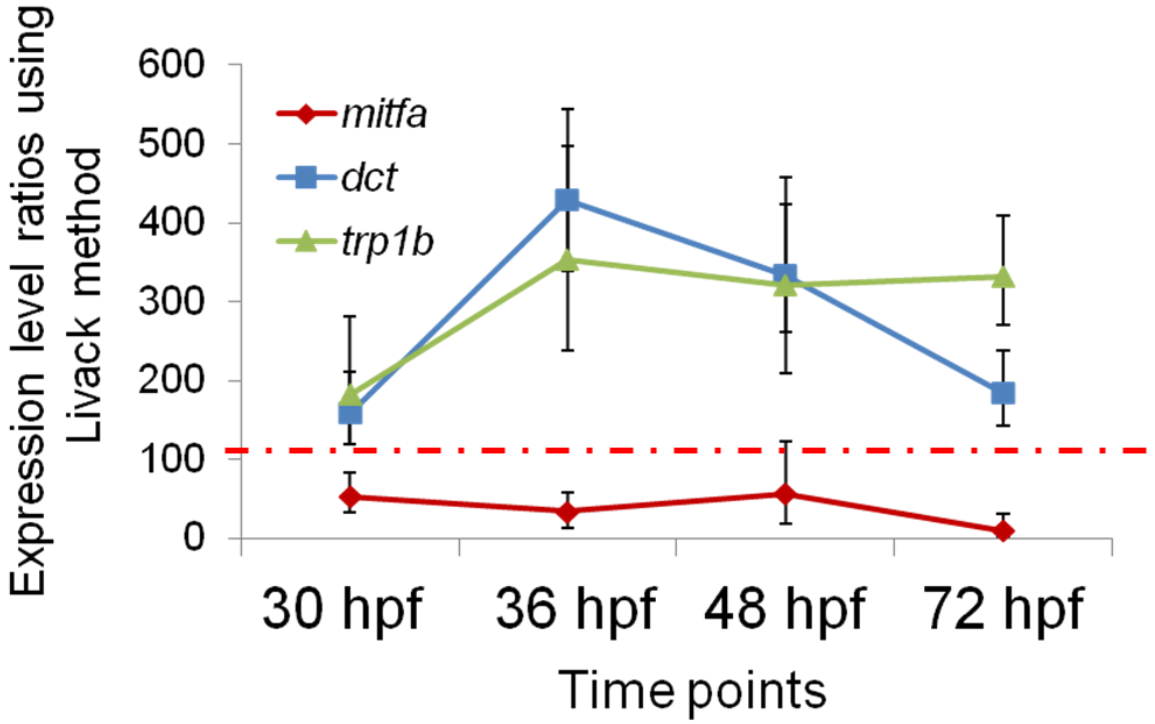

Figure 4.25: Graphs summarising the changes of average expression levels for *mitfa, dct a*nd *tyrp1b* in fifty pooled embryos using the Livack analysis methods.

Average expression level at 30 hpf, 36 hpf, 48 hpf and 72 hpf for each gene, after correction for the reference gene *gapdh* and using the 23 hpf expression level as a baseline (the red dotted line represent expression level at 23 hpf which was the baseline for comparison of gene expression at each timepoint). Bars represent standard deviation at each timepoint.

Table 4.3: p-values associated to the statistical test (REST 2009) comparing gene expression to the level of expression of the gene at the"calibrator" timepoint, 23 hpf.

	p-value at 30 hpf	p-value at 36 hpf	p-value at 48 hpf	p-value at 72 hpf
mitfa	0.003	0.031	0.067	0.033
dct	0.080	0.030	0.020	0.048
trp1b	0.049	0.044	0.025	0.016

4.2.4 Investigating whether gene expression level in pools of five cells is correlated with the variance in gene expression

In the next experiments, we investigated gene expression in five cell pools to describe expression on a finer scale and to evaluate expression variability in the two cell populations. For the first step, to assess the reliability of the technical replicates at low levels of detection, we tested the correlation between gene expression level and gene expression variability. More precisely, we tested whether the variability observed in the measurements of gene expression could be attributed to the technical unreliability and difficulty of measuring low expression levels. It was crucial to assess whether the variability of low gene expression was correlated to the fact that expression was low. A linear regression was used to test statistically whether or not technical difficulties in measuring low expression levels were responsible for the variability or not.

The objective of this test was to determine whether low expression level was significantly associated with high variances. Gene expression was measured in each of the ten samples of five cells at each of five timepoints and absolute and relative expression levels were determined in each case. The series of Ct(s) collected for both relative and absolute quantification experiments were plotted against their variances. Figure 4.26 shows the results of the linear regression tests for each gene at each timepoint. The results are presented in the graphs (each point shown on the graph corresponds to the test applying the average gene expression level in the ten samples collected for both relative and absolute quantification analyses (shown as the average Ct) against the variance of this series of values); the p-values which allow assessing for the significance of the test; and the R^2 values which indicate how much of the variation in expression level was explained by the expression level. The graphs show the line corresponding to the linear model. Further to the results of the linear regression, it is important to take account of the distribution of the data points on, and between, the graphs as the distribution of the data gives a sense of the relative sizes of variance and expression compared between the genes.

When data were taken altogether, no significant correlations between the variances and expression levels were found ($p = 0.1319$, $R^2 = 5.66$ %) (data not shown). When plotted individually, the test showed no significant correlation between the variances and expression levels for the low expression genes; *sox10* ($p = 0.6352$, $R^2 = 9.19$ %); *mitfa* ($p = 0.051$, $R^2 = 32.99$ %); *trp1b* (*trp1b* $p = 0.7291$, $R^2 = 10.72$ %). Interestingly for *gapdh* ($p = 0.003$ $R^2 = 65.43$ %) and *dct* ($p = 0.006$ $R^2 = 58.53$ %) the test showed a significant correlation between gene expression level and variance of gene expression. These genes were expressed at "high" levels (Ct(s) are grouped in the lowest part of graph for *gapdh*, under 40 in samples of five cells, and under 52 for *dct)* meaning that this correlation did not relate to the fact that high variances were associated to low expression levels. The plot corresponding to *gapdh* test in Figure 4.26 shows that all points were grouped together suggesting that the variances and the levels of expression (the series of Ct(s)) at each timepoint varied within a very tight spectrum (this confirmed previous analysis of the variability of *gapdh* in section 4.2.2). The information shown in the graph explains the significant p-value found here by suggesting that the Ct(s) and the variances of the series

were both very low. This result did not suggest that there was technical difficulty for the reproducibility of measurements for *gapdh*. The results for *dct* showed that three series of values seemed to show high variance, however, the expression level were not particularly low (Ct(s) all under 52 in five cell samples). Consequently, this correlation was not an indicator of the loss of reproducibility when measuring gene expression at lower levels but rather it is likely the result of a low number of data points. However, it remains possible that the variability of *dct* expression had been partly related to detection therefore, in the analyses of *dct* expression level measurements and *dct* variability, this point will be discussed. Altogether, these data suggest that technical detection of low expression level was not a major factor affecting the measurement of biological variability in these genes' expression.

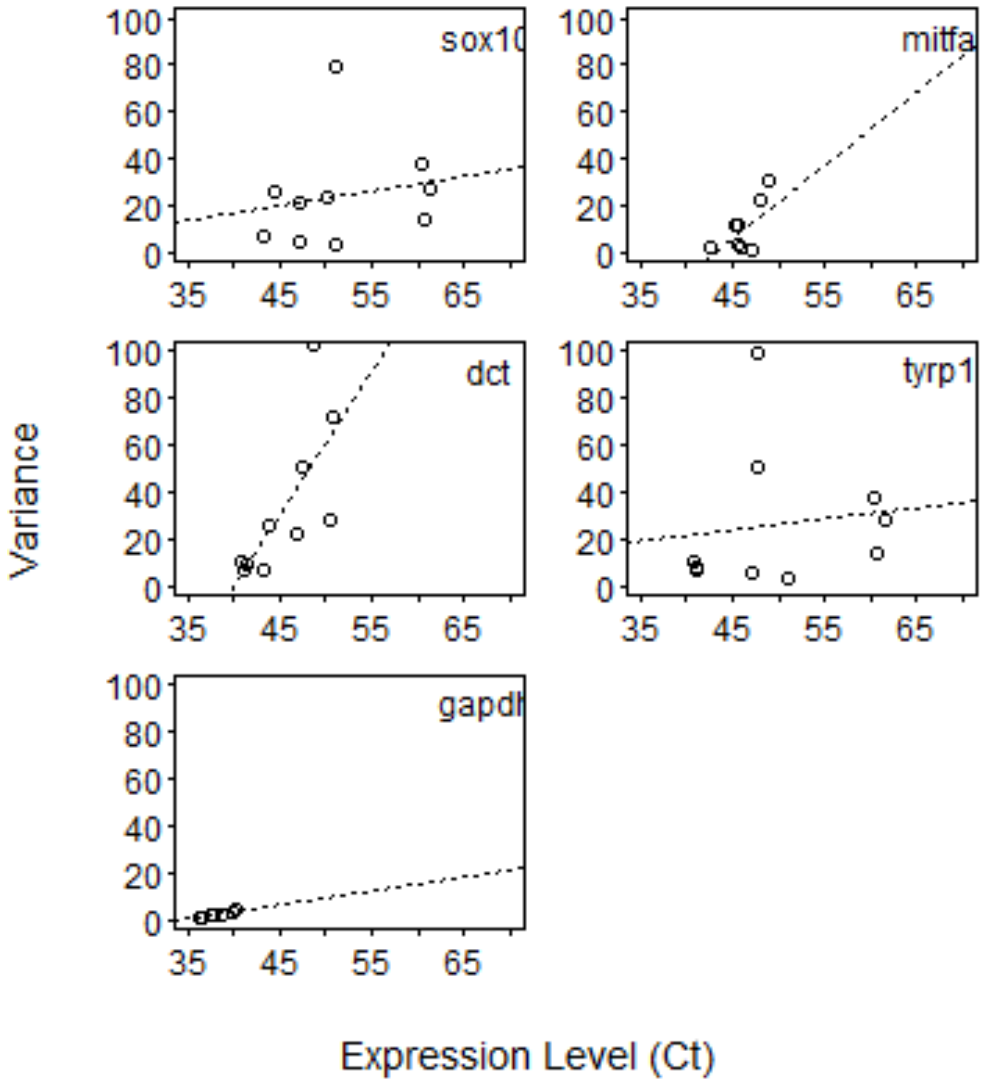

Figure 4.26: Test of correlation between expression levels and variances for each gene.

The series of gene expression levels (Ct(s)) measured in ten samples for both absolute and relative quantification experiments, at each timepoint (23 hpf, 30 hpf, 36 hpf, 48 hpf and 72 hpf) were used to determine averages and variances of each series [2 $_{(\text{series of ten samples})}$ * 5 $_{(\text{timepoints})}$ = 10 $_{(\text{series in total for each gene})}$)]. The variance of each series was then plotted against the average of each series and linear regression was used for each gene. The lines correspond to a projection of the best model fit from the linear regression. Top left panel *sox10* ($p = 0.5842$, $R^2 = 8.10$ %), top right panel, *mitfa* ($p = 0.05$, $R^2 = 32.99$ %), second panel left, *dct (*$p = 0.0161$ (*), $R^2 = 47.76$ %), second right panel, *tyrp1b* ($p = 0.7207$, $R^2 = 10.6$ %), lower panel, *gapdh* ($p = 0.003$, $R^2 = 65.43$ %).

4.2.5 Determining the heterogeneity of melanocytic gene expression in the NC cell population and in the melanocyte population

4.2.5.a. Investigating variability of gene expression through time

The variability of gene expression was statistically tested using the method of stochastic profiling as described in Quaranta *et al.*, (2010). A random selection of *sox10*-GFP NC positive cells (presumably including melanoblasts, glioblast and other precursors), were selected at 23 hpf and 30 hpf from transgenic fish , whereas at 36 hpf, 48 hpf and 72 hpf we specifically selected melanocytes (i.e. melanin+ cells) at (Dutton *et al.*, 2001)). At early stages (23 hpf, 30 hpf) the cell population was expected to be highly heterogeneous for melanocytic genes. In contrast, the variability of the genes in melanocytes, at later stages, 36 hpf, 48 hpf and 72 hpf was expected to be decreased.

To establish the variability of gene expression, we used both the cycle data Ct collected from the relative quantification experiment and from absolute quantification experiment. The differences of variances of the series of data were tested against the variance of gapdh at each time point for each gene. Differences in variances were statistically tested using Fisher test (one-tailed in R (Crawley, 2007). Variances were significantly different (i.e. displaying heterogeneity of expression) when the ratio of the (*gapdh* variance) / (gene tested variance) was greater than 3.7, which was the critical value defined by the test from the data (with DF=9, α=0.05, critical value: 3.7 from Fisher's F probability distribution tables). Figure 4.27 shows both graphs for analysis of relative and absolute quantification expression. The graphs allow us to visualise the significance by the three lines which correspond to different levels of significance of p-values ($p = 0.05$, $p = 0.01$ and $p = 0.001$). All the values plotted above these lines indicate a significant result i.e. that gene's expression is more variable in the 5 cell pools than the housekeeping control gene, and thus that the cells are likely heterogeneous for expression of that gene (Figure 4.27).

Both analyses using the Ct(s) collected for absolute and the relative quantification showed similar results when testing the significance of the test. At 23 hpf, only s*ox10* expression was stable in samples. *dct* and *trp1b* expression variances were significantly varying compared to *gapdh* and *mitfa* expression was also significantly different. This result suggested that at this stage, *mitfa*, *dct* and *tr1pb* were heterogeneous in the *sox10*-GFP cell population. At 30 hpf, only *dct* and *trp1b* were significantly varying compared to *gapdh*. Whether this result could suggest that both *mitfa* and s*ox10* expressions were restricted to the same precursor cells could be discussed. However it seems that *dct* and *trp1b* expressions remained significantly variable in the *sox10*-GPF (+) cell population suggesting that at this stage, more than one precursor type could exist in this population.

At 36 hpf, in the melanocyte population, the variances of *sox10* expression, *dct* expression and *trp1b* expression were significantly different from *gapdh*'s variance to a lesser extent. This result suggested that *dct* and *trp1b* expressions remained heterogeneously expressed in the melanised cells. In contrast, *mitfa* was not varying

significantly ($p>0.05$) when using the Ct(s) collected from absolute expression quantification, whereas, it was borderline when using Ct(s) of relative quantification experiment. These results showed that in melanised cells at 36 hpf, expression of *mitfa* was rather homogeneous while *sox10* expression was significantly heterogeneous. This result suggests that the melanised cell population could potentially be in a transition phase characterised by the stabilisation of *mitfa* and destabilisation of *sox10* expression. The low level of variability of *dct* and *trp1b* expressions suggests that the melanocyte population was not yet genetically settled at this stage. At 48 hpf, *sox10*, *mitfa* and *trp1b* were just above the first significance line ($p<0.05$) which corresponds to low, but significant level of heterogeneity compared to *gapdh.* The most variable gene was *dct* ($p<0.001$). *sox10* was expressed at low levels which suggested that its expression was decreased in the whole melanised cell population at this stage. *mitfa* expression was also decreased at this stage. This destabilisation of expression could suggest that an unknown regulatory event (epigenetic or presence of a new factor) was modifying the steady-state level of *mitfa* expression, to a new lower value. Analysing relative quantification data collected at 72 hpf showed that all genes seemed to be homogeneously expressed in the melanised cell population except *sox10* ($p<0.001$) (with *dct* borderline, just above threshold 0.05). Analysing the variances of Ct(s) collected for absolute quantification, *trp1b* and *dct* variances were weakly significantly ($p<0.05$) different from *gapdh* variance. These results could suggest that at 72 hpf, melanocytes had reached a relative stable state with relatively stable and high expression of *dct* and *trp1b*, and with stable and low expression of *mitfa* and unstable and low *sox10* expression.

In both experiments, these tests showed that the variances of melanocytic gene expression were reduced during melanocyte development implicating a decrease of heterogeneity of gene expression during lineage restriction. In contrast, s*ox10* expression heterogeneity was increased in melanocytes.

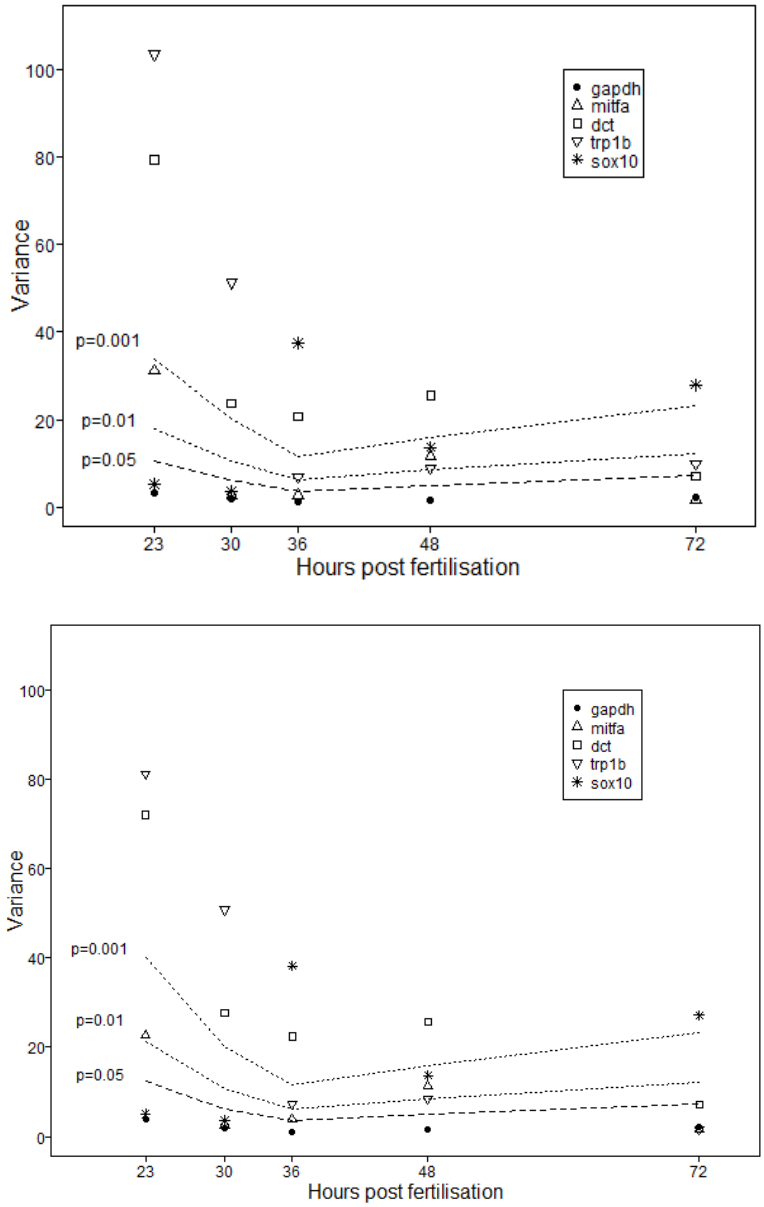

Figure 4.27: Testing *sox10* and melanocytic gene expressions heterogeneity during melanocyte lineage restriction.

The plots show the variances of gene expression data series (Ct(s)) at each timepoint. Analysis of the absolute quantification experiment is presented in the top panel and analysis of the relative quantification experiment is shown in the lower panel. The Fisher test shows the results of comparing the variances of each series (*mitfa*, *dct*, *trp1b* and *sox10* at each timepoint for both experiments) to the variance of *gapdh* at each timepoint. The dotted lines represent different levels of significance for the Fisher test (p = 0.05, p = 0.01 and p = 0.001). When the data points are above the line, variances were significantly different from those of *gapdh* at that level.

4.2.6 Quantifying gene expression level in five cell samples in both the NC cell population and the melanocyte populations

Quantification of gene expression during specification and differentiation in the small cell pools is presented here. In this experiment, qRT-PCR measurements were used to determine gene expression levels in repeated samples of five cells. Expression levels of *mitfa, sox10, dct* and *tyrp1b* were measured in ten independent 5-cell samples at 23 hpf, 30 hpf, 36 hpf, 48 hpf and 72 hpf. As before, *sox10*-GFP(+) NC cells were analysed at early stages (23 hpf and 30 hpf) and melanised cells were analysed at later stages (36 hpf, 48 hpf and 72 hpf). Data are shown in five graphs (Figures, 4.28. (23 hpf), 4.29. (30 hpf), 4.30 (36 hpf), 4.31 (48 hpf), 4.32 (72 hpf)). These graphs show the relative expression levels for each gene in each of the ten samples (1-10), and using *gapdh* as a reference gene. Each sample was run in duplicate and both values are presented in the graphs.

In most samples, the expression level measured in duplicates were highly consistent, suggesting good technical reproducibility. However, in ten cases (over the 200 duplicates presented, meaning in 5 % of the samples), the values for the duplicates were less consistent: at 23 hpf, for *sox10*, in sample 1, and *trp1b* in sample 6; at 30 hpf, for *trp1b* in sample 2 and 4 and *mitfa* in sample 1; at 36 hpf, for *trp1b* in sample 2 and 4; at 48 hpf for *trp1b* in sample 1 and 10, as well as *dct* in sample 7.

4.2.6.a Relative quantification of gene expression at 23 hpf in neural crest cells

sox10-GFP (+) cells were selected at 23 hpf and expression levels were measured in ten pools of five cells by qRT-PCR. Figure 4.28 shows relative expression levels in the ten samples. At this stage, *sox10* marks the NC cell population which probably contains several precursors, such as neuroglioblasts and melanoblasts in the specification phase. Consistent with this, there was considerable variation in the expression levels observed between samples. *trp1b* expression level was high in sample 1 (mean fold change ± s.e) (2300 ± 659)- sample 5 (1010 ± 20)- sample 6 (1750 ± 469) – and sample 8 (1000 ± 173), whereas *dct* expression was only highly expressed in sample 9 (1250 ± 264). *sox10* expression was particularly highly expressed in sample 1 (1550 ± 482). *mitfa* expression levels (from 100 ± 28 to 500 ± 132) seemed to be always close to *dct* expression level except in sample 9.

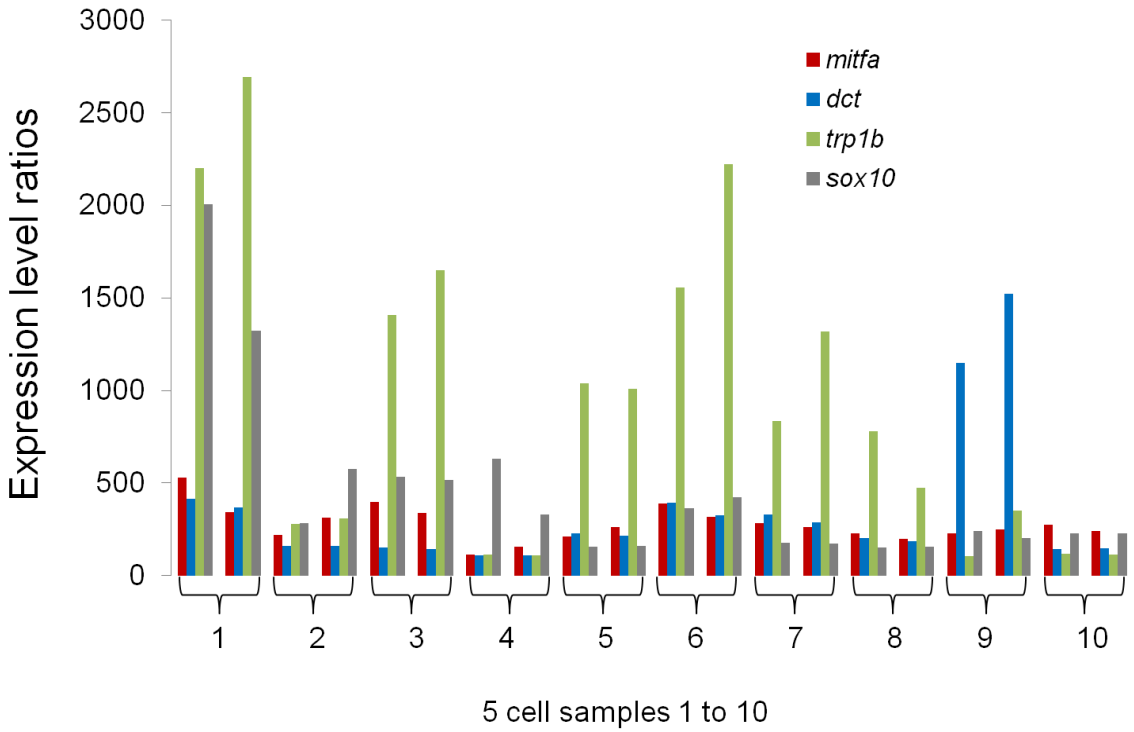

Figure 4.28: Relative quantification of *mitfa, dct, tyrp1b* and *sox10* by qRT-PCR in ten samples of five *sox10*-GPF+ cells, at 23 hpf.

Samples are numbered 1-10, and relative expression levels are shown (fold change), calculated as $1/\Delta(1/Ct)$ ($y = 1/\Delta(1/Ct)$), where $\Delta(1/Ct) = 1/Ct$ gene of interest – $1/Ct$ reference gene (*gapdh*). Samples were run in duplicates. The expression levels determined for each gene in each replicate are shown.

4.2.6.b Relative quantification of gene expression at 30 hpf in Neural Cest cells

At 30 hpf, *sox10*-GFP positive cells were selected and then expression levels were measured in ten pools of five cells by qRT-PCR. Figure 4.29 shows relative expression levels in the ten samples. At this stage, *sox10* remained expressed in glial and other precursors such as melanoblasts which had probably started differentiating. In sample 2 (mean fold change ± s.e), (900 ± 633) – sample 4 (550 ± 400) and sample 7 (700 ± 102), *trp1b* expression level was high whereas *dct* expression was only highly expressed in sample 6 (818 ± 38). In contrast with the results from 23 hpf, here *sox10* expression seemed to be weakly expressed (from 100 ± 5 to 270 ± 17) and m*itfa* expression levels were high (from 300 ± 68 to 1200 ± 356) particularly in samples 1-2-6-7.

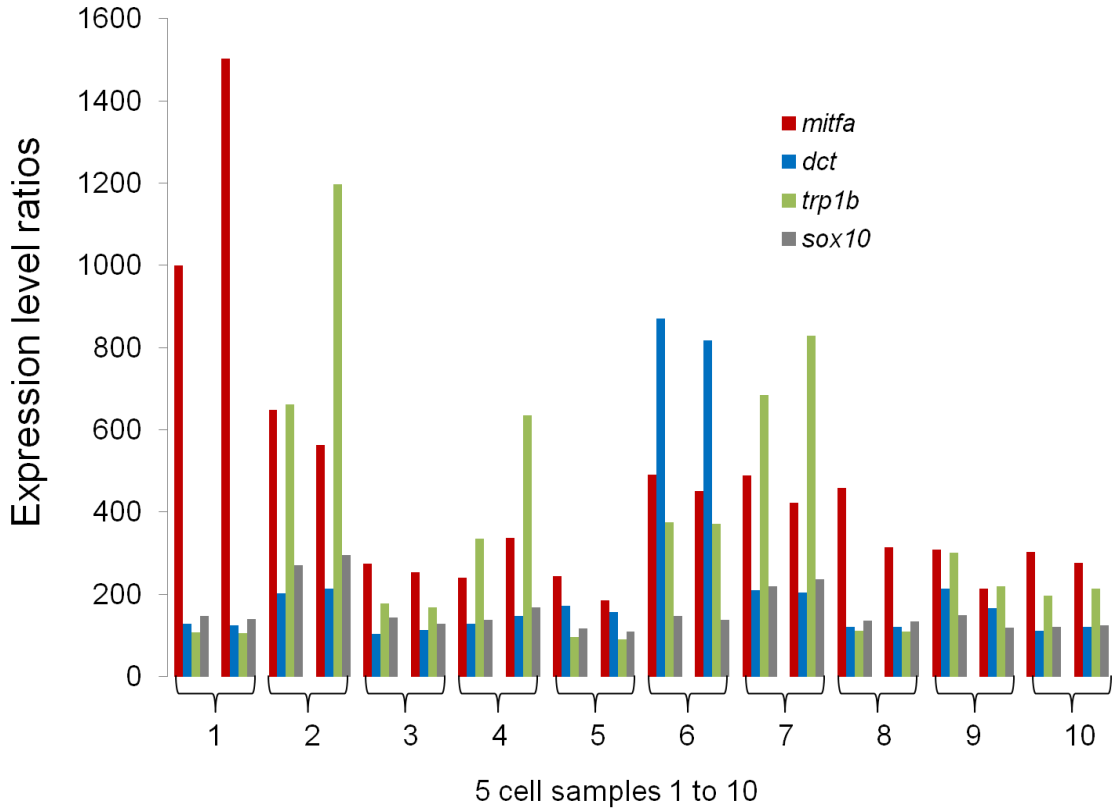

Figure 4.29: Relative quantification of *mitfa, dct, tyrp1b* and *sox10* by qRT-PCR in ten samples of five *sox10*-GPF+ cells, at 30 hpf.

Samples are numbered 1-10, and relative expression levels are shown (fold change), calculated as $1/\Delta(1/Ct)$ ($y = 1/\Delta(1/Ct)$), where $\Delta(1/Ct) = 1/Ct$ gene of interest – $1/Ct$ reference gene (*gapdh*). Samples were run in duplicates. The expression levels determined for each gene in each replicate are shown.

4.2.6.c. Relative quantification of gene expression at 36 hpf in melancoytes

Melanised cells were selectively analysed at 36 hpf and expression levels were measured in ten pools of five cells by qRT-PCR. Figure 4.30 shows relative expression levels in the ten samples. At this stage cells selected were differentiating melanocytes. In sample 4 (mean fold change ± s.e), (850 ± 519)- sample 5 (630 ± 17)- and sample 6 (1100 ± 356), *trp1b* expression level was high whereas *dct* expression was only highly expressed in sample 5 (680 ± 120). *sox10* expression was weakly expressed (from 70 ± 0.6 to 100 ± 7.3) in all samples and *mitfa*, as well as, *dct* (except in sample 5) was expressed at a consistent level (190 ± 26 to 210 ± 5).

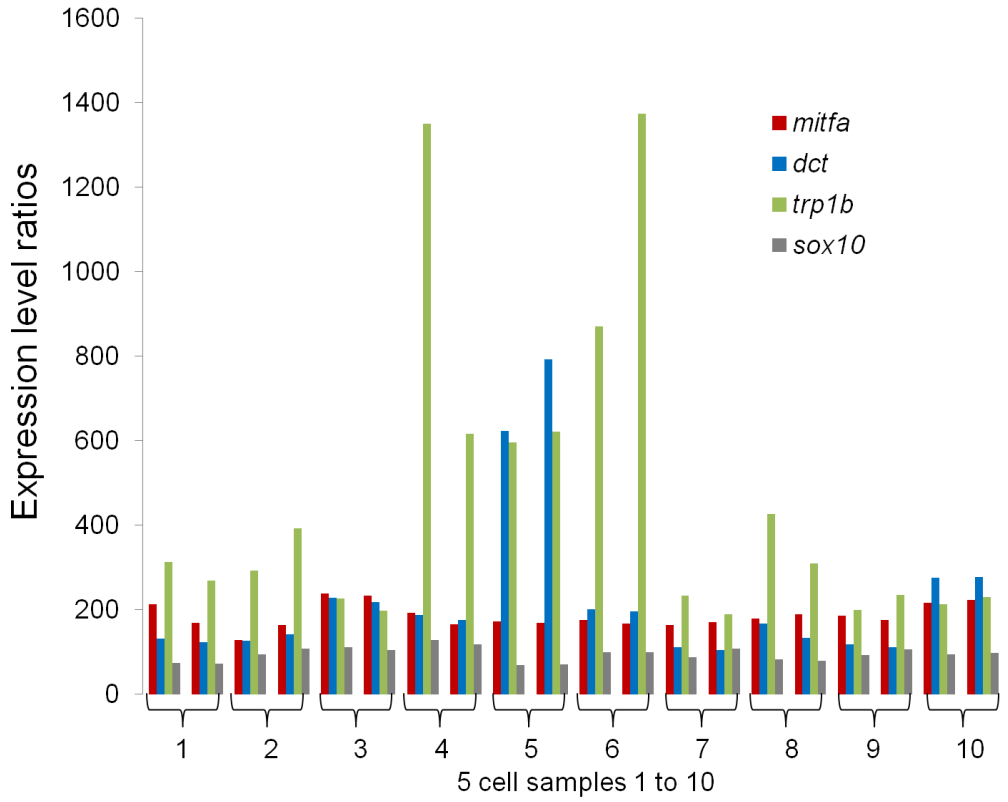

Figure 4.30: Relative quantification of *mitfa, dct, tyrp1b* and *sox10* by qRT-PCR in ten samples of five melanised cells, at 36 hpf.

Samples are numbered 1-10, and relative expression levels are shown (fold change), calculated as $1/\Delta(1/Ct)$ ($y = 1/\Delta(1/Ct)$), where $\Delta(1/Ct) = 1/Ct$ gene of interest – $1/Ct$ reference gene (*gapdh*). Samples were run in duplicates. The expression levels determined for each gene in each replicate are shown.

4.2.6.d Relative quantification of gene expression at 48 hpf in melanocytes

At 48 hpf, melanised cells were analysed and expression level were measured in ten pools of five cells by qRT-PCR. Figure 4.31 shows relative expression levels in the ten samples. At this stage, melanocytes are still differentiating, increasing melanin content, for instance. In sample 1 (mean fold change ± s.e = 2010 ± 816), sample 5 (1400 ± 117)- and sample 8 (1200 ± 299), *trp1b* expression level was high whereas *dct* expression was expressed in a consistent manner (from 150 ± 10 to 490 ± 186) except in sample 7 (980 ± 546) in which it was expressed at higher level. *sox10* expression remained low in each sample (around 100 ± 17). *mitfa* expression seemed consistently expressed (from 200 ± 0.2 to 400 ± 241) at levels comparable to *dct* but slightly lower.

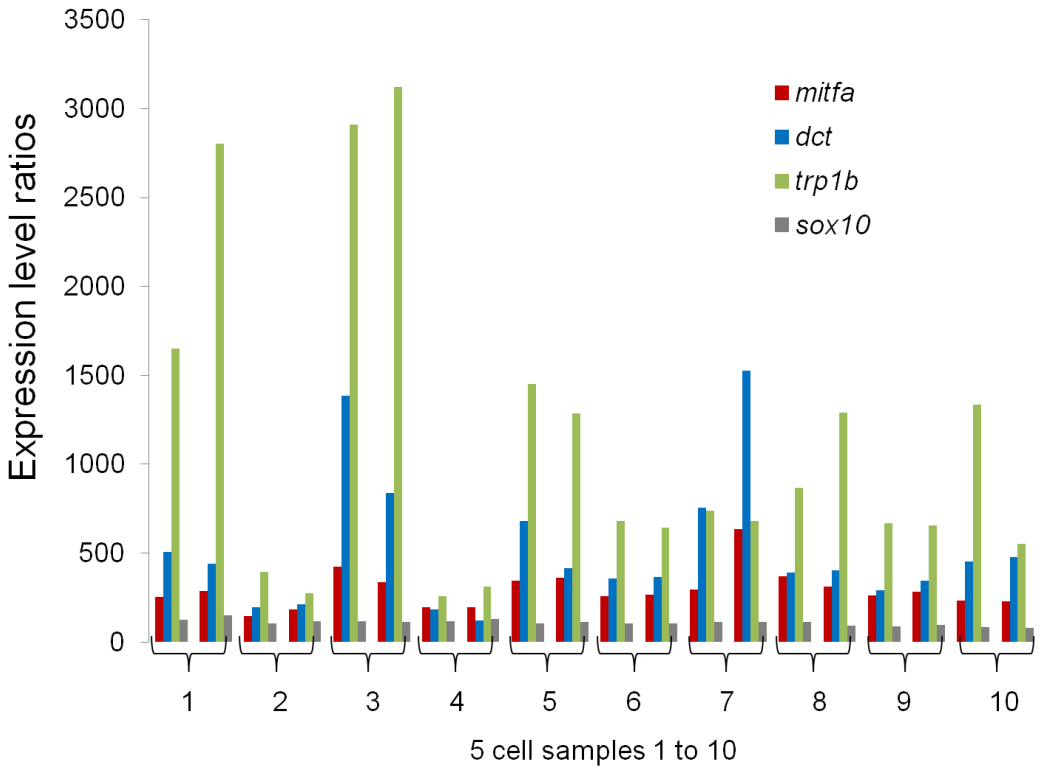

Figure 4.31: Relative quantification of *mitfa, dct, tyrp1b* and *sox10* by qRT-PCR in ten samples of five melanised cells, at 48 hpf.

Samples are numbered 1-10, and relative expression levels are shown (fold change), calculated as $1/\Delta(1/Ct)$ ($y = 1/\Delta(1/Ct)$), where $\Delta(1/Ct) = 1/Ct$ gene of interest – $1/Ct$ reference gene (*gapdh*). Samples were run in duplicates. The expression levels determined for each gene in each replicate are shown.

4.2.6.e Relative quantification of gene expression at 72 hpf in melanocytes

Melanised cells were selected at 72 hpf and expression levels were measured in ten pools of five cells by qRT-PCR. Figure 4.32 shows relative expression levels in the ten samples. At this stage, embryonic melanocytes are considered to be fully differentiated. In sample 7, (mean fold change ± s.e) (1210 ± 29) – sample 9 (1580 ± 255) – and sample 10 (1300 ± 255), *trp1b* expression level was high. Expression of *dct* remained consistent (from 100 ± 1.2 to 500 ± 30), whereas, expression of *mitfa* was decreased compared to expression at 48 hpf (around 250 ± 46). *sox10* expression remained low in each sample as at 48 hpf (around 100 ± 30).

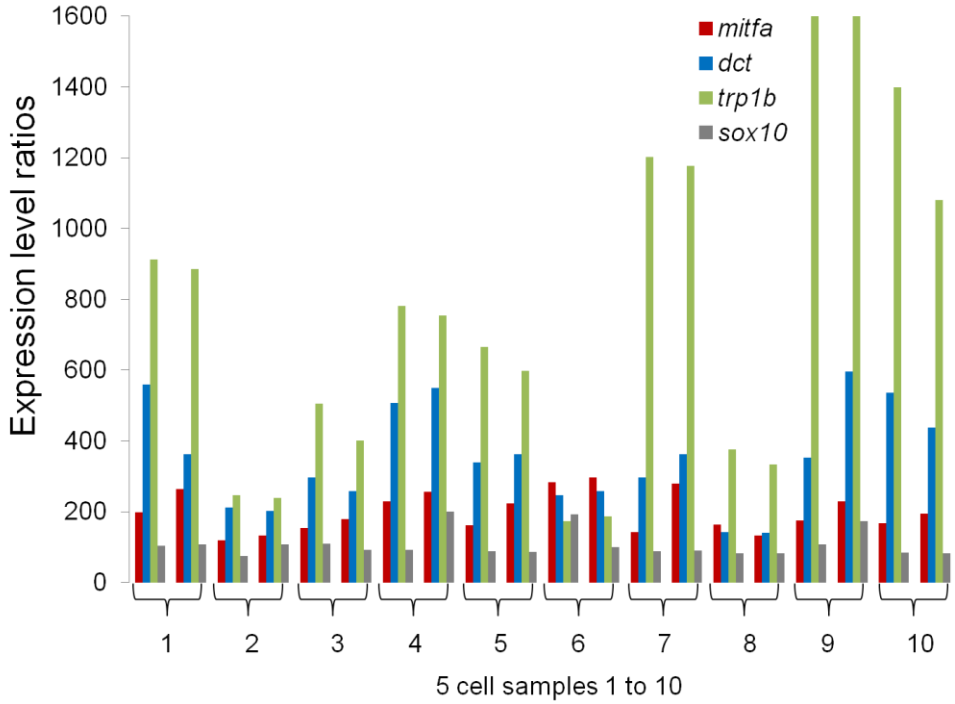

Figure 4.32: Relative quantification of *mitfa, dct, tyrp1b* and *sox10* by qRT-PCR in ten samples of five melanised cells, at 72 hpf.

Samples are numbered 1-10, and relative expression levels are shown, calculated as $1/\Delta(1/Ct)$ ($y = 1/\Delta(1/Ct)$), where $\Delta(1/Ct)$ = 1/Ct gene of interest – 1/Ct reference gene (*gapdh*). Samples were run in duplicates. The expression levels determined for each gene in each replicate are shown.

4.2.6.f Summarising relative expression level measured in five cell pools

The data collected here are summarised to better understand the changes in expression levels at each timepoint through the cell population (Figure 4.33). Gene expression levels measured for each gene were averaged at each timepoint for the ten samples, the standard deviation (bars) is shown for each series in the graph. To interpret these data, it is crucial to keep in mind that measurements were undertaken in NC cells at 23 hpf and 30 hpf and in melanocytes after 36 hpf.

At 23 hpf we observed that *trp1b* seemed highly expressed but with a high level of variability. At 30 hpf *trp1b* expression had decreased in NC cells. *sox10* expression decreased slightly from 23 hpf to 30 hpf. In contrast *mitfa* expression seemed to be slightly elevated. *dct* expression was relatively stable from 23 hpf to 30 hpf when averaging the data. To summarise these results, in NC cells we saw that *trp1b* expression seemed to be variable in the cell population (high and low levels), as was previously determined (section 4.2.5.). We observed that *sox10* expression seemed to be lowered in the cells. The boost of *mitfa* expression at 30 hpf compared to 23 hpf was not found in the study of *mitfa* expression in whole embryos. Therefore, whether this result could correspond to a fine boost of *mitfa* which was not detected in the whole embryo would have to be verified. *dct* expression seemed to be expressed at the same level, at 23 hpf and 30 hpf, which could suggest that *dct* was expressed in melanoblasts since 23 hpf.

As previously observed in whole embryo, *sox10* expression was low in melanocytes, after 36 hpf and *mitfa* expression was decreased. As expected, *trp1b* and *dct* expression levels were increased in melanocytes compared to when investigating NC cells. Their expression level increase was also observed in whole embryo as well as their stabilisation for *trp1b* and a light decrease for *dct*. Therefore these results are consistent with the previous observation in whole embryos.

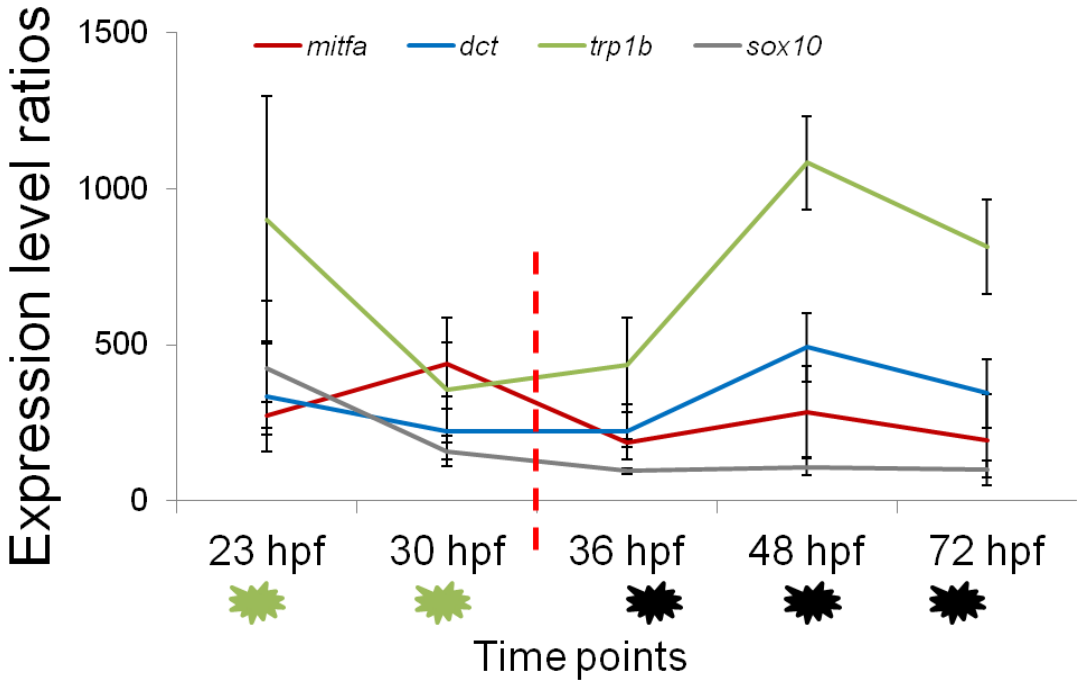

Figure 4.33: Graphs summarising *mitfa, dct, tyrp1*b and *sox10* relative expression levels in 10 samples at five time points during melanoblasts/melanocyte development.

These graphs show a decrease of *sox10* expression over time but also a decrease of *mitfa* expression at 72 hpf. *trp1b* expression increase from 30 hpf and remained stable and high by 48 hpf. *dct* expression seemed to be increased at 36 hpf and stabilised by 72 hpf. Bars show the standard deviation. The green cells remind that at 23 hpf and 30 hpf cells analysed were *sox10*-GFP(+) cells, whereas, at 36 hpf, 48 hpf, 72 hpf, cells selected were melanocytes (black cells). The red line on the lower graph also reminds the change in cell population type.

4.2.7 Determining *mitfa, tyrp1b, dct* and *sox10* mRNA copy number in five cell samples

In previous experiments, the relative gene expression levels were determined in five cell pools. Here, the objective was to determine the absolute copy number of *mitfa, sox10, dct* and *tyrp1b* cDNA in ten different pools of five cells after RT-qPCR. As for relative quantification cells were analysed through specification and differentiation phases at 23 hpf, 30 hpf, 36 hpf, 48 hpf, and 72 hpf.

The data collected here present an estimation of gene expression, at a certain timepoint, under the conditions of the experiments. The data obtained at 23 hpf and 30 hpf will have to be analysed in the context of the NC cell population. The data collected from melanocytes should reflect gene expression in a cell population gaining in stability and homogeneity as suggested by the analysis of its variability previously presented (fully homogeneous population was assessed at 72 hpf in the previous experiment).

Figure 4.34 shows the results for *mitfa, dct, tyrp1b, sox10* and *gapdh* (for comparison) at 23 hpf, 30 hpf, 36 hpf, 48 hpf, and 72 hpf, respectively. At each timepoint, a graph for each gene is presented summarising expression level for each gene in each sample (each sample was run in triplicates). The stability of *gapdh* expression has been previously studied (section 2.2). From 23 hpf to 72 hpf, *gapdh* expression was comprised of between (mean copy number in samples ± s.d = 4500 ± 56 and 8100 ± 72 transcript copies in samples.

Results shown in Figure 4.35 summarise this experiment and present the mean of transcript copy number found for each gene at each time point. In the *sox10*-GFP(+), *sox10* expression was always detected, as in relative quantification experiments. *mitfa* expression seemed to be slightly increased from 23 hpf to 30 hpf which could suggest, as in the relative quantification analysis, that a higher proportion of *sox10*-GFP cells could be melanoblasts at 30 hpf compared to 23 hpf. This result was not observed when looking at *mitfa* in whole embryos which could suggest that even if *mitfa* expression was more restricted to the melanocyte lineage by 30 hpf, a higher proportion of *mitfa* (+) cells colocalised with *sox10*-GFP cells at 30 hpf than at 23 hpf. This hypothesis will be further developed in the cross-validation section of this Chapter (section 4.2.9). In contrast with the results obtained with relative quantification expression, *trp1b* expression was low at 23 hpf and slightly increased by 30 hpf. The variations in the level of *trp1b* expression from an experiment to another might be related to the fact that the expression of *trp1b* is variable at this stage in the NC cell population as suggested by our test of variability presented in section 4.2.5. *dct* expression, as in relative quantification analysis, seemed to be maintained at the same level of expression (maybe expressed in the same proportion of cells) at 23 hpf and 30 hpf.

In melanocytes, *mitfa* expression was at its highest at 36 hpf and then decreased until at least 72 hpf. This result is consistent with the relative quantification analysis of *mitfa* expression. Further consistency with the relative quantification analysis, is the decrease of *sox10* expression we observed here. At 36 hpf, *tyrp1b* and *dct* expression levels

were expressed at a high level compared to what observed in NC cells which is consistent with the fact that we are selectively analysing melanocytes. However, in contrast with the relative quantification experiment in pools of cells and in whole embryos, their expression kept increasing after 36 hpf and until 72 hpf. Whether the stabilisation of *dct* and *trp1b* expression was not observed here because of the lack of expression correction by a reference gene (reflect irrelevant changes in transcription) or whether this increase was crucial in the biology and the differentiation of melanocytes will have to be further explored.

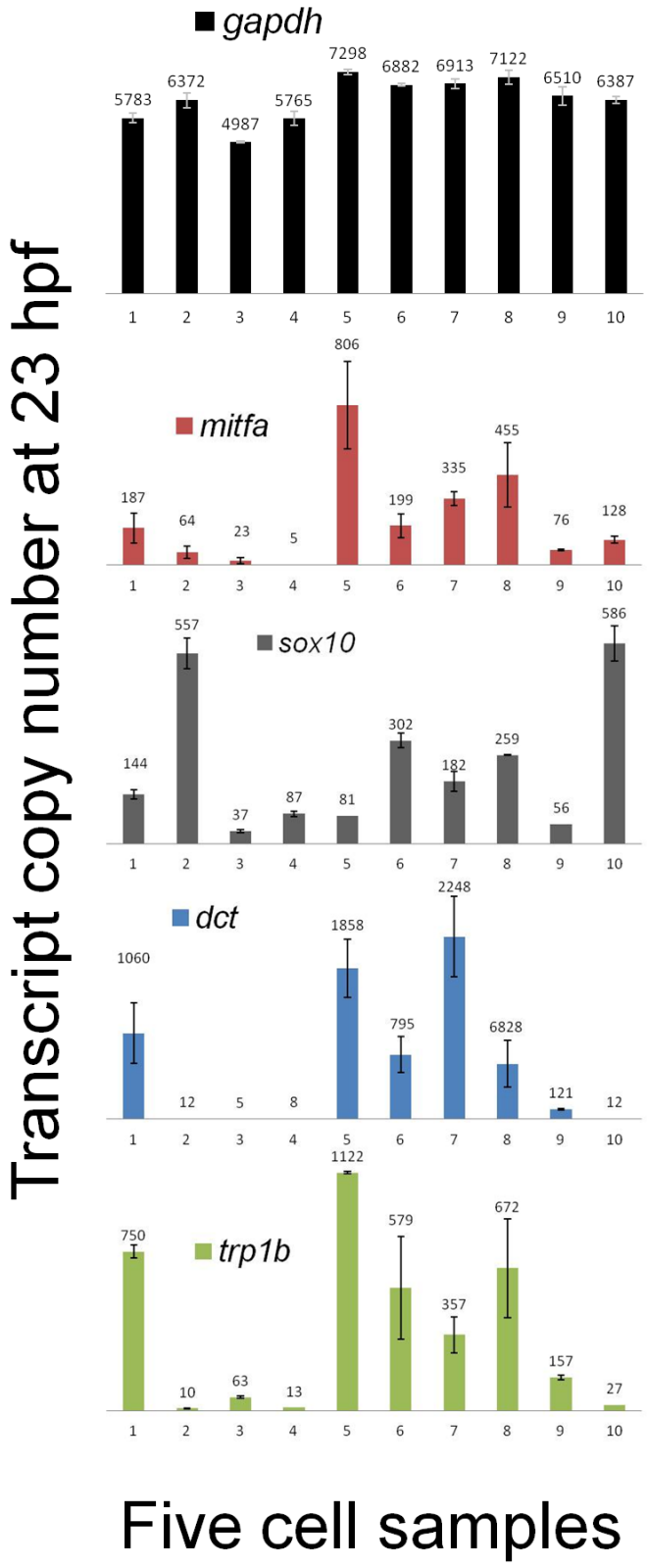

Figure 4.34: Absolute quantification (copy number) of *mitfa, sox10, dct* and *tyrp1b* at 23 hpf, 30 hpf, 36 hpf, 48 hpf, 72 hpf in ten samples (1-10) of 5 cells by qRT-PCR. See legend on page 212.

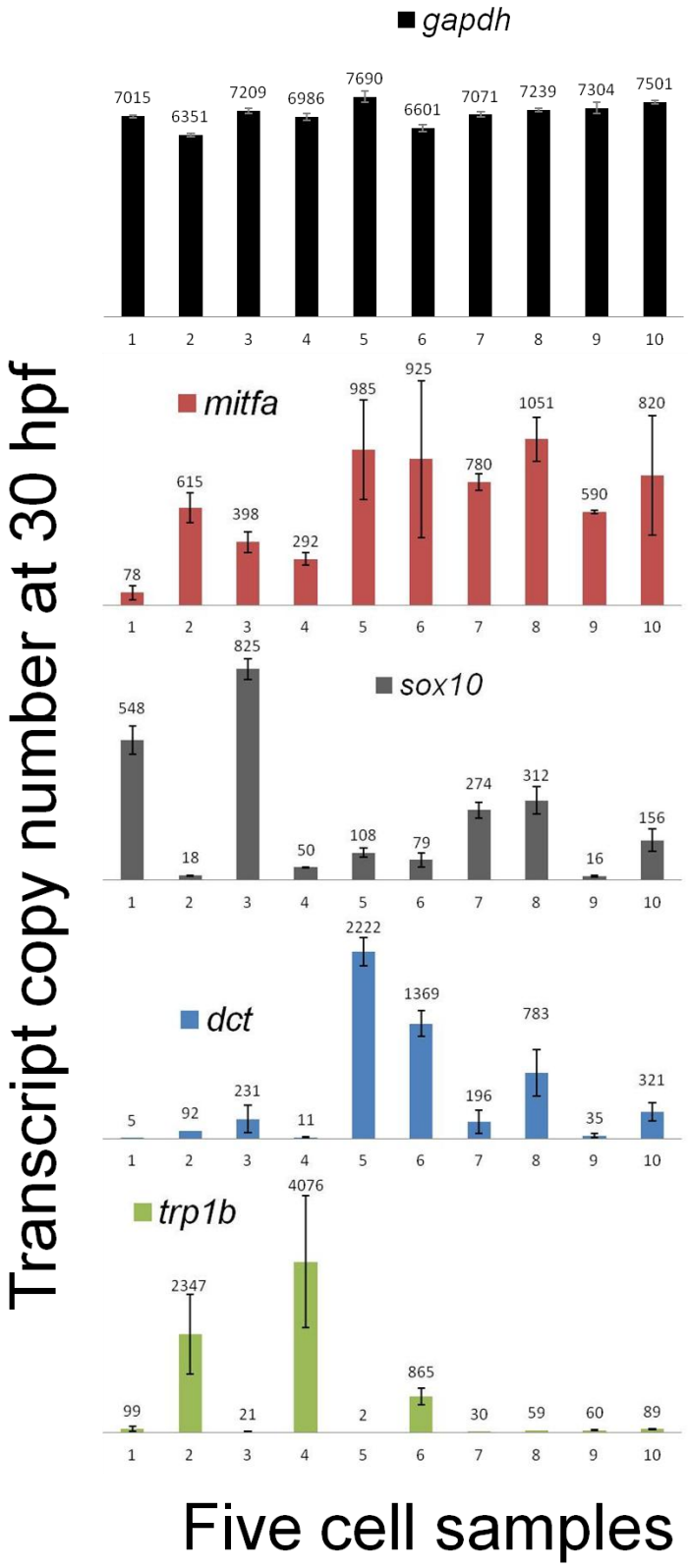

Figure 4.34: Absolute quantification (copy number) of *mitfa, sox10, dct* and *tyrp1b* at 23 hpf, 30 hpf, 36 hpf, 48 hpf, 72 hpf in ten samples (1-10) of 5 cells by qRT-PCR. See legend on page 212.

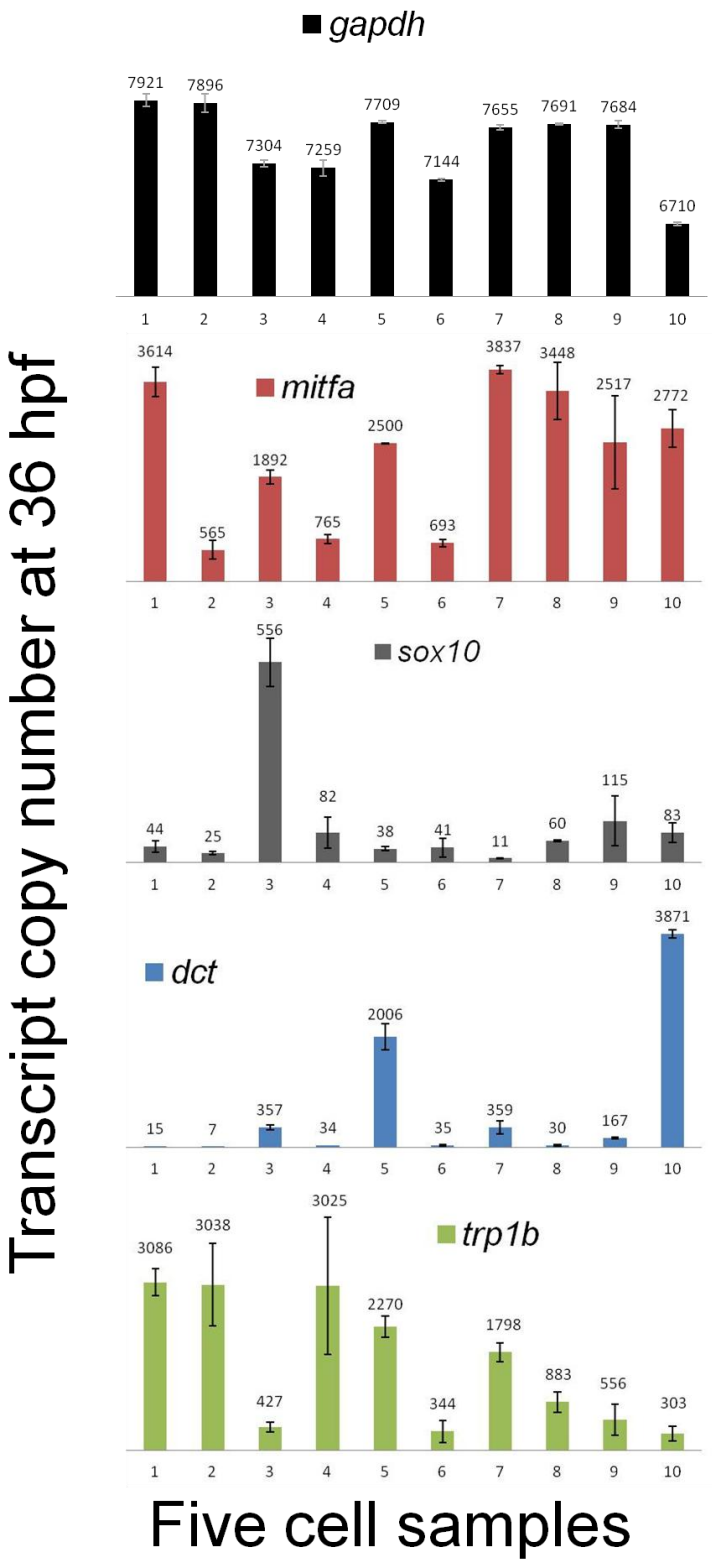

Figure 4.34: Absolute quantification (copy number) of *mitfa, sox10, dct* and *tyrp1b* at 23 hpf, 30 hpf, 36 hpf, 48 hpf, 72 hpf in ten samples (1-10) of 5 cells by qRT-PCR. See legend on page 212.

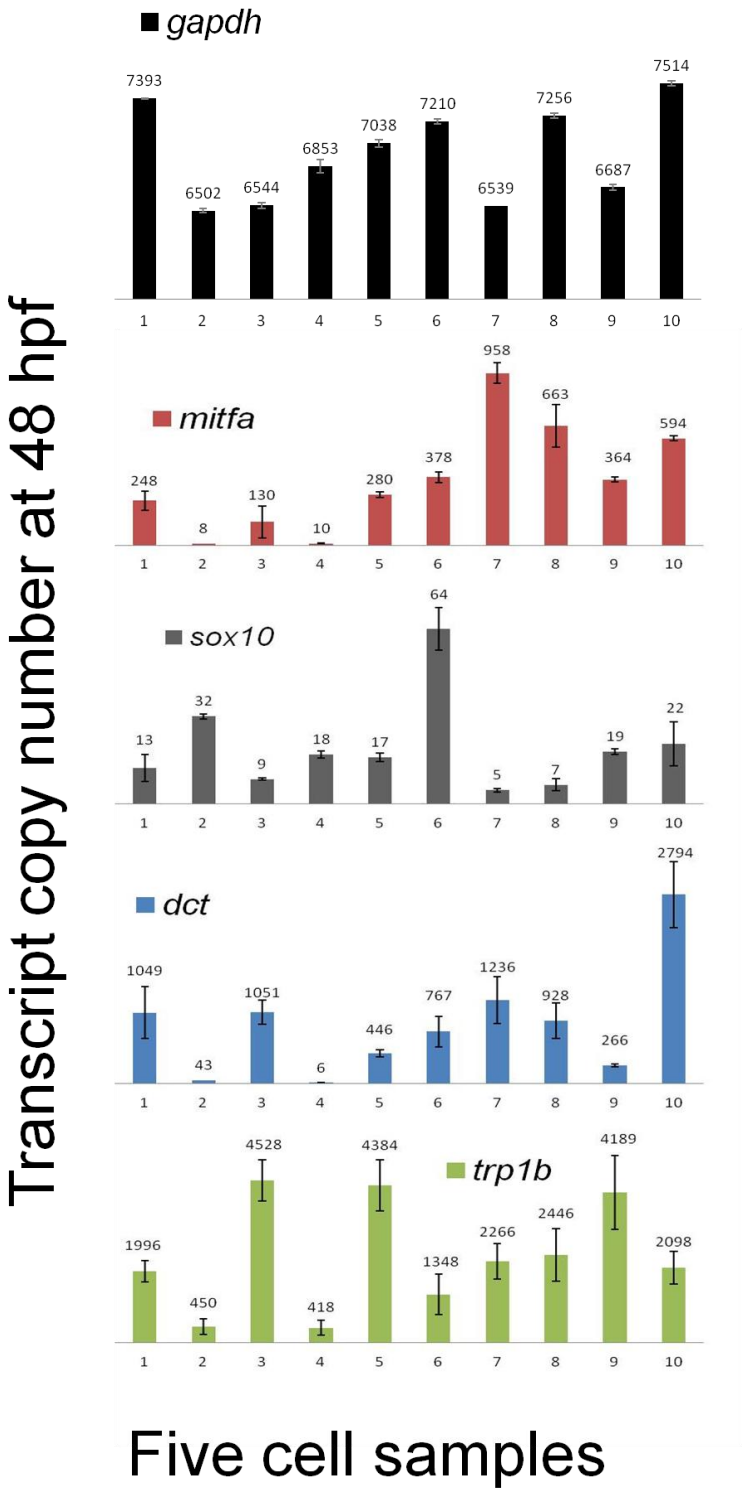

Figure 4.34: Absolute quantification (copy number) of *mitfa, sox10, dct* and *tyrp1b* at 23 hpf, 30 hpf, 36 hpf, 48 hpf, 72 hpf in ten samples (1-10) of 5 cells by qRT-PCR. See legend on page 2012

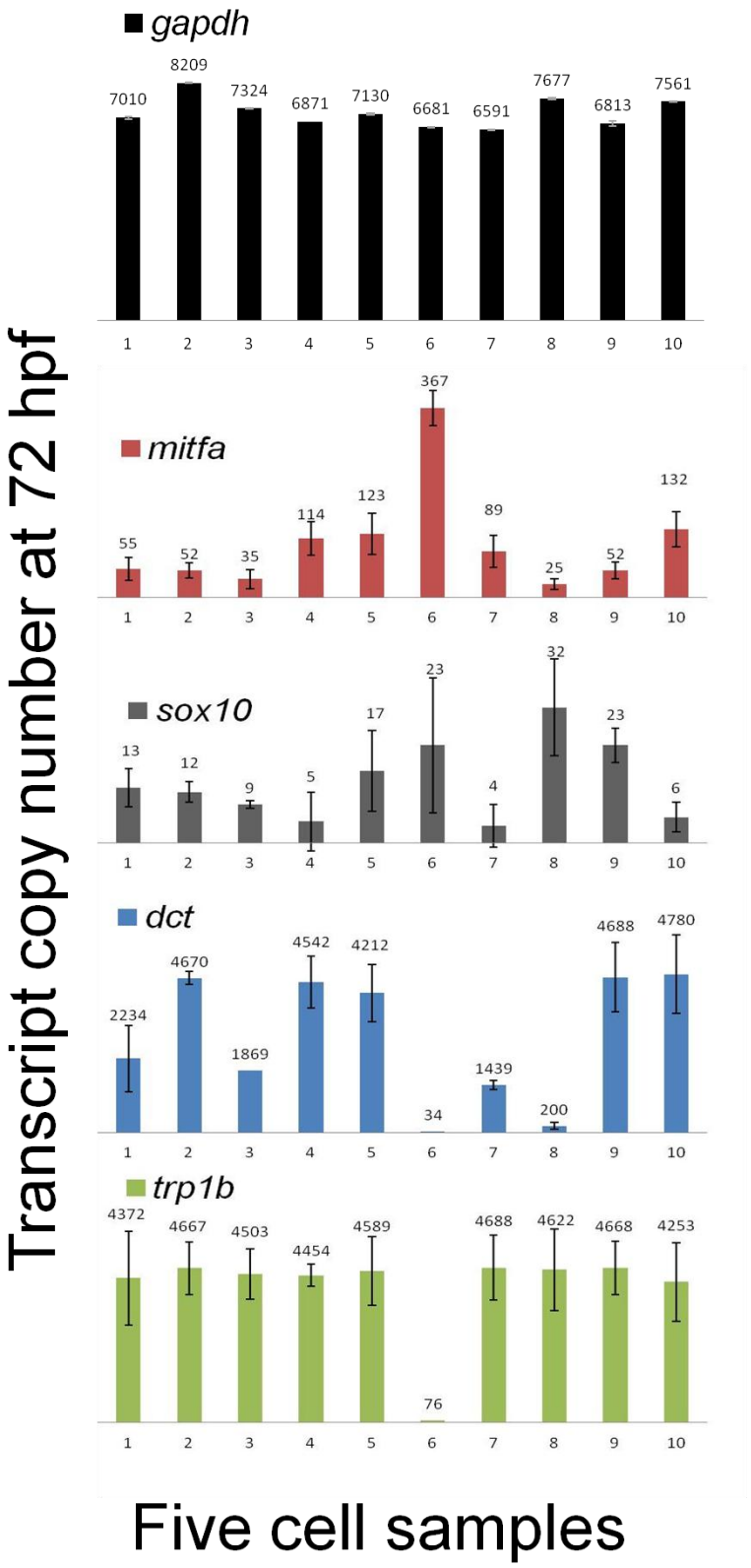

Figure 4.34: Absolute quantification (copy number) of *mitfa, sox10, dct* and *tyrp1b* at 23 hpf, 30 hpf, 36 hpf, 48 hpf, 72 hpf in ten samples (1-10) of 5 cells by qRT-PCR. See legend on the next page.

Figure 4.34: Absolute quantification (copy number) of *mitfa, sox10, dct* and *tyrp1b* at 23 hpf, 30 hpf, 36 hpf, 48 hpf, 72 hpf in ten samples (1-10) of 5 cells by qRT-PCR.

mRNA copy number in five cell samples (1-10) shown graphically (bars correspond to standard deviation).

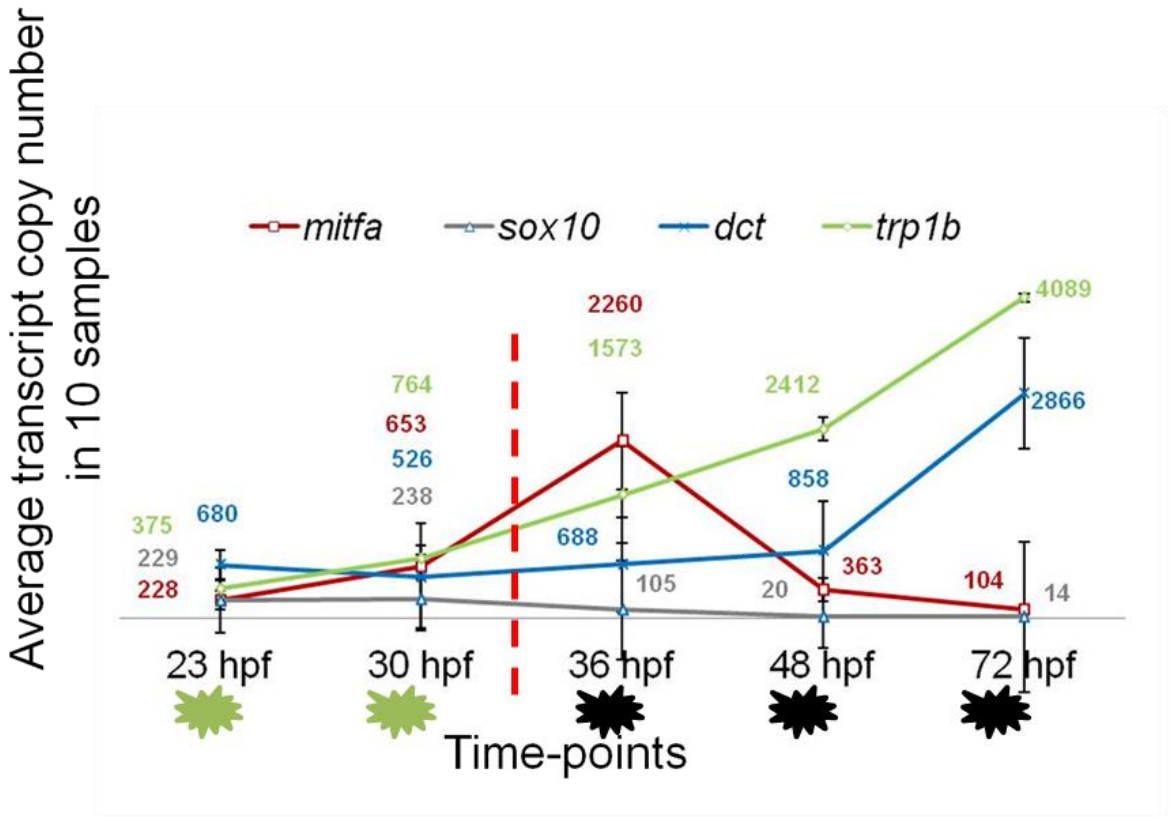

Figure 4.35: Average gene copy number for 10 samples of five cells at five time points.

Graph showing mean of gene copy number determined by absolute quantification after RT-qPCR in ten 5-cell pools at 23 hpf, 30 hpf (both *sox10*-GFP (+) cells as reminded by the green cells on x axis), 36 hpf , 48 hpf and 72 hpf (melanised cells as reminded by the black cells on x axis). The transition between the two different cell populations is shown by the dotted res line on the graph. The bars represent standard deviation for each mean. An increase in *mitfa* expression can be observed from 23 hpf to 36 hpf with a peak at 36 hpf. An increase in *tyrp1b* and *dct* copy number could also be observed. However, *tyrp1b* and *dct* expression kept increasing until at least 72 hpf while *mitfa* expression decreased from 36 hpf and until at least 72 hpf. *sox10* expression remained low until 36 hpf and decreased until 72 hpf at least .

4.2.8 Single cell analysis of melanocyte gene expression

4.2.8 a Using single cell analysis to test for existence of a chromatoblast expressing *mitfa* at 23 hpf

The hypothesis of the existence of a chromatoblast has already been suggested but was never tested *in vivo* (Bagnara *et al.*, 1979, Lacosta *et al.*, 2007, Minchin and Hughes, 2008, Lopes *et al.*, 2008). Recent work proposed that, in an early phase (around 23 hpf), *ltk* expression might mark a chromatoblast-like cell-type (Lopes *et al.*, 2008). Given the extensive expression of *mitfa* in the NC at this stage, we hypothesise that *ltk* and *mitfa* expression would overlap in a substantial proportion of cells which could be chromatoblasts (Curran *et al.*, 2009). However, later, such as at 72 hpf, the genes would not be co-expressed since *ltk* would only be detected in differentiated iridophores and *mitfa* only in differentiated melanocytes. From as early as 36 hpf, expression of *ltk* and expression of melanocyte markers do not overlap (Nikaido *et al.*, in preparation). In this experiment, the objective was to test this hypothesis in zebrafish at 23 hpf.

To test the co-expression of *mitfa* and *ltk* in NC cells at early stages, the expression of *ltk* and *mitfa* was investigated by nested RT- PCR technique at 23 hpf in 40 individual GFP+ NC cells from *sox10:GFP(+)*. To investigate the likelihood of false positive detection at 23 hpf, the experiment was repeated at 72 hpf when *mitfa* was restricted to the melanocyte lineage and *ltk* to the iridophore lineage.

Single cell reverse transcription and PCR were processed according to the protocol described in Bengtsson *et al.*, (2008). Nested PCR consisted of two rounds of amplification. This method allowed the amplification of expression from single cell cDNA. *sox10*-GFP (+) cells were selected at 23 hpf, and melanised cells were selected at 72 hpf. We attempted to use *β-actin* as a positive control for detection at both timepoints. Unfortunately, *β-actin* expression could only be detected in 80 % of samples. This could be due to variations of *β-actin* expression in some samples or to failure of detection. As shown in subsequent experiments, *β-actin* expression was variable in melanocyte populations which probably explains these results. In retrospect, a more appropriate control gene, such as *gapdh*, would have been a better choice, as demonstrated in section 4.2.2. However, at 72 hpf, *mitfa*, which is exclusively expressed in melanocyte at this stage, could replace *β-actin* as a positive control for detection. In contrast, as *ltk* would not be expressed in differentiated melanocytes, it could be used as a control for false positive.

Figure 4.37 shows the results at 72 hpf. Although *β-actin* expression was detected in 35/40 (88 %) of cells analysed at this stage, in practice essentially all isolated melanocytes (39/40; 98 %) could be shown to express *mitfa*, whereas, only 2.5 % (1/40) showed a band corresponding to the iridophore marker *ltk*. This false positive band could correspond to random weak activation of *ltk*, or to an error in the selection of the cell which could be an iridophore (*actin*(+)/*mitfa*(-)*ltk*(+)) as under incident light iridophores can be difficult to distinguish from melanocytes. Several faint bands were also observed in the *ltk* agarose gel. The presence of these light bands was not investigated as they were not the expected size for the amplified fragment. Taken together, these results showed that *ltk*

was not significantly expressed in *mitfa (+)* melanised melanocytes at 72 hpf and that gene expression detection by single cell RT-nested PCR protocol could be used to investigate expression of *ltk* and *mitfa* at 23 hpf**.** Interestingly, this result also shows that *mitfa* remains expressed in most melanocytes by 72 hpf, even if its expression level is low and difficult to detect by other methods. This result will be later discussed in the context of the cross-validation of results (section 4.2.9).

Figure 4.38 presents the RT- nested -PCR on forty single cells investigating *ltk*, *mitfa* and *β-actin* at 23 hpf. The housekeeping gene, *β-actin,* was detected in 73 % (31/40 cells) of cells analysed. This result suggested that *β-actin* was not expressed homogeneously in these cells and/or that its detection was not reliable. This experiment would have to be repeated using another control gene such as *gapdh*. Furthermore, wells 6, 7, 10, 11, 13, 15, 19, 30, showed a higher band which corresponded to the genomic DNA *β-actin* (confirmed by band size and by direct sequencing, data not shown). At 23 hpf, 90 % (36/40 cells) of the *sox10*-GFP(+) cells expressed *mitfa* and half (20/40 cells) of the *sox10*-GFP(+) cells expressed the iridoblast marker, *ltk*. Furthermore, 100 % of cells expressing *ltk,* expressed *mitfa,* and additionally, 64.5 % (20/31 cells) of *mitfa* expressing cells expressed *lkt*.

These results showed that *mitfa* was broadly expressed in *sox10*-GFP(+) cell population at 23 hpf and that more than half of these *mitfa* expressing cells also expressed *ltk*. The results also suggest that two different populations of *mitfa (+*) cells could co-exist at 23 hpf, a *sox10(+)/mitfa(+)/ltk(+)* population and a *sox10(+)/mitfa(+)/ltk(-)* population which is consistent with descriptions in the literature (Lopes *et al.*, 2008).

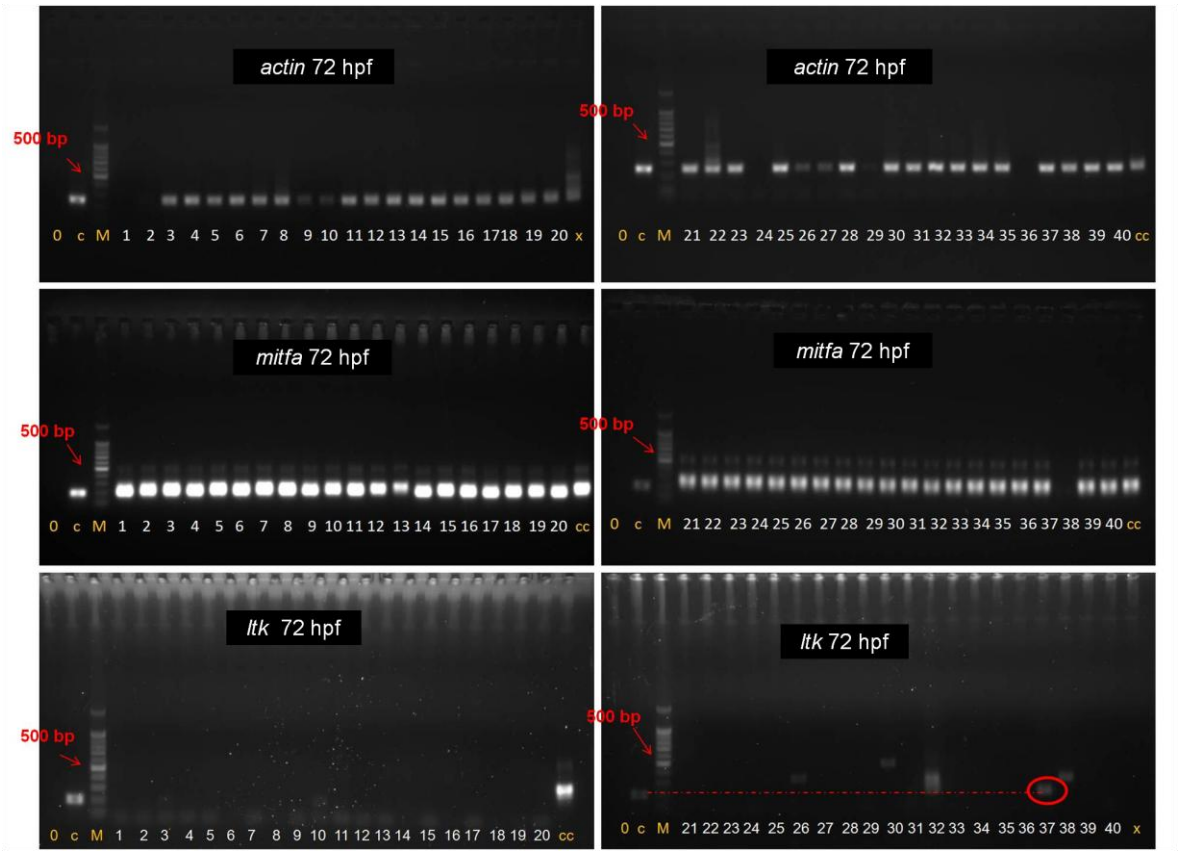

Figure 4.37: Single cell nested RT-PCR for *β-actin, mitfa* and *ltk* mRNA in 40 melanised cells at 72 hpf.

Each well (1-40) corresponds to a single cell tested. Two negative controls were run, the negative control without cDNA template (0) and the negative control corresponding to a non-melanised cell (x). Two positive controls are shown, the positive control with total 23 hpf embryo cDNA (one round amplification) (c), and the nested PCR positive control (two rounds amplification) (cc). The 100 bp DNA marker (Promega) is shown in (M).

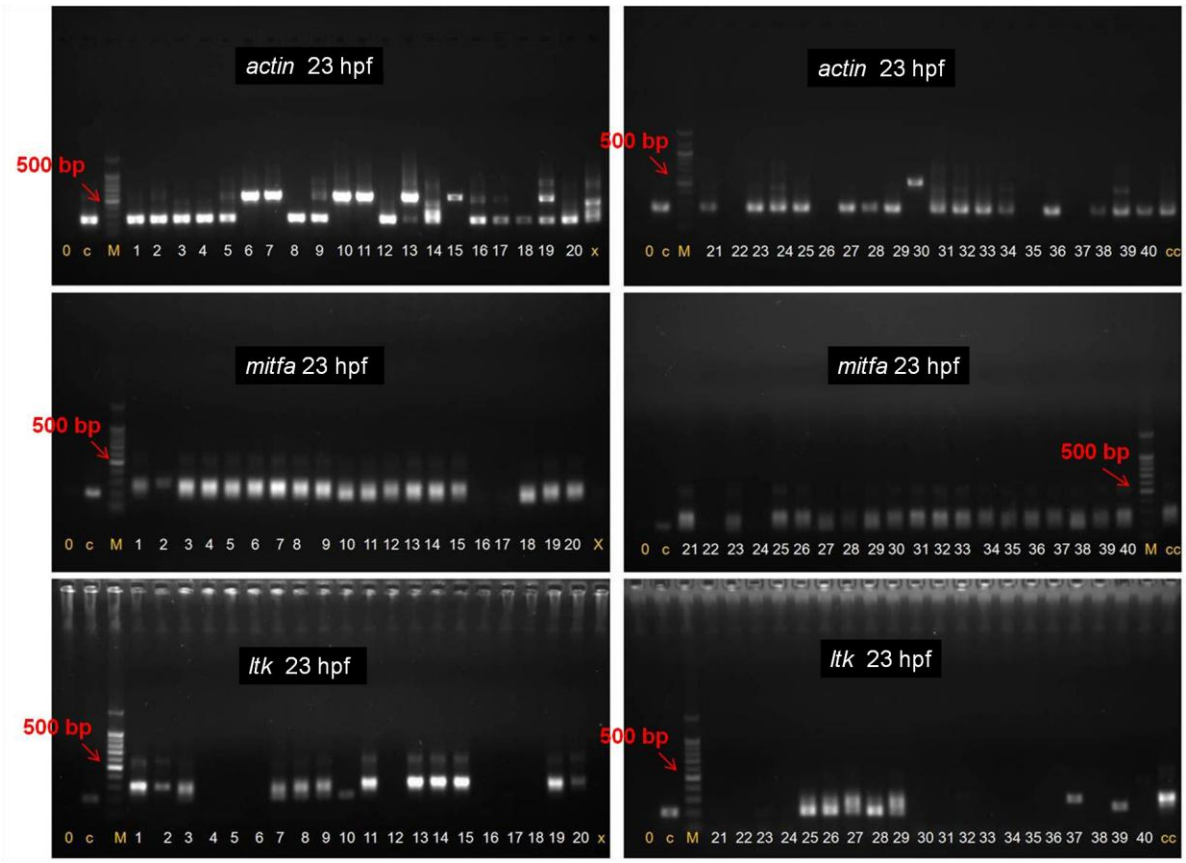

Figure 4.38: Single cell nested RT-PCR for *β-actin, mitfa* and *ltk* mRNA in 40 *sox10*:GFP positive cells from 23 hpf.

Each well (1-40) corresponds to a single cell tested. Two negative controls were run, the negative control without cDNA template (0), and the negative control corresponding to a non-melanised cell (x). Two positive controls are shown, the positive control with total 23 hpf embryo cDNA (one round amplification) (c), and the nested PCR positive control (two rounds amplification) (cc). The 100 bp DNA marker (Promega) is shown in (M).

4.2.8 b Developing single cell qRT-PCR

In the previous experiment, gene expression was assessed in single cells using the method of RT-nested-PCR. The previous experiment did not allow us to investigate the difference in gene expression level for *mitfa* in the *mitfa+/ltk+* cells and in the *mitfa+/ltk-* cells at 23 hpf. In this experiment, the objective was to go further in the quantification of gene expression by attempting to use the RT-qPCR technique at the single cell level.

The method of RT was used in combination with qPCR analysis (Bengtsson *et al.*, 2008). As a first control for acceptable amplification of the signal, it was key to observe the exponential linear amplification phase. Secondly, it was important to verify that the melting curve showed a peak at a temperature specific to the targeted sequence. In order to optimise the detection of gene expression, the final cDNA volume obtained after RT was reduced and the totality of this volume was used to test for expression of only one gene, in duplicate (instead of five genes as in the qRT-PCR of whole embryos). Consequently, the concentration of cDNA was maximised and used to run the qPCR with an increased probability of detecting low concentration of the target cDNA sequences.

As a test case, the absolute expression levels of a highly expressed gene, *dct*, was tested at 48 hpf in ten melanocytes. The results showed that the exponential linear amplification was observed in only three samples (cells 2, 7 and 10 see Appendix 2). This result suggested that gene amplification occurred correctly in only three samples. Exponential amplification, as well as melting curve analysis, both confirmed that only these three samples revealed amplification of the targeted *dct* sequence. The level of expression was measured in an absolute way using the absolute standard curve and copy numbers were determined for these samples (see Appendix 2). This method requires further optimisation to be used in the future.

4.2.8.c Gene expression estimation in single cells

In previous experiments, gene expression levels were determined in pools of five cells. In this section, the objective was to use these data to determine gene expression level in single cells. For this, we used the data previously collected by Yang and Johnson (2006) which describes the number of *dct* (+) cells at each timepoint in zebrafish (*dct* (+) cells at 36 hpf: 190 ± 10, at 48 hpf: 250 ± 13, at 72 hpf: 300 ± 15). This data, in combination with our data in melanoblasts/melanocytes, could be used to estimate the number of transcripts for each gene in single cells. This estimation could then be used to evaluate the mean expression levels for *mitfa, tyrp1b,* and *dct* in single cells from the relative and absolute quantification experiments. Curran *et al.,* (2009) showed that around 26 hpf, 50 % of the *mitfa* (+) cells express *dct* however, because it remains unclear what type of cells express *mitfa* at early stages and whether the proportion of *dct* (+) could increase within the *mitfa* (+) cells, this analysis was only valuable at later stages, after 36 hpf in melanocytes.

Table 4.4 shows estimations of transcript copy number in single cells from the absolute quantification experiment, and Table 4.5 presents relative estimation of expression level in single cells from the total embryo relative quantification experiment.

The disparities observed within these two tables could be related to the differences of analysis between absolute and relative quantification and the differences in measuring expression in pools of cells or in whole embryos. Further investigation is required to establish whether these results are contradictory or not. A value of 100 copies of mRNA in a cell is often considered to be the threshold underneath which stochatsic and probabilistic effects may become important. Our data suggest that from 48 hpf, stochastic effects be could part of *mitfa* activation as we found that less than 100 mRNA copies were probably present in single cells. This result suggests that it could be interesting to investigate the stochastic aspect of *mitfa* transcriptional activition in melanocytes at late stages. *sox10* expression was also found to be very low, less than 10 copies in single cells after 48 hpf. However, whether this decrease reflects a loss of expression or whether *sox10* expression is maintained at a very low level by a probabilistic effect is also unknown.

Table 4.4: Estimation of transcript number for each gene, at each timepoint in single melancoytes.

This estimation was calculated using data collected in absolute quantification experiments. The mean of values (mean ± s.d) in the 10 samples of five cells was used to calculate the mean copy number in single cells, at each timepoint.

	mitfa	***sox10***	***dct***	***tyrp1b***
36 hpf	452 ± 117	21 ± 15	137.6 ± 120	314.6 ± 114
48 hpf	72.6 ± 27	4 ± 1.6	117 ± 76	482.4 ± 131
72 hpf	20.8 ± 9	2.8 ± 0.8	573.2 ± 182	817.8 ± 134

Table 4.5: Estimation of relative quantification (calibrated to *gapdh* expression) in single melanocytes.

This estimation was calculated using *dct* (+) cells number at each time point, found in Yang and Johnson, (2006), and relative expression for each gene in whole embryo.

	mitfa	***dct***	***tyrp1b***
36 hpf	0.09615	2.07692	1.23077
48 hpf	0.18182	1.27273	1.09091
72 hpf	0.01667	0.76667	1.01667

4.2.9 Combined analysis of expression results

In the previous sections, quantitative and qualitative data were collected. Expressions of melanocytic genes were studied in whole embryos (section 4.2.3) and in small pools of cells (section 4.2.6 and section 4.2.7). We used both the relative quantification (section 4.2.6) and absolute quantification (section 4.2.7) methods to analyse expression levels in pools of cells. The variability of gene expression was determined in these pools (section 4.2.5), and additionally, we tested whether technical difficulties of detection could have been responsible for the variations observed at low levels and found that it was not the case (4.2.2). Furthermore, we investigated gene expression in individual cells at 23 hpf in *sox10*-GFP cells and at 72 hpf in melanocytes (section 4.2.8). The data collected in the *sox10*-GFP (+) cells and in the melanocyte populations have to be analysed in two different contexts. First, they were analysed in the context of a precursor mixture cell population, and second, in the context of a specific cell population differentiating. The cross-analysis of this study is complex because different techniques were used, such as nested RT-qPCR, whole embryo RT-qPCR and five cell pools RT-qPCR, but also because two reference cell populations and different scales of analysis were studied (the whole embryos, small pools of cells, the *sox10*-GFP cells or the melanocytes).

At 23 hpf, it has been suggested that NC- *sox10*-GFP cells could consist of different unknown types of precursors (chromatoblasts, glioblasts, neuroglioblasts). The study of melanocytic gene expression variability (section 4.2.5) suggested that *dct*, *trp1b*, and *mitfa* were highly variable in this cell population at this stage. The high standard deviation observed when analysing *trp1b* expression in small pools of cells with the relative quantification method could be related to the variability at this stage (section 4.2.6). Combined with the results obtained by RT-nested-PCR in individual cells (showing that 65 % of the cells expressing *mitfa* also expressed the iridoblast marker, *ltk*, at this stage) these data support the hypothesis of the existence of various precursors at 23 hpf. One in particular could be a chromatoblast, as shown here (65 %: *sox10*(+)/*mitfa*(+)/*ltk*(+)) and *trp1b* would be expressed in a subset of cells that are already beginning melanocyte differentiation.

Throughout the development of NC, precursors enter specification and commitment. Consequently, the population present at 30 hpf in the *sox10*-GFP cell population was more likely to contain a mixture of precursors at different stage of differentation compared to 23 hpf. These precursors might include melanoblasts, glioblasts or neuroblasts. By 30 hpf, in the *sox10*-GFP cell population, *dct* and *trp1b* remained variable (section 4.2.5), whereas, the variability of *mitfa* was decreased compared to the one at 23 hpf. Knowing that in whole embryo analysis, *mitfa* expression was decreased at 30 hpf compared to 23 hpf, and conversely, it was increased in small pools of cells, it seemed that comparing whole embryos (4.2.3) to small pools of cells showed apparently contradictory results. However, this apparent contradiction can be explained by taking into consideration the difference between investigating gene expression in a growing whole embryo (increased number of cells in total) and in a specific cell population (becoming more restricted) (Figure 4.39). The *sox10*-GFP cell population becomes more restricted

from 23 hpf to 30 hpf (expressed in less cell types at 30 hpf than at 23 hpf), in contrast, in the same time period the whole embryo increases in cell number. Therefore, considering that the number of melanoblasts present at 23 hpf could be close to the number of melanoblasts present at 30 hpf and that the rest of the *mitfa* (+) precursors present at 23 hpf will switch off *mitfa* expression, we find that *mitfa* expression appears decreased when testing it in whole embryos. In contrast, it seemed increased when measuring it in the specific *sox10*-GFP cell population (Figure 4.39). Consequently, these results were not contradictory, but rather, the context in which we were testing gene expression was different.

Melanocyte differentiation is a continuing process from 36 hpf to 72 hpf. The experiment investigating genetic variability suggested that the melanocyte population was only genetically homogeneous by 72 hpf. The fact that in all experiments, *dct* and *trp1b* expressions were higher at each of the three timepoints measured during cell differentiation (36 hpf, 48 hpf and 72 hpf), compared to 23 hpf and 30 hpf, is coherent with the fact that melanocytes were selectively chosen at later stages and indicates increasing expression per cell. However, in all experiments we observed that *mitfa* expression remained quite low, and specially decreased at 72 hpf. This could suggest that *mitfa* is expressed at low level in fully differentiated cells. Therefore, this data suggest that *mitfa*, consistent with its role as a transcription factor, is never highly expressed in cells. However, the results of single cell RT-nested-PCR showed that all melanocytes expressed *mitfa* at 72 hpf, suggesting that *mitfa* did not disappear in cells, consistent with evidence for the ongoing role of Mitfa (Johnson *et al.*, 2010).

sox10 expression had been suggested to be lost in melanocytes. All experiments described here suggest the decrease of *sox10* expression which confirmed the data found in the previous study in Greenhill *et al.*, (2011), although as is perhaps to be expected, using the more sensitive technique of qRT-PCR *sox10* expression remains detectable, albeit at very low levels.

Expression levels of *dct* and *trp1b* in melanocytes were mostly consistent through the study. However, the whole embryo analysis as well as the relative quantification experiment in small pools of cells showed that *dct* and *trp1b* are perhaps reaching a plateau by 72 hpf (and a slight decrease was observed in small pools of cells) whereas, in absolute quantification analysis, *dct* and *trp1b* expressions seemed to always increase until 72 hpf. It remains to be tested whether the expression level reached for *dct* and *trp1b* at 72 hpf in absolute quantification experiment is due to parameters which were irrelevant to the melanocyte biology during cell differentiation, such as cell growth in embryo, and which were not corrected by this technique.

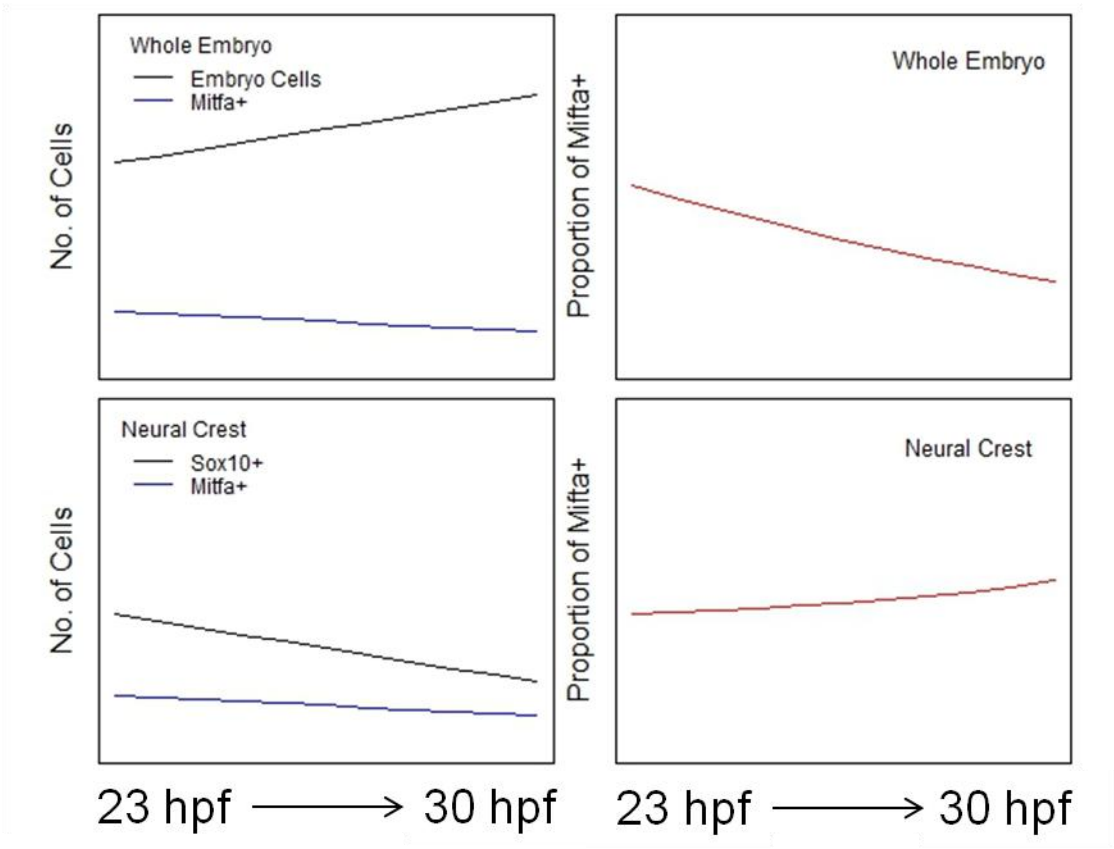

Figure 4.39: Observing *mitfa* expression in whole embryo shows a decrease while it seems to be increased when measuring expression in *sox10* (+) cells.

mitfa is expressed in an unknown but large proportion of NC cells at 23 hpf (on both top and bottom left panels, *mitfa* expression is represented by the blue line) whereas it is restricted to melanoblasts at 30 hpf (hypothesis of a slight decrease of *mitfa* expression from 23 hpf to 30 hpf as melanoblasts division also occurs). The number of NC cells (*sox10* (+) cells at 23 hpf and 30 hpf, black line on the bottom left panel) decreases (most precursors differentiate, *sox10* expression is maintained in melanoblasts and glioblasts only and expression levels drop in some early differentiating cells) whereas the number of cells in the whole embryo increases as the embryo grows (black line, top left panel, number of cells increases through time). Consequently, when measuring the proportion of *mitfa* expression level in the whole embryo (red line, top right panel), we observe a decrease of *mitfa* expression. When looking at gene expression in the *sox10* (+) cell population, we observe a slight increase of expression (red line, bottom right panel). Thus the apparent disparities observed in the result of our experiment (23 hpf to 30 hpf) are in fact related to the reference point of the experiments which vary from an experiment to another (see text).

4.3 Discussion

The results presented in this Chapter consist of a preliminary study for developing a new approach to the melanocyte GRN. It has been well described that cell-to-cell variations and gene expression level variations in apparently isogenic populations, were essential parameters to evaluate for understanding cell specification from a multipotent pool (Elowitz *et al.*, 2002, Peccoud and Jacob, 1996, Quaranta and Garbett, 2010, Fournier *et al.*, 2007, Raser and O'Shea, 2005, Janes *et al.*, 2010). We showed it is possible to design a method to investigate gene expression in five cells and to use it to investigate gene expression level and gene expression heterogeneity. We used this method to measure the genetic variability of melanocytic genes in the NC cell population and in the melanocyte lineage. These results are intended to contribute to both developing refined techniques for quantification of melanocyte gene expression *in vivo* and better understanding of the heterogeneity of expression of melanocytic genes.

4.3.1 The advantages of the stochastic profiling method

In these experiments, we used the stochastic profiling method. In contrast with measuring gene expression in a single sample from the whole embryo, investigating gene expression in small pools of cells allowed us to observe biological variation in gene expression within the cell population (ten random samples containing five melancoytes randomly selected). The stochastic profiling method, combined with statistical analyses of the gene expression variances allowed us to analyse the heterogeneity of melanocytic genes through time. Previous experiments such as the ones presented in Greenhill *et al.*, (2011) investigated gene expression at different timepoints. The study presented here took this investigation further by assessing the characteristics of gene expression variations within the cell population at certain times and through time.

Altogether, the results showed that:

- Around 23 hpf, melanocytic genes were heterogeneously expressed in NC cells suggesting the existence of a population of precursors.
- One such precursor at this stage co-expresses *mitfa* and *ltk*, as well as *sox10*, and is likely to be a chromatoblast.
- *tyrp1b* and *dct* expression levels stabilise relatively late in melanocyte differentiation.
- *mitfa* expression decreases as melanocytes differentiate, but remains detectable.
- The decrease of *sox10* expression observed in whole embryos in Greenhill *et al.*, (2011), was confirmed quantitatively.

In Janes *et al.*, (2005), as in Quaranta *et al.*, (2008), the stochastic profiling method, associated with the Monte Carlo simulation in MATLAB software, was used to model their

data to understand cell heterogeneity. However, other methods could be used to investigate gene expression heterogeneity in cells. Tang *et al,* (2006) used microarray analysis to understand the variability of gene expression in cell populations. Hernandez *et al.,* (2012) investigated, via microarray analysis, the heterogeneity of expression of factors increasing invasiveness in ductal carcinomas and in breast cancer cells. Other studies used the correlation of gene expression to show the heterogeneity of gene expression in cells and to observe cell variability. For instance, Schulz *et al.,* (2007) studied the variability of the channel proteins expressed in neuronal cells by testing pairwise expression correlation of channel protein genes using the Pearson correlation. They showed a qualitative and a quantitative specificity of channel genes expressed in each cell as well as a high variability of gene expression levels in the neuronal cell population.

4.3.2 Measuring gene expression in small pools of cells

Thanks to the protocol of cDNA production adapted to low material amounts (published by Bengtsson *et al.,* (2008)) and to a rigorous qPCR standardisation process, we have here developed a technique to measure gene expression in pools of five cells freshly *ex vivo*. For the first time we could investigate the levels of melanocytic gene expression in pools of five cells. This technique is now available for further investigations, such as, quantifying the heterogeneity of *dct* and *trp1b* in the *mitfa*-GFP cell population around 23 hpf to determine whether *mitfa* only marked melanoblasts at this stage. Furthermore, it could be used to examine the existence of precursors such as chromatoblasts by investigating the co-expression of key genes such as *id2, ltk (*iridoblasts markers) *mitfa, dct* (melanoblast markers), and *pax7* (xanthoblasts marker) in *sox10*-GFP(+) cells.

One limitation of this technique was that mRNA transcription was considered but protein translation was not. This is a substantial limitation, since not all mRNA molecules might be translated to protein and the translation process is also susceptible to bursting, meaning that many proteins are produced from one mRNA copy, before translation is silenced (McAdams and Arkin, 1997, Li and Xie, 2011). Consequently, mRNA expression is likely to not reflect protein levels perfectly. Furthermore, transcript stability might be fluctuating which could result in translation kinetics bias. Besides, transcripts have different "life times" in cytoplasm, allowing the translation for variable time periods. In contrast with bacterial systems, in mammalian and zebrafish, mRNA and protein lifetimes are comparable (Golding *et al.,* 2005, Li and Xie, 2011). However, measuring protein levels would not be feasible at this stage because antibodies were not available in zebrafish. Hence, despite its limitations, mRNA quantification was a feasible approach to begin to understand cel-to-cell variability in the NC.

In future, these preliminary data could be used to investigate gene expression correlation by testing some of the known features of the GRN described in the modelling. For instance, whether the variations of *mitfa* expression could explain the variations of *dct* and *trp1b* could be tested.

4.3.3 Understanding the decrease of *mitfa* expression in melanocytes

The single cell analysis at 72 hpf suggested that *mitfa* expression remained detectable at 72 hpf in melanocytes. However, the decrease of *mitfa* expression was measured in all experiments presented. Consequently, it could be suggested that the transcription factor, *mitfa*, is expressed at low levels in differentiated melanocytes. This could simply reflect the change from a differentiating state, where transcription of melanocyte-specific products is highly active, to a maintenance state where homeostasis is the main demand. Alternatively, this result might suggest a different role for *mitfa* during late melanocyte differentiation. In one case, *mitfa* could remain the main gene responsible for maintenance of melanocytes; perhaps the mechanism involving Factor Y (described in the Chapter 3) is set to allow maintenance of *mitfa* expression but only at a decreased level.

Alternatively, the decrease of *mitfa* expression could suggest that *mitfa* was no longer directly the gene responsible for maintenance of the differentiated melanocyte phenotype and might suggest the existence of a new factor in the network. Such an idea was first described in Model A (Figure 4.40): a factor called Factor X could be activated to relay *mitfa'*s role in melanocyte differentiation (Greenhill *et al.*, 2011). This factor would ensure melanocyte development after the decrease of *mitfa*. Factor X would then be described as a *mitfa*-dependent factor, induced in melanocytes around 36 hpf in zebrafish and which would have the property to maintain melanocyte differentiation. Factor X could activate *dct* expression as well as other melanocytic genes such as *tyrosinase*. If Factor X exists, once turned on, it would replace *mitfa* and its expression would be maintained either via another activation loop either by low levels of *mitfa*. This hypothesis suggests that after a certain timepoint, maintaining Factor X would be sufficient to maintain melanocyte development, in the absence of *mitfa.*

It would be interesting to test the hypothesis of the existence of Factor X, however, no candidate factors are known yet and there is no other evidence for its existence other than the observation of *mitfa* expression decrease in embryos and cell pools after 48 hpf. Factor X would be a transcription factor carrying at least an M-box in its regulatory sequence. If it exists, whether Factor X could be activated early in melanoblasts or only during cell differentiation cannot be determined from the hypothesis here. Interestingly, in *mitfa*^{w2} mutants, melanocyte maintenance fails if *mitfa* is inactivated in late differentiation even after 72 hpf, suggesting that Mitfa itself continues to be required, and rather negating the value of the hypothetical factor X (Johnson *et al.*, 2010). Postulating the existence of Factor X, would not rescue the original model A from Greenhill *et al.*, (2011). A new version of the model, even taking into account this unexpected decrease of *mitfa* expression, would still require the presence of a factor to maintain *mitfa* expression at a later stage, during differentiation. In the future, improving characterisation of *mitfa* and *sox10* expression dynamics would allow better evaluation of the network.

Combining two approaches could allow testing for the existence of Factor X by: 1) running a genome sequence analysis looking at genes responsive to Mitfa and carrying M-boxes in their promoter would allow the creation of an initial candidate gene list. 2) ChIP experiments could permit the identification of transcription factor genes activated by Mitfa

during melanocyte differentiation. A list of candidate transcription factors combining results found by these analyses could then be tested in several ways. A microarray screening study based on MITF targets described by Hoek *et al.*, (2008) could also be referred to. To reduce candidate factors, it could be interesting to investigate *dct* or *tyrosinase* promoters for specific binding sites. As a last step, *in vivo* tests could then be run by designing probes for WISH to test if a candidate gene could be expressed during melanocyte differentiation, as around 36 hpf in partly PTU treated embryos. Finally, a functional test activating or repressing the gene candidate's expression could show the existence or the absence of a Factor X.

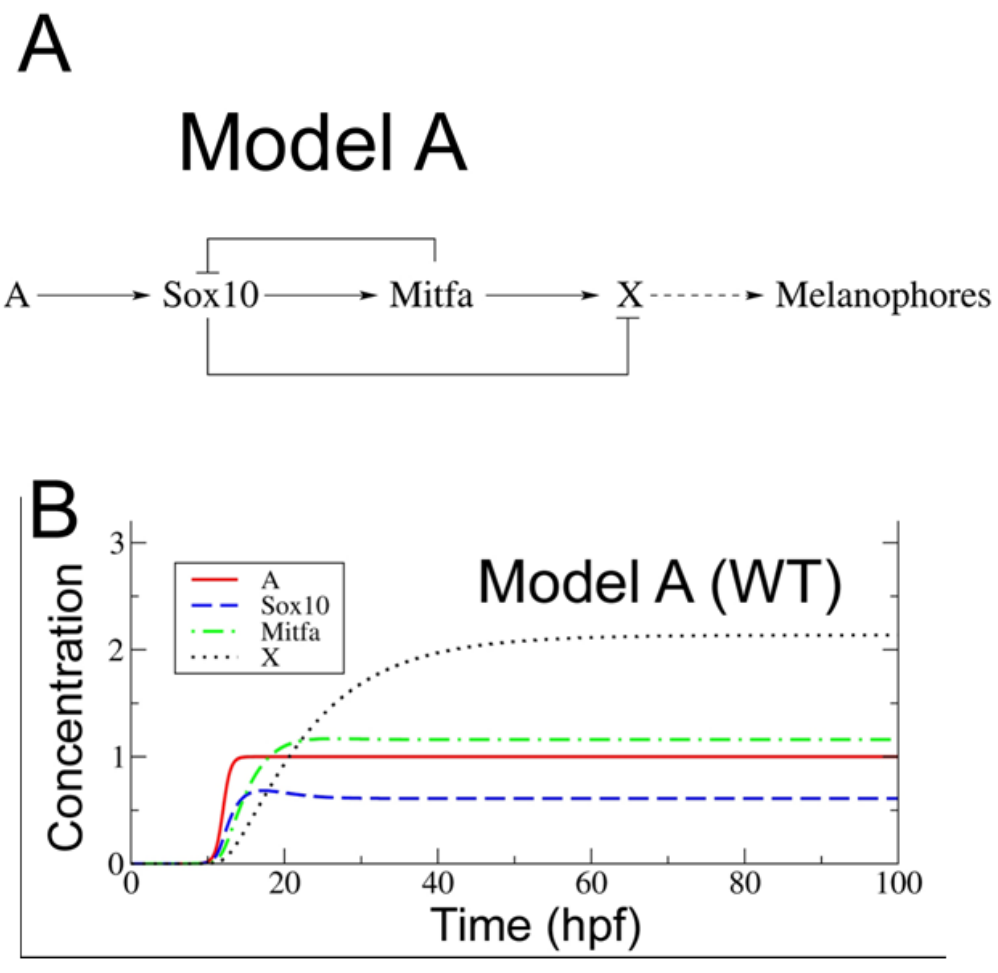

Figure 4.40: Model A described Factor X as an important factor for melanocyte differentiation downstream Mitfa

The model A shows that after activation of *mitfa*, by Sox10 (which was first activated by factor called A), Mitfa can both repress *sox10* expression and activated Factor X (A). In the model, Sox10 could also downregulated Factor X before activation of *mitfa* (A). The prediction for the timecourses of expression of *sox10*, Factor A, *mitfa* and Factor X, when this model was envisaged, are presented in (B). The model suggested then that a Factor X would be highly expressed compared to *mitfa* (B). A new model including Factor should now also include other tested parameters as the decrease of *sox10* and *mitfa* expressions. (reproduced with the kind permission of Greenhill *et al.*, (2011)).

4.3.3 Better definition of the precursor population at early stages

In our experiments the NC pool was studied at 23 hpf and 30 hpf. In this cell population, several precursors were present. Single RT-nested PCR experiments showed that about 65 % of *sox10*-GFP(+)/*mitfa(*+) cell were also *ltk* (+) at 23 hpf. The result showed that *mitfa* expressing cells were heterogeneous at this stage. Whether *ltk* and *mitfa* were 100 % co-expressed earlier than 23 hpf in NC cells remains to be tested. Furthermore, whether the variability of *mitfa* expression observed at 23 hpf could reflect a functional difference between two cells with low or high levels of *mitfa* remains to be addressed. Then high *mitfa* could mark a certain type of precursor (melanoblasts for instance) while low *mitfa* could mark another kind of precursor (melanoglioblast for instance). Alternatively, it could also be suggested that this phase of variability was inevitably following *mitfa* first activation. Whether some *sox10* (+) cells were *mitfa* (-) was not tested here.

At 30 hpf, cells selected were *sox10*-GFP positive cells which would be expected to include glial precursors (Dutton *et al.*, 2001). This could suggest that *mitfa* was also turned on in these cells at this stage before being inhibited by a *sox10* dependent repressor such as the forkhead box D3 (*foxd3)* (Carney *et al.*, 2006, Dutton *et al.*, 2001). *foxd3* is activated by *sox10* in glioblast/melanoblast and it has been described as a repressor of *mitfa* and of melanocyte fate (Ignatius *et al.*, 2008). Mechanisms involved in *foxd3* dependent inhibition of *mitfa* remain unclear. In these experiments, no glioblast markers other than *sox10* were tested. It would be interesting to determine and to compare the heterogeneity of *foxd3* expression in cells to that of *mitfa* at 30 hpf in the *sox10*-GFP(+) cell population. Also, it would be interesting to know whether *foxd3* and *mitfa* are co-expressed at this timepoint in *sox10*-GFP (+) cells and to determine whether changes in these expression levels could be correlated with fate acquisition.

More experiments could be performed to test the hypothesis of the existence of a chromatoblast, in zebrafish, by investigating expression of several markers in early *sox10*(+) (glioblast marker, as described in Carney *et al.*, (2006)), and in *mitfa* (+) cells (Lister *et al.*, 1999)). Investigating expression of *pax7* to test for xanthoblast marker, and *ltk* to test for an iridoblast marker could show the existence of a precursor at early stages (15 hpf to 30 hpf) (Lopes *et al.*, 2008, Lacosta *et al.*, 2007, Minchin and Hughes, 2008). Lastly, the analysis of cell tracing using *mitfa*-GFP transgenic fish could be interesting in order to track cells from 23 hpf to 36 hpf when a potential precursor could be described.

4.3.4 Further testing of gene expression correlations in the GRN

Further statistical analysis and experiments *in vivo* would have to be carried out to better understand the results presented here. For instance, we could observe that expression level of *mitfa*, *dct* and *trp1b* could be varying similarly in some samples (section 4.2.7, Figure 4.34, for instance at 23 hpf, samples 2-3-4). Analysis of correlation could help determine whether these data could reflect the proximity of regulatory relationship in the GRN. Furthermore, testing direct activation and repression of these genes using ChIP experiments looking for binding of *mitfa* and *sox10* on *dct*, *trp1b*, s*ox10* and *mitfa*, at each timepoint would be fundamental. Furthermore, testing the role of epigenetic markers, such as, acetylation, methylation and chromatin state, for each gene in individual cells at each timepoint, could also allow to better understanding of variations in gene expression. These results, combined with accurate measurements of gene expression in cells at each timepoint, could permit further understanding of the GRN dynamics and mechanisms.

4.3.5 Further evaluation of noise and gene expression stochasticity involved in melanocyte development

Systems biology and computational approaches are used to capture biological variations in complex biological systems to achieve more realistic representations of the system. Many studies have statistically analysed and modelled gene expression in cellular systems, but using different methods (Guo *et al.*, 2003, Fournier *et al.*, 2007, Elowitz *et al.*, 2002, Nygaard *et al.*, 2005, Mao and Resat, 2004, M.Sriram Iyengar, 2011, Hubbell *et al.*, 2002). Gene expression fluctuations can be explained by many biological phenomena such as stochasticity of gene transcription, deterministic gene expression and biological noise (Paulsson, 2004, Elowitz *et al.*, 2002, Raser and O'Shea, 2004). Stochasticity allows the activation, the repression and the plasticity of gene expression whereas the deterministic approach does not. Recently, there has been an increasing evidence to support stochastic (probabilistic) mechanisms of gene regulation. In a review, Li and Xie, (2011) showed the crucial role of stochasticity in gene expression and activation. It would be important to better define the part of stochasticity in melanocyte gene expression (Li and Xie, 2011). This aspect of melanocyte development is poorly documented and it could be important to investigate to help understand the instability of other systems such as melanoma (Goding, 2000, Uong and Zon, 2009, Mao and Resat, 2004). Our data suggest that around 48 hpf and later, stochastic effects could play an important role in activation or maintenance of low *mitfa* expression levels.

In the future, three key parameters would have to be investigated to better define the stochasticity of the system; the rates of transcription; chromatin state for target genes; and the distance between promoters. Then, it would be possible to determine whether stochasticity could have been responsible for genetic variability in the multipotent cell pool. Several regulatory events could be involved in causing gene expression variability in melanoblasts. The transition from a precursor state to a differentiated melanocyte steady state involved important changes in the GRN which could cause variability in cells.

Testing the fine tuning of *mitfa* and *sox10* in cells and assessing the role of background noise in melanocyte precursors will be crucial in the future.

4.3.6 Absolute quantification and the limitation of measurements

Absolute quantification consists of measuring the absolute gene expression concentration in each sample without normalising it. Optimisation of the method is of importance to minimise experimental variations such as tube variability due to experimental set up, as well as background amplification noise. In our experiments, relative quantification of gene expression was assessed using both the ΔΔCt method with the associated statistics and by the REST 2009 software developed by Pfaffl *et al.,* (2002). Absolute quantification was determined as transcript copy numbers in five cell pools. According to the manufacturer and to studies, gene detection with SYBR Green I is sensitive enough to detect gene expression down to 10 copies (Colborn *et al.*, 2008, Steuerwald *et al.*, 1999, Budhia *et al.*, 2006). However, when gene expression was lower than 10 copies per sample, it was considered to be too low to be confidently assessed.

Thanks to several quantitative techniques, many studies have investigated gene copy number in cells (Kelso *et al.*, 1999, Diercks *et al.*, 2009). mRNA represent 2 % of total RNA in a cell corresponding to 0.5 to 1 pg of material (Brady, 2000). According to Taniguchi *et al.,* (2009), this would correspond to about 106 transcripts per cell. In another study, Nygaard *et al.,* (2005) measured absolute gene expression in samples of carcinoma Hela cells and reported that 8116 genes per cell were expressed in a range from 0.3 to 40,000 per cell with over 90 % of these genes being represented in low copy number, from 1 to 15 copies (Nygaard *et al.*, 2005, Brady, 2000). These experiments showed that only about 20 genes were expressed at high to very high levels in single cells, meaning up to 40,000 copies per cell. These observations are interesting as they give a sense of transcriptional activity in a cell. However, it seemed that gene copy numbers could vary a lot depending on different cell types, genes and cell developmental stage and state. The data we collected in this experiment (section 4.2.7) fitted the ranges presented here, with low expression for those encoding transcription factors and higher expression level for enzymes. However, it will be key to further study the biological significance of this absolute numbers to define their relevance. In our study, the lack of resolution under 10 copies per sample was a limitation to measure very low copy numbers. To overcome this limitation, single cell mRNA analysis could be performed using mRNA sequencing analysis with has a better resolution.

Peccoud *et al.,* (1996) used "monte carlo" simulation to estimate confidence intervals for detecting targets by including the initial number of molecules present to detect. They showed that relative uncertainty of detection ranged from 10 % to 25 % when initial copy number was 100. This correlation (measured by the slope in calibration experiments) has been shown to be lost depending on the ratio between the level of gene expression in the sample and the sample size (Nygaard *et al.,* 2005). Nygaard *et al.,* (2005) applied an ANOVA approach to examine the effects of variation with reduced amount of total RNA in first round of amplified RNA production. Nygaard *et al.,* (2005) showed that

a critical level of expression was observed where stochastic fluctuations became significant and prevented reliable measurements. They also showed that this level was sample size dependent meaning that there was a correlation between the threshold and sample size. In Karanth *et al.,* (2009) data were analysed using the Pfaffl method. Karanth *et al.,* (2009) could determine the relative steady-state of *fatty-acid binding protein* (*fabp*) gene, in zebrafish, depending on different diets. For this, Karanth *et al.,* (2009) first calculated gene copy number according to Bustin *et al.,* (2005) and used copy number ratio of *fabp* and reference gene to determine steady-sates. In another study, Wacker *et al.,* (2008) used the ΔCt method associated with a student t-test to analyse single cells, muscle fibers gene expression. The variety of methods used for establishing a qPCR technique and analyzing the qPCR is related to the variety of models study. It is essential to chose and apply the appropriate method with strong statistical analysis for each specific experiments as we did in this Chapter for each different measurements.

4.3.7 Investigating gene expression in single cells

In this chapter single-cell expression could be assessed by RT-nested PCR but not by RT-qPCR. The technique of single cell RT-nested PCR has been used in several studies (Phillips and Lipski, 2000, Dixon *et al.*, 2000, Kelso *et al.*, 1999). Phillips and Lipski, (2000) showed the robustness of the technique using multiplex amplification in a first round and specific amplification in a second round, to study heterogeneity of cells of the autonomic regions of the nervous system. Several protocols described the methods to process to small material amount RNA extraction and reverse transcription avoiding contamination, loss and RNAse degradation in samples (Kurimoto *et al.*, 2006, Hartshorn *et al.*, 2005, Bengtsson *et al.*, 2008). Hartshorn *et al.*, (2005) described a method to detect gene expression in big single cells such as blastomeres. For this study, the protocol described in Bengston *et al.,* (2008) was used as it was best suited protocol for this experiment. This protocol allowed us to extract RNA from single cells and convert RNA to cDNA for amplifying gene expression by PCR, qPCR or nested PCR.

The nested qPCR results allowed us to better characterise *mitfa* (+) cells at 23 hpf. However, the reference gene used, *β-actin*, could not be detected in all samples suggesting that the experiment should be repeated using *gapdh* as a reference gene. It has been shown to be expressed in homogeneous manner in the melanocyte population (Pei *et al.*, 2007). mRNA amplification has become a widely used approach (Kelso *et al.*, 1999, Taniguchi *et al.*, 2009, Phillips and Lipski, 2000). We tested the single cell RT-qPCR in *ex-vivo* in zebrafish melanocytes. The technique did not work due to lack of detection with the set up and with the kit used. Optimisation using a more appropriate set up and machine could allow detection of gene expression in single cells. As previously explained, an important concern in qPCR experiments is the reliability of results obtained in reflecting concentration or level of expression of starting material (Cookson *et al.*, 2005, Colborn *et al.*, 2008). This problem is amplified when working with very low quantities of input RNA, where stochastic effects and background amplification due to template dilution may also have created bias in gene expression detection. However, in the future, it would be

interesting to develop a single cell assay with accurate quantification of expression in order to validate and push further the analysis of single cell heterogeneity.

Experiments of live imaging, following multiple messengers and using time-lapse for example, could allow observation of the variability in gene expression through time and space in single cells. However, it remains difficult to combine this sort of approach with quantitative techniques. Single cell expression could also be quantified using serial analysis of gene expression (SAGE) method or RNA seq also called "Whole Transcriptome Shotgun Sequencing" or single cell microarray (Kurimoto *et al.*, 2006).

4.3.9 Conclusion

This preliminary study allowed us to investigate key points of the GRN: the characterisation of the melanoblast and melanocyte population showed the heterogeneity of early *mitfa(+)* cell populations; as well as the decrease of *mitfa* expression in melanocytes at 72 hpf. Furthermore, our results suggest the existence of a chromatoblast at early stages. The combination of biological data and statistical analyses permitted the observation of the GRN within a different and new approach, stochastic profiling and will contribute to deciphering the quantitative features of the GRN. In conclusion, the stochastic profiling approach seemed appropriate to achieving quantification of variation in gene expression, even if the accuracy of techniques for reading gene expression in small pools of cells is difficult to achieve. This can be overcome by increasing sample size, and in the future, using more accurate techniques for gene expression measurements in single cells.

Chapter 5. Insights into *sox10* and *mitfa* regulation

5.1 Introducing the complex regulation between the two transcription factors Sox10 and Mitfa in melanocytes.

Two transcription factors, *Sox10* and *Mitf,* have been found to be crucial for melanocyte development in several species such as mouse, human, *Xenopus* and zebrafish (Lister *et al.*, 1999, Elworthy *et al.*, 2003b, Jiao *et al.*, 2004, Kumasaka *et al.*, 2005, Hou *et al.*, 2006). However, several aspects of the interactions between these factors remain unclear, for example, the role of Sox10 in differentiation of melanocytes in zebrafish compared to mouse, and the role of Mitfa as a repressor of *sox10* in zebrafish during cell differentiation. In this Chapter, aspects of *sox10* and *mitfa* inter-dependent regulation were tested *in vivo* in order to investigate caveats of the melanocyte GRN.

5.1.1 The role and the regulation of *sox10* during melanocyte development

The role of *sox10* in early melanocyte development does not appear consistent from one species to another. For example, in zebrafish, *in vivo* data suggested that there was no requirement for an ongoing role of *sox10* in melanocyte for differentiation. In contrast, *in vitro* data in mouse suggested that *Sox10* might contribute to the expression of melanocyte differentiation genes, *Dct* and *Tyr* (Murisier *et al.*, 2007, Hou *et al.*, 2006). In *Sox10*-mutant mice primary NC cultures, *Mitf* expression was neither sufficient to rescue pigmentation nor to induce *Tyrosinase* expression in cell culture in the absence of the factor SOX10, suggesting that SOX10 was required to act alongside MITF to activate *Tyrosinase* expression (Hou *et al.*, 2006). In zebrafish, *sox10* over-expression induced ectopic *mitfa* expression and thanks to *mitfa* induction, pigmentation was fully rescued. In contrast, loss of *sox10* expression in zebrafish embryos resulted in the loss of *mitfa* expression and pigment cell types (Dutton *et al.*, 2001, Elworthy *et al.*, 2003b). Consequently, in zebrafish the essential function of *sox10* in the melanocyte lineage is mediated by the transcriptional regulation of *mitfa* (Elworthy *et al.*, 2003b). Furthermore, a previous study based on immunohistochemistry and WISH, showed that *sox10* expression was lost upon early melanocyte differentiation in zebrafish *in vivo* (Greenhill *et al.*, 2011). Therefore, in contrast to what observed in zebrafish, SOX10 was maintained in the melanocytic lineage of mammalian species and might control melanocyte differentiation in addition to fate specification in the mouse (Dutton *et al.*, 2001, Hou *et al.*, 2006).

Together, the data indicated a crucial role for *sox10* in melanocyte specification although its precise role during differentiation remains controversial throughout species (Hou *et al.*, 2006, Aoki *et al.*, 2003, Carney *et al.*, 2006, Elworthy *et al.*, 2003b, Kelsh, 2006b, Dutton *et al.*, 2001, Potterf *et al.*, 2001). A GRN was constructed from previous experimental data in order to better understand the influence of different factors in the melanocyte GRN in zebrafish. The study of zebrafish mutants, particularly *sox10*^{t3} and *mitfa*^{w2} mutants, has been crucial for the collection of data and the testing of key hypotheses. In the mutant *sox10*^{t3}, the *sox10* allele contains a 1397 bp insertion which interrupts the *sox10*-coding sequence upstream of the HMG domain and adds eight novel amino acids before prematurely truncating the protein. The *mitfa*^{w2} mutant allele contains a single base substitution which creates a premature stop codon and results in a truncated protein (Lister *et al.*, 1999). Testing the expression of *sox10, mitfa, tyrp1b, dct* and *silva* in these mutants has allowed the evaluation of the repressive effects of Sox10 on some genes downstream Mitfa in zebrafish. In our experiments, one objective was to quantitatively assess the role of Sox10 in the regulation of genes downstream of Mitfa in zebrafish and to understand the mechanisms involved in the loss of *sox10* during melanocyte differentiation.

5.1.2 Sox10 can repress the expression of genes downstream of Mitfa

Melanocyte specification in zebrafish is based upon activation of *mitfa* by Sox10. In turn, Mitfa activates the expression of the genes responsible for melanin synthesis. Importantly, previous experiments have shown a clear distinction between the effects of *sox10* and *mitfa* over-expression in zebrafish. Improved understanding of these differences would allow better definition of the regulatory role of both transcription factors in melanocyte development in zebrafish.

Testing gene expression induction ectopically can demonstrate potential activatory and repressive regulatory interactions between factors. For this, the ectopic activation of gene expression had to be tested before the endogenous gene expression was activated in embryos. In zebrafish embryos, *sox10* expression is activated at 11 hpf in NC and *mitfa* is activated around 18 hpf in a potential precursor cell population in NC (Dutton *et al.*, 2001). Consequently, induction of gene expression, such as *mitfa* or *sox10*, could be tested ectopically by injecting mRNA at the one cell stage and by testing probable direct gene expression activation before activation of endogenous expression (at 6 hpf). Detectable responses from direct activation are considered to result from protein synthesis and gene expression activation. Indirect activation would appear later. It would be caused by protein translation and transcriptional activation of another factor which in turn would be translated and would then activate gene expression.

Ectopic expression of *mitfa* or *sox10* gene expression in zebrafish embryo has been tested previously. When ectopically over-expressed in one cell stage embryos, the wild-type *mitfa* mRNA caused a strong expression of all melanocyte differentiation genes tested by 6 hpf. This suggested direct activation of their expression by Mitfa. In contrast, by 6 hpf, wild-type *sox10* mRNA induced *mitfa* expression however no expression of melanocyte differentiation genes could be detected. Interestingly, by 10.5 hpf, *tyrp1b* was

activated while *dct, tyr* and *silva* were not. This suggested an indirect activation of *tyrp1b* via activation of *mitfa* by Sox10 (Greenhill *et al.*, 2011). This interpretation is confirmed by the failure to activate *tyrp1b* expression by injecting *sox10* mRNA in *mitfa*^{w2} mutant. This result suggested that *tyrp1b* expression was strictly *mitfa*-dependent in zebrafish and that in the presence of high *sox10* expression, low *mitfa* expression could not activate all melanocytic genes (Greenhill *et al.*, 2011). It was then suggested that Sox10 could have repressive effects on expression of some melanocytic genes, except *tyrp1b*. Importantly, these results were consistent with the previous observation of residual melanin in *sox10* mutant fish (Figure 5.01). The de-repression of expression of the genes responsible for melanin synthesis led to the production of residual melanin in the dorsal part of embryos up to 40 hpf even in the absence of *mitfa* (Figure 5.01) (Greenhill *et al.*, 2011). This residual melanin appeared later than in WT embryos (presumably due to the lack of *mitfa* and the low levels of melanocytic gene expression). From 40 hpf, and up to 56 hpf, it was possible to quantify the increase in the number of melanised cells, and additionally in some cases, it was possible to assess the changes of aspect of residual melanin from fainted and spread, at 41 hpf, to dense and round, at 43 hpf (Figure 5.01).

Sox10 is a factor involved in NC specification and in maintenance of pluripotency (Kim *et al.*, 2003, Kelsh, 2006b). Therefore, there is a potential this repressive effect could be enhanced in non-melanoblast cells and be reinforced by the absence of *mitfa*. Consequently, it would be difficult to observe the weak repressive effect directly in WT condition in melanoblasts. However, WISH experiments investigating the expression of *dct, tyrp1b, silva, mitfa* and *sox10* in *sox10*^{t3} mutant, but also in *mitfa*^{w2} mutant, and additionally the double *sox10*^{t3}/ *mitfa*^{w2} mutant, showed detectable *sox10* dependent downstream repression of *dct* and *silva* and *tyrosinase* at 24 hpf and 36 hpf (Figure 5.02, Table 5.01) (Greenhill *et al.*, 2011). Table 5.01 shows the de-repression of *dct, silva* and *tyrosinase* in most *sox10*^{t3} mutant embryos from 24 hpf to 42 hpf whereas fewer embryos showed residual gene expression in *mitfa*^{w2} mutants (Greenhill *et al.*, 2011). The quantitative aspect of de-repression of genes downstream Mitfa was not assessed in these experiments.

In this Chapter, complementary analyses were carried out to investigate quantitatively melanocytic gene expression in *mitfa*^{w2} and *sox10*^{t3} mutants in order to assess the level of de-repression of genes downstream of Mitfa in the absence of Sox10. The expression of *tyrp1b, dct, mitfa* and *sox10* were assessed in pooled embryos at three different time points, 30 hpf, 36 hpf and 72 hpf by quantitative RT-PCR. We tested whether the de-repression of *dct* could be observed in the *sox10*^{t3} mutants compared to *dct* expression in *mitfa*^{w2} mutant particularly around 30 hpf. Whether *tyrp1b* expression, which was not repressed by Sox10 in the previous experiment, was differently affected in *mitfa*^{w2} and *sox10*^{t3} mutants was also investigated. These experiments allowed the quantification of gene expression in mutant lines, and additionally, evaluation of the changes in expression level that were predicted by the model during cell differentiation in zebrafish.

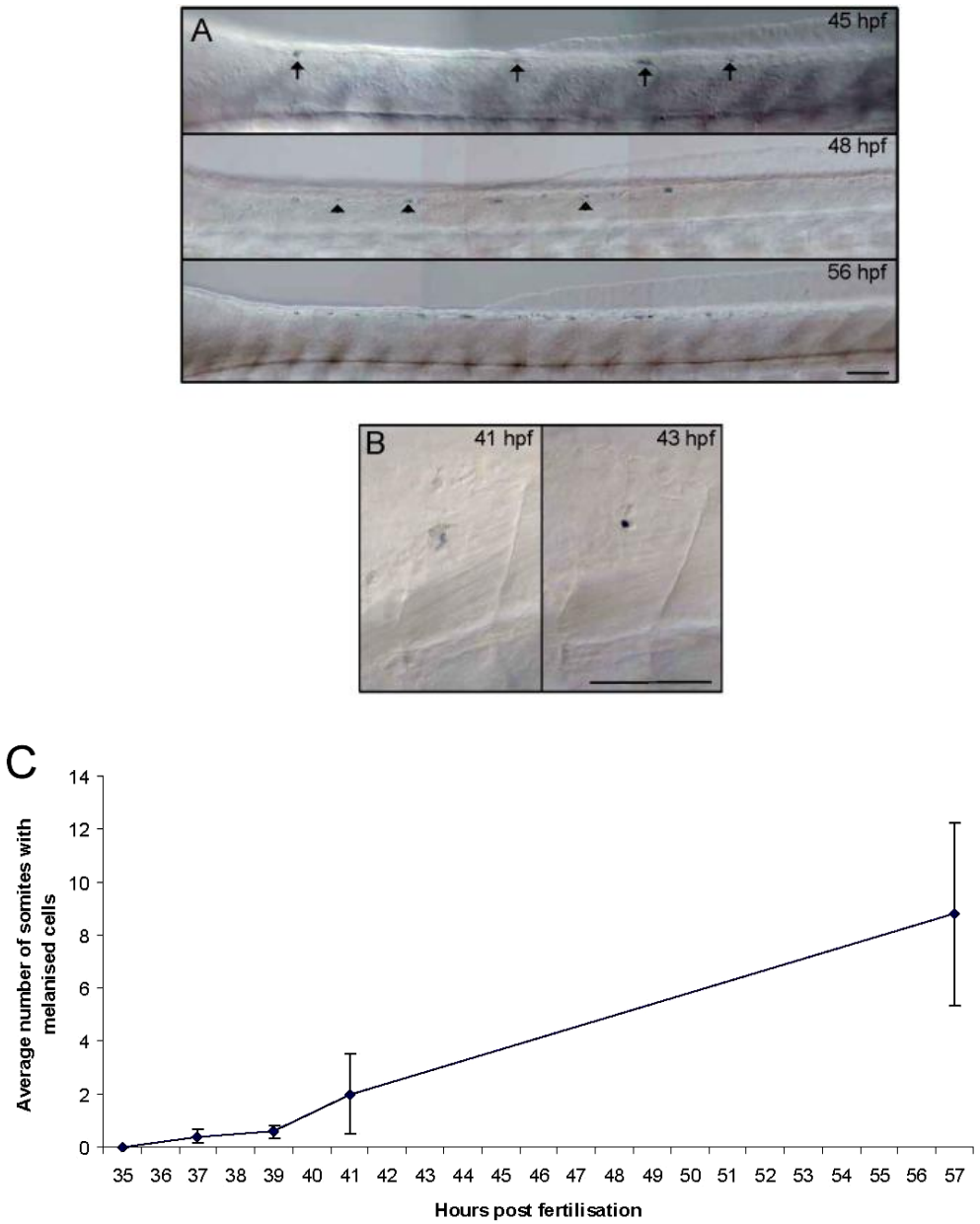

Figure 5.01: Residual melanin is observed in somites in *sox10*^{t3} mutants

Residual melanised cells appeared in zebrafish *sox10*^{t3} mutants around 40 hpf and increase until 56 hpf. The dorsal trunk of a single embryo shows the dynamic changes in residual melanised cells from 45 hpf to 56 hpf (A, arrowheads show residual melanised cells). Note how initially many cells show diffuse melanin (arrowheads at 45 hpf) and how new melanised cells appear with time (arrowheads at 48 hpf) and until 56 hpf. A single melanised cell at 41 hpf and 43 hpf shows the change from diffuse melanin (41 hpf) to a tiny, dense spot (43 hpf) (B). The graphical plot shows the increase of the mean (±s.e.) number of segments containing residual melanised cells from a typical series of embryos (n=19), from 35 hpf to 57 hpf (C), (reproduced with the kind permission of Greenhill *et al.*, 2011).

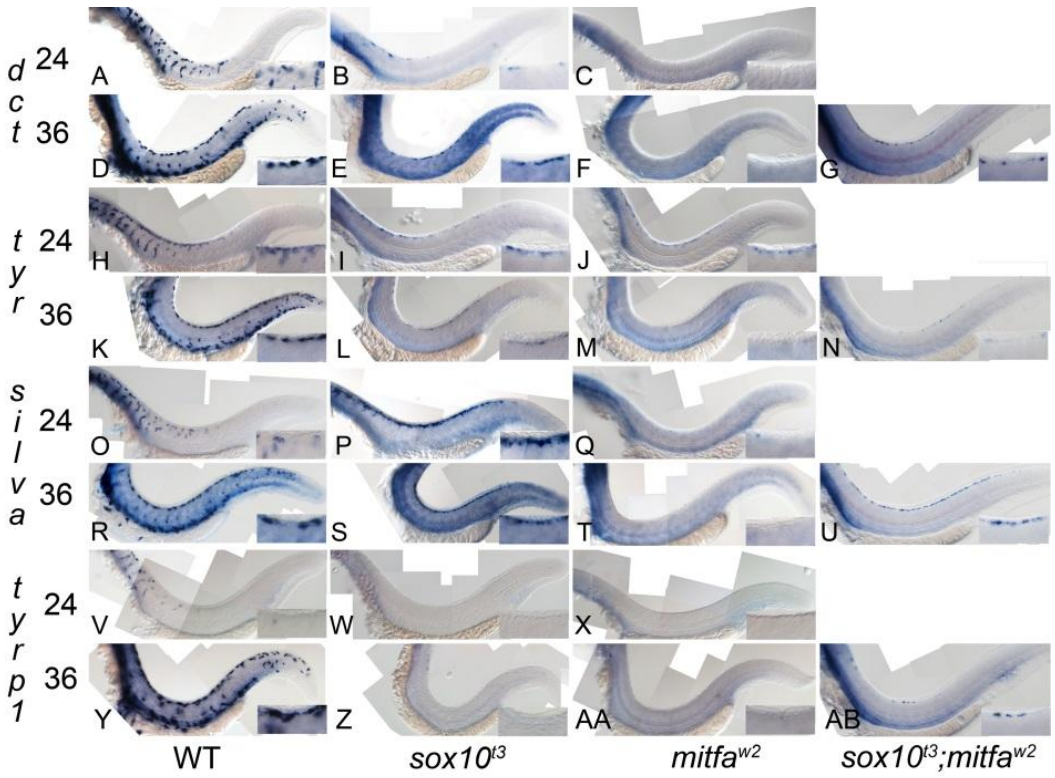

Figure 5.02: De-repression of *silva, dct* and *tyr* observed in somites of *sox10* ^{t3}, *mitfa*^{w2} and *sox10* ^{t3};*mitfa* ^{w2} zebrafish mutants

WISH showing expression of *dct*, *tyr*, *silva* and *tyrp1* in the lateral trunk of wild-type (WT), *sox10*^{t3}, *mitfa*^{w2} and *sox10*^{t3}; *mitfa*^{w2} mutants are presented at 24 and 36 hpf as indicated (A-AB). Insets in each panel show enlargement of area of dorsal posterior trunk. Note the pronounced de-repression of *silva* and *dct*, mild de-repression of *tyr*, and minimal residual expression of *tyrp1*. Note that all WISH were over-developed in order to detect low level expression, (reproduced with the kind permission of Greenhill *et al.*, 2011).

Table 5.01: Quantification of zebrafish mutant embryos showing residual marker gene expression.

Residual expression for *silva*, *dct*, *tyrosinase* and *tyrp1b* was assessed in *sox10*^{t3} and *mitfa*^{w2} mutants from 24 hpf to 60 hpf. Colour coding reflects percentage with residual expression: 90-100%; 20-89%; 0-19%, n.d: not determined. (Reproduced with the kind permission of Greenhill *et al.*, 2011).

Marker	Genotype	24 hpf	30 hpf	36 hpf	42 hpf	48 hpf	54 hpf	60 hpf
silva	*sox10*	10/10	12/12	14/14	14/14	18/20	12/16	0/11
	mitfa	2/6	5/12	0/7	n.d.	n.d.	n.d.	n.d.
dct	*sox10*	14/14	12/12	14/15	8/8	8/16	1/11	0/12
	mitfa	0/6	5/12	0/10	n.d.	n.d.	n.d.	n.d.
tyrosinase	*sox10*	11/11	17/17	10/11	15/17	5/13	3/16	0/11
	mitfa	6/6	10/10	0/8	n.d.	n.d.	n.d.	n.d.
tyrp1b	*sox10*	12/12	8/8	7/9	7/7	2/6	0/1	0/8
	mitfa	6/9	0/11	0/11	n.d.	n.d.	n.d.	n.d.

5.1.3 The GRN predicts that the decrease of *sox10* expression during melanocyte development is Mitfa dependent

5.1.3.a The transcription factor Mitfa activates *sox10* expression ectopically

In zebrafish, in contrast with observations in the mouse model, *sox10* expression seems to be decreased during melanocyte differentiation (Hou *et al.*, 2006, Harris *et al.*, 2010, Greenhill *et al.*, 2011). Interestingly, ectopic injections of *mitfa* mRNA in transgenic *Tg(-7.2sox10:GFP)* embryos showed strong activation of GFP in embryos at both 6 hpf and 10.5 hpf suggesting direct activation of expression (Table 5.02). As a positive control, *sox10* mRNA was injected. As a negative controls two constructs were injected; the version of the *sox10* allele containing a non-conservative substitution (L142Q) of a fully-conserved residue in the HMG domain, *sox10* (L142Q), and *mitfa*^{w2} mRNA. This resulted in no activation of GFP (Figure 5.03).

The results showed that *mitfa* mRNA injection could ectopically activate s*ox10* expression in zebrafish. Consequently, ectopic *mitfa* expression could activate *sox10* expression suggesting that Mitfa could directly or indirectly activate *sox10* promoter (Figure 5.03, Table 5.02) (Greenhill *et al.*, 2011). To narrow the region of the *sox10* promoter which could be bound by Mitfa, the experiment was repeated in *Tg(-4.9sox10:GFP)* line in which the farthest 5' region, including three M-boxes, was absent. No activation of GFP could be seen at 6 hpf in embryos injected with *mitfa* mRNA (Greenhill *et al.*, 2011). These results suggested that Mitfa might activate *sox10* expression by binding one or more of the 3' M-boxes in the promoter of *sox10*. From these observations, the hypothesis was suggested that *sox10* decrease would be Mitfa dependent in zebrafish *in vivo*. The recruitment or the presence of a negative co-regulator of Mitfa, *in vivo* in NC, would cause this to become a repressive interaction (Greenhill *et al.*, 2011). The hypothesis was suggested that Hdac1 could be this co-repressor.

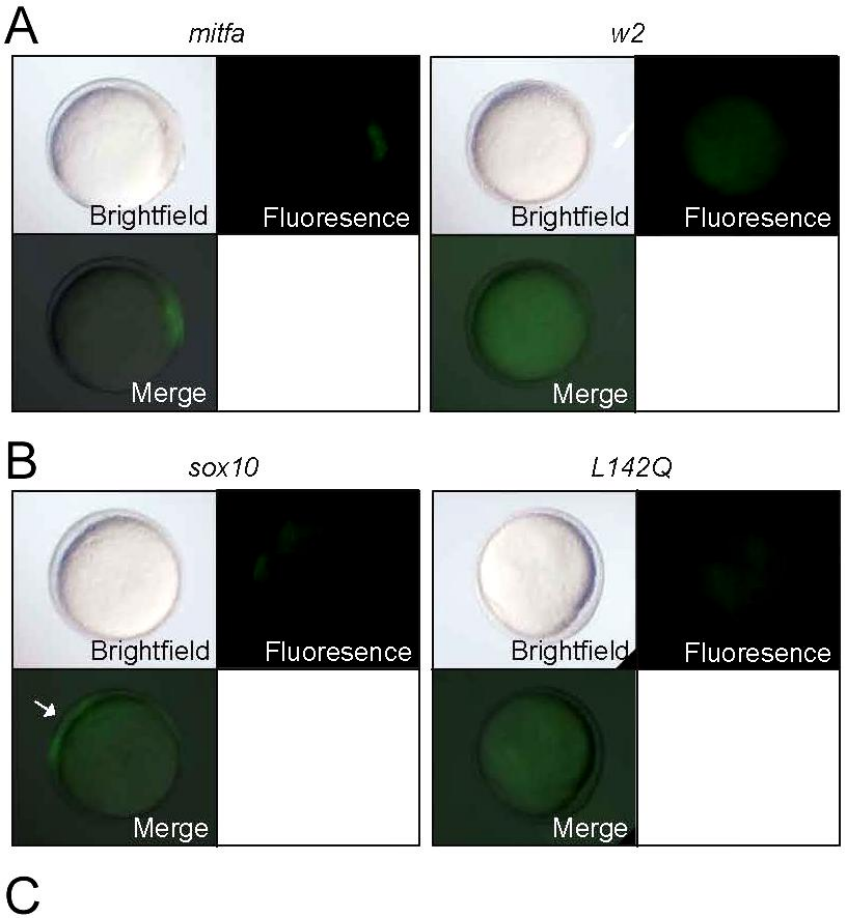

Figure 5.03: Ectopic injection of *mitfa* mRNA in one-cell stage embryos can activate GFP in *Tg*(-7.2*sox10:GFP*) by 6 hpf.

Embryos are shown in lateral view in bright field, or fluorescence, as indicated. *Tg*(-7.2*sox10:GFP*) embryos were injected with RNA encoding wild-type (A, left panel) or *mitfa*^{w2} mutant *mitfa* (A, right panel) or *sox10* wild-type mRNA (B, left panel) or *sox10(L142Q)* mutant (B, right panel). Representative embryos are shown at 10.5 hpf, with GFP expression detectable in those injected with wild-type, but not mutant forms, (reproduced with the kind permission of Greenhill *et al.*, 2011).

Table 5.02: Proportion of embryos from *Tg(-7.2sox10:GFP)* outcross showing expression of GFP at 6 hpf and 10 .5 hpf after injection of with indicated mRNA.

(NB: Only 50 % of embryos from this cross would be transgenic, thus maximum percentage GFP+ embryos expected is 50 %. At 6 hpf and 10.5 hpf, both series of embryos injected with WT mRNA showed expression of GFP whereas negative controls tests injecting mutant mRNA version of the genes showed no GFP expression (reproduced with the kind permission of Greenhill *et al.*, 2011).

RNA	6 hpf		10.5 hpf	
mitfa	94/257	37%	68/152	45%
mitfa(w2)	0/118	0%	0/78	0%
sox10	20/319	6%	95/193	49%
sox10(L142Q)	0/120	0%	0/80	0%

5.1.3.b Mitfa and Hdac1 could be responsible for the repression of *sox10* expression in melanocytes

It has been suggested that a co-repressor present *in vivo* in NC cells could be recruited by Mitfa to repress *sox10* and allow the differentiation of melanocytes (Greenhill *et al.*, 2011). In this study, we tested the hypothesis that Hdac is a co-repressor for Mitfa to downregulate *sox10* expression in melanocytes.

Hdac1 is a protein of the histone deacetylase family which are proteins involved in chromatin deacetylation which is a key mechanism of epigenetic gene silencing (Harrison *et al.*, 2011, Cunliffe, 2004). *hdac1* expression is ubiquitous in zebrafish during development until 19 hpf. After this timepoint, *hdac1* expression is not spatially restricted but it is strongly maintained in head and more weakly expressed in dorsal and ventral stripe at 36 hpf (Thisse, 2004). In zebrafish, *histone deactylase 1* (*hdac1)* function has been shown to be involved in the process of development of the central nervous system. Particularly, it has been shown to be necessary for the specification and patterning of neurones and myelinating glial cells, via regulating the transcription of key genes for early neurogenesis such as *achaete-scute complex-like 1b (ascl1b)* (Harrison *et al.*, 2011).

In the context of the *hdac1/colgate* mutant analysis, a small molecule inhibitor of Hdacs, Trichostatin A (TSA), was used to test the our hypothesis. TSA treatments were used at different time periods focusing on *sox10* expression and development of melanocytes, especially during melanocyte differentiation. The study of the *colgate*/*hdac1* zebrafish mutant showed two interesting features. Firstly, melanocytes exhibited developmental retardation during differentiation with reduced melanised cells suggesting defective melanocyte development from 27 hpf until at least 72 hpf (Figure 5.04). Secondly, a persistent *sox10* expression was observed in the dorsal part of embryos at 52 hpf (Figure 5.05) (Ignatius *et al.*, 2008). Interestingly, *sox10* expression was not changed at 24 hpf in mutant (Figure 5.05). Furthermore *mitfa* expression was firstly reduced in *colgate/hdac1* mutant at 25 hpf, but then recovered and was increased at 48 hpf compared to its expression in WT (Figure 5.06). *dct* and *c-kit* expressions remained greatly reduced in mutant embryos from 25 hpf to 48 hpf at least, whereas *foxd3* expression was boosted at 24 hpf in premigratory NC cells and in the somites (Ignatius *et al.*, 2008). To explain these results, Ignatius *et al.*, (2008), suggested that Hdac1 could be a repressor of *foxd3*.

In our experiments, we explored the phenotype of loss of melanocyte differentiation in the *colgate*/*hdac1* zebrafish mutant and the persistence of *sox10* expression at 48 hpf. According to our hypothesis, the phenotype of elevation of *mitfa* at 52 hpf in the *colgate/hdac1* mutant could be explained by the persistence of *sox10* in *colgate/hdac1* mutants. Also, this persistence of expression could cause a repression, or a delay of *dct* expression (due to the previously described repressive effects of Sox10 on *dct*).

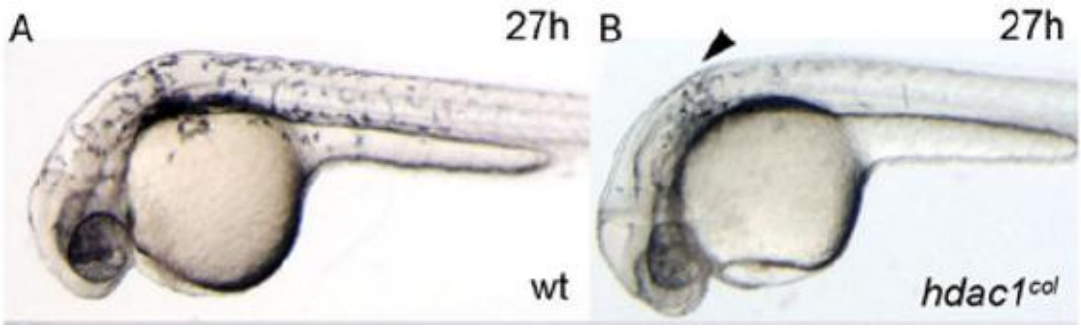

Figure 5.04 Melanocyte differentiation is disrupted in the *colgate/hdac1* zebrafish mutant by 27 hpf

27 hpf WT (A) and *hdac1/colgate* mutant (B) embryos in lateral view. In WT embryos, melanocytes can be observed posterior to the eye and otic vesicle while some are migrating over the flank of the embryo (A). In contrast, in mutant embryos fewer melanocytes can be observed and cells seemed to accumulate posterior to the otic vesicle (arrowheads in B points at melanocytes posterior to the otic vesicle), very few migrating melanocytes can be seen (B), (reproduced with the kind permission of Ignatius *et al.*, 2008).

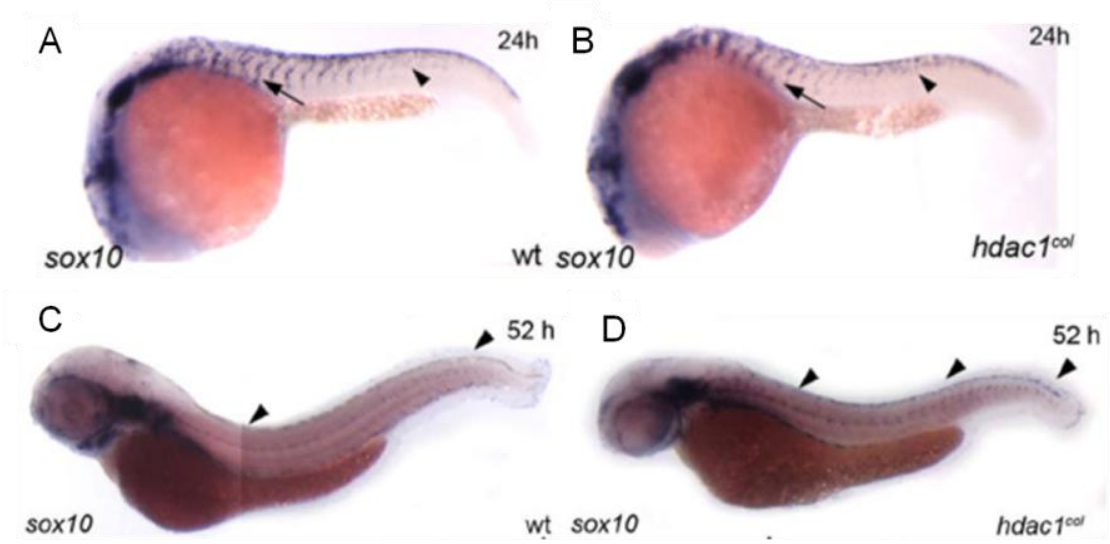

Figure 5.05: *sox10* expression is reduced at 24 hpf but persistent at 52 hpf in *colgate/hdac1* zebrafish embryos

WISH investigating *sox10* expression in WT (A,C) and *colgate/hdac1* mutant (B,D) embryos. 24 hpf embryos (A-B) and 52 hpf embryos (C-D) are presented in lateral view. At 24 hpf, no differences could be observed in the expression of *sox10* in number of cranial and trunk NC cells ((A-B) arrowheads). At 52 hpf *sox10* expression was persistent and robust in the dorsal stripe of *colgate/hdac1* mutants, while expression in wild-type is absent to faint ((C-D) arrowheads), (reproduced with the kind permission of Ignatius *et al.*, 2008).

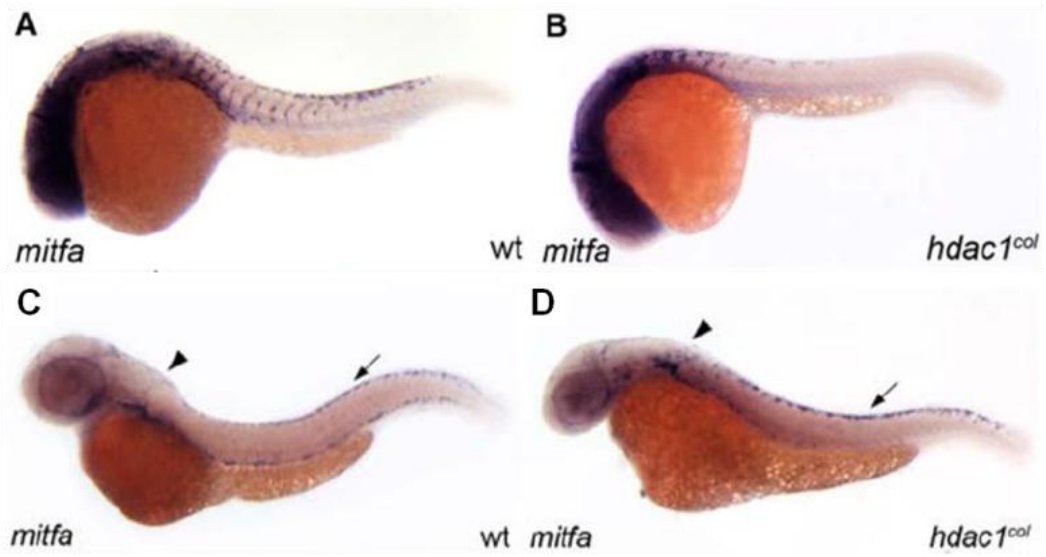

Figure 5.06: *mitfa* expression is reduced at 25 hpf and activated by 48 hpf in melanocytes in *colgate/hdac1* zebrafish mutants.

WISH investigating *mitfa* expression in WT (A,C) and *colgate/hdac1* mutant (B,D) embryos at 25 hpf (A-B) and 48 hpf (C-D). Embryos are presented in lateral view. At 25 hpf, fewer *mitfa*-positive melanoblasts were specified in *colgate/hdac1* mutants as compared to WT. At 48 hpf *mitfa* expression is decreased in differentiating melanoblasts in wild-type however it is robustly expressed in melanoblasts in *colgate/hdac1* in dorsal region (C and D arrowheads), (reproduced with the kind permission of Ignatius *et al.*, 2008).

5.1.4 The role and the regulation of *mitfa* in melanocyte development

One aspect of the *Mitfa* regulatory network which remains unclear is its auto-regulation. It has been shown *in vitro* that MITF might activate its own expression (Saito *et al.*, 2002). However, this hypothesis has not been assessed using *in vivo* data and it remains unclear if and when Mitf could be responsible for its own activation. In this Chapter, to clarify whether or not it is plausible that Mitfa could activate its own expression, we tested *mitfa* transcription response to ectopic *mitfa* mRNA induction in zebrafish at one cell stage.

5.1.5 Aims and approach

The objective of these experiments was to better understand the dynamic interactions between *sox10* and *mitfa,* focusing especially on the melanocyte differentiation phase.

- We investigated expression levels of *mitfa, sox10, dct* and *tyrp1b* by RT-qPCR at three timepoints in $sox10^{t3}$ and $mitfa^{w2}$ mutants to quantify the degree of de-repression of *dct* in *sox10* mutants (Greenhill *et al.*, 2011).
- Hdac-mediated repression of *sox10* expression was tested by investigating the effects of Hdac inhibition on *sox10* expression. This experiment was critical to test the hypothesis that Mitfa and Hdac could be co-repressing *sox10* expression during melanocyte differentiation.
- Mitfa dependent activation of *mitfa* was tested ectopically *in vivo* to assess whether Mitfa could activate its own expression,

Altogether these experiments should help to clarify the regulatory interactions which associate Sox10 and Mitfa during melanocyte differentiation and contribute to the testing of the GRN.

5.2 Results

5.2.1 Melanocytic gene expression was tested by RT-qPCR in *sox10*^{t3} and *mitfa*^{w2} mutants

Previous WISH experiments have described the decrease of *sox10*, *mitfa*, *dct* and *tyrp1b* expressions in zebrafish *sox10*^{t3} mutant and the decrease of *dct*, *mitfa* and *tyrp1b* in *mitfa*^{w2} mutant (Greenhill *et al.*, 2011). The results showed the de-repression of *dct* expression, but not of *tyrp1b* expression in the *sox10*^{t3} mutant. However, these experiments did not quantitatively assess the level of expression of the genes in the *sox10*^{t3} and *mitfa*^{w2} mutants. In the experiments presented here, we used the quantitative technique of RT-qPCR to measure *dct*, *tyrp1b* and *mitfa* expressions in *sox10*^{t3} and *mitfa*^{w2} mutants at 30 hpf, 36 hpf and 72 hpf (Figure 5.07). Five samples of fifty embryos of each genotype, homozygous *mitfa*^{w2} and homozygous *sox10*^{t3} were analysed. Heads were removed using forceps to avoid detection of *dct* expression from eyes or *sox10* expression from otic vesicle. RNA was extracted using tri-reagent (Sigma) and RT-qPCR were run (Livak and Schmittgen, 2001). The results were normalised to the expression level of the reference gene *gapdh*, and expression level of genes in *mitfa*^{w2} and *sox10*^{t3} were compared statistically. Data were analysed using the ΔΔCt method (Livak and Schmittgen, 2001).

The results of gene expression quantification by RT-qPCR in mutants are presented in Figure 5.07 - expression levels are reported as a proportion of the expression levels found in WT at each timepoint. The results of the statistical analysis (p-values) are presented in Table 5.03. The results showed that gene expression for all genes examined was greatly reduced at each timepoint in both *mitfa*^{w2} and *sox10*^{t3} mutants compared to WT. At each timepoint, the expression of *mitfa* was significantly higher in *mitfa*^{w2} mutants compared to *sox10*^{t3} mutants as the non-functional mRNA could be produced in *mitfa*^{w2} mutants whereas no *mitfa* mRNA was produced in *sox10*^{t3} mutants. Importantly, the level of *mitfa* expression in *mitfa*^{w2} mutants was less than in WT, which indicates that the *sox10*-dependent activation of *mitfa* is not sufficient to explain fully the level of *mitfa* in the WT. In other words, there is some sort of Mitfa-dependent activation of *mitfa* at these stages. A significantly higher level of *tyrp1b* in *sox10*^{t3} mutant compared to *mitfa*^{w2} mutant was also observed, however, in both mutants the levels of expression remained very low. Investigating the level of expression of *dct* at the early time-point, 30 hpf, showed that *dct* expression was significantly higher (about five times) in the *sox10*^{t3} mutant compared to expression in the *mitfa*^{w2} mutant, whereas this was not the case for *tyrp1b*. This data are consistent with the de-repression of *dct* expression in *sox10*^{t3} mutant suggested by the model. Consequently, this experiment suggested that previous results showing the *sox10* de-repression of *dct*, but not of *tyrp1b* expression, could be confirmed and quantified. Together the data support the suggestion that *sox10* is a weak repressor of some but not all genes downstream to Mitfa in zebrafish melanocytes.

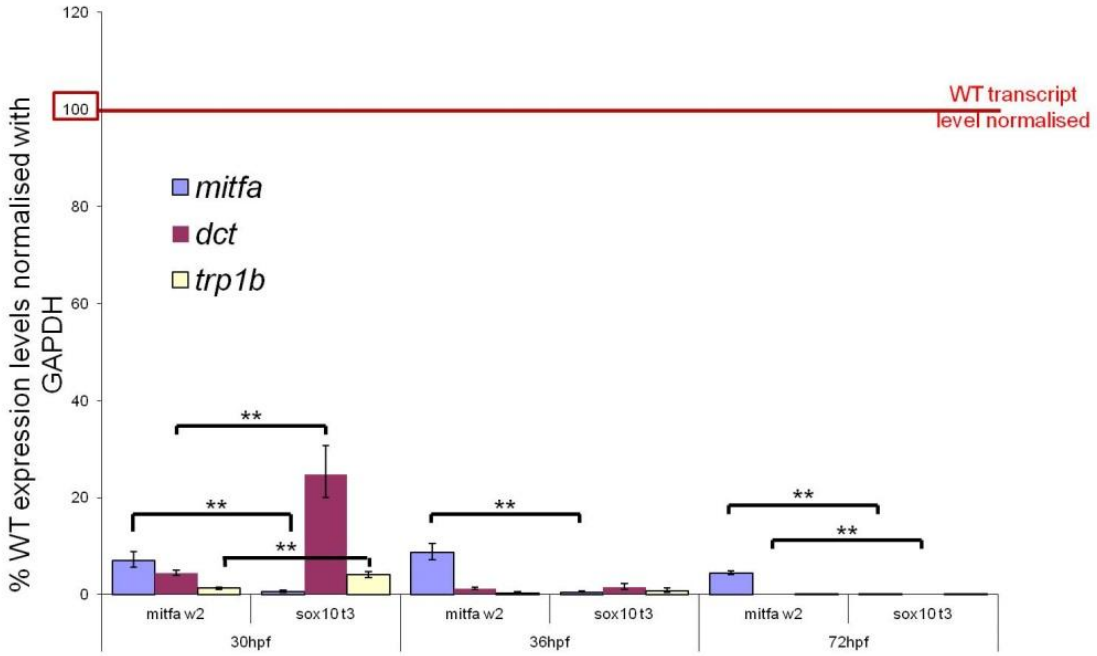

Figure 5.07: RT-quantitative PCR of *mitfa, dct* and *tyrp1b* expression in zebrafish wild-type (WT), *mitfa*^{w2} mutants and *sox10*^{t3} mutants.

Values shown are means (bars show standard deviation), at 30 hpf, 36 hpf and 72 hpf. Expression levels in WT controls were normalised to *gapdh* expression for each sample and expression is shown as a percentage of WT transcript expression levels normalised to *gapdh* expression. The differences in gene expression levels in *sox10* mutants compared with *mitfa* mutants were tested and significant results are indicated on the graph (one-tailed t-test with Bonferroni correction for multiple comparisons,**). (reproduced with the kind permission of Greenhill *et al.*, 2011).

Table 5.03: Result of the statistical analysis (p-values) of the comparison of gene expression in *mitfa*^{w2} mutant and *sox10*^{t3} mutant.
Student t-test with Boniferroni correction for multiple comparison was used to determine p-values and after correction. The results were significant when p-value < 0.017. For each condition, gene expression was determined in five samples of fifty pooled embryos.

gene	***mitfa***	***dct***	***trp1b***
30 hpf	0.0116	0.0117	0.0071
36 hpf	0.0026	0.0348	0.0248
72 hpf	0.0127	0.0069	0.0344

5.2.2 Testing Hdac as a Mitfa dependent co-repressor of *sox10*

We investigated a mechanism for *sox10* downregulation in melanocyte during the differentiation phase. In regards to the analysis of the *colgate*/*hdac1* mutant (maintenance of *sox10* in melanocytes at 48 hpf and melanocyte development retardation), the hypothesis was that Hdac1 could be a Mitfa dependent inhibitor of *sox10* during melanocyte differentiation. This co-regulation could be happening via a complex Mitfa/Hdac1 or alternatively, via the recruitment of Hadc1, by Mitfa, to the regulatory sequences on *sox10* promoter.

The objective of these experiments was to phenocopy the effects of melanocyte differentiation loss and *sox10* expression persistence at 48 hpf, observed in *colgate/hdac1* mutant with the TSA treatments (Ignatius *et al.*, 2008). Consequently, the focus of the experiments was to observe effects of inhibiting Hdac(s) on *sox10* expression persistence in the dorsal part of embryos and on disruption of melanocyte differentiation at about 48 hpf zebrafish embryos. If Hdac(s) are involved in inhibiting *sox10* expression in a Mitfa dependent manner, we would expect to observe a persistence of *sox10* expression in melanocytes in TSA treated embryos and in *mitfa*^{w2} mutant. If Mitfa and Hdac(s) work together as co-repressors, we would expect no effects of TSA treatments on *mitfa* expression levels and no effects of the TSA treatments in absence of Mitfa. Embryos were treated from 12 hpf, 24 hpf, 30 hpf and 36 hpf to 48 hpf covering both the specification and differentiation phases of melanocyte development.

5.2.2.a Hdac inhibitor treatments caused melanocyte development disruption

The phenotype of the *colgate*/*hdac1* zebrafish mutant has been described by Ignatius *et al.*, (2008). Compared to 27 hpf wild-type (WT) embryos, where the melanocytes were posterior to the eye and otic vesicle and migrating over the flank of the embryo, the *colgate*/*hdac1* mutant had fewer melanocytes with most located posterior to the otic vesicle and there was no observation of migrating melanocytes. Importantly, Ignatius *et al.,* (2008) showed that NC induction and migration of non-melanogenic cells were unaffected in the mutant. Furthermore, in WT, by 72 hpf, melanocytes were present in four stripes whereas, in *colgate*/*hdac1* mutants, melanocyte numbers remained low (Ignatius *et al.*, 2008). Ignatius *et al.,* (2008) suggested that melanocytes present in *colgate*/*hdac1* mutant failed to migrate and were mainly localized to the dorsal stripe and to a patch of melanocytes posterior to the otic vesicle (Ignatius *et al.*, 2008). Cells which did migrate ventrally in *colgate/hdac1* mutants were present in the anterior ventral stripe over the yolk extension. In the experiments described in this Chapter, we saw no evidence for impairment of cell migration and therefore it was not investigated.

Embryos were treated with TSA during four time periods and the changes on melanocyte differentiation were assessed. The results of TSA treatments on melanocyte differentiation are presented in Figures 5.08 and 5.09. We observed that all TSA treatments from 12-48 hpf, 24-48 hpf, 30-48 hpf and 36-48 hpf, clearly resulted in developmental retardation in fish (Figure 5.08). Zebrafish development and morphological changes are

very well described at these stages, therefore, assessment of embryonic retardation can be readily achieved (Kimmel *et al.*, 1995). Zhu *et al.*, (2011) also described this type of developmental retardation phenotype when treating fish with TSA. This suggests that these effects could be the result of inhibition of Hdac proteins involved in early development, by TSA, as it was not observed in *colgate/hdac1* embryos. Consequently, to compensate for this developmental retardation, treated embryos were staged on general morphology and the melanocyte phenotypes (e.g. melanisation, cell shape or number of cells) were observed and compared to the phenotype of melanocytes in a stage-matched embryo.

We found that TSA treatments led to disruption/inhibition of melanocyte differentiation. TSA treatment from 12 hpf to 48 hpf caused reduced pigmentation (reduced melanised cell number) and strong developmental retardation as seen by the reduced development of head structures such as eyes, and by a reduction of body size (Figure 5.08). Embryos treated from 30-48 hpf and 36-48 hpf showed developmental retardation, although, the number of melanised cells did not seem to be affected compared to the phenotype in the 24-48 hpf treated fish (Figures 5.08). We found that after treatment 48 hpf embryos could be morphologically staged as equivalent to 36 hpf embryos. Therefore, to compare the melanisation and melanocyte development between treated and untreated fish, the 36 hpf staged embryos were used as a control (Figure 5.09). The results showed that treating embryos from 24 - 48 hpf led to an important decrease of melanised cells compared to the 36 hpf stage control (Figure 5.09). This reduction of melanised cells could be due to the reduction or loss of cell melanisation (Figure 5.09). This observation suggested that the developmental retardation and the pigment phenotype were two independent phenomena. It also suggested that Hdac was important in the time period of 24 to 30 hpf for melanisation and melanocyte development. However, it remains to be investigated whether Hdac could be involved in *sox10* regulation at early stages.

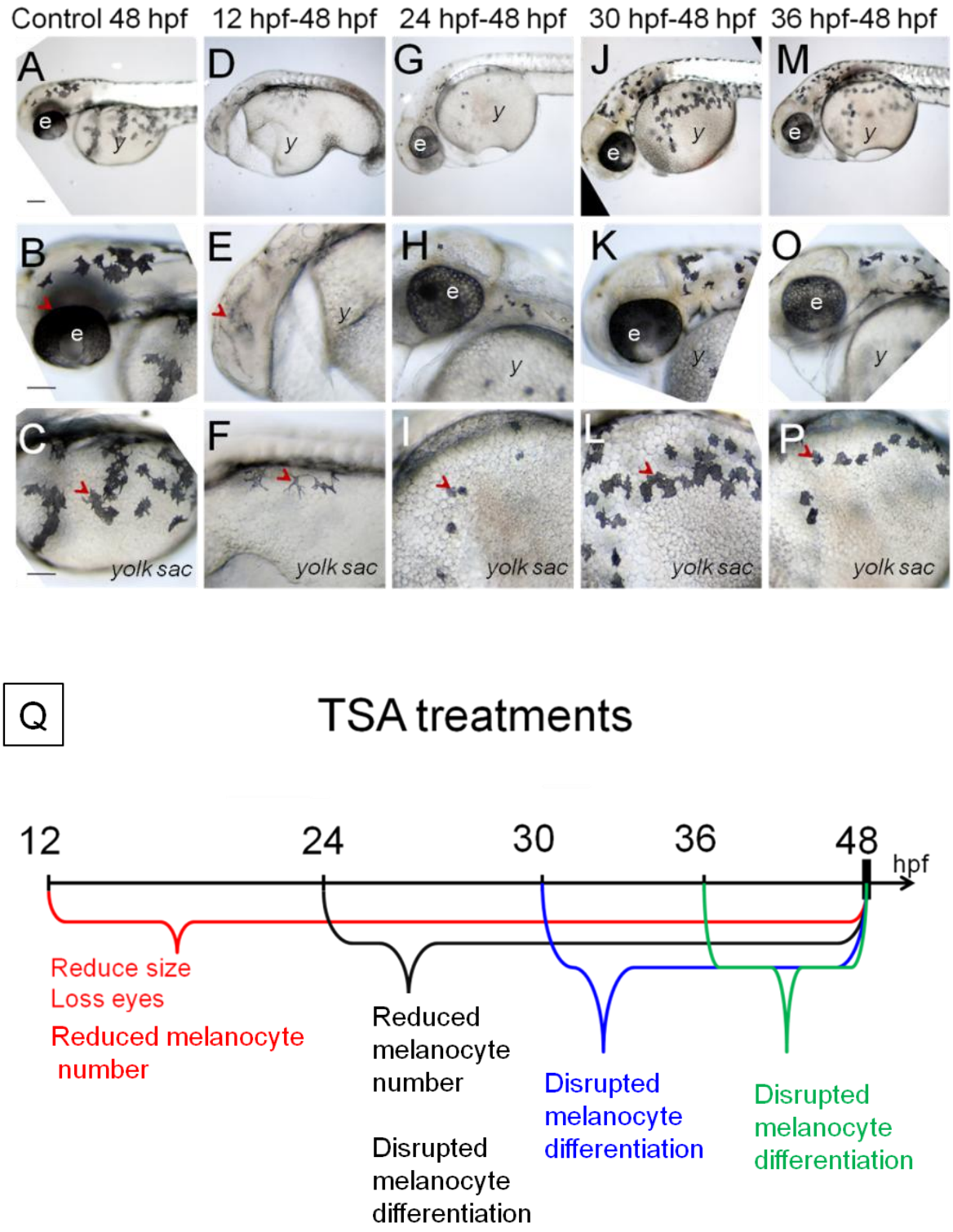

Figure 5.08: Hdac inhibitory treatments lead to developmental retardation of the zebrafish embryo and to disruption of melanocyte differentiation. See legend on the next page.

Figure 5.08: Hdac inhibitory treatments lead to developmental retardation of the zebrafish embryo and to disruption of melanocyte differentiation.

Embryos were treated with Trichostatin A (TSA) (1 µM concentration) for four different time windows, 12-48 hpf, 24-48 hpf, 30-48 hpf and 36-48 hpf. Embryos treated from 12-48 hpf (D-F), show drastic decrease melanocyte number (not quantified, only observed), lack of eye structure (in B arrowheads points eyes whereas in E, arrowheads points the lack of eye), short body size and developmental retardation. Embryos treated from 24, 30 and 36 to 48 hpf (G-P) show developmental retardation compare to 48 hpf DMSO treated control (A-C). Embryos treated from 24-48 hpf also seem to show decrease melanocyte number (not quantified, only observed)). Treated embryos (G-P) were staged as morphologically equivalent to 36 hpf (Kimmel *et al.*, 1995) (in C,F,I,L,P, arrowheads points at melanocytes. Embryos are shown in lateral view. e: eyes; y: yolk sac, Scale bar: 100 µm. For each condition, 160 fish were tested and observed and representative phenotypes are shown here. (Q) The scheme summarises the effects and the timing of the different TSA treatments in embryos and melanocyte development.

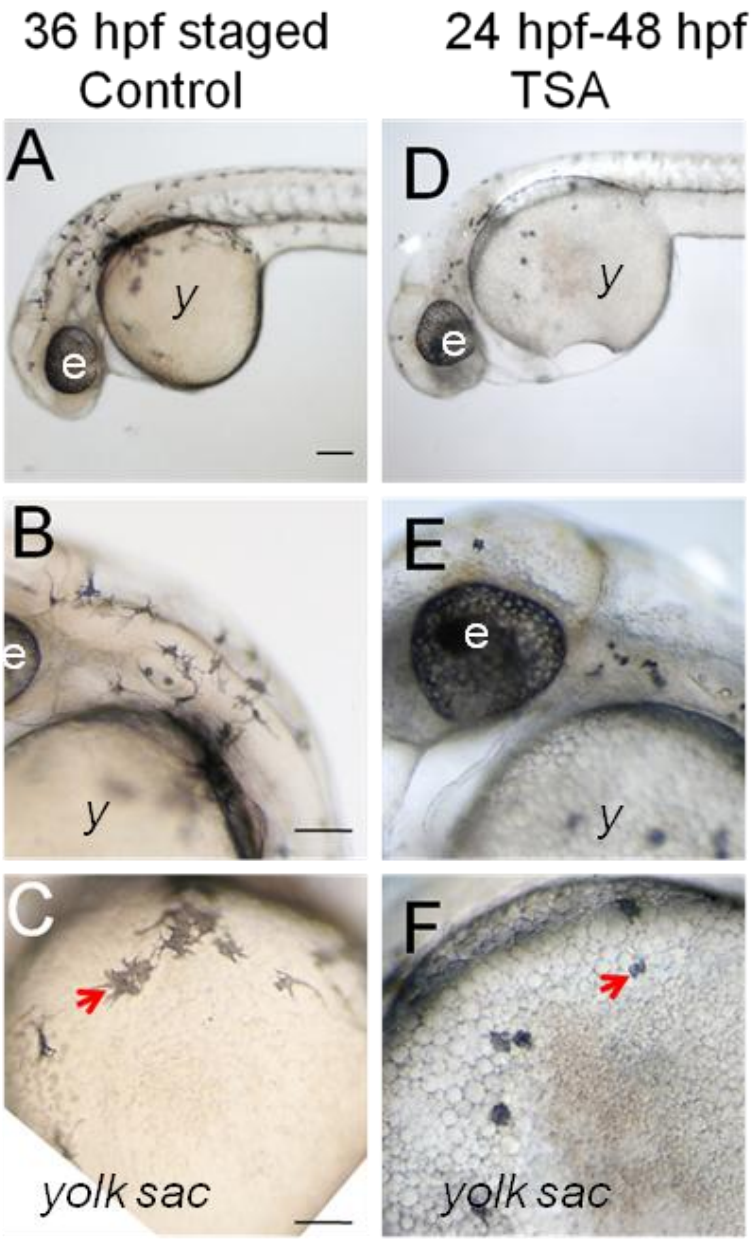

Figure 5.09: Treating zebrafish embryos with TSA from 24 to 48 hpf causes disruption of melanocyte differentiation and reduced melanised cell number.

Embryos were treated with Trichostatin A (TSA) (1 µM concentration), from 24 to 48 hpf and shown in lateral view (D-F). Embryos were staged as 36 hpf and melanocyte number as well as shape or size of melanocytes was reduced as shown in (D-F) compare to stage-matched control (A-C). (A,D) show embryos in lateral view, (B,E) show heads and anterior trunk in lateral view and (C,F) show yolk sac in lateral view (arrowheads point at melanocytes). For each condition, 160 fish were tested and observed and representative phenotypes are shown here. e: eyes ; y: yolk sac. Scale bar: 100 µm.

5.2.2.b Hdac inhibitor treatments caused persistence of *sox10* expression in melanocytes

For the next step in investigating Hdac as an Mitfa-dependent repressor of *sox10* expression during melanocyte differentiation, we assessed the effects of TSA treatments on *sox10* expression. Dutton *et al.*, (2001) described the time course of *sox10* expression in zebrafish from the five-somite stage to 60 hpf. Until about 23 hpf *sox10* expression is a NC cell marker. Later it is downregulated in most derivatives, until its expression becomes strictly restricted to glial cells (Potterf *et al.*, 2001, Carney *et al.*, 2006, Drerup *et al.*, 2009, Kelsh, 2006b, Dutton *et al.*, 2001). From five-somite stage to fourteen-somite stage, *sox10* is expressed in most cranial and trunk premigratory NC cells. From eighteen-somite stage, *sox10* is strongly expressed in the premigratory and migrating NC cells and in the otic vesicle. By 24 hpf, *sox10* expression is associated with cranial ganglia and posterior lateral line nerve, but also with the otic vesicle and migrating NC cells throughout the trunk and in premigratory crest. Then, cells expressing *sox10* extend along the posterior lateral line nerve, and in some migrating cells of the rostral trunk. At 36 hpf weak *sox10* expression was reported in some melanocytes in some cells of the dorsal stripe. At 40 hpf, *sox10* was detected in cells adjacent to the notochord in segmentally arranged lines which were presumed to be glial cells. By 60 hpf *sox10* was expressed in the enteric nervous system of embryos.

colgate/hdac1 mutant embryos showed persistence of *sox10* expression in the dorsal region of embryos at 48 hpf (staged as 36 hpf) in NC derived cells. These cells are likely to be glioblasts and melanoblasts according to positioning and staining with *sox10* (Ignatius *et al.*, 2008). In the experiment described here, TSA-treated embryos were staged at 36 hpf and *sox10* expression was investigated by WISH after TSA treatments.

The results shown in Figure 5.10 demonstrate that embryos treated with TSA from 24-48 hpf had elevated *sox10* expression in dorsal position, the position of premigratory NC cells. However, to test whether *sox10* expression was boosted in melanocytes, the experiment was repeated reducing the dose of PTU treatment to avoid total inhibition of melanin synthesis in cells. Cells of the dorsal stripe were then observed carefully to test for co-localisation of the WISH signal and melanin (Figure 5.11). Our results clearly showed that *sox10* expression was boosted in brown melanised cells in embryos treated from 24 - 48 hpf compared to staged control embryos. The blue signal was weaker and even sometimes absent from melanised brown cells in controls, whereas it was co-localised in melanocytes of treated embryos.

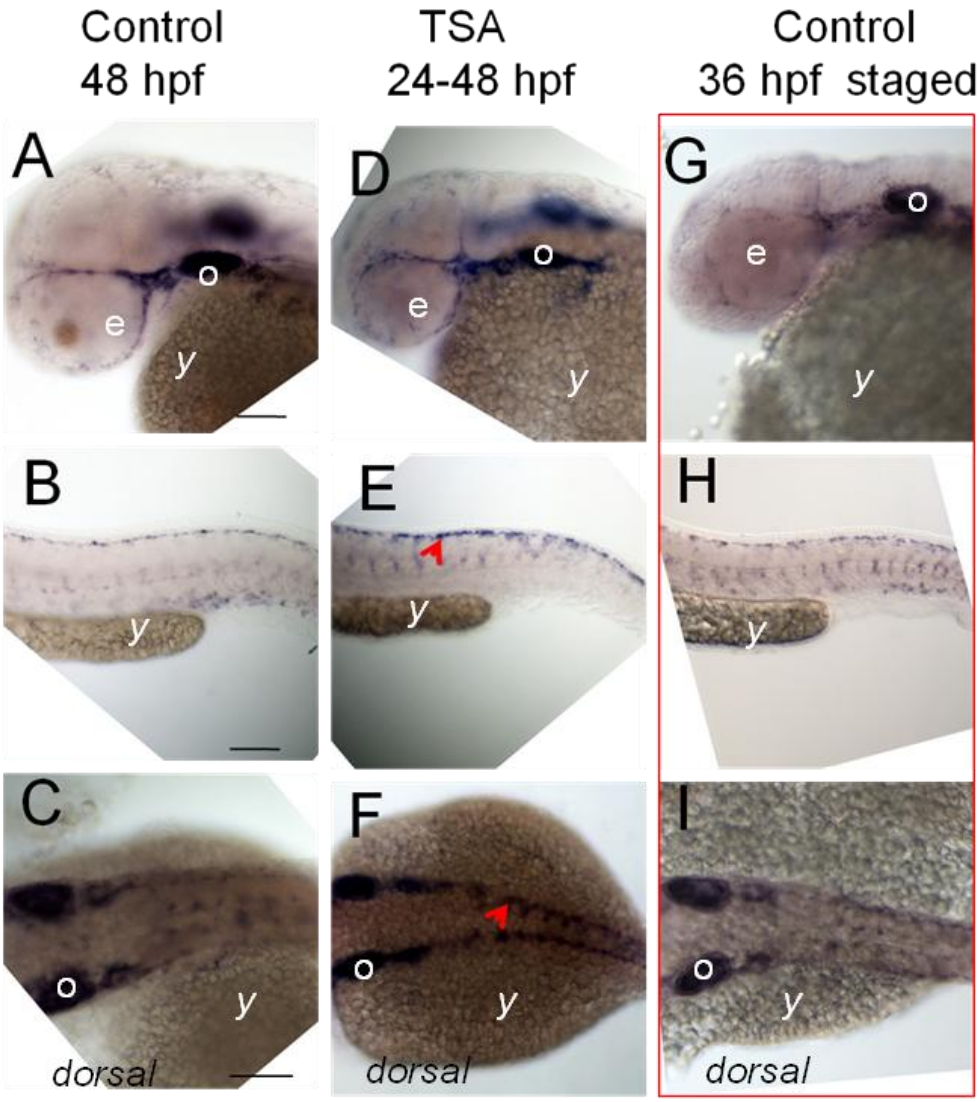

Figure 5.10: *sox10* expression is boosted in premigratory NC derived cells in 24-48 hpf TSA treated zebrafish embryos.

Embryos were treated with PTU and Trichostatin A (1 µM concentration) from 24-48 hpf (D-F). WISH with *sox10* probe shows an elevated *sox10* expression in premigratory (the arrowhead in E shows the cells marked by the signal in the dorsal part of the embryo's trunk) and migrating NC derived cells (probably melanoglioblasts according to the stage) of treated embryos (E-F, the arrowhead shows the cells marked by the signal) compared to staged DMSO treated control (H-I). (A,D,G) show dorsolateral view of heads, (B,E,H) show lateral view of trunk and (C,F,I) show dorsal view of trunk. 80 embryos were observed and analysed for each condition and representative embryos were shown here. e: eyes ; y: yolk sac ; o: otic vesicle. Scale bar: 100 µm.

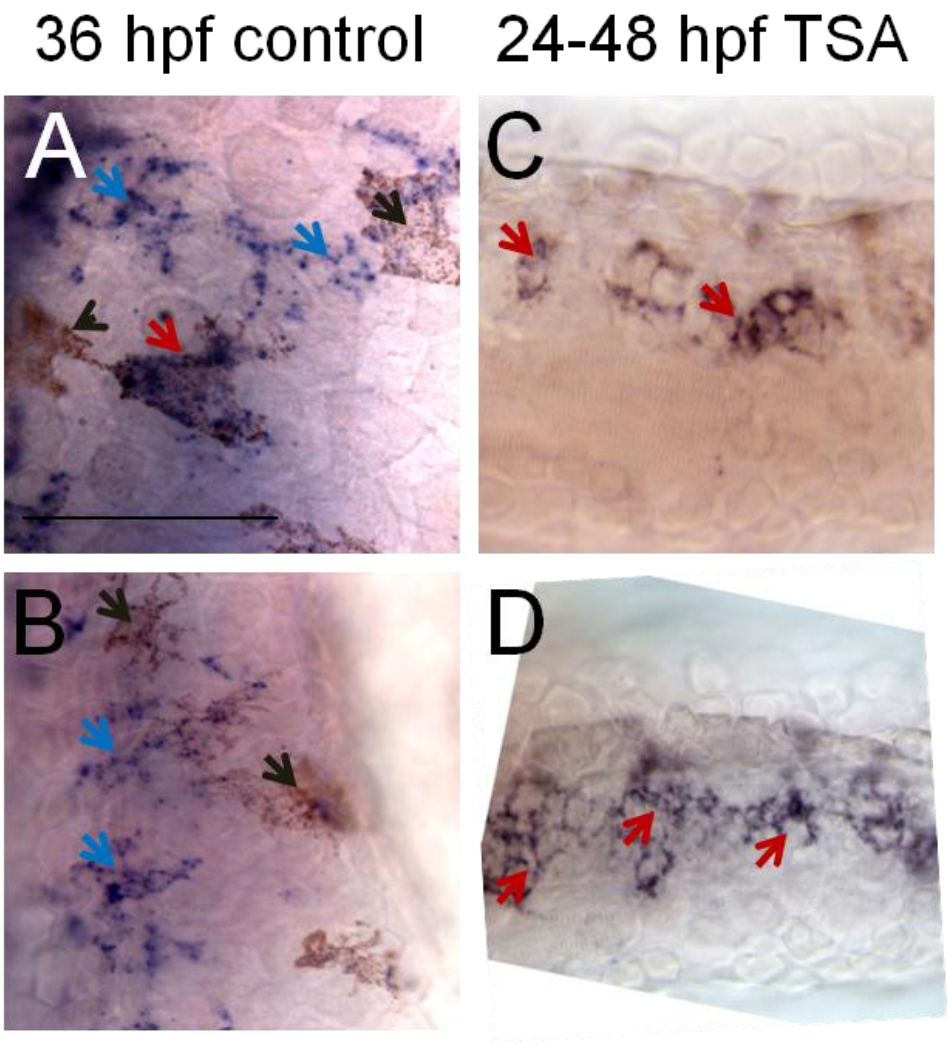

Figure 5.11: *sox10* expression is boosted in melanocytes after 24-48 hpf *hdac* inhibition by TSA treatment in zebrafish embryos.

Embryos were treated with low dose PTU (70 %) allowing only light production of melanin. WISH investigating *sox10* expression shows that Trichostatin A (1 µM) treated embryos (C,D) from 24 hpf to 48 hpf present increased *sox10* expression in melanocytes (B,D red arrows showing co-localisation of brown cells and blue signal) compare to 36 hpf staged control (A,B, the blue arrowheads show blue signal (*sox10* expression) outside of melanised cells (the black arrowheads show melanocytes that lack detectable blue signal) - note that co-localisation of blue signal and melanin is less frequent in controls than in treated embryos). Fifteen embryos of each condition were observed in close up and representative phenotypes were documented here, however, no quantification were realised. All pictures were taken in dorsal view in dorsal trunk in dorsal stripe. Scale bar: 100 µm.

5.2.2.c The persistence of *sox10* expression is observed in *mitfa*^{w2} mutant

The Mitfa and Hdac1 co-repressor of *sox10* hypothesis suggested that the lack of one of the two factors would result in disruption of the inhibitory mechanism. Consequently, *mitfa*^{w2} mutant lacking *mitfa* expression should phenocopy the persistence of *sox10* expression observed both, in dorsal region of *colgate/hdac1* mutant around 48 hpf, and in TSA treated embryos stages at 36 hpf. Furthermore, *mitfa*^{w2} mutant did not produce the functional Mitfa protein, therefore, TSA treatment should not trigger any changes in *sox10* expression compared to expression observed in untreated *mitfa*^{w2} mutant embryos. We tested these predictions, and the results are presented in Figure 5.12.

WT TSA treated embryos and DMSO treated *mitfa*^{w2} mutant embryos both showed the persistence of *sox10* expression in the dorsal region of the trunk. In addition, TSA treated *mitfa*^{w2} mutant embryos presented the same phenotype as staged DMSO *mitfa*^{w2} mutant embryos. This suggested that the TSA treatment did not cause any changes on *sox10* expression in the absence of *mitfa*. Furthermore, loss of *mitfa* in *mitfa*^{w2} mutant could also phenocopy the phenotype of persistence of *sox10* expression observed in *colgate/hdac1* mutant. This result could suggest that TSA dependent increase of *sox10* required the factor Mitfa. This suggested that both the lack of Mitfa and the inhibition of Hdac in WT embryos, led to activation of *sox10* expression in melanocyte.

5.2.2.d Summarising the effects of TSA on melanocyte differentiation and *sox10* expression during melanocyte development.

Altogether, these results suggested that inhibition of Hdacs repressed melanocyte differentiation while also boosting *sox10* expression in melanised cells. In the context of the study described in Ignatius *et al.,* (2008), these results also suggested that Mitfa and Hdacs proteins could work together as a repressor of *sox10*. An alternative hypothesis could be that Mitfa was required to activate *Hdac* trancription which in turn would have a repressive effect on *sox10*. However, *in situ* hybridisation experiments investigating *hdac1* expression showed that it was ubiquitously expressed from an early developmental stage in zebrafish. In contrast, *mitfa* is expressed only in melanocytes at 48 hpf, therefore, *mitfa* expression is the spatial limiting factor and does not seem to activate *hdac1* transcriptional expression. Whether Mitfa could activate another Hdacs protein has not been reported. Previous data have suggested the possibility that Mitfa might directly bind the *sox10* promoter; it is plausible, therefore, that Mitfa might help target Hdac activity to the *sox10* promoter, thus resulting in repression of *sox10*.

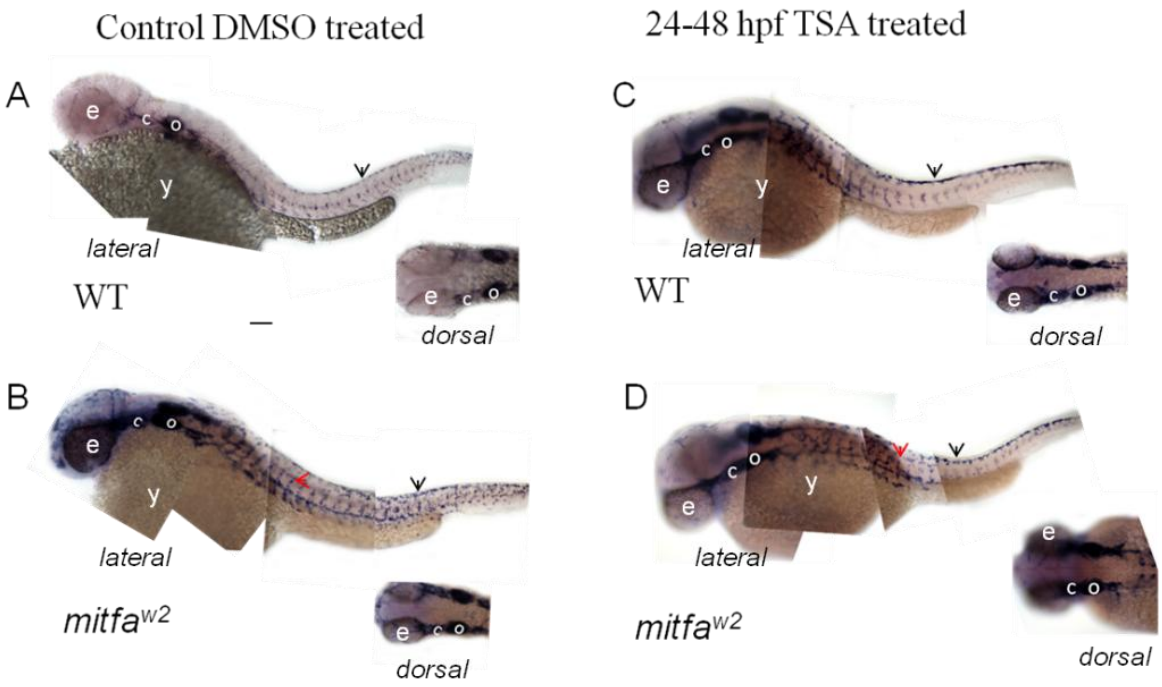

Figure 5.12: Trichostatin A treatment did not change *sox10* expression in *mitfa*^{w2} mutant embryos.

In situ hybridisation investigating *sox10* expression in WT and *mitfa*^{w2} mutant embryos treated with DMSO (control) (A-B) or Hdac inhibitor (TSA, 1 µM concentration) (C-D) from 24 hpf to 48 hpf. Embryos are shown in lateral view and a dorsal view of head is presented for each case showing elevation of the typical *sox10* expression in cranial ganglia (c) and in otic vesicle (o) in untreated mutant (B) and treated embryos both WT (C) and mutant (D) compared to the control (A). Elevated *sox10* expression in premigratory cells (black arrowheads in external dorsal part of trunk show these cells in B,C,D) and migrating NC cells (red arrowheads in middle trunk in B,C,D) can be observed in DMSO treated and TSA treated *mitfa*^{w2} mutant fish as well as in WT TSA treated embryos compare to WT untreated condition for which staining of migrating cells is particularly faint (no red arrow in A). For each condition 80 embryos were analysed and representative phenotypes are represented here. e: eyes ; y: yolk sac; c: cranial ganglia. Scale bar: 100 µm.

5.2.3 Mitfa-dependent maintenance of *mitfa* expression

In vitro experiments reported in Saito *et al.* (2002) have shown that *Mitf* might regulate its own expression in a process involving the Wnt signalling effector, LEF-1, as a non-binding cofactor. However, no *in vivo* experiments have yet demonstrated this mechanism. The GRN model for melanocyte development in zebrafish was described previously. It did not rule out the hypothesis that Mitfa could activate its own expression in a feedback loop and actually predicted this feature as a direct or indirect self-activation. As a preliminary investigation of this hypothesis, we tested the capacity of *mitfa* to activate its own expression.

To test whether Mitfa could drive *mitfa* expression, the *mitfa* mRNA was ectopically injected in embryos at the one cell stage. Both *mitfa* and *dct* expression were investigated by WISH at 6 hpf and 10.5 hpf after injections. *dct* being a direct target of Mitfa, activation of *dct* was used as a positive control for activity of the *mitfa* mRNA injected construct and efficiency of Mitfa activity after injections. For detection of induced *mitfa* expression, we had to avoid detecting the injected construct. Consequently, the probe used for WISH was designed to the 3'UTR region of the endogenous gene, outside of the sequence used to synthesise the injected construct. The $mitfa^{b692}$ mutant was used as a negative control (Lister *et al.*, 2001). In the $mitfa^{b692}$ mutant, a single base change creates an amino acid substitution replacing the conserved isoleucine at position 215 in the first helix of the helix–loop–helix dimerization domain for serine, as described in Lister *et al.*, (2001). This allele causes the inability of Mitfa to activate the transcription through its cognate binding site and to rescue melanophore development when expressed in the *mitfa* mutant embryos (Lister *et al.*, 2001). Expression of *mitfa* was first investigated by WISH in fish from an incross of heterozygous $mitfa^{b692}$ mutants. The expected c 25% of the progeny showed decreased *mitfa* expression compare to WT as shown at 30 hpf, and were assumed to be homozygous $mitfa^{b692}$ mutants (Figure 5.13). As a negative control, endogenous *mitfa* (3'UTR) expression and *dct* expression were tested at 6 hpf and 10.5 hpf after injecting the $mitfa^{b692}$ mutated RNA form. In these embryos we expected neither induction of *dct* nor *mitfa* after injection of the $mitfa^{b692}$ mutated RNA form.

Embryos were photographed in animal pole view or lateral view (description of orientation on Figure 5.14) at 6 hpf which corresponded to the gastrula phase also called the shield stage (corresponding to 50-75 % epiboly) (Figure 5.14). 10.5 hpf, corresponds to the end of gastrulation and very early segmentation (Figure 5.14). After injection of the *mitfa* mRNA at one cell stage, expression induced at 6 hpf was likely to show direct activation of gene expression whereas expression at 10.5 hpf could more likely relate to indirect activation.

Figure 5.15 presents the results of the WISH investigating *dct* and *mitfa* (3'UTR probe) expression in embryos at 6 hpf and 10.5 hpf after injection of WT *mitfa* mRNA and $mitfa^{b692}$ mutated RNA form at one cell stage. Embryos injected at one cell stage with synthesised WT *mitfa* mRNA showed strong ectopic expression of *mitfa* and *dct* at 6 hpf (Figure 5.15 A-B, animal pole view, dotted blue/dark purple signal in cells of the blastomere) and at 10.5 hpf (Figure 5.15, E-F, lateral view, dotted blue/purple signal in the

margin blastomeres/yolk cells). Interestingly, at 10.5 hpf, the signal corresponding to *dct* and *mitfa* (3'UTR) was not as widespread in the embryo as observed in embryos at 6 hpf. However, the expression observed at 10.5 hpf was weaker than observed at 6 hpf. It could be suggested that this low activation at 10.5 hpf showed that only some of the cells activating the endogenous Mitfa factor at 6 hpf were able to perpetuate activation of the gene later. Consistently with this, expression of *dct* was also reduced at 10.5 hpf compared to 6 hpf. It could be tested whether a feedback loop was only activated in a certain proportion of cells causing maintenance of *mitfa*, and in turn, of *dct* expression, in these cells. Alternatively, it is possible that *in vivo* in melanocytes a cofactor of Mitfa normally drives efficient feedback activation of *mitfa* by Mitfa. Figure 5.15 showed that embryos injected with *mitfa*^{b692} mutant mRNA did not activate expression of *dct* nor *mitfa* at either 6 hpf or 10.5 hpf in blastomeres. Neither did these embryos show expression in yolk cells in the lateral view nor in animal pole view (lateral views of embryos in the Figure) as the blue/purple signal was not detected.

Altogether, these experiments showed that *mitfa* could drive its own expression when ectopically activated in zebrafish embryos. It remains to be tested whether *mitfa* activates its own expression in melanocytes during development.

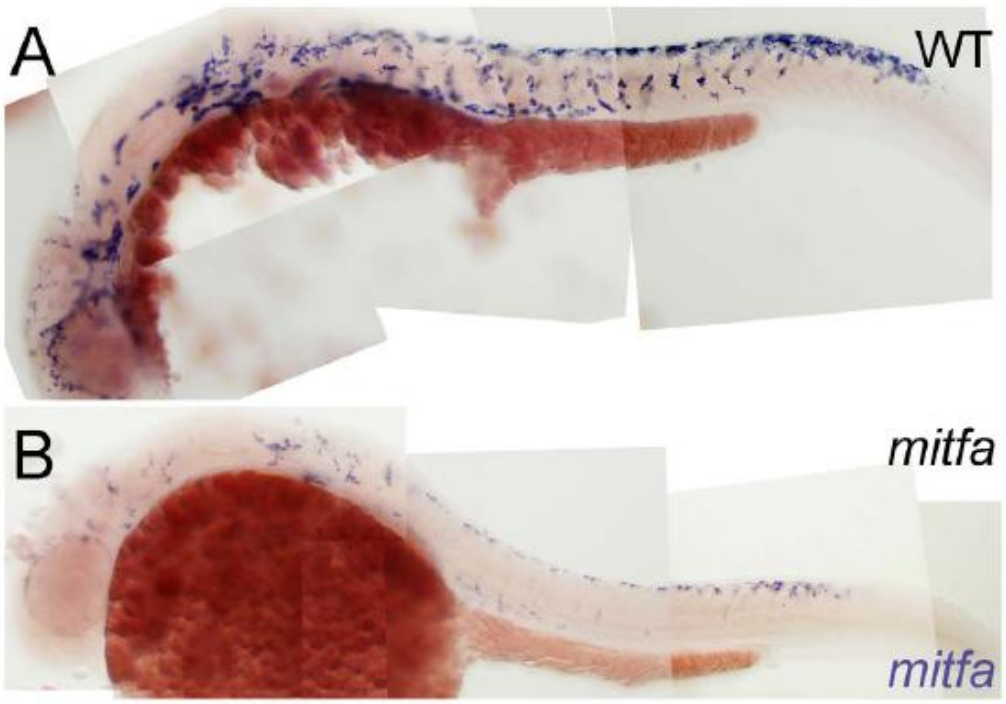

Figure 5.13: *mitfa* expression is reduced in *mitfa*^{b692} mutant.

WISH investigating *mitfa* expression in WT (A) and *mitfa*^{b692} mutant (B). Embryos from incross of *mitfa* heterozygotes were treated with PTU and processed for *in situ* hybridization with *mitfa* probes at 30 hpf stage. A majority (53/69; 73 %) showed normal strong *mitfa* expression and were presumed wild-type siblings (A, WT), whereas 33/124 (27 %) had weakened expression and were presumed *mitfa* mutants (B). (Reproduced with the kind permission of Greenhill *et al.*, 2011).

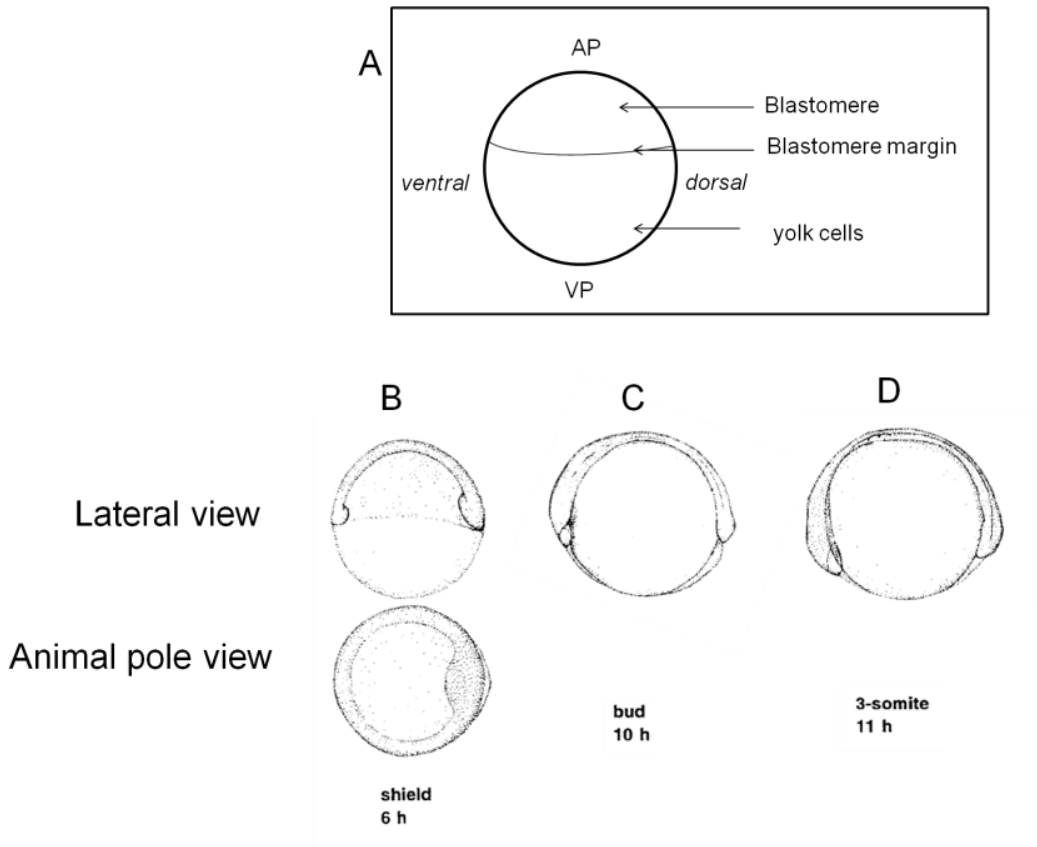

Figure 5.14: Zebrafish embryo orientation and stage description at 6 hpf and 10.5 hpf.

At early stages of development, embryos can be orientated as in (A) the blastomeres is developing in the animal pole (AP: animal pole) while the yolk cells are beneath the blastomeres margin in the vegetal pole, (VP: vegetal pole) then the ventral and dorsal sides can be defined. The 6 hpf shield stage is represented in (B) in lateral view and animal pole view while the bud stage (C, 10 hpf) and the 5 somites stage (D,11 hpf) are only represented in lateral view. Adapted from Kimmel *et al.*, (1995).

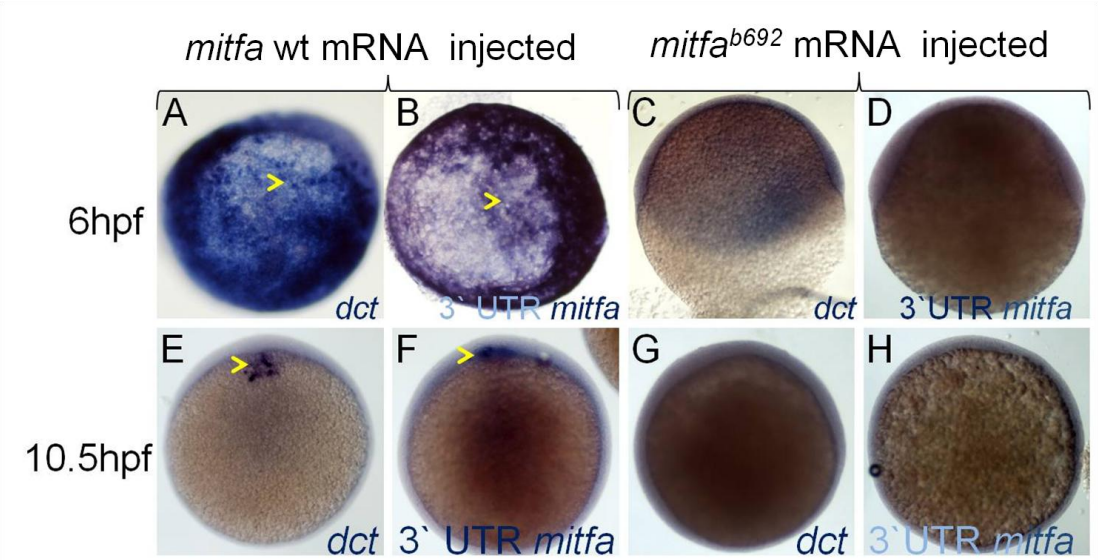

Figure 5.15: Injection of mRNA encoding WT *mitfa* drives ectopic expression of *dct* and *mitfa* at both 6 hpf and 10.5 hpf in zebrafish embryos.

Injection of WT *mitfa* mRNA drives ectopic expression of *dct* (A,E, arrowhead) and *mitfa* (B,F, widespread blue signal (dots as shown by arrowheads)) at 6 hpf (A,B, animal pole view, blue signal shown by arrowheads) and 10.5 hpf (lateral view). In contrast no expression could be detected in embryos injected with RNA encoding the *mitfa*^{b692} mutant form (C,G,D,H, embryos are shown in lateral view). Expression of the endogenous *mitfa* gene is detected using an anti-sense probe corresponding to the 3'UTR of the gene, a sequence absent from the injected RNA. 200 embryos were analysed for each condition and embryos presented here show the representative phenotype. A volume of 1 nL of 0.25 ng.µL^{-1} concentrated mRNA was injected. (Reproduced with the kind permission of Greenhill *et al.*, 2011).

5.3 Discussion

In this Chapter, several aspects of the GRN were investigated and we showed that:

- Hdac could be involved, with Mitfa, as a co-repressor of *sox10* in melanocytes. More particularly, Hdac1 remains the best candidate for this feature.
- We could quantify the de-repression effect of *sox10* on *dct* expression as well as confirm expression of melanocytic genes, in *mitfa* and *sox10* mutants, according to the melanocyte GRN in zebrafish.
- Mitfa could be a potential activator of its own expression *in vivo*.

5.3.1 Hdac1 might be an important factor for melanocyte development

The mathematical modelling predicted that *sox10* downregulation in melanocytes would be *mitfa* dependent (Greenhill *et al.*, 2011). Consistent with this prediction, *hdac1* mutants showed both persistent *sox10* expressions in NC cells and poor melanocyte differentiation, although, the connection between these phenotypes was not addressed. The data collected here allowed further characterisation of the melanocyte differentiation disruption associated with the persistent *sox10* expression. Chemical inhibition of the histone deacetylase function at the time of early melanocyte differentiation allowed us to show that blocking Hdac activity in melanocytes led to poor melanocyte differentiation and correlated with persistence of *sox10* expression.

Hdac1 seems to be an important factor for melanocyte development, however, it is still unclear what mechanisms are in play and what its role is *in vivo*. One limitation in this experiment was that the small molecule used, Trichostatin A (TSA), is a Hdac inhibitor, therefore, it was not specific to Hdac1. This molecule has already been utilised in zebrafish to test the role of hdac4 in development at 36 hpf and 6 dpf (Zhu *et al.*, 2011). However, only Hdac1 has been shown to have a role in melanoblast development in zebrafish. In order to test specific inactivation of Hdac1, it would be essential to investigate this hypothesis in *colgate*/*hdac1* mutants, however, it would not be possible to control for temporal changes in roles of Sox10, Mitfa and Hadc1. Alternatively, a new conditional transgenic line could be created which would express a truncated or dominant negative, version of Hdac1 to test conditional blocking of the protein in melanocytes during differentiation. It would be interesting to use qPCR analyses in purified NC cells or melanoblasts to assess and compare elevation and persistence of *sox10* expression in the following; WT TSA treated embryos; in $mitfa^{w2}$ embryos; and in $mitfa^{w2}$ TSA treated embryos. Furthermore, ChIP experiments looking for Mitfa/Hdac1 complexes on *sox10* promoter would allow verification of the presence of both proteins during melanocyte differentiation as direct regulators of *sox10*. Analysis of s*ox10* epigenetic markers and particularly the acetylation during cell differentiation would also be informative.

The model presented in Figure 5.16 summarises the hypothesis proposed here. Hdac1 and Mitfa together would form a complex to allow dowregulation of *sox10* expression in melanocytes and perhaps of *foxd3* expression, as suggested in Ignatius *et al.*, (2008). In this model, losing Hdac1 or Mitfa would cause maintenance of *sox10* and of *foxd3* in melanocytes and would explain the *colgate*/*hdac1* phenotype described in Ignatius *et al.*, (2008) as well as the results described here. As described in the Figure 5.26, the maintenance of *foxd3* would firstly cause *mitfa* expression to be decreased as described in *colgate/hdac1* mutant. Reduced *mitfa* expression would thus explain reduced activation of *dct* expression in a first instance as observed in *colgate/hdac1* mutant. However, the *mitfa* dependent *kit* signalling would allow the survival of melanocytes and later, the persistence of *sox10* would permit boosting *mitfa* expression, as observed in *colgate/hdac1* mutants. In this model, blocking *foxd3* with a morpholino would rescue *mitfa* expression at early stages and therefore would allow recovery of *dct* expression in melanocytes at early stages, as described in the *colgate/hdac1* mutant.

5.3.2 The role of Hdac1 as a repressor of *foxd3* in melanocytes

foxd3 is known as a direct repressor of *mitfa* expression in NC and it has been suggested to be involved in glial/melanoblast fate choice by turning off *mitfa* expression in cells (Lister *et al.*, 2006, Curran *et al.*, 2009, Ignatius *et al.*, 2008). The mechanism involved in *foxd3* dependent repression of *mitfa* is not understood yet. Cooper *et al.*, (2009) suggested that *foxd3* could be downregulated by the *kit* signalling in melanocytes. A loss of activation of *kit* signalling would then cause the maintenance of *foxd3* which would result in the repression of *mitfa* (Cooper *et al.*, 2009). In WT, *foxd3* expression might be kept low in melanocytes so that *foxd3* and *mitfa* were never observed to be co-expressed (Thomas and Erickson, 2009, Dottori *et al.*, 2001, Curran *et al.*, 2009). Interestingly, the study of *foxd3* mutants showed that defects of melanocyte pigmentation caused by the loss of Foxd3 (such as *mitfa* expression delay at 24 hpf or increase melanocyte number) could be compensated after cell differentiation (Stewart *et al.*, 2006). Stewart *et al.* (2006) studied the *sym1* mutation, a nucleotide deletion which disrupted the forkhead DNA-binding domain of the *foxd3* gene, introducing a premature stop codon and therefore deactivating *foxd3* (Stewart *et al.*, 2006, Yuan *et al.*, 2006). This study showed that loss of *foxd3* resulted in migration delays in NC derivatives migrating on the medial pathway (e.g. neuronal, glial or melanocyte precursors) in zebrafish (Stewart *et al.*, 2006). Furthermore, in the study, the loss of *foxd3* resulted in a delay of *mitfa* and *dct* expression as well as a delay in melanocyte differentiation. Interestingly, all these phenomena were later compensated and no abnormal phenotype was observed in melanocyte number at 3 dpf suggesting there was no crucial role for *foxd3* in melanocyte development.

In *colgate/hdac1* mutants, *foxd3* expression was increased in somites. Furthermore, an increase in the number of cranial satellite glia in the pre-otic and post-otic placodes could be observed in this mutant as well as a reduced melanocyte number compared to WT. The melanocyte phenotype did not recover until at least 3.5 dpf (Ignatius *et al.*, 2008). Interestingly, Ignatius *et al.* (2008) showed that blocking *foxd3* by morpholino injection could rescue the melanocyte phenotype in *colgate/hdac1* mutant. Looking at WISH

investigating *foxd3* expression in *colgate/hdac1* mutant, it seemed that in the absence of Hdac1, *foxd3* was expressed in melanocytes. Consequently, extended expression of *foxd3* was suggested as an explanation for reduced melanocytes in *colgate/hdac1* mutant. However, extended expression of *foxd3* did not explain persistence expression of *sox10* in melanocytes. It seems that the persistence of *sox10* expression was a defect of the melanocyte GRN itself, due to the lack of Hdac1. Together, these experimental data in *sym1* and *colgate/hdac1* mutants showed that loss of *foxd3* does not seem to affect melanocyte development in a critical manner. Although, its prolonged expression could prevent normal melanocyte development and differentiation, it did not explain *sox10* persistence at 48 hpf in *colgate/hdac1* mutants.

The role of *foxd3* was not investigated in our study. However, the boost of *foxd3* at 24 hpf could explain the reduction of *mitfa* in mutant embryos at 25 hpf, whereas, *sox10* expression persistence in *colgate/hdac1* mutant at 48 hpf could explain the elevated *mitfa* expression in the dorsal region. It is then plausible that Hdac1 repression of *foxd3* would be *mitfa* dependent. It would be important to clarify the timing for *foxd3* downregulation in melanocytes or *mitfa* (+) cells and the role of a potential Mitfa/Hdac1 complex in this process. Ignatius *et al.*, (2008) suggested that Hdac1 was a repressor of *foxd3*. Consequently, in a future experiment, it would be interesting to test this hypothesis by comparing the epigenetic state of *foxd3* DNA in *foxd3* expressing and non-expressing cells (silencing by acetylation) and by testing the presence of Hdac1 on the regulatory sequences of *foxd3* in melanocytes. *foxd3* expression could also be investigated in *mitfa*^{w2} mutants during melanocyte differentiation (24 hpf to 48 hpf) to test for increased /prolonged *foxd3* at these stages.

Interestingly, one mechanism suggested for Foxd3 dependent repression of *mitfa* is through a co-repressor, CtBP2 (Liang *et al.*, 2011). In zebrafish, Liang *et al.* (2011) showed that morpholino knockdown of CtBP2a and CtBPP2b led to increased melanocyte number at 3 dpf as well as increased *mitfa* expression at 24 hpf in *mitfa*-GFP transgenic fish which was confirmed by qPCR analysis (Liang *et al.*, 2011). Whether or not CtBP2 will be a *mitfa* co-inhibitor for *Foxd3*, around 24 hpf, still needs to be tested.

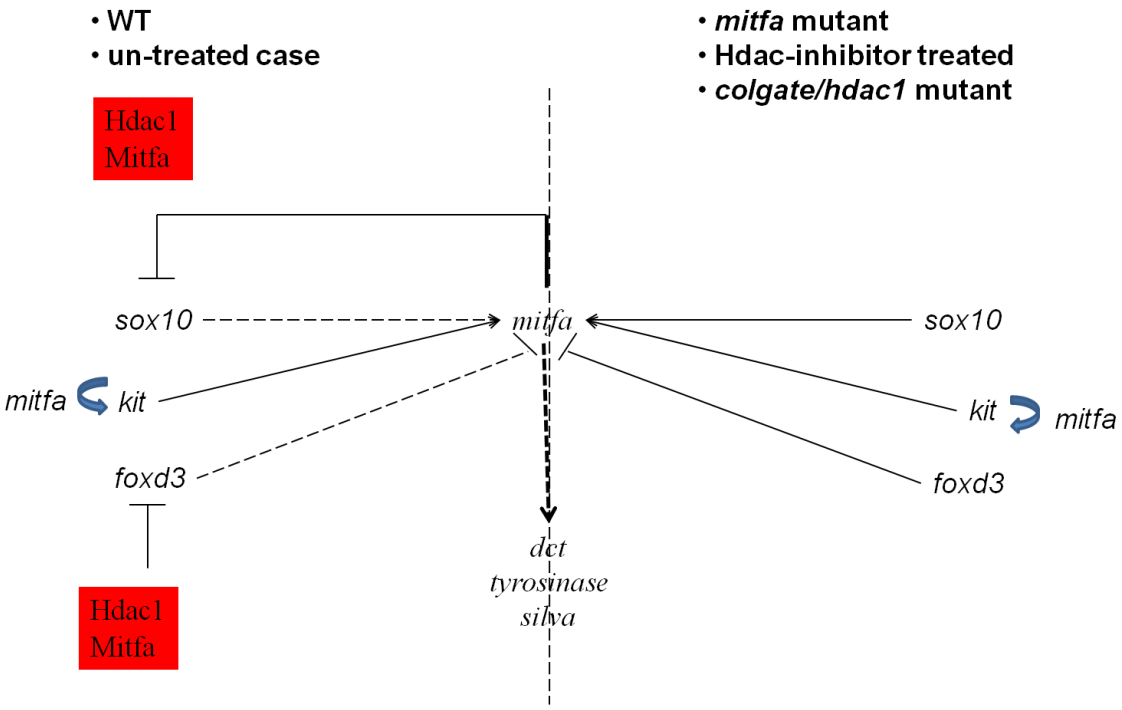

Figure 5.16: Hdac1 and Mitfa together can repress *sox10* and *foxd3* in melanocytes.

In WT and un-treated cases (left panel), Hdac1 and Mitfa form a complex (red) which represses *sox10* and *foxd3* expression in melanocytes. Therefore, *sox10* and *foxd3* expression are lost in melanocytes as observed *in vivo* (the black dotted lines represent the interaction which only take place before Hdac1/Mitfa repression effect.). The *kit* signalling (*mitfa* dependent as indicated by blue arrow) could allow melanocyte survival against the *foxd3* repressive effect in the left panel. However, when one of the two components of the complex is missing (*mitfa* mutant, Hdac-inhibitor treated embryos, *colgate*/*hdac1* mutant embryos, shown the right panel), *sox10* expression is persistent in melanocytes (as observed *in vivo* in *colgate/hdac1* mutant, in Hdac-inhibitor treated embryos and in *mitfa*^{w2} mutant embryos) and *foxd3* expression is boosted (as observed *in vivo* in *colgate/hdac1* mutant). In these cases, the kit signalling also allows survival of melanocytes however, cell differentiation is impaired by maintenance of *foxd3* and persistence of *sox10* expression in cells.

5.3.3 A strategy to better understand *mitfa* and *sox10* regulation in melanocyte development.

In order to quantitatively test the GRN model, we quantified expressions of *sox10, dct, tyrp1b* and *mitfa* in embryos at 30 hpf, 36 hpf and 72 hpf in *sox10* and *mitfa* mutants. These experiments confirmed Sox10's negative effect on some genes downstream of Mitfa, such as *dct*, but not *tyrp1b*. The results of *mitfa* expression quantification in *sox10* and *mitfa* mutants, showed that *sox10* activation was not sufficient to generate normal levels of *mitfa* expression in WT. This result could suggest that another factor of regulatory mechanism, absent in *mitfa* mutant, could be important for *mitfa* activation. Wnt signalling has been shown to be required with Sox10 for *mitfa* activation; interestingly, Chen *et al.*, (2000) have described a LEF-1 and Mitf dependent mechanism of co-activation of *Mitf*. Thus, our data are consistent with Mitfa associated with a co-activator such as Lef-1.

In the future, RNA sequencing or microarray studies should allow investigation of other factors in play during the regulation of *sox10* and *mitfa*. These analyses could allow deciphering new factors downstream of Mitfa and/or Sox10. Consequently, it would be possible to identify candidate factors for better establishing the regulatory network responsible for interactions and expression timecourse of these crucial factors in melanocytes in zebrafish. Whether or not more differences between mouse and zebrafish could be in play *in vivo* would have to be investigated further. It would also be interesting to quantify expression levels of *mitfa, sox10, dct* and *tyrp1b* in melanocyte in mouse through time to compare results to the zebrafish model.

5.3.4 Investigating the role of Mitfa in *mitfa* expression

The model predicted that factors other than *sox10* could be involved in *mitfa* regulation. The role of *mitfa* as a self-regulator has never been addressed *in vivo*. Here, *mitfa* expression was investigated by ectopically injecting embryos with *mitfa* mRNA in order to preliminarily test the possibility that Mitfa could activate its own expression.

The observation of low *mitfa* activation in $mitfa^{w2}$ mutant, combined with predictions of the GRN model, suggested that Mitfa could activate *mitfa* expression. The results of the experiment we presented suggested that Mitfa would potentially directly or indirectly activate the expression of *mitfa*. Our experiments focused on ectopic expression, and not in melanocytes. However, these data support the hypothesis that Mitfa alone or with a cofactor (possibly Lef-1, (Saito *et al.*, 2003)) could be involved in a positive feedback loop to maintain its expression. It would be interesting to investigate whether Lef-1 could have been recruited in embryos at 6 hpf, which could suggest that Mitfa also recruits Lef-1 in melanocytes.

Mechanisms of negative and positive feedback loops have often been described as features of GRNs in eukaryotes. These feedback loops can allow a very simple network of just two genes to exhibit non-trivial behaviours like changes in cell fates (Schlitt and Brazma, 2007, Becskei *et al.*, 2001). *Mitf* promoter did not seem to carry M-boxes which are Mitf DNA binding sites (Saito *et al.*, 2002). To assess this question further in zebrafish, the Zebrafish DNA *mitfa* genome sequence (gi|76666366|emb|BX927362.10|) (from clone CH211-170N20 in linkage group 6, complete sequence) was investigated looking for M-box sites (AGTCATGTGCT) using BLAST® software and found no matches. This suggests that neither the promoter, nor the first intron of *mitfa* genome sequence, carry a Mitfa binding site. Consequently, the regulation of its own expression could be indirect or allowed by recruiting a cofactor which could bind *Mitf*'s promoter or alternatively it could be due to activation via a remote enhancer. Further experiments would be required to test *in vivo* whether Mitfa could drive *mitfa* expression. One suggestion would be to generate a new zebrafish line: a *sox10* mutant line expressing *mitfa* under a heat-shock promoter. In these fish, inducing a first temperature dependent activation of *mitfa* at about 30 hpf should be sufficient to engage a feedback loop which would trigger constant expression of *mitfa*. Expression of *mitfa* could then be tested later, at several timepoint, 32, 36, 40, 48 hpf, by WISH or qPCR and compared to a no heat-shock control. Furthermore, ChIP experiments testing for the recruitment of both Lef-1/Mitfa or Mitfa alone in melanocyte during differentiation would allow us to assess the role of Mitfa in its own expression in melanocytes *in vivo*.

5.3.5 Conclusion

Altogether these experiments permitted us to go further with our understanding of the fine regulation of the GRN. For example, quantifying gene expression in both *sox10* and *mitfa*

mutants added further support to the interpretation of previous experiments. Specifically we confirmed the hypothesis of *sox10's* role in melanocyte differentiation in zebrafish and their differences from the described data in mouse. Our experiments also suggest focusing future experiments on testing two potential co-regulating complexes involving Mitfa. Firstly, the Hdac1/Mitfa complex could be involved in *sox10* repression with Mitfa as a binding factor, and secondly, the Lef-1/Mitfa complex could be an activator of Mitfa with Lef-1 as a binding factor. It would be crucial to determine the epigenetic status of both *mitfa* and *sox10* during cell differentiation as well as investigating factors binding promoters by ChIP experiments to test these hypotheses.

Chapter 6. Discussion

6.1 Overview

In this thesis, I have presented and contributed knowledge on the genetics of melanocyte development. Some of the key findings are as follows:

- *mitfa* expression was maintained in melanocytes in an Mitfa-dependent fashion (Chapter 4 and 5) suggesting the existence of a positive feedback loop on Mitfa involving a Factor Y.

- Wnt signalling remained activated in melanocytes after cell specification. It was not limiting for melanisation, although it may play a role in other aspects of melanocyte differentiation, including cell adhesion/patterning. Thus, whilst Wnt signalling may contribute to Factor Y, it is likely only one of several factors that act here (Chapter 3).

- We showed that melanocytic gene expression could be quantified in whole embryos, and in pools of five cells in the NC cell population and in melanocytes using stochastic profiling (Chapter 4). This method allowed us to observe an unexpected decrease of *mitfa* expression in melanocytes at late stages (Chapter 4).

- Single cell PCR showed the co-expression of *mitfa* and *ltk* in a substantial proportion of *sox10*+ NC cells, consistent with the proposed partially-restricted pigment cell progenitor (chromatoblast) discussed in Lopes et al (2008).

- Inhibiting Hdac in zebrafish embryos suggested that Hdac could be a Mitfa-dependent co-repressor of *sox10* (Chapter 5). This could explain the decrease of *sox10* expression in melanocytes, which was confirmed by stochastic profiling of *sox10* expression in melanocytes (Chapter 4).

This research used NC in zebrafish to investigate melanocyte development and has broad implications as melanocytes are found widely in vertebrates, including human. This also contributes, in a wider sense, to knowledge in the fields of zebrafish development, NC development, stem cell biology, developing techniques for the study of expression variation, cell heterogeneity and fate restriction and melanocytic diseases.

6.2 Defining *mitfa* expressing cells at early stages

For the melanocyte lineage, the known determining factors are *mitfa* and *sox10* but the results of our study suggested that in zebrafish, not all *mitfa/sox10* positive cells at 23 hpf would become melanocytes (Dutton *et al.*, 2001). Observing the co-expression of an iridoblast marker such as *ltk* in *sox10(+)mitfa(+)* cells at 23 hpf suggested that the existence of a chromatoblast should be further tested in zebrafish before 30 hpf. Lineage restriction study could allow the following of cells from early to late stages to determine the potentiality of *mitfa (+)* cells at 23 hpf. From 23 hpf to 30 hpf, the NC cell pool is heterogeneous and both characterising the precursor types present and identifying the mechanisms causing genetic heterogeneity would allow us to better define fate restriction in NC. Developing a zebrafish NC cell culture from single cells could help understand the potentiality of cells at each time point.

6.3 MITF as a co-factor for many potential factors

Our results suggested that Mitfa could recruit a co-inhibitor, Hdac, for downregulation of *sox10* expression and perhaps also a co-activator (e.g. Lef-1), for its auto-activation. Interestingly, MITF has been shown to bind other protein factors in mammals, including SOX10, LEF1, PAX3, CREB, GLI2, OC-2, CtBP2 and MITF (Kim *et al.*, 2000b, Liang *et al.*, 2011, Saito *et al.*, 2003, Bondurand *et al.*, 2000). Other factors could bind MITF such as Rab27a, a member of the RAS oncogene family involved in melanosome transport in mouse (Sestakova *et al.*, 2010, Kawasaki *et al.*, 2008). These analyses show that Mitfa is at the centre of a protein interaction network, allowing complex regulation of gene expression.

One example of a co-regulation mechanism involving Mitfa has been tested here as a feature of the network: the role of Hdac as a Mitfa-dependent co-repressor of *sox10* expression. The study of *colgate/hdac1* mutant combined with our study of effects of Hdac inhibition suggested that, in this case, *sox10* downregulation could be explained by the activity of Hdac, and particularly Hdac1, as a co-repressor for Mitfa in melanocytes (Ignatius *et al.*, 2008). Several crucial aspects of this mechanism remains to be tested: whether Mitfa and Hdac1 both directly interact; whether this complex could also recruit other factors; whether this complex remains attached to the *sox10* promoter after differentiation. As described in Turner, (2000), Hdacs have the ability to trigger long-term epigenetic changes. Thus, interaction between Hdac1 and Mitfa at *mitfa* DNA binding site on *sox10* promoter might cause long term/permanent downregulation of *sox10* expression in melanocytes. It would be interesting to perform ChIP analysis looking for Mitfa/Hdac1 interacting on *sox10* promoter. This could be complemented by measurements of chromatin acetylation levels at the *sox10* gene before and after 48 hpf. We predict acetylation levels would be higher before Hdac was active in melanocytes, before 48 hpf, and would then decrease.

Our analysis also raises the hypothesis that *foxd3* could be inhibited by Hdac1 in a Mitfa dependent manner in *colgate/hdac1* mutant. *foxd3* is required for NC cell development and several studies in zebrafish, *Xenopus* and mouse, suggested that *foxd3*

had an important role in regulating melanocyte specification (Curran *et al.*, 2010, Wang *et al.*, 2011, Kos *et al.*, 2001, Honore *et al.*, 2003). Ignatius *et al.*, (2008) observed an increase of *foxd3* expression in *colgate/hdac1* zebrafish mutant and thus suggested that Hdac1 could be a negative regulator of *foxd3* in melanocytes. Knowing that *foxd3* expression is inhibited in melanocytes and that Mitfa can probably recruit co-factors such as Hdac1, it is plausible that *foxd3* expression could be inhibited by Hdac1 in a Mitfa dependent manner in *colgate/hdac1* mutant. Investigating whether or not and in which cells the expression of *foxd3* is boosted in *mitfa*^{w2} mutant and if *mitfa* expression is activated in *foxd3* mutant, could help understanding the regulation between these two factors.

6.4 *mitfa* is lowly expressed in melanocyte differentiation in zebrafish

Together, the data collected and analysed in Chapters 3-5 have allowed us to observe and suggest improvements to the core melanocyte GRN published in Greenhill *et al.*, (2012) and more particularly for the role of *mitfa* in this process. Melanocyte differentiation relies on *mitfa* expression, but our experiments suggest that it is maintained only at a low level in melanocytes. Weakly maintaining *mitfa* expression (weak role of Factor Y) could directly or indirectly allow the system to firstly activate another factor which was previously described as Factor X, which remains to be determined. Here we discuss the mechanisms involved in the decrease of *mitfa* expression and the potential existence of Factor X.

6.4.1 Mitfa expression is decreased but maintained in melanocytes

Our data quantifying *mitfa* expression in single cells showed that *mitfa* remained expressed in melanocytes at 72 hpf (Chapter 4). However, the decrease of absolute and relative expression of *mitfa* in melanocytes by 72 hpf suggested that the genetic or epigenetic mechanisms involved in its maintenance are also involved or play a part in this decrease (Chapter 4). Consequently, in this hypothesis, Factor Y would be an ensemble of factors which allow the maintenance of *mitfa* but at a low level of expression.

The hypothesis raised by the model suggests that Mitfa itself could be a regulator of *mitfa* expression is supported by the result of activation of *mitfa* by Mitfa in an ectopic context *in vivo* (Chapter 5). However, this prediction of the model also raises another key question, whether Mitfa acts alone or via another factor. We have not directly addressed this question is this study but it will be important to investigate it in the future. It would first be important to test if this feedback interaction existed *in vivo* in melanocytes, and if it did, would it be sufficient to maintain *mitfa* expression during melanocyte differentiation. Mitfa can recruit co-factors, to re-direct or to cause activation or inhibition of gene expression. Here, Mitfa could perhaps activate its own expression using a co-factor such as, Lef-1, as suggested by Saito *et al.*, (2003). In this hypothesis, Mitfa/Lef1 would work together to maintain a low level of *mitfa* expression and melanocyte differentiation. This is supported by the data we collected showing that Wnt signalling remained lowly activated

in melanocytes after cell specification (Chapter 3). However, boosting Wnt signalling did not cause dramatic effects on melanocyte differentiation even if *mitfa* expression was boosted. This data suggest that Wnt signalling was not limiting for cell differentiation. In this hypothesis, both the co-activation of *mitfa* by Mitfa/co-activator of *mitfa* (Lef-1?), and other unknown factors or mechanisms, would be responsible for the maintenance of low levels of *mitfa* expression. Furthermore, in this hypothesis, this low level of *mitfa* expression would be key for maintenance of melanocyte differentiation. Interestingly, this has been verified in Johnson *et al.,* (2010) where a conditional loss of *mitfa* in melanocytes after 48 hpf, in zebrafish caused loss of cell differentiation with loss of melanisation, loss of cell dendricity, reduced melanised cell number.

6.4.2 Mitfa and Factor X could be important for melanocyte differentiation GRN

Alternatively, the decrease of *mitfa* observed in melanocytes could suggest that Mitfa could be activating another key factor in the process of melanocyte differentiation. This other factor could be a factor previously suggested, Factor X, and its first activation could be Mitfa dependent. In this hypothesis, Factor Y could actively maintain low levels of *mitfa* expression in cells as in the previous hypothesis, however, here, after activation of Factor X, Mitfa would only be key for activating Factor X. The existence of Factor X had already been suggested by Greenhill *et al*., (2011) (called model A), however, the observation of *mitfa* expression decrease in cells is the first potential biological evidence for its existence. As discussed in Chapter 4, these observations would not rescue the original model A which was too simplistic and also had other flaws such as, it could not explain the *sox10*-independent maintenance of *mitfa* expression we observe *in vivo*, nor the *mitfa*-dependent decrease of *sox10* expression suggested by *in vivo* data (Greenhill *et al.*, 2011, Elworthy *et al.*, 2003b). A new version of the model, taking into account this unexpected decrease of *mitfa* expression, would include the presence of a factor to relay *mitfa* expression at a later stage, during differentiation, together with other parameters described in model C and here (Greenhill *et al.*, 2011). Testing if Wnt signalling was Factor Y caused a boost of *mitfa* expression during melanocyte differentiation, however, this did not dramatically affect melanocyte differentiation. This result could also suggest that Mitfa is the only not key factor after 48 hpf in melanocytes. The Figure 6.03 summarises the new proposal for the melanocyte GRN at both specification and differentiation states, including the Factor X hypothesis. It would be interesting to test the hypothesis of the existence of Factor X, however, no candidate factors are currently known from zebrafish. Investigating transcription factors responding to Mitfa could help finding appropriate candidates.

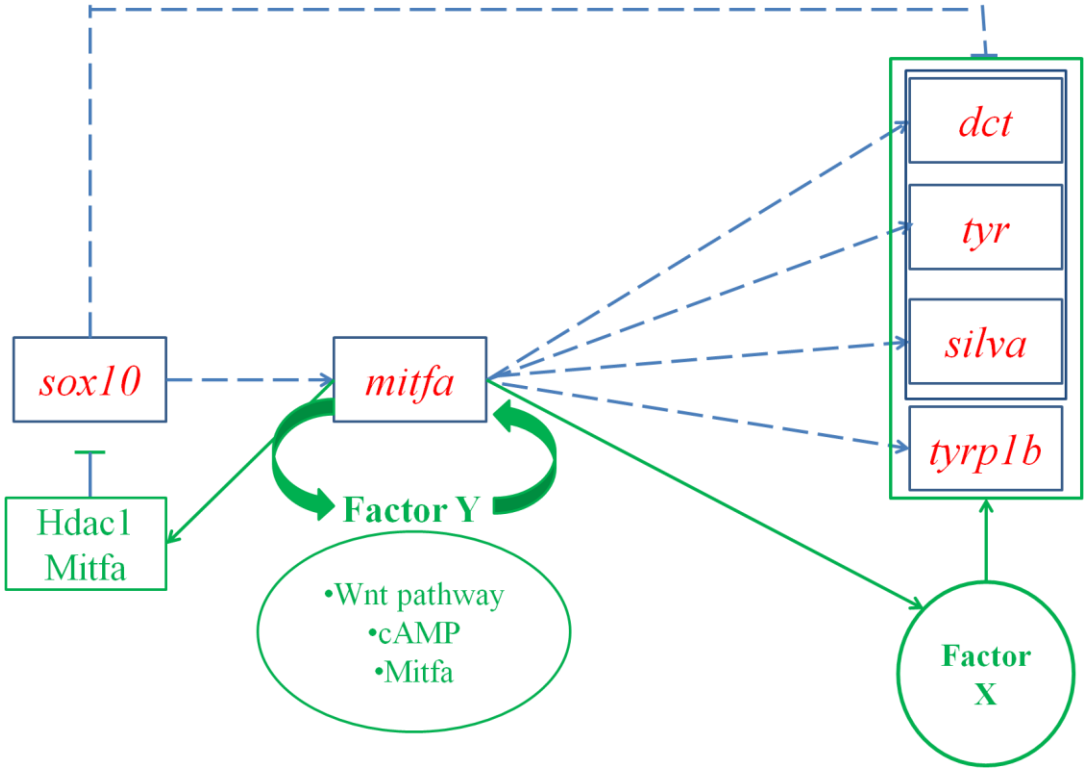

Figure 6.03: Factor Y as a factor to maintain low levels of mitfa expression and Factor X as a key factor for melanocyte differentiation first activated by Mitfa.

The blue dashed arrows and the blue cadre show the GRN in place during melanocyte specification (Greenhill *et al.*, 2011). The green arrows (feedback Factor Y/Mitfa), the green cadres (co-inhibition of *sox10* by Mitfa/Hdac1) and the green circles (Factor Y= Wnt signalling with cAMP pathway and/or Mitfa itself and existence of Factor X as a Mitfa dependent factor activator of melanocytic genes) show the potential new features of the GRN for melanocyte differentiation in regards of the results presented in this study.

6.5 New factors interacting with *mitfa* for melanocyte differentiation

In this study, we found that Wnt signalling was not limiting for melanocyte differentiation, consequently, new candidate factors should be investigated. Furthermore, going further with the GRN involved in melanocyte development means finding new factors involved in the GRN, or, identifying new mechanisms involved in maintaining the differentiated state. As described in Levy *et al.,* (2011), Dicer could be a potential factor involved in melanocyte development. Levy *et al.,* (2011) showed that protein and mRNA levels of microRNA and DICER were upregulated in melanocytes during development in human primary melanocytes and suggested that *Mitf* could be responsible for this increase. MITF could then activate *Dicer* expression via two E-boxes on *Dicer* promoter. Importantly, in their experiment, *Dicer* knockdown caused a loss of hair follicle melanocytes. In zebrafish, the orthologue *dicer1* is active on processing miRNA, however, its role in *mitfa* regulation or in melanocytes has not been investigated yet. To test Dicer1 involvement in *mitfa* regulation, it would be interesting to use morpholinos against *dicer1*, as in Cifuentes *et al.,* (2010) and look at melanocyte development at 30 hpf and *mitfa* WISH around 20 hpf.

Another study has shown the role of *Transcription factor AP-2*, Tfap2a and Tfap2e in melanocyte differentiation in zebrafish via regulation of *mitfa* activity (Van Otterloo *et al.,* 2012). The study showed that knockdown of both *tfap2a* and *tfap2e* in zebrafish triggered downregulation of *dct, tyrosinase* and *tyrp1b* expression as well as cell autonomous changes such as a reduction of melanocyte melanin content and reduced cell number at 36 and 48 hpf (Van Otterloo *et al.,* 2012). Their study suggested that the role of Tfap2 could be to modulate Mitfa transcriptional activation of target genes via direct phosphorylation of Mitfa, or via phosphorylation of a factor which in turn would regulate Mitfa activity (Van Otterloo *et al.,* 2012). It would be important to better test the timing of activity of Tfap2a and Tfap2e for melanocyte development to understand whether it is required for melanocyte specification and later for differentiation and finally if it affects genes other than *mitfa.* For this, it would be possible to utilise a conditional approach using a dominant null allele of *tfap2a*, under a heat-shock promoter, inducible at a specific temperature. Then, conditional knockdown of the gene at different time of melanocyte differentiation would allow for the testing of the effects of decreased *tfap2a* on melanocyte development.

6.6 The study of Mitfa and Sox10 expression in zebrafish has important implications for melanoma research

The role, the regulation and the expression level variations of *mitfa* and *sox10* we described in our study in zebrafish are relevant to the better understanding of melanoma. The oncogenic role of the gene *MITF* has been described as well as its pro-proliferation effect depending on its level of expression (Kido *et al.,* 2009). This justifies the study of the regulatory mechanisms activating or inhibiting *MITF*. In this study we showed that *mitfa*

expression was decreased in melanocytes during cell differentiation however, its expression remained maintained. *Mitf* has been found to be involved in melanoma progression in several studies implicating different pathways such as the MAPK/MERK pathway as shown in B16 melanoma cells *in vitro* in Englaro *et al.,* (1998). A study in melanoma cell lines has shown that BRAF is involved in enhancing melanoma response to MITF and therefore, suggested that *Mitf* and BRAF could both be the targets for melanoma treatments (Kido *et al.,* 2009). It would be interesting to investigate whether the activation of the MAPK/MERK pathway in melanocytes could be indirectly Mitfa dependent and is therefore decreased during normal cell differentiation.

In our experiments in normal melanocyte development, we observed a decrease of *sox10* expression in melanocytes. Interestingly, in melanoma cells in culture, it has been suggested that the factor Tyro3 could play a role in activating Mitf, via Sox10. Indeed, it has been suggested that *Tyro3* could activate *Mitf* expression in a *Sox10* dependent manner and by bypassing BRAF in melanocyte and melanoma backgrounds (Zhu *et al.*, 2009, Easty *et al.*, 2011). Ectopic expression of *Tyro3* could activate, or downregulate (*Tyro3* shRNA infection) *Mitf* expression by redirecting SOX10 to the nucleus. Therefore, in cell culture *Tyro3* knockdown led to reduced melanoma and in contrast, *Tyro3* overactivation led to increased melanoma and the levels of *Tyro3* measured by RT-PCR in melanoma cells were found to be increased by 3 folds in 50 % of samples studied compared to normal skin tissue (Zhu *et al.*, 2009, Easty *et al.*, 2011). A clear mechanism for this interaction remains to be described *in vivo* and the role of Tyro3 in normal melanocyte development remains to be described in zebrafish. It would be interesting to test whether B-raf or Tyro3 could activate *sox10* during melanocyte development in zebrafish.

Altogether, these studies suggested that over-activation of *Sox10* could be key in the increase of *Mitf* observed in melanoma cells. They suggested that the *Sox10* expression increase could be related to the MAPK pathway via several routes such as P38 kinase or BRAF but also that the epigenetic state of *Sox10* and *Mitf* could be crucial in this misregulation. Factors and pathways such as *p38, Braf, Mc1r,* PKA, cAMP, *Gsk3β, Nfat, Disc1, CtBP2, Sox2, Dicer* or *Tyro3* have been suggested to be important actors in the network and they also will have to be investigated in fish to improve our understanding of the GRN of both normal melanocyte and melanoma (Kido *et al.*, 2009, McGill *et al.*, 2002, Gross *et al.*, 2009, Drerup *et al.*, 2009, Saha *et al.*, 2006, Zhu *et al.*, 2009, Liang *et al.*, 2011, Adameyko *et al.*, 2011, Levy *et al.*, 2011).

6.7 Measuring transcriptional variation may help to better characterise melanocyte development and perhaps melanoma development

In this study we developed a technique to measure cell heterogeneity in a population. Heterogeneity can be biologically critical for the emergence and/or the survival of different cell types during cell specification and differentiation but also for the survival of cancer cells in a population. Going further in the development of techniques to measure cell to cell

heterogeneity would help understand the role of different cell clones in melanoma tumor formation.

Our experiments now show that it is possible to investigate gene expression in melanocytes in pools of five zebrafish cells. In the future, further development of the technique could allow us to investigate gene expression at the single cell level, *ex vivo*. Single cells analysis could also allow us to measure expression levels of key genes in melanoma cells compared to normal cells at different timepoint of the melanoma tumor progression. The technical difficulty of measuring gene expression in a low amount of material remains a major obstacle for this research. Various techniques have been described and several machines and kits have been developed to permit a better approach to this problem. New methods such as the one developed by the Xie Group of the University of Harvard allow probing of single molecules in cells (Friedman *et al.*, 2006). Another technological approach was used in Narsinh *et al.*, (2011) for studying the role of cell heterogeneity in pluripotency. This technology developed by Fluidigm DELTAgene Assays, consists of high-quality, rapid, and robust single cell qPCR. Such approaches could be tested with the objective to design an assay for detection of very low material amount in zebrafish cells.

The heterogeneity within cells seems to play an important role in the maintenance, the survival and the progression of melanoma cells. *In vivo*, melanoma cells have also been shown to be heterogeneous (Sieber-Blum and Hu, 2008). Also they have been shown to be characterised by the heterogeneity of signalling pathways and factors also involved in melanocyte development (Croteau *et al.*, 2012, Busca *et al.*, 2000, La Porta and Zapperi, 2012, Schatton and Frank, 2008). This heterogeneity is not well defined from one tumor to another and it is a crucial parameter to better understand cancers *in vivo*. Croteau *et al.*, (2012) described striking intra-tumor heterogeneity by measuring gene expression in two clonal tumors which were distinguished after isolation from a same parental tumor. The study showed high heterogeneity of metalloproteinase-1 (MMP-1) in melanoma cells which was involved in aggressiveness, and interestingly, the heterogeneity of *Braf* was also observed. The two clonal populations rapidly showed different characteristics of growth, survival and invasiveness (Croteau *et al.*, 2012). Studies in melanoma cells reported that *Mitf* expression level could be either increased or decreased relating heterogeneity of its expression (Easty *et al.*, 2011, Rebecca *et al.*, 2012, Yancovitz *et al.*, 2012).

Other studies have described stochasticity in cancer cell population with a stochastic Markov model (Gupta *et al.*, 2011). This model assumed that the changes in cell states, called the interconversion rates, only depend on the cell's current state and remains constant under fixed environmental conditions. In this study, Gupta *et al.*, (2011) showed the role of stochasticity in single cell behaviour promoting phenotypic equilibrium in the cancer cell population. In cancer cell populations, this equilibrium allowed the maintenance of some specific cell-surface markers profiles across many divisions in cell culture (Gupta *et al.*, 2011).

6.8 Zebrafish is a new tool for developing drugs against melanocyte-related disease in human

In this study we used zebrafish as a model to study melanocyte development and the results we collected for normal development of the cell can be used for understanding abnormal development such as in neurocristopathies and melanoma. Furthermore this knowledge can be extrapolated in human and used for engineering new therapeutic strategies.

Melanoma is associated with mis-regulation and an increase of *β*-catenin, B-RAF/B-RAS and the cAMP pathway as shown in B16 melanoma cells (Goding, 2000, Rubinfeld *et al.*, 1997, Van Dyke and Merlino, 2012, Busca *et al.*, 2000, Dumaz, 2012). Ceol *et al.*, (2011) studied genes involved in melanoma in the zebrafish model. They used a transgenic line *Tg(mitfa:BRAFV600E*) which over expresses the oncogene BRAF in melanocytes, in a *p53(lf)* mutant background, to investigate genes involved in activating tumor formation (Ceol *et al.*, 2011). In the transgenic *Tg(mitfa:BRAFV600E*); *p53(lf)* mutant, the melanocyte and tumor formation were suppressed by another mutation, the *mitfa(lf).* Consequently, *Tg(mitfa:BRAFV600E*); *p53*(*lf*); *mitfa(lf)* fish did not show melanised pigmentation. After identifying candidates for tumor formation from studies of human tumor samples, Ceol *et al.*, (2011) cloned the candidate sequences into a transposon vector and injected it at one cell stage in transgenic *Tg(mitfa:BRAFV600E*); *p53(lf); mitfa(lf)* fish. Melanocyte production and melanoma could be rescued in adult fish injected with mRNA coding for the enzyme SETDB1. Consequently, using this strategy, Ceol *et al.*, (2011) showed that enzyme SETDB1, which methylates the histone H3 on lysine 9 (H3K9), could accelerate melanoma tumor formation in fish. These results could be used to investigate this enzyme and target it for drug design in human.

Zebrafish is an acceptable model for the study of melanoma as shown in Ignatius and Langenau, (2009), Patton and Zon, (2005), Feitsma and Cuppen, (2008), Mione and Trede, (2010) and Ceol *et al.*, (2011). Combining the possibilities offered by new technologies to the available analysis of melanocyte cells in zebrafish brings the right conditions for establishing new efficient methods to test new therapeutic drugs or assays.

6.9 Future experiments

In addition to the other experiments suggested in Chapter 3-5, future possibilities could also be found with transgenic lines, such as *mitfa*-GFP, *sox10*-GFP, *ltk*-GFP or *TOP;d*GFP, which will help to fully test the new hypotheses and improve the understanding of the underlying melanocyte genetics. The regulation of *mitfa* and *sox10* in melanocytes as well as the discovery of new factors involved in their regulatory process through cell development remains a central node. The existence of a chromatoblast should be further tested and in this aim, single cell transcriptome analysis could be performed.

6.10 Conclusion

In conclusion, these experiments have allowed us to answer some important questions and to propose new research directions in the context of melanocyte development. The fundamental aspect of melanocyte developmental research is particularly relevant for developing the understanding of the mechanisms involved in several congenital and aggressive human diseases. The development of applied research for developing drugs tested in cell culture, in mouse, or in zebrafish, is then closely related and based upon the fundamental study of genetic regulatory networks such as the one presented here.

References

Abitua, P. B., Wagner, E., Navarrete, I. A. & Levine, M. (2012), Identification of a rudimentary neural crest in a non-vertebrate chordate. Nature, *492*, 104-7.

Abramoff, M. D., Magalhaes, P.J., Ram, S.J. (2004), Image Processing with ImageJ. Biophotonics International, *11*, 36-42.

Adameyko, I., Lallemend, F., Aquino, J. B., Pereira, J. A., Topilko, P., Muller, T., Fritz, N., Beljajeva, A., Mochii, M., Liste, I., et al. (2009), Schwann cell precursors from nerve innervation are a cellular origin of melanocytes in skin. Cell, *139*, 366-79.

Adameyko, I., Lallemend, F., Furlan, A., Zinin, N., Aranda, S., Kitambi, S. S., Blanchart, A., Favaro, R., Nicolis, S., Lubke, M., et al. (2011), Sox2 and Mitf cross-regulatory interactions consolidate progenitor and melanocyte lineages in the cranial neural crest. Development, *139*, 397-410.

Alkhateeb, A., Fain, P. R. & Spritz, R. A. (2005), Candidate functional promoter variant in the FOXD3 melanoblast developmental regulator gene in autosomal dominant vitiligo. J Invest Dermatol, *125*, 388-91.

Ando, H., Kondoh, H., Ichihashi, M. & Hearing, V. J. (2007), Approaches to identify inhibitors of melanin biosynthesis via the quality control of tyrosinase. J Invest Dermatol, *127*, 751-61.

Antonellis, A., Bennett, W. R., Menheniott, T. R., Prasad, A. B., Lee-Lin, S. Q., Green, E. D., Paisley, D., Kelsh, R. N., Pavan, W. J. & Ward, A. (2006), Deletion of long-range sequences at Sox10 compromises developmental expression in a mouse model of Waardenburg-Shah (WS4) syndrome. Hum Mol Genet, *15*, 259-71.

Aoki, H. & Moro, O. (2002), Involvement of microphthalmia-associated transcription factor (MITF) in expression of human melanocortin-1 receptor (MC1R). Life Sci, *71*, 2171-9.

Aoki, T., Ohnishi, H., Oda, Y., Tadokoro, M., Sasao, M., Kato, H., Hattori, K. & Ohgushi, H. (2010), Generation of induced pluripotent stem cells from human adipose-derived stem cells without c-MYC. Tissue Eng Part A, *16*, 2197-206.

Aoki, Y., Saint-Germain, N., Gyda, M., Magner-Fink, E., Lee, Y. H., Credidio, C. & Saint-Jeannet, J. P. (2003), Sox10 regulates the development of neural crest-derived melanocytes in Xenopus. Dev Biol, *259*, 19-33.

Atack, J. R., Prior, A. M., Fletcher, S. R., Quirk, K., Mckernan, R. & Ragan, C. I. (1994), Effects of L-690,488, a prodrug of the bisphosphonate inositol monophosphatase inhibitor L-690,330, on phosphatidylinositol cycle markers. J Pharmacol Exp Ther, *270*, 70-6.

Avissar, S., Schreiber, G., Danon, A. & Belmaker, R. H. (1988), Lithium inhibits adrenergic and cholinergic increases in GTP binding in rat cortex. Nature, *331*, 440-2.

Aybar, M. J., Nieto, M. A. & Mayor, R. (2003), Snail precedes slug in the genetic cascade required for the specification and migration of the Xenopus neural crest. Development, *130*, 483-94.

Badner, J. A., Sieber, W. K., Garver, K. L. & Chakravarti, A. (1990), A genetic study of Hirschsprung disease. Am J Hum Genet, *46*, 568-80.

Bagnara, J. T. (1999), The emergence of pigment cell biology: a personal view. Pigment Cell Res, *12*, 48-65.

Bagnara, J. T., Matsumoto, J., Ferris, W., Frost, S. K., Turner, W. A., Jr., Tchen, T. T. & Taylor, J. D. (1979), Common origin of pigment cells. Science, *203*, 410-5.

Bandarchi, B., Jabbari, C. A., Vedadi, A. & Navab, R. (2013), Molecular biology of normal melanocytes and melanoma cells. J Clin Pathol.

Bar, T., Kubista, M. & Tichopad, A. (2011), Validation of kinetics similarity in qPCR. Nucleic Acids Res.

Barker, N. (2008), The canonical Wnt/beta-catenin signalling pathway. Methods Mol Biol, *468*, 5-15.

Baroffio, A., Dupin, E. & Le Douarin, N. M. (1988), Clone-forming ability and differentiation potential of migratory neural crest cells. Proc Natl Acad Sci U S A, *85*, 5325-9.

Baroffio, A., Dupin, E. & Le Douarin, N. M. (1991), Common precursors for neural and mesectodermal derivatives in the cephalic neural crest. Development, *112*, 301-5.

Baynash, A. G., Hosoda, K., Giaid, A., Richardson, J. A., Emoto, N., Hammer, R. E. & Yanagisawa, M. (1994), Interaction of endothelin-3 with endothelin-B receptor is essential for development of epidermal melanocytes and enteric neurons. Cell, *79*, 1277-85.

Becskei, A., Seraphin, B. & Serrano, L. (2001), Positive feedback in eukaryotic gene networks: cell differentiation by graded to binary response conversion. EMBO J, *20*, 2528-35.

Bellei, B., Flori, E., Izzo, E., Maresca, V. & Picardo, M. (2008), GSK3beta inhibition promotes melanogenesis in mouse B16 melanoma cells and normal human melanocytes. Cell Signal, *20*, 1750-61.

Bellei, B., Pitisci, A., Catricala, C., Larue, L. & Picardo, M. (2010), Wnt/beta-catenin signaling is stimulated by alpha-melanocyte-stimulating hormone in melanoma and melanocyte cells: implication in cell differentiation. Pigment Cell Melanoma Res, *24*, 309-25.

Bengtsson, M., Hemberg, M., Rorsman, P. & Stahlberg, A. (2008), Quantification of mRNA in single cells and modelling of RT-qPCR induced noise. BMC Mol Biol, *9*, 63.

Benned-Jensen, T., Mokrosinski, J. & Rosenkilde, M. M. (2011), The E92K melanocortin 1 receptor mutant induces cAMP production and arrestin recruitment but not ERK activity indicating biased constitutive signaling. PLoS One, *6*, e24644.

Berridge, M. J., Downes, C. P. & Hanley, M. R. (1989), Neural and developmental actions of lithium: a unifying hypothesis. Cell, *59*, 411-9.

Bertolotto, C. & Ballotti, R. (2009), Functional role of MITF phosphorylation. In vivo veritas? Pigment Cell Melanoma Res, *22*, 703-4.

Bertolotto, C., Busca, R., Abbe, P., Bille, K., Aberdam, E., Ortonne, J. P. & Ballotti, R. (1998), Different cis-acting elements are involved in the regulation of TRP1 and TRP2 promoter activities by cyclic AMP: pivotal role of M boxes (GTCATGTGCT) and of microphthalmia. Mol Cell Biol, *18*, 694-702.

Boissy, R. E. & Nordlund, J. J. (1997), Molecular basis of congenital hypopigmentary disorders in humans: a review. Pigment Cell Res, *10*, 12-24.

Bondurand, N., Pingault, V., Goerich, D. E., Lemort, N., Sock, E., Le Caignec, C., Wegner, M. & Goossens, M. (2000), Interaction among SOX10, PAX3 and MITF, three genes altered in Waardenburg syndrome. Hum Mol Genet, *9*, 1907-17.

Bosch, F., Gomez-Foix, A. M., Arino, J. & Guinovart, J. J. (1986), Effects of lithium ions on glycogen synthase and phosphorylase in rat hepatocytes. J Biol Chem, *261*, 16927-31.

Brady, G. (2000), Expression profiling of single mammalian cells--small is beautiful. Yeast, *17*, 211-7.

Breslauer, K. J., Frank, R., Blocker, H. & Marky, L. A. (1986), Predicting DNA duplex stability from the base sequence. Proc Natl Acad Sci U S A, *83*, 3746-50.

Bronner-Fraser, M. (2003), Hierarchy of events regulating neural crest induction. Harvey Lect, *99*, 129-44.

Bronner-Fraser, M. & Fraser, S. E. (1988), Cell lineage analysis reveals multipotency of some avian neural crest cells. Nature, *335*, 161-4.

Bronner-Fraser, M. & Fraser, S. E. (1991), Cell lineage analysis of the avian neural crest. Development, *Suppl 2*, 17-22.

Budhia, S., Haring, L. F., Mcconnell, I. & Blacklaws, B. A. (2006), Quantitation of ovine cytokine mRNA by real-time RT-PCR. J Immunol Methods, *309*, 160-72.

Burstyn-Cohen, T. & Kalcheim, C. (2002), Association between the cell cycle and neural crest delamination through specific regulation of G1/S transition. Dev Cell, *3*, 383-95.

Busa, W. B. & Gimlich, R. L. (1989), Lithium-induced teratogenesis in frog embryos prevented by a polyphosphoinositide cycle intermediate or a diacylglycerol analog. Dev Biol, *132*, 315-24.

Busca, R., Abbe, P., Mantoux, F., Aberdam, E., Peyssonnaux, C., Eychene, A., Ortonne, J. P. & Ballotti, R. (2000), Ras mediates the cAMP-dependent activation of extracellular signal-regulated kinases (ERKs) in melanocytes. EMBO J, *19*, 2900-10.

Bustin, S. A. (2000), Absolute quantification of mRNA using real-time reverse transcription polymerase chain reaction assays. J Mol Endocrinol, *25*, 169-93.

Carney, T. J., Dutton, K. A., Greenhill, E., Delfino-Machin, M., Dufourcq, P., Blader, P. & Kelsh, R. N. (2006), A direct role for Sox10 in specification of neural crest-derived sensory neurons. Development, *133*, 4619-30.

Carreira, S., Goodall, J., Aksan, I., La Rocca, S. A., Galibert, M. D., Denat, L., Larue, L. & Goding, C. R. (2005), Mitf cooperates with Rb1 and activates p21Cip1 expression to regulate cell cycle progression. Nature, *433*, 764-9.

Carreira, S., Goodall, J., Denat, L., Rodriguez, M., Nuciforo, P., Hoek, K. S., Testori, A., Larue, L. & Goding, C. R. (2006), Mitf regulation of Dia1 controls melanoma proliferation and invasiveness. Genes Dev, *20*, 3426-39.

Ceol, C. J., Houvras, Y., Jane-Valbuena, J., Bilodeau, S., Orlando, D. A., Battisti, V., Fritsch, L., Lin, W. M., Hollmann, T. J., Ferre, F., et al. (2011), The histone methyltransferase SETDB1 is recurrently amplified in melanoma and accelerates its onset. Nature, *471*, 513-7.

Cerny, R., Lwigale, P., Ericsson, R., Meulemans, D., Epperlein, H. H. & Bronner-Fraser, M. (2004), Developmental origins and evolution of jaws: new interpretation of "maxillary" and "mandibular". Dev Biol, *276*, 225-36.

Chan, T. M., Longabaugh, W., Bolouri, H., Chen, H. L., Tseng, W. F., Chao, C. H., Jang, T. H., Lin, Y. I., Hung, S. C., Wang, H. D., et al. (2009), Developmental gene regulatory networks in the zebrafish embryo. Biochim Biophys Acta, *1789*, 279-98.

Cheli, Y., Ohanna, M., Ballotti, R. & Bertolotto, C. (2012), Fifteen-year quest for microphthalmia-associated transcription factor target genes. Pigment Cell Melanoma Res, *23*, 27-40.

Chen, H., Jiang, L., Xie, Z., Mei, L., He, C., Hu, Z., Xia, K. & Feng, Y. Novel mutations of PAX3, MITF, and SOX10 genes in Chinese patients with type I or type II Waardenburg syndrome. Biochem Biophys Res Commun, *397*, 70-4.

Chen, R. H., Ding, W. V. & Mccormick, F. (2000), Wnt signaling to beta-catenin involves two interactive components. Glycogen synthase kinase-3beta inhibition and activation of protein kinase C. J Biol Chem, *275*, 17894-9.

Chen, W., Chen, M. & Barak, L. S. (2010), Development of small molecules targeting the Wnt pathway for the treatment of colon cancer: a high-throughput screening approach. Am J Physiol Gastrointest Liver Physiol, *299*, G293-300.

Chomczynski, P. & Sacchi, N. (1987), Single-step method of RNA isolation by acid guanidinium thiocyanate-phenol-chloroform extraction. Anal Biochem, *162*, 156-9.

Cifuentes, D., Xue, H., Taylor, D. W., Patnode, H., Mishima, Y., Cheloufi, S., Ma, E., Mane, S., Hannon, G. J., Lawson, N. D., et al. (2010), A novel miRNA processing pathway independent of Dicer requires Argonaute2 catalytic activity. Science, *328*, 1694-8.

Colas, J. F. & Schoenwolf, G. C. (2001), Towards a cellular and molecular understanding of neurulation. Dev Dyn, *221*, 117-45.

Colborn, J. M., Byrd, B. D., Koita, O. A. & Krogstad, D. J. (2008), Estimation of copy number using SYBR Green: confounding by AT-rich DNA and by variation in amplicon length. Am J Trop Med Hyg, *79*, 887-92.

Cookson, S., Ostroff, N., Pang, W. L., Volfson, D. & Hasty, J. (2005), Monitoring dynamics of single-cell gene expression over multiple cell cycles. Mol Syst Biol, *1*, 2005 0024.

Cooper, C. D., Linbo, T. H. & Raible, D. W. (2009), Kit and foxd3 genetically interact to regulate melanophore survival in zebrafish. Dev Dyn, *238*, 875-86.

Crawley, M. J. (2007), The R book, (Chichester, Wiley).

Cronin, J. C., Wunderlich, J., Loftus, S. K., Prickett, T. D., Wei, X., Ridd, K., Vemula, S., Burrell, A. S., Agrawal, N. S., Lin, J. C., et al. (2009), Frequent mutations in the MITF pathway in melanoma. Pigment Cell Melanoma Res, *22*, 435-44.

Croteau, W., Jenkins, M. H., Ye, S., Mullins, D. W. & Brinckerhoff, C. E. (2012), Differential mechanisms of tumor progression in clones from a single heterogeneous human melanoma. J Cell Physiol, *228*, 773-80.

Cunliffe, V. T. (2004), Histone deacetylase 1 is required to repress Notch target gene expression during zebrafish neurogenesis and to maintain the production of motoneurones in response to hedgehog signalling. Development, *131*, 2983-95.

Curran, K., Lister, J. A., Kunkel, G. R., Prendergast, A., Parichy, D. M. & Raible, D. W. (2010), Interplay between Foxd3 and Mitf regulates cell fate plasticity in the zebrafish neural crest. Dev Biol, *344*, 107-18.

Curran, K., Raible, D. W. & Lister, J. A. (2009), Foxd3 controls melanophore specification in the zebrafish neural crest by regulation of Mitf. Dev Biol, *332*, 408-17.

Deardorff, M. A., Tan, C., Saint-Jeannet, J. P. & Klein, P. S. (2001), A role for frizzled 3 in neural crest development. Development, *128*, 3655-63.

Delaurier, A., Nakamura, Y., Braasch, I., Khanna, V., Kato, H., Wakitani, S., Postlethwait, J. H. & Kimmel, C. B. Histone deacetylase-4 is required during early cranial neural crest development for generation of the zebrafish palatal skeleton. BMC Dev Biol, *12*, 16.

Diercks, A., Kostner, H. & Ozinsky, A. (2009), Resolving cell population heterogeneity: real-time PCR for simultaneous multiplexed gene detection in multiple single-cell samples. PLoS One, *4*, e6326.

Dixon, A. K., Richardson, P. J., Pinnock, R. D. & Lee, K. (2000), Gene-expression analysis at the single-cell level. Trends Pharmacol Sci, *21*, 65-70.

Dominguez, I., Itoh, K. & Sokol, S. Y. (1995), Role of glycogen synthase kinase 3 beta as a negative regulator of dorsoventral axis formation in Xenopus embryos. Proc Natl Acad Sci U S A, *92*, 8498-502.

Don, P., Iuga, A., Dacko, A. & Hardick, K. (2006), Treatment of vitiligo with broadband ultraviolet B and vitamins. Int J Dermatol, *45*, 63-5.

Donoghue, P. C., Graham, A. & Kelsh, R. N. (2008), The origin and evolution of the neural crest. Bioessays, *30*, 530-41.

Dorsky, R. I., Moon, R. T. & Raible, D. W. (1998), Control of neural crest cell fate by the Wnt signalling pathway. Nature, *396*, 370-3.

Dorsky, R. I., Moon, R. T. & Raible, D. W. (2000a), Environmental signals and cell fate specification in premigratory neural crest. Bioessays, *22*, 708-16.

Dorsky, R. I., Raible, D. W. & Moon, R. T. (2000b), Direct regulation of nacre, a zebrafish MITF homolog required for pigment cell formation, by the Wnt pathway. Genes Dev, *14*, 158-62.

Dorsky, R. I., Sheldahl, L. C. & Moon, R. T. (2002), A transgenic Lef1/beta-catenin-dependent reporter is expressed in spatially restricted domains throughout zebrafish development. Dev Biol, *241*, 229-37.

Dottori, M., Gross, M. K., Labosky, P. & Goulding, M. (2001), The winged-helix transcription factor Foxd3 suppresses interneuron differentiation and promotes neural crest cell fate. Development, *128*, 4127-38.

Drerup, C. M., Wiora, H. M., Topczewski, J. & Morris, J. A. (2009), Disc1 regulates foxd3 and sox10 expression, affecting neural crest migration and differentiation. Development, *136*, 2623-32.

Dumaz, N. (2012), Mechanism of RAF isoform switching induced by oncogenic RAS in melanoma. Small GTPases, *2*, 289-292.

Dunn, K. J., Williams, B. O., Li, Y. & Pavan, W. J. (2000a), Neural crest-directed gene transfer demonstrates Wnt1 role in melanocyte expansion and differentiation during mouse development. Proc Natl Acad Sci U S A, *97*, 10050-10055.

Dunn, K. J., Williams, B. O., Li, Y. & Pavan, W. J. (2000b), Neural crest-directed gene transfer demonstrates Wnt1 role in melanocyte expansion and differentiation during mouse development. Proc Natl Acad Sci U S A, *97*, 10050-5.

Dunn, O. J. (1961), Multiple Comparisons Among Means. Journal of the American Statistical Association, *56*, 52-64.

Dupin, E., Calloni, G., Real, C., Goncalves-Trentin, A. & Le Douarin, N. M. (2007), Neural crest progenitors and stem cells. C R Biol, *330*, 521-9.

Dupin, E., Glavieux, C., Vaigot, P. & Le Douarin, N. M. (2000), Endothelin 3 induces the reversion of melanocytes to glia through a neural crest-derived glial-melanocytic progenitor. Proc Natl Acad Sci U S A, *97*, 7882-7887.

Dupin, E., Real, C., Glavieux-Pardanaud, C., Vaigot, P. & Le Douarin, N. M. (2003), Reversal of developmental restrictions in neural crest lineages: transition from Schwann cells to glial-melanocytic precursors in vitro. Proc Natl Acad Sci U S A, *100*, 5229-33.

Dupin, E., Sextier-Sainte-Claire Deville, F., Nataf, V. & Le Douarin, N. M. (1993), The ontogeny of the neural crest. C R Acad Sci III, *316*, 1062-81.

Dutton, K. A., Pauliny, A., Lopes, S. S., Elworthy, S., Carney, T. J., Rauch, J., Geisler, R., Haffter, P. & Kelsh, R. N. (2001), Zebrafish colourless encodes sox10 and specifies non-ectomesenchymal neural crest fates. Development, *128*, 4113-25.

Easty, D. J., Gray, S. G., O'byrne, K. J., O'donnell, D. & Bennett, D. C. (2011), Receptor tyrosine kinases and their activation in melanoma. Pigment Cell Melanoma Res, *24*, 446-61.

Egeblad, M. & Werb, Z. (2002), New functions for the matrix metalloproteinases in cancer progression. Nat Rev Cancer, *2*, 161-74.

Eisen, J. S. & Weston, J. A. (1993), Development of the neural crest in the zebrafish. Dev Biol, *159*, 50-9.

Elowitz, M. B., Levine, A. J., Siggia, E. D. & Swain, P. S. (2002), Stochastic gene expression in a single cell. Science, *297*, 1183-6.

Elworthy, S., Lister, J. A., Carney, T. J., Raible, D. W. & Kelsh, R. N. (2003a), Transcriptional regulation of mitfa accounts for the sox10 requirement in zebrafish melanophore development. Development, *130*, 2809-2818.

Elworthy, S., Lister, J. A., Carney, T. J., Raible, D. W. & Kelsh, R. N. (2003b), Transcriptional regulation of mitfa accounts for the sox10 requirement in zebrafish melanophore development. Development, *130*, 2809-18.

Englaro, W., Bertolotto, C., Busca, R., Brunet, A., Pages, G., Ortonne, J. P. & Ballotti, R. (1998), Inhibition of the mitogen-activated protein kinase pathway triggers B16 melanoma cell differentiation. J Biol Chem, *273*, 9966-70.

Erickson, C. A. (1985), Control of neural crest cell dispersion in the trunk of the avian embryo. Dev Biol, *111*, 138-57.

Feitsma, H. & Cuppen, E. (2008), Zebrafish as a cancer model. Mol Cancer Res, *6*, 685-94.

Florczyk, L. M. F. A. S. J. (2007), Exploring the cross-talk between p38 MAPK and canonical Wnt signaling pathways. The Journal of Immunology, *178, 94.15*.

Fournier, T., Gabriel, J. P., Mazza, C., Pasquier, J., Galbete, J. L. & Mermod, N. (2007), Steady-state expression of self-regulated genes. Bioinformatics, *23*, 3185-92.

Friedman, N., Cai, L. & Xie, X. S. (2006), Linking stochastic dynamics to population distribution: an analytical framework of gene expression. Phys Rev Lett, *97*, 168302.

Gammill, L. S. & Bronner-Fraser, M. (2003), Neural crest specification: migrating into genomics. Nat Rev Neurosci, *4*, 795-805.

Garcia-Borron, J. C., Sanchez-Laorden, B. L. & Jimenez-Cervantes, C. (2005), Melanocortin-1 receptor structure and functional regulation. Pigment Cell Res, *18*, 393-410.

Garcia-Castro, M. I., Marcelle, C. & Bronner-Fraser, M. (2002), Ectodermal Wnt function as a neural crest inducer. Science, *297*, 848-51.

Garg, A., Mohanram, K., Di Cara, A., De Micheli, G. & Xenarios, I. (2009), Modeling stochasticity and robustness in gene regulatory networks. Bioinformatics, *25*, i101-9.

Garraway, L. A., Widlund, H. R., Rubin, M. A., Getz, G., Berger, A. J., Ramaswamy, S., Beroukhim, R., Milner, D. A., Granter, S. R., Du, J., et al. (2005), Integrative genomic analyses identify MITF as a lineage survival oncogene amplified in malignant melanoma. Nature, *436*, 117-22.

Gillespie, D. T. (2009), Deterministic limit of stochastic chemical kinetics. J Phys Chem B, *113*, 1640-4.

Goding, C. R. (2000), Mitf from neural crest to melanoma: signal transduction and transcription in the melanocyte lineage. Genes Dev, *14*, 1712-28.

Goding, C. R. (2007), Melanocytes: the new Black. Int J Biochem Cell Biol, *39*, 275-9.

Golding, I., Paulsson, J., Zawilski, S. M. & Cox, E. C. (2005), Real-time kinetics of gene activity in individual bacteria. Cell, *123*, 1025-36.

Greenhill, E. R., Rocco, A., Vibert, L., Nikaido, M. & Kelsh, R. N. (2011), An iterative genetic and dynamical modelling approach identifies novel features of the gene regulatory network underlying melanocyte development. PLoS Genet, *7*, e1002265.

Gross, J. B., Borowsky, R. & Tabin, C. J. (2009), A novel role for Mc1r in the parallel evolution of depigmentation in independent populations of the cavefish Astyanax mexicanus. PLoS Genet, *5*, e1000326.

Guo, X., Qi, H., Verfaillie, C. M. & Pan, W. (2003), Statistical significance analysis of longitudinal gene expression data. Bioinformatics, *19*, 1628-35.

Gupta, P. B., Fillmore, C. M., Jiang, G., Shapira, S. D., Tao, K., Kuperwasser, C. & Lander, E. S. (2011), Stochastic state transitions give rise to phenotypic equilibrium in populations of cancer cells. Cell, *146*, 633-44.

Halaban, R., Moellmann, G., Tamura, A., Kwon, B. S., Kuklinska, E., Pomerantz, S. H. & Lerner, A. B. (1988), Tyrosinases of murine melanocytes with mutations at the albino locus. Proc Natl Acad Sci U S A, *85*, 7241-5.

Hall, B. K. (2008), The neural crest and neural crest cells: discovery and significance for theories of embryonic organization. J Biosci, *33*, 781-93.

Hall, C., Flores, M. V., Murison, G., Crosier, K. & Crosier, P. (2006), An essential role for zebrafish Fgfrl1 during gill cartilage development. Mech Dev, *123*, 925-40.

Hallsson, J. H., Haflidadottir, B. S., Stivers, C., Odenwald, W., Arnheiter, H., Pignoni, F. & Steingrimsson, E. (2004), The basic helix-loop-helix leucine zipper transcription factor Mitf is conserved in Drosophila and functions in eye development. Genetics, *167*, 233-41.

Hanken, J. & Gross, J. B. (2005), Evolution of cranial development and the role of neural crest: insights from amphibians. J Anat, *207*, 437-46.

Hans, S., Kaslin, J., Freudenreich, D. & Brand, M. (2009), Temporally-controlled site-specific recombination in zebrafish. PLoS One, *4*, e4640.

Hari, L., Miescher, I., Shakhova, O., Suter, U., Chin, L., Taketo, M., Richardson, W. D., Kessaris, N. & Sommer, L. (2012), Temporal control of neural crest lineage generation by Wnt/beta-catenin signaling. Development, *139*, 2107-17.

Harris, M. L., Baxter, L. L., Loftus, S. K. & Pavan, W. J. (2010), Sox proteins in melanocyte development and melanoma. Pigment Cell Melanoma Res, *23*, 496-513.

Harrison, M. R., Georgiou, A. S., Spaink, H. P. & Cunliffe, V. T. (2011), The epigenetic regulator Histone Deacetylase 1 promotes transcription of a core neurogenic programme in zebrafish embryos. BMC Genomics, *12*, 24.

Hartshorn, C., Anshelevich, A. & Wangh, L. J. (2005), Rapid, single-tube method for quantitative preparation and analysis of RNA and DNA in samples as small as one cell. BMC Biotechnol, *5*, 2.

Hearing, V. J. & Jimenez, M. (1987), Mammalian tyrosinase--the critical regulatory control point in melanocyte pigmentation. Int J Biochem, *19*, 1141-7.

Heasman, J., Crawford, A., Goldstone, K., Garner-Hamrick, P., Gumbiner, B., Mccrea, P., Kintner, C., Noro, C. Y. & Wylie, C. (1994), Overexpression of cadherins and underexpression of beta-catenin inhibit dorsal mesoderm induction in early Xenopus embryos. Cell, *79*, 791-803.

Hedstrand, H., Ekwall, O., Olsson, M. J., Landgren, E., Kemp, E. H., Weetman, A. P., Perheentupa, J., Husebye, E., Gustafsson, J., Betterle, C., et al. (2001), The transcription factors SOX9 and SOX10 are vitiligo autoantigens in autoimmune polyendocrine syndrome type I. J Biol Chem, *276*, 35390-5.

Henrique, D., Adam, J., Myat, A., Chitnis, A., Lewis, J. & Ish-Horowicz, D. (1995), Expression of a Delta homologue in prospective neurons in the chick. Nature, *375*, 787-90.

Hernandez, L., Wilkerson, P. M., Lambros, M. B., Campion-Flora, A., Rodrigues, D. N., Gauthier, A., Cabral, C., Pawar, V., Mackay, A., A'hern, R., et al. (2012), Genomic and

mutational profiling of ductal carcinomas in situ and matched adjacent invasive breast cancers reveals intra-tumour genetic heterogeneity and clonal selection. J Pathol.

Higuchi, R., Fockler, C., Dollinger, G. & Watson, R. (1993), Kinetic PCR analysis: real-time monitoring of DNA amplification reactions. Biotechnology (N Y), *11*, 1026-30.

Hirata, M., Nakamura, K., Kanemaru, T., Shibata, Y. & Kondo, S. (2003), Pigment cell organization in the hypodermis of zebrafish. Dev Dyn, *227*, 497-503.

Hodgkin, A. L. & Huxley, A. F. (1952), A quantitative description of membrane current and its application to conduction and excitation in nerve. J Physiol, *117*, 500-44.

Hodgkinson, C. A., Moore, K. J., Nakayama, A., Steingrimsson, E., Copeland, N. G., Jenkins, N. A. & Arnheiter, H. (1993), Mutations at the mouse microphthalmia locus are associated with defects in a gene encoding a novel basic-helix-loop-helix-zipper protein. Cell, *74*, 395-404.

Hoek, K. S., Schlegel, N. C., Eichhoff, O. M., Widmer, D. S., Praetorius, C., Einarsson, S. O., Valgeirsdottir, S., Bergsteinsdottir, K., Schepsky, A., Dummer, R., et al. (2008), Novel MITF targets identified using a two-step DNA microarray strategy. Pigment Cell Melanoma Res, *21*, 665-76.

Hoerter, J. D., Bradley, P., Casillas, A., Chambers, D., Denholm, C., Johnson, K. & Weiswasser, B. (2012), Extrafollicular dermal melanocyte stem cells and melanoma. Stem Cells Int, *2012*, 407079.

Honore, S. M., Aybar, M. J. & Mayor, R. (2003), Sox10 is required for the early development of the prospective neural crest in Xenopus embryos. Dev Biol, *260*, 79-96.

Hou, L., Arnheiter, H. & Pavan, W. J. (2006), Interspecies difference in the regulation of melanocyte development by SOX10 and MITF. Proc Natl Acad Sci U S A, *103*, 9081-5.

Hou, L., Panthier, J. J. & Arnheiter, H. (2000), Signaling and transcriptional regulation in the neural crest-derived melanocyte lineage: interactions between KIT and MITF. Development, *127*, 5379-89.

Hou, L. & Pavan, W. J. (2008), Transcriptional and signaling regulation in neural crest stem cell-derived melanocyte development: do all roads lead to Mitf? Cell Res, *18*, 1163-76.

Hubbell, E., Liu, W. M. & Mei, R. (2002), Robust estimators for expression analysis. Bioinformatics, *18*, 1585-92.

Hultman, K. A., Bahary, N., Zon, L. I. & Johnson, S. L. (2007), Gene Duplication of the zebrafish kit ligand and partitioning of melanocyte development functions to kit ligand a. PLoS Genet, *3*, e17.

Hultman, K. A., Budi, E. H., Teasley, D. C., Gottlieb, A. Y., Parichy, D. M. & Johnson, S. L. (2009), Defects in ErbB-dependent establishment of adult melanocyte stem cells reveal

independent origins for embryonic and regeneration melanocytes. PLoS Genet, *5*, e1000544.

Hur, E. M. & Zhou, F. Q. (2010), GSK3 signalling in neural development. Nat Rev Neurosci, *11*, 539-51.

Ignatius, M. S. & Langenau, D. M. (2009), Zebrafish as a model for cancer self-renewal. Zebrafish, *6*, 377-87.

Ignatius, M. S., Moose, H. E., El-Hodiri, H. M. & Henion, P. D. (2008), colgate/hdac1 Repression of foxd3 expression is required to permit mitfa-dependent melanogenesis. Dev Biol, *313*, 568-83.

Ikenouchi, J., Matsuda, M., Furuse, M. & Tsukita, S. (2003), Regulation of tight junctions during the epithelium-mesenchyme transition: direct repression of the gene expression of claudins/occludin by Snail. J Cell Sci, *116*, 1959-67.

Ikeya, M., Lee, S. M., Johnson, J. E., Mcmahon, A. P. & Takada, S. (1997), Wnt signalling required for expansion of neural crest and CNS progenitors. Nature, *389*, 966-70.

Imai, K. S., Hino, K., Yagi, K., Satoh, N. & Satou, Y. (2004), Gene expression profiles of transcription factors and signaling molecules in the ascidian embryo: towards a comprehensive understanding of gene networks. Development, *131*, 4047-58.

Ishizaki, H., Spitzer, M., Wildenhain, J., Anastasaki, C., Zeng, Z., Dolma, S., Shaw, M., Madsen, E., Gitlin, J., Marais, R., et al. (2010), Combined zebrafish-yeast chemical-genetic screens reveal gene-copper-nutrition interactions that modulate melanocyte pigmentation. Dis Model Mech, *3*, 639-51.

Ito, S. & Wakamatsu, K. (2003), Quantitative analysis of eumelanin and pheomelanin in humans, mice, and other animals: a comparative review. Pigment Cell Res, *16*, 523-31.

Ito, S. & Wakamatsu, K. (2008), Chemistry of mixed melanogenesis--pivotal roles of dopaquinone. Photochem Photobiol, *84*, 582-92.

Janes, K. A., Wang, C. C., Holmberg, K. J., Cabral, K. & Brugge, J. S. (2010), Identifying single-cell molecular programs by stochastic profiling. Nat Methods, *7*, 311-7.

Jeffery, W. R., Strickler, A. G. & Yamamoto, Y. (2004), Migratory neural crest-like cells form body pigmentation in a urochordate embryo. Nature, *431*, 696-9.

Jiao, Z., Mollaaghababa, R., Pavan, W. J., Antonellis, A., Green, E. D. & Hornyak, T. J. (2004), Direct interaction of Sox10 with the promoter of murine Dopachrome Tautomerase (Dct) and synergistic activation of Dct expression with Mitf. Pigment Cell Res, *17*, 352-62.

Jin, E. J. & Thibaudeau, G. (1999), Effects of lithium on pigmentation in the embryonic zebrafish (Brachydanio rerio). Biochim Biophys Acta, *1449*, 93-9.

Jin, Y., Mailloux, C. M., Gowan, K., Riccardi, S. L., Laberge, G., Bennett, D. C., Fain, P. R. & Spritz, R. A. (2007), NALP1 in vitiligo-associated multiple autoimmune disease. N Engl J Med, *356*, 1216-25.

Johnson, S. L., Nguyen, A. N. & Lister, J. A. (2010), mitfa is required at multiple stages of melanocyte differentiation but not to establish the melanocyte stem cell. Dev Biol, *350*, 405-13.

Kabbarah, O. & Chin, L. (2006), Advances in malignant melanoma: genetic insights from mouse and man. Front Biosci, *11*, 928-42.

Kaern, M., Elston, T. C., Blake, W. J. & Collins, J. J. (2005), Stochasticity in gene expression: from theories to phenotypes. Nat Rev Genet, *6*, 451-64.

Kalcheim, C. (2000), Mechanisms of early neural crest development: from cell specification to migration. Int Rev Cytol, *200*, 143-96.

Kalcheim, C. & Burstyn-Cohen, T. (2005), Early stages of neural crest ontogeny: formation and regulation of cell delamination. Int J Dev Biol, *49*, 105-16.

Kamme, F. & Erlander, M. G. (2003), Global gene expression analysis of single cells. Curr Opin Drug Discov Devel, *6*, 231-6.

Kao, K. R. & Elinson, R. P. (1988), The entire mesodermal mantle behaves as Spemann's organizer in dorsoanterior enhanced Xenopus laevis embryos. Dev Biol, *127*, 64-77.

Karanth, S., Lall, S. P., Denovan-Wright, E. M. & Wright, J. M. (2009), Differential transcriptional modulation of duplicated fatty acid-binding protein genes by dietary fatty acids in zebrafish (Danio rerio): evidence for subfunctionalization or neofunctionalization of duplicated genes. BMC Evol Biol, *9*, 219.

Kawa, Y., Soma, Y., Nakamura, M., Ito, M., Kawakami, T., Baba, T., Sibahara, K., Ohsumi, K., Ooka, S., Watabe, H., et al. (2005), Establishment of a kit-negative cell line of melanocyte precursors from mouse neural crest cells. Pigment Cell Res, *18*, 188-95.

Kawakami, A. & Fisher, D. E. (2011), Key discoveries in melanocyte development. J Invest Dermatol, *131*, E2-4.

Kawasaki, A., Kumasaka, M., Satoh, A., Suzuki, M., Tamura, K., Goto, T., Asashima, M. & Yamamoto, H. (2008), Mitf contributes to melanosome distribution and melanophore dendricity. Pigment Cell Melanoma Res, *21*, 56-62.

Kelly, C., Chin, A. J., Leatherman, J. L., Kozlowski, D. J. & Weinberg, E. S. (2000), Maternally controlled (beta)-catenin-mediated signaling is required for organizer formation in the zebrafish. Development, *127*, 3899-911.

Kelsh, R. N. (2004), Genetics and evolution of pigment patterns in fish. Pigment Cell Res, *17*, 326-36.

Kelsh, R. N. (2006a), Sorting out Sox10 functions in neural crest development. Bioessays, *28*, 788-798.

Kelsh, R. N. (2006b), Sorting out Sox10 functions in neural crest development. Bioessays, *28*, 788-98.

Kelsh, R. N., Brand, M., Jiang, Y. J., Heisenberg, C. P., Lin, S., Haffter, P., Odenthal, J., Mullins, M. C., Van Eeden, F. J., Furutani-Seiki, M., et al. (1996a), Zebrafish pigmentation mutations and the processes of neural crest development. Development, *123*, 369-89.

Kelsh, R. N., Brand, M., Jiang, Y. J., Heisenberg, C. P., Lin, S., Haffter, P., Odenthal, J., Mullins, M. C., Van Eeden, F. J., Furutani-Seiki, M., et al. (1996b), Zebrafish pigmentation mutations and the processes of neural crest development. Development, *123*, 369-89.

Kelsh, R. N. & Eisen, J. S. (2000), The zebrafish colourless gene regulates development of non-ectomesenchymal neural crest derivatives. Development, *127*, 515-25.

Kelsh, R. N., Harris, M. L., Colanesi, S. & Erickson, C. A. (2009), Stripes and belly-spots -- a review of pigment cell morphogenesis in vertebrates. Semin Cell Dev Biol, *20*, 90-104.

Kelsh, R. N., Schmid, B. & Eisen, J. S. (2000), Genetic analysis of melanophore development in zebrafish embryos. Dev Biol, *225*, 277-93.

Kelso, A., Groves, P., Ramm, L. & Doyle, A. G. (1999), Single-cell analysis by RT-PCR reveals differential expression of multiple type 1 and 2 cytokine genes among cells within polarized CD4+ T cell populations. Int Immunol, *11*, 617-21.

Kido, K., Sumimoto, H., Asada, S., Okada, S. M., Yaguchi, T., Kawamura, N., Miyagishi, M., Saida, T. & Kawakami, Y. (2009), Simultaneous suppression of MITF and BRAF V600E enhanced inhibition of melanoma cell proliferation. Cancer Sci, *100*, 1863-9.

Kim, C. H., Oda, T., Itoh, M., Jiang, D., Artinger, K. B., Chandrasekharappa, S. C., Driever, W. & Chitnis, A. B. (2000a), Repressor activity of Headless/Tcf3 is essential for vertebrate head formation. Nature, *407*, 913-6.

Kim, J., Lo, L., Dormand, E. & Anderson, D. J. (2003), SOX10 maintains multipotency and inhibits neuronal differentiation of neural crest stem cells. Neuron, *38*, 17-31.

Kim, J., Lu, J. & Quinn, P. G. (2000b), Distinct cAMP response element-binding protein (CREB) domains stimulate different steps in a concerted mechanism of transcription activation. Proc Natl Acad Sci U S A, *97*, 11292-6.

Kim, J. H., Sohn, K. C., Choi, T. Y., Kim, M. Y., Ando, H., Choi, S. J., Kim, S., Lee, Y. H., Lee, J. H., Kim, C. D., et al. (2010), Beta-catenin regulates melanocyte dendricity through the modulation of PKCzeta and PKCdelta. Pigment Cell Melanoma Res, *23*, 385-93.

Kim, S., Kim, S. H., Kim, H., Chung, A. Y., Cha, Y. I., Kim, C. H., Huh, T. L. & Park, H. C. (2008), Frizzled 8a function is required for oligodendrocyte development in the zebrafish spinal cord. Dev Dyn, *237*, 3324-31.

Kimmel, C. B., Ballard, W. W., Kimmel, S. R., Ullmann, B. & Schilling, T. F. (1995), Stages of embryonic development of the zebrafish. Dev Dyn, *203*, 253-310.

Klein, C. A., Zohlnhofer, D., Petat-Dutter, K. & Wendler, N. (2003), Gene expression analysis of a single or few cells. Curr Protoc Mol Biol, *Chapter 25*, Unit 25B 8.

Klein, P. S. & Melton, D. A. (1996), A molecular mechanism for the effect of lithium on development. Proc Natl Acad Sci U S A, *93*, 8455-9.

Klymkowsky, M. W., Rossi, C. C. & Artinger, K. B. (2010), Mechanisms driving neural crest induction and migration in the zebrafish and Xenopus laevis. Cell Adh Migr, *4*, 595-608.

Kofahl, B. & Wolf, J. (2010), Mathematical modelling of Wnt/beta-catenin signalling. Biochem Soc Trans, *38*, 1281-5.

Korinek, V., Barker, N., Morin, P. J., Van Wichen, D., De Weger, R., Kinzler, K. W., Vogelstein, B. & Clevers, H. (1997), Constitutive transcriptional activation by a beta-catenin-Tcf complex in APC-/- colon carcinoma. Science, *275*, 1784-7.

Kos, R., Reedy, M. V., Johnson, R. L. & Erickson, C. A. (2001), The winged-helix transcription factor FoxD3 is important for establishing the neural crest lineage and repressing melanogenesis in avian embryos. Development, *128*, 1467-79.

Kumasaka, M., Sato, S., Yajima, I., Goding, C. R. & Yamamoto, H. (2005), Regulation of melanoblast and retinal pigment epithelium development by Xenopus laevis Mitf. Dev Dyn, *234*, 523-34.

Kurimoto, K., Yabuta, Y., Ohinata, Y., Ono, Y., Uno, K. D., Yamada, R. G., Ueda, H. R. & Saitou, M. (2006), An improved single-cell cDNA amplification method for efficient high-density oligonucleotide microarray analysis. Nucleic Acids Res, *34*, e42.

La Porta, C. A. & Zapperi, S. (2012), Human breast and melanoma cancer stem cells biomarkers. Cancer Lett.

Labonne, C. & Bronner-Fraser, M. (1998), Neural crest induction in Xenopus: evidence for a two-signal model. Development, *125*, 2403-14.

Labonne, C. & Bronner-Fraser, M. (1999), Molecular mechanisms of neural crest formation. Annu Rev Cell Dev Biol, *15*, 81-112.

Labonne, C. & Bronner-Fraser, M. (2000), Snail-related transcriptional repressors are required in Xenopus for both the induction of the neural crest and its subsequent migration. Dev Biol, *221*, 195-205.

Lacosta, A. M., Canudas, J., Gonzalez, C., Muniesa, P., Sarasa, M. & Dominguez, L. (2007), Pax7 identifies neural crest, chromatophore lineages and pigment stem cells during zebrafish development. Int J Dev Biol, *51*, 327-31.

Lacosta, A. M., Muniesa, P., Ruberte, J., Sarasa, M. & Dominguez, L. (2005), Novel expression patterns of Pax3/Pax7 in early trunk neural crest and its melanocyte and non-melanocyte lineages in amniote embryos. Pigment Cell Res, *18*, 243-51.

Lamers, C. H., Rombout, J. W. & Timmermans, L. P. (1981), An experimental study on neural crest migration in Barbus conchonius (Cyprinidae, Teleostei), with special reference to the origin of the enteroendocrine cells. J Embryol Exp Morphol, *62*, 309-23.

Lang, D., Chen, F., Milewski, R., Li, J., Lu, M. M. & Epstein, J. A. (2000), Pax3 is required for enteric ganglia formation and functions with Sox10 to modulate expression of c-ret. J Clin Invest, *106*, 963-71.

Lang, D., Lu, M. M., Huang, L., Engleka, K. A., Zhang, M., Chu, E. Y., Lipner, S., Skoultchi, A., Millar, S. E. & Epstein, J. A. (2005), Pax3 functions at a nodal point in melanocyte stem cell differentiation. Nature, *433*, 884-7.

Larionov, A., Krause, A. & Miller, W. (2005), A standard curve based method for relative real time PCR data processing. BMC Bioinformatics, *6*, 62.

Le Douarin, N. (1980), Migration and differentiation of neural crest cells. Curr Top Dev Biol, *16*, 31-85.

Le Douarin, N. (2001), [The neural crest and evolution of vertebrates]. Bull Mem Acad R Med Belg, *156*, 521-31.

Le Douarin, N., Dulac, C., Dupin, E. & Cameron-Curry, P. (1991), Glial cell lineages in the neural crest. Glia, *4*, 175-84.

Le Douarin, N. A. K., C. (1999), The Neural Crest. *Cambridge University Press.*

Le Douarin, N. M. (2008), Developmental patterning deciphered in avian chimeras. Dev Growth Differ, *50 Suppl 1*, S11-28.

Le Douarin, N. M., Creuzet, S., Couly, G. & Dupin, E. (2004), Neural crest cell plasticity and its limits. Development, *131*, 4637-50.

Le Douarin, N. M. & Dupin, E. (2003), Multipotentiality of the neural crest. Curr Opin Genet Dev, *13*, 529-36.

Le Douarin, N. M., Dupin, E. & Ziller, C. (1994), Genetic and epigenetic control in neural crest development. Curr Opin Genet Dev, *4*, 685-95.

Lee, B. W., Schwartz, R. A., Hercogova, J., Valle, Y. & Lotti, T. M. (2012), Vitiligo road map. Dermatol Ther, *25 Suppl 1*, S44-56.

Lee, H. C., Tsai, J. N., Liao, P. Y., Tsai, W. Y., Lin, K. Y., Chuang, C. C., Sun, C. K., Chang, W. C. & Tsai, H. J. (2007), Glycogen synthase kinase 3 alpha and 3 beta have distinct functions during cardiogenesis of zebrafish embryo. BMC Dev Biol, *7*, 93.

Lee, H. Y., Kleber, M., Hari, L., Brault, V., Suter, U., Taketo, M. M., Kemler, R. & Sommer, L. (2004), Instructive role of Wnt/beta-catenin in sensory fate specification in neural crest stem cells. Science, *303*, 1020-3.

Lee, M., Goodall, J., Verastegui, C., Ballotti, R. & Goding, C. R. (2000), Direct regulation of the Microphthalmia promoter by Sox10 links Waardenburg-Shah syndrome (WS4)-associated hypopigmentation and deafness to WS2. J Biol Chem, *275*, 37978-83.

Lei, J. (2009), Stochasticity in single gene expression with both intrinsic noise and fluctuation in kinetic parameters. J Theor Biol, *256*, 485-92.

Levsky, J. M. & Singer, R. H. (2003), Gene expression and the myth of the average cell. Trends Cell Biol, *13*, 4-6.

Levy, C., Khaled, M., Robinson, K. C., Veguilla, R. A., Chen, P. H., Yokoyama, S., Makino, E., Lu, J., Larue, L., Beermann, F., et al. (2011), Lineage-specific transcriptional regulation of DICER by MITF in melanocytes. Cell, *141*, 994-1005.

Lewis, J. L., Bonner, J., Modrell, M., Ragland, J. W., Moon, R. T., Dorsky, R. I. & Raible, D. W. (2004), Reiterated Wnt signaling during zebrafish neural crest development. Development, *131*, 1299-308.

Li, G. W. & Xie, X. S. (2011), Central dogma at the single-molecule level in living cells. Nature, *475*, 308-15.

Li, X., Zhao, X., Fang, Y., Jiang, X., Duong, T., Fan, C., Huang, C. C. & Kain, S. R. (1998), Generation of destabilized green fluorescent protein as a transcription reporter. J Biol Chem, *273*, 34970-5.

Li, Y., Zhu, X., Yang, L., Li, J., Lian, Z., Li, N. & Deng, X. (2010), Expression and network analysis of genes related to melanocyte development in the Silky Fowl and White Leghorn embryos. Mol Biol Rep, *38*, 1433-41.

Liang, H., Fekete, D. M. & Andrisani, O. M. (2011), CtBP2 downregulation during neural crest specification induces expression of Mitf and REST, resulting in melanocyte differentiation and sympathoadrenal lineage suppression. Mol Cell Biol, *31*, 955-70.

Ling, D. & Salvaterra, P. M. (2011), Robust RT-qPCR data normalization: validation and selection of internal reference genes during post-experimental data analysis. PLoS One, *6*, e17762.

Lipniacki, T., Paszek, P., Marciniak-Czochra, A., Brasier, A. R. & Kimmel, M. (2006), Transcriptional stochasticity in gene expression. J Theor Biol, *238*, 348-67.

Lister, J. A. (2012), Melanocytes and melanoma: hooked on elongation. Pigment Cell Melanoma Res, *24*, 397-8.

Lister, J. A., Close, J. & Raible, D. W. (2001), Duplicate mitf genes in zebrafish: complementary expression and conservation of melanogenic potential. Dev Biol, *237*, 333-44.

Lister, J. A., Cooper, C., Nguyen, K., Modrell, M., Grant, K. & Raible, D. W. (2006), Zebrafish Foxd3 is required for development of a subset of neural crest derivatives. Dev Biol, *290*, 92-104.

Lister, J. A., Robertson, C. P., Lepage, T., Johnson, S. L. & Raible, D. W. (1999), nacre encodes a zebrafish microphthalmia-related protein that regulates neural-crest-derived pigment cell fate. Development, *126*, 3757-67.

Liu, X., Long, F., Peng, H., Aerni, S. J., Jiang, M., Sanchez-Blanco, A., Murray, J. I., Preston, E., Mericle, B., Batzoglou, S., et al. (2009), Analysis of cell fate from single-cell gene expression profiles in C. elegans. Cell, *139*, 623-33.

Livak, K. J. & Schmittgen, T. D. (2001), Analysis of relative gene expression data using real-time quantitative PCR and the 2(-Delta Delta C(T)) Method. Methods, *25*, 402-8.

Lopes, S. S., Yang, X., Muller, J., Carney, T. J., Mcadow, A. R., Rauch, G. J., Jacoby, A. S., Hurst, L. D., Delfino-Machin, M., Haffter, P., et al. (2008), Leukocyte tyrosine kinase functions in pigment cell development. PLoS Genet, *4*, e1000026.

Lucky, P. A. & Nordlund, J. J. (1985), The biology of the pigmentary system and its disorders. Dermatol Clin, *3*, 197-216.

M.Sriram Iyengar, P. (2011), Symbolic Systems Biology, Theory and Methods. Sudbury, Mass. : Jones and Bartlett Learning.

Ma, L., Swalla, B. J., Zhou, J., Dobias, S. L., Bell, J. R., Chen, J., Maxson, R. E. & Jeffery, W. R. (1996), Expression of an Msx homeobox gene in ascidians: insights into the archetypal chordate expression pattern. Dev Dyn, *205*, 308-18.

Mansky, K. C., Sankar, U., Han, J. & Ostrowski, M. C. (2002), Microphthalmia transcription factor is a target of the p38 MAPK pathway in response to receptor activator of NF-kappa B ligand signaling. J Biol Chem, *277*, 11077-83.

Mao, L. & Resat, H. (2004), Probabilistic representation of gene regulatory networks. Bioinformatics, *20*, 2258-69.

Marchant, L., Linker, C., Ruiz, P., Guerrero, N. & Mayor, R. (1998), The inductive properties of mesoderm suggest that the neural crest cells are specified by a BMP gradient. Dev Biol, *198*, 319-29.

Maresca, V., Flori, E., Bellei, B., Aspite, N., Kovacs, D. & Picardo, M. (2010), MC1R stimulation by alpha-MSH induces catalase and promotes its re-distribution to the cell periphery and dendrites. Pigment Cell Melanoma Res, *23*, 263-75.

Marklund, L., Moller, M. J., Sandberg, K. & Andersson, L. (1996), A missense mutation in the gene for melanocyte-stimulating hormone receptor (MC1R) is associated with the chestnut coat color in horses. Mamm Genome, *7*, 895-9.

Mayor, R., Morgan, R. & Sargent, M. G. (1995), Induction of the prospective neural crest of Xenopus. Development, *121*, 767-77.

Mayor, R., Young, R. & Vargas, A. (1999), Development of neural crest in Xenopus. Curr Top Dev Biol, *43*, 85-113.

Mcadams, H. H. & Arkin, A. (1997), Stochastic mechanisms in gene expression. Proc Natl Acad Sci U S A, *94*, 814-9.

Mcgill, G. G., Horstmann, M., Widlund, H. R., Du, J., Motyckova, G., Nishimura, E. K., Lin, Y. L., Ramaswamy, S., Avery, W., Ding, H. F., et al. (2002), Bcl2 regulation by the melanocyte master regulator Mitf modulates lineage survival and melanoma cell viability. Cell, *109*, 707-18.

Mcmahon, A. P. & Bradley, A. (1990), The Wnt-1 (int-1) proto-oncogene is required for development of a large region of the mouse brain. Cell, *62*, 1073-85.

Mellgren, E. M. & Johnson, S. L. (2004), A requirement for kit in embryonic zebrafish melanocyte differentiation is revealed by melanoblast delay. Dev Genes Evol, *214*, 493-502.

Metz, J. R., Peters, J. J. & Flik, G. (2006), Molecular biology and physiology of the melanocortin system in fish: a review. Gen Comp Endocrinol, *148*, 150-62.

Meulemans, D. & Bronner-Fraser, M. (2004), Gene-regulatory interactions in neural crest evolution and development. Dev Cell, *7*, 291-9.

Minchin, J. E. & Hughes, S. M. (2008), Sequential actions of Pax3 and Pax7 drive xanthophore development in zebrafish neural crest. Dev Biol, *317*, 508-22.

Mione, M. C. & Trede, N. S. (2010), The zebrafish as a model for cancer. Dis Model Mech, *3*, 517-23.

Monsoro-Burq, A. H., Wang, E. & Harland, R. (2005), Msx1 and Pax3 cooperate to mediate FGF8 and WNT signals during Xenopus neural crest induction. Dev Cell, *8*, 167-78.

Murisier, F., Guichard, S. & Beermann, F. (2007), The tyrosinase enhancer is activated by Sox10 and Mitf in mouse melanocytes. Pigment Cell Res, *20*, 173-84.

Nakagawa, S. & Takeichi, M. (1995), Neural crest cell-cell adhesion controlled by sequential and subpopulation-specific expression of novel cadherins. Development, *121*, 1321-32.

Narsinh, K. H., Sun, N., Sanchez-Freire, V., Lee, A. S., Almeida, P., Hu, S., Jan, T., Wilson, K. D., Leong, D., Rosenberg, J., et al. (2011), Single cell transcriptional profiling reveals heterogeneity of human induced pluripotent stem cells. J Clin Invest, *121*, 1217-21.

Naysmith, L., Waterston, K., Ha, T., Flanagan, N., Bisset, Y., Ray, A., Wakamatsu, K., Ito, S. & Rees, J. L. (2004), Quantitative measures of the effect of the melanocortin 1 receptor on human pigmentary status. J Invest Dermatol, *122*, 423-8.

Nelson, W. J. & Nusse, R. (2004), Convergence of Wnt, beta-catenin, and cadherin pathways. Science, *303*, 1483-7.

Nikaido, M., Law, E. W. & Kelsh, R. N. (2013), A Systematic Survey of Expression and Function of Zebrafish frizzled Genes. PLoS One, *8*, e54833.

Nishimura, E. K., Jordan, S. A., Oshima, H., Yoshida, H., Osawa, M., Moriyama, M., Jackson, I. J., Barrandon, Y., Miyachi, Y. & Nishikawa, S. (2002), Dominant role of the niche in melanocyte stem-cell fate determination. Nature, *416*, 854-60.

Novak, A. & Dedhar, S. (1999), Signaling through beta-catenin and Lef/Tcf. Cell Mol Life Sci, *56*, 523-37.

Nygaard, V., Holden, M., Loland, A., Langaas, M., Myklebost, O. & Hovig, E. (2005), Limitations of mRNA amplification from small-size cell samples. BMC Genomics, *6*, 147.

Odenthal, J., Rossnagel, K., Haffter, P., Kelsh, R. N., Vogelsang, E., Brand, M., Van Eeden, F. J., Furutani-Seiki, M., Granato, M., Hammerschmidt, M., et al. (1996), Mutations affecting xanthophore pigmentation in the zebrafish, Danio rerio. Development, *123*, 391-8.

Olsson, M. J. & Juhlin, L. (2002), Long-term follow-up of leucoderma patients treated with transplants of autologous cultured melanocytes, ultrathin epidermal sheets and basal cell layer suspension. Br J Dermatol, *147*, 893-904.

Osawa, M., Egawa, G., Mak, S. S., Moriyama, M., Freter, R., Yonetani, S., Beermann, F. & Nishikawa, S. (2005), Molecular characterization of melanocyte stem cells in their niche. Development, *132*, 5589-99.

Oshima, N. (2001), Direct reception of light by chromatophores of lower vertebrates. Pigment Cell Res, *14*, 312-9.

Parichy, D. M., Mellgren, E. M., Rawls, J. F., Lopes, S. S., Kelsh, R. N. & Johnson, S. L. (2000a), Mutational analysis of endothelin receptor b1 (rose) during neural crest and pigment pattern development in the zebrafish danio rerio. Dev Biol, *227*, 294-306.

Parichy, D. M., Ransom, D. G., Paw, B., Zon, L. I. & Johnson, S. L. (2000b), An orthologue of the kit-related gene fms is required for development of neural crest-derived xanthophores and a subpopulation of adult melanocytes in the zebrafish, Danio rerio. Development, *127*, 3031-44.

Parichy, D. M., Rawls, J. F., Pratt, S. J., Whitfield, T. T. & Johnson, S. L. (1999), Zebrafish sparse corresponds to an orthologue of c-kit and is required for the morphogenesis of a subpopulation of melanocytes, but is not essential for hematopoiesis or primordial germ cell development. Development, *126*, 3425-36.

Pathy, A. L., Helm, T. N., Elston, D., Bergfeld, W. F. & Tuthill, R. J. (1993), Malignant melanoma arising in a blue nevus with features of pilar neurocristic hamartoma. J Cutan Pathol, *20*, 459-64.

Patton, E. E., Mathers, M. E. & Schartl, M. (2011), Generating and analyzing fish models of melanoma. Methods Cell Biol, *105*, 339-66.

Patton, E. E. & Zon, L. I. (2005), Taking human cancer genes to the fish: a transgenic model of melanoma in zebrafish. Zebrafish, *1*, 363-8.

Paulsson, J. (2004), Summing up the noise in gene networks. Nature, *427*, 415-8.

Peccoud, J. & Jacob, C. (1996), Theoretical uncertainty of measurements using quantitative polymerase chain reaction. Biophys J, *71*, 101-8.

Pei, D. S., Sun, Y. H., Chen, S. P., Wang, Y. P., Hu, W. & Zhu, Z. Y. (2007), Zebrafish GAPDH can be used as a reference gene for expression analysis in cross-subfamily cloned embryos. Anal Biochem, *363*, 291-3.

Peixoto, A., Monteiro, M., Rocha, B. & Veiga-Fernandes, H. (2004), Quantification of multiple gene expression in individual cells. Genome Res, *14*, 1938-47.

Pfaffl, M. W. (2001), A new mathematical model for relative quantification in real-time RT-PCR. Nucleic Acids Res, *29*, e45.

Pfaffl, M. W. (2009), REST 2009 Software User Guide.

Phillips, J. K. & Lipski, J. (2000), Single-cell RT-PCR as a tool to study gene expression in central and peripheral autonomic neurones. Auton Neurosci, *86*, 1-12.

Phung, B., Sun, J., Schepsky, A., Steingrimsson, E. & Ronnstrand, L. (2011), C-KIT signaling depends on microphthalmia-associated transcription factor for effects on cell proliferation. PLoS One, *6*, e24064.

Pietrzak, A., Bartosinska, J., Hercogova, J., Lotti, T. M. & Chodorowska, G. (2012), Metabolic syndrome in vitiligo. Dermatol Ther, *25 Suppl 1*, S41-3.

Potterf, S. B., Furumura, M., Dunn, K. J., Arnheiter, H. & Pavan, W. J. (2000), Transcription factor hierarchy in Waardenburg syndrome: regulation of MITF expression by SOX10 and PAX3. Hum Genet, *107*, 1-6.

Potterf, S. B., Mollaaghababa, R., Hou, L., Southard-Smith, E. M., Hornyak, T. J., Arnheiter, H. & Pavan, W. J. (2001), Analysis of SOX10 function in neural crest-derived melanocyte development: SOX10-dependent transcriptional control of dopachrome tautomerase. Dev Biol, *237*, 245-57.

Prasad, M. S., Sauka-Spengler, T. & Labonne, C. (2012), Induction of the neural crest state: control of stem cell attributes by gene regulatory, post-transcriptional and epigenetic interactions. Dev Biol, *366*, 10-21.

Price, E. R., Horstmann, M. A., Wells, A. G., Weilbaecher, K. N., Takemoto, C. M., Landis, M. W. & Fisher, D. E. (1998), alpha-Melanocyte-stimulating hormone signaling regulates expression of microphthalmia, a gene deficient in Waardenburg syndrome. J Biol Chem, *273*, 33042-7.

Price, L. H. & Heninger, G. R. (1994), Lithium in the treatment of mood disorders. N Engl J Med, *331*, 591-8.

Quaranta, V. & Garbett, S. P. (2010), Not all noise is waste. Nat Methods, *7*, 269-72.

Quigley, I. K. & Parichy, D. M. (2002), Pigment pattern formation in zebrafish: a model for developmental genetics and the evolution of form. Microsc Res Tech, *58*, 442-55.

Raible, D. W., Wood, A., Hodsdon, W., Henion, P. D., Weston, J. A. & Eisen, J. S. (1992), Segregation and early dispersal of neural crest cells in the embryonic zebrafish. Dev Dyn, *195*, 29-42.

Raj, A. & Van Oudenaarden, A. (2008), Nature, nurture, or chance: stochastic gene expression and its consequences. Cell, *135*, 216-26.

Raser, J. M. & O'shea, E. K. (2004), Control of stochasticity in eukaryotic gene expression. Science, *304*, 1811-4.

Raser, J. M. & O'shea, E. K. (2005), Noise in gene expression: origins, consequences, and control. Science, *309*, 2010-3.

Rawls, J. F. & Johnson, S. L. (2003), Temporal and molecular separation of the kit receptor tyrosine kinase's roles in zebrafish melanocyte migration and survival. Dev Biol, *262*, 152-61.

Real, C., Glavieux-Pardanaud, C., Le Douarin, N. M. & Dupin, E. (2006), Clonally cultured differentiated pigment cells can dedifferentiate and generate multipotent progenitors with self-renewing potential. Dev Biol, *300*, 656-69.

Rebecca, V. W., Sondak, V. K. & Smalley, K. S. (2012), A brief history of melanoma: from mummies to mutations. Melanoma Res, *22*, 114-22.

Roberts, E., Magis, A., Ortiz, J. O., Baumeister, W. & Luthey-Schulten, Z. (2011), Noise contributions in an inducible genetic switch: a whole-cell simulation study. PLoS Comput Biol, *7*, e1002010.

Rodrigues, F. S., Doughton, G., Yang, B. & Kelsh, R. N. (2012), A novel transgenic line using the Cre-lox system to allow permanent lineage-labeling of the zebrafish neural crest. Genesis.

Roose, J., Molenaar, M., Peterson, J., Hurenkamp, J., Brantjes, H., Moerer, P., Van De Wetering, M., Destree, O. & Clevers, H. (1998), The Xenopus Wnt effector XTcf-3 interacts with Groucho-related transcriptional repressors. Nature, *395*, 608-12.

Rubinfeld, B., Robbins, P., El-Gamil, M., Albert, I., Porfiri, E. & Polakis, P. (1997), Stabilization of beta-catenin by genetic defects in melanoma cell lines. Science, *275*, 1790-2.

Rutledge, R. G. & Cote, C. (2003), Mathematics of quantitative kinetic PCR and the application of standard curves. Nucleic Acids Res, *31*, e93.

Saha, B., Singh, S. K., Sarkar, C., Bera, R., Ratha, J., Tobin, D. J. & Bhadra, R. (2006), Activation of the Mitf promoter by lipid-stimulated activation of p38-stress signalling to CREB. Pigment Cell Res, *19*, 595-605.

Saint-Jeannet, J. P., He, X., Varmus, H. E. & Dawid, I. B. (1997a), Regulation of dorsal fate in the neuraxis by Wnt-1 and Wnt-3a. Proc Natl Acad Sci U S A, *94*, 13713-8.

Saint-Jeannet, J. P., He, X., Varmus, H. E. & Dawid, I. B. (1997b), Regulation of dorsal fate in the neuraxis by Wnt-1 and Wnt-3a. Proc Natl Acad Sci U S A, *94*, 13713-8.

Saito, H., Yasumoto, K., Takeda, K., Takahashi, K., Fukuzaki, A., Orikasa, S. & Shibahara, S. (2002), Melanocyte-specific microphthalmia-associated transcription factor isoform activates its own gene promoter through physical interaction with lymphoid-enhancing factor 1. J Biol Chem, *277*, 28787-94.

Saito, H., Yasumoto, K., Takeda, K., Takahashi, K., Yamamoto, H. & Shibahara, S. (2003), Microphthalmia-associated transcription factor in the Wnt signaling pathway. Pigment Cell Res, *16*, 261-5.

Sambrook, J., Russell,D (2001), Molecular Cloning: A Laboratory Manual. .

Santoriello, C., Anelli, V., Alghisi, E. & Mione, M. (2012), Highly penetrant melanoma in a zebrafish model is independent of ErbB3b signaling. Pigment Cell Melanoma Res, *25*, 287-9.

Sato, S., Tanaka, M., Miura, H., Ikeo, K., Gojobori, T., Takeuchi, T. & Yamamoto, H. (2001), Functional conservation of the promoter regions of vertebrate tyrosinase genes. J Investig Dermatol Symp Proc, *6*, 10-8.

Sauka-Spengler, T. & Bronner-Fraser, M. (2006), Development and evolution of the migratory neural crest: a gene regulatory perspective. Curr Opin Genet Dev, *16*, 360-6.

Sauka-Spengler, T. & Bronner-Fraser, M. (2008a), Evolution of the neural crest viewed from a gene regulatory perspective. Genesis, *46*, 673-82.

Sauka-Spengler, T. & Bronner-Fraser, M. (2008b), A gene regulatory network orchestrates neural crest formation. Nat Rev Mol Cell Biol, *9*, 557-68.

Schatton, T. & Frank, M. H. (2008), Cancer stem cells and human malignant melanoma. Pigment Cell Melanoma Res, *21*, 39-55.

Schepsky, A., Bruser, K., Gunnarsson, G. J., Goodall, J., Hallsson, J. H., Goding, C. R., Steingrimsson, E. & Hecht, A. (2006), The microphthalmia-associated transcription factor Mitf interacts with beta-catenin to determine target gene expression. Mol Cell Biol, *26*, 8914-27.

Schilling, T. F., Piotrowski, T., Grandel, H., Brand, M., Heisenberg, C. P., Jiang, Y. J., Beuchle, D., Hammerschmidt, M., Kane, D. A., Mullins, M. C., et al. (1996), Jaw and branchial arch mutants in zebrafish I: branchial arches. Development, *123*, 329-44.

Schlitt, T. & Brazma, A. (2007), Current approaches to gene regulatory network modelling. BMC Bioinformatics, *8 Suppl 6*, S9.

Schneider, R. A. (1999), Neural crest can form cartilages normally derived from mesoderm during development of the avian head skeleton. Dev Biol, *208*, 441-55.

Schneider, S., Steinbeisser, H., Warga, R. M. & Hausen, P. (1996), Beta-catenin translocation into nuclei demarcates the dorsalizing centers in frog and fish embryos. Mech Dev, *57*, 191-8.

Schulz, D. J., Goaillard, J. M. & Marder, E. E. (2007), Quantitative expression profiling of identified neurons reveals cell-specific constraints on highly variable levels of gene expression. Proc Natl Acad Sci U S A, *104*, 13187-91.

Schumacher, J. A., Hashiguchi, M., Nguyen, V. H. & Mullins, M. C. (2011), An intermediate level of BMP signaling directly specifies cranial neural crest progenitor cells in zebrafish. PLoS ONE, *6*, e27403.

Serbedzija, G. N., Fraser, S. E. & Bronner-Fraser, M. (1990), Pathways of trunk neural crest cell migration in the mouse embryo as revealed by vital dye labelling. Development, *108*, 605-12.

Sestakova, B., Ondrusova, L. & Vachtenheim, J. (2010), Cell cycle inhibitor p21/ WAF1/ CIP1 as a cofactor of MITF expression in melanoma cells. Pigment Cell Melanoma Res, *23*, 238-51.

Shibahara, S., Takeda, K., Yasumoto, K., Udono, T., Watanabe, K., Saito, H. & Takahashi, K. (2001), Microphthalmia-associated transcription factor (MITF): multiplicity in structure, function, and regulation. J Investig Dermatol Symp Proc, *6*, 99-104.

Sieber-Blum, M. & Hu, Y. (2008), Epidermal neural crest stem cells (EPI-NCSC) and pluripotency. Stem Cell Rev, *4*, 256-60.

Sineva, G. S. & Pospelov, V. A. (2010), Inhibition of GSK3beta enhances both adhesive and signalling activities of beta-catenin in mouse embryonic stem cells. Biol Cell, *102*, 549-60.

Sommer, L. (2011), Generation of melanocytes from neural crest cells. Pigment Cell Melanoma Res, *24*, 411-21.

Southard-Smith, E. M., Angrist, M., Ellison, J. S., Agarwala, R., Baxevanis, A. D., Chakravarti, A. & Pavan, W. J. (1999), The Sox10(Dom) mouse: modeling the genetic variation of Waardenburg-Shah (WS4) syndrome. Genome Res, *9*, 215-25.

Southard-Smith, E. M., Kos, L. & Pavan, W. J. (1998), Sox10 mutation disrupts neural crest development in Dom Hirschsprung mouse model. Nat Genet, *18*, 60-4.

Stachel, S. E., Grunwald, D. J. & Myers, P. Z. (1993), Lithium perturbation and goosecoid expression identify a dorsal specification pathway in the pregastrula zebrafish. Development, *117*, 1261-74.

Stahlberg, A. & Bengtsson, M. (2010), Single-cell gene expression profiling using reverse transcription quantitative real-time PCR. Methods, *50*, 282-8.

Staroscik, A. (2004), Calculator for determining the number of copies of a template.

Steingrimsson, E., Copeland, N. G. & Jenkins, N. A. (2004), Melanocytes and the Microphthalmia Transcription Factor Network. Annu Rev Genet, *38*, 365-411.

Stemple, D. L. & Anderson, D. J. (1992), Isolation of a stem cell for neurons and glia from the mammalian neural crest. Cell, *71*, 973-85.

Steuerwald, N., Cohen, J., Herrera, R. J. & Brenner, C. A. (1999), Analysis of gene expression in single oocytes and embryos by real-time rapid cycle fluorescence monitored RT-PCR. Mol Hum Reprod, *5*, 1034-9.

Steventon, B. & Mayor, R. (2012), Early neural crest induction requires an initial inhibition of Wnt signals. Dev Biol, *365*, 196-207.

Stewart, R. A., Arduini, B. L., Berghmans, S., George, R. E., Kanki, J. P., Henion, P. D. & Look, A. T. (2006), Zebrafish foxd3 is selectively required for neural crest specification, migration and survival. Dev Biol, *292*, 174-88.

Stolovicki, E. & Braun, E. (2011), Collective dynamics of gene expression in cell populations. PLoS One, *6*, e20530.

Summers, C. G. (2009), Albinism: classification, clinical characteristics, and recent findings. Optom Vis Sci, *86*, 659-62.

Tachibana, M., Takeda, K., Nobukuni, Y., Urabe, K., Long, J. E., Meyers, K. A., Aaronson, S. A. & Miki, T. (1996), Ectopic expression of MITF, a gene for Waardenburg syndrome type 2, converts fibroblasts to cells with melanocyte characteristics. Nat Genet, *14*, 50-4.

Takada, S., Stark, K. L., Shea, M. J., Vassileva, G., Mcmahon, J. A. & Mcmahon, A. P. (1994), Wnt-3a regulates somite and tailbud formation in the mouse embryo. Genes Dev, *8*, 174-89.

Takahashi, A. & Kawauchi, H. (2006), Evolution of melanocortin systems in fish. Gen Comp Endocrinol, *148*, 85-94.

Takeda, K., Yasumoto, K., Takada, R., Takada, S., Watanabe, K., Udono, T., Saito, H., Takahashi, K. & Shibahara, S. (2000a), Induction of melanocyte-specific microphthalmia-associated transcription factor by Wnt-3a. J Biol Chem, *275*, 14013-6.

Takeda, K., Yasumoto, K., Takada, R., Takada, S., Watanabe, K., Udono, T., Saito, H., Takahashi, K. & Shibahara, S. (2000b), Induction of melanocyte-specific microphthalmia-associated transcription factor by Wnt-3a. J Biol Chem, *275*, 14013-6.

Tang, F., Hajkova, P., Barton, S. C., O'carroll, D., Lee, C., Lao, K. & Surani, M. A. (2006), 220-plex microRNA expression profile of a single cell. Nat Protoc, *1*, 1154-9.

Taniguchi, K., Kajiyama, T. & Kambara, H. (2009), Quantitative analysis of gene expression in a single cell by qPCR. Nat Methods, *6*, 503-6.

Theveneau, E. & Mayor, R. (2012), Neural crest delamination and migration: from epithelium-to-mesenchyme transition to collective cell migration. Dev Biol, *366*, 34-54.

Thiery, J. P., Duband, J. L. & Delouvee, A. (1982), Pathways and mechanisms of avian trunk neural crest cell migration and localization. Dev Biol, *93*, 324-43.

Thisse, B., Thisse, C (2004), Fast Release Clones: A High Throughput Expression Analysis.

Thisse, C. & Thisse, B. (2008), High-resolution in situ hybridization to whole-mount zebrafish embryos. Nat Protoc, *3*, 59-69.

Thomas, A. J. & Erickson, C. A. (2008), The making of a melanocyte: the specification of melanoblasts from the neural crest. Pigment Cell Melanoma Res, *21*, 598-610.

Thomas, A. J. & Erickson, C. A. (2009), FOXD3 regulates the lineage switch between neural crest-derived glial cells and pigment cells by repressing MITF through a non-canonical mechanism. Development, *136*, 1849-58.

Trentin, A., Glavieux-Pardanaud, C., Le Douarin, N. M. & Dupin, E. (2004), Self-renewal capacity is a widespread property of various types of neural crest precursor cells. Proc Natl Acad Sci U S A, *101*, 4495-500.

Tribulo, C., Aybar, M. J., Nguyen, V. H., Mullins, M. C. & Mayor, R. (2003), Regulation of Msx genes by a Bmp gradient is essential for neural crest specification. Development, *130*, 6441-52.

Tseng, A. S., Engel, F. B. & Keating, M. T. (2006), The GSK-3 inhibitor BIO promotes proliferation in mammalian cardiomyocytes. Chem Biol, *13*, 957-63.

Turner, B. M. (2000), Histone acetylation and an epigenetic code. Bioessays, *22*, 836-45.

Ungar, A. R. & Calvey, C. R. (2002), Zebrafish frizzled7b is expressed in prechordal mesoderm, brain and paraxial mesoderm. Mech Dev, *118*, 165-9.

Uong, A. & Zon, L. I. (2009), Melanocytes in development and cancer. J Cell Physiol, *222*, 38-41.

Van De Wetering, M., Cavallo, R., Dooijes, D., Van Beest, M., Van Es, J., Loureiro, J., Ypma, A., Hursh, D., Jones, T., Bejsovec, A., et al. (1997), Armadillo coactivates transcription driven by the product of the Drosophila segment polarity gene dTCF. Cell, *88*, 789-99.

Van Dyke, T. & Merlino, G. (2012), beta-catenin in metastatic melanoma--the smoking gun reloaded. Pigment Cell Melanoma Res, *25*, 125-6.

Van Lookeren Campagne, M. M., Wang, M., Spek, W., Peters, D. & Schaap, P. (1988), Lithium respecifies cyclic AMP-induced cell-type specific gene expression in Dictyostelium. Dev Genet, *9*, 589-96.

Van Otterloo, E., Li, W., Garnett, A., Cattell, M., Medeiros, D. M. & Cornell, R. A. (2012), Novel Tfap2-mediated control of soxE expression facilitated the evolutionary emergence of the neural crest. Development, *139*, 720-30.

Vanhaecke, T., Papeleu, P., Elaut, G. & Rogiers, V. (2004), Trichostatin A-like hydroxamate histone deacetylase inhibitors as therapeutic agents: toxicological point of view. Curr Med Chem, *11*, 1629-43.

Vassilatis, D. K., Hohmann, J. G., Zeng, H., Li, F., Ranchalis, J. E., Mortrud, M. T., Brown, A., Rodriguez, S. S., Weller, J. R., Wright, A. C., et al. (2003), The G protein-coupled receptor repertoires of human and mouse. Proc Natl Acad Sci U S A, *100*, 4903-8.

Vickaryous, M. K. & Sire, J. Y. (2009), The integumentary skeleton of tetrapods: origin, evolution, and development. J Anat, *214*, 441-64.

Villanueva, S., Glavic, A., Ruiz, P. & Mayor, R. (2002), Posteriorization by FGF, Wnt, and retinoic acid is required for neural crest induction. Dev Biol, *241*, 289-301.

Von Ahsen, N., Wittwer, C. T. & Schutz, E. (2001), Oligonucleotide melting temperatures under PCR conditions: nearest-neighbor corrections for Mg(2+), deoxynucleotide triphosphate, and dimethyl sulfoxide concentrations with comparison to alternative empirical formulas. Clin Chem, *47*, 1956-61.

Wacker, M. J., Tehel, M. M. & Gallagher, P. M. (2008), Technique for quantitative RT-PCR analysis directly from single muscle fibers. J Appl Physiol, *105*, 308-15.

Wada, S. & Saiga, H. (2002), HrzicN, a new Zic family gene of ascidians, plays essential roles in the neural tube and notochord development. Development, *129*, 5597-608.

Walker, M. B. & Trainor, P. A. (2006), Craniofacial malformations: intrinsic vs extrinsic neural crest cell defects in Treacher Collins and 22q11 deletion syndromes. Clin Genet, *69*, 471-9.

Wang, W. D., Melville, D. B., Montero-Balaguer, M., Hatzopoulos, A. K. & Knapik, E. W. (2011), Tfap2a and Foxd3 regulate early steps in the development of the neural crest progenitor population. Dev Biol, *360*, 173-85.

Wen, B., Chen, Y., Li, H., Wang, J., Shen, J., Ma, A., Qu, J., Bismuth, K., Debbache, J., Arnheiter, H., et al. (2010), Allele-specific genetic interactions between Mitf and Kit affect melanocyte development. Pigment Cell Melanoma Res, *23*, 441-7.

Westerfield, M. (2000), The zebrafish book. A guide for the laboratory use of zebrafish (Danio rerio). . *University of Oregon Press, Eugene.* .

Weston, J. A. (1970), The migration and differentiation of neural crest cells. Adv Morphog, *8*, 41-114.

White, R. M. & Zon, L. I. (2008), Melanocytes in development, regeneration, and cancer. Cell Stem Cell, *3*, 242-52.

Widlund, H. R. & Fisher, D. E. (2003), Microphthalamia-associated transcription factor: a critical regulator of pigment cell development and survival. Oncogene, *22*, 3035-41.

Winer, J., Jung, C. K., Shackel, I. & Williams, P. M. (1999), Development and validation of real-time quantitative reverse transcriptase-polymerase chain reaction for monitoring gene expression in cardiac myocytes in vitro. Anal Biochem, *270*, 41-9.

Wittwer, C. T., Ririe, K. M., Andrew, R. V., David, D. A., Gundry, R. A. & Balis, U. J. (1997), The LightCycler: a microvolume multisample fluorimeter with rapid temperature control. Biotechniques, *22*, 176-81.

Wong, M. L. & Medrano, J. F. (2005), Real-time PCR for mRNA quantitation. Biotechniques, *39*, 75-85.

Wu, D. Y., Ugozzoli, L., Pal, B. K., Qian, J. & Wallace, R. B. (1991), The effect of temperature and oligonucleotide primer length on the specificity and efficiency of amplification by the polymerase chain reaction. DNA Cell Biol, *10*, 233-8.

Wu, J., Yang, J. & Klein, P. S. (2005), Neural crest induction by the canonical Wnt pathway can be dissociated from anterior-posterior neural patterning in Xenopus. Dev Biol, *279*, 220-32.

Yajima, I., Kumasaka, M. Y., Thang, N. D., Goto, Y., Takeda, K., Iida, M., Ohgami, N., Tamura, H., Yamanoshita, O., Kawamoto, Y., et al. (2011), Molecular Network Associated with MITF in Skin Melanoma Development and Progression. J Skin Cancer, *2011*, 730170.

Yamaguchi, Y., Passeron, T., Watabe, H., Yasumoto, K., Rouzaud, F., Hoashi, T. & Hearing, V. J. (2007), The effects of dickkopf 1 on gene expression and Wnt signaling by melanocytes: mechanisms underlying its suppression of melanocyte function and proliferation. J Invest Dermatol, *127*, 1217-25.

Yancovitz, M., Litterman, A., Yoon, J., Ng, E., Shapiro, R. L., Berman, R. S., Pavlick, A. C., Darvishian, F., Christos, P., Mazumdar, M., et al. (2012), Intra- and inter-tumor heterogeneity of BRAF(V600E))mutations in primary and metastatic melanoma. PLoS One, *7*, e29336.

Yanfeng, W., Saint-Jeannet, J. P. & Klein, P. S. (2003), Wnt-frizzled signaling in the induction and differentiation of the neural crest. Bioessays, *25*, 317-25.

Yang, C. T. & Johnson, S. L. (2006), Small molecule-induced ablation and subsequent regeneration of larval zebrafish melanocytes. Development, *133*, 3563-73.

Yasumoto, K., Takeda, K., Saito, H., Watanabe, K., Takahashi, K. & Shibahara, S. (2002), Microphthalmia-associated transcription factor interacts with LEF-1, a mediator of Wnt signaling. Embo J, *21*, 2703-14.

Yost, C., Torres, M., Miller, J. R., Huang, E., Kimelman, D. & Moon, R. T. (1996), The axis-inducing activity, stability, and subcellular distribution of beta-catenin is regulated in Xenopus embryos by glycogen synthase kinase 3. Genes Dev, *10*, 1443-54.

Yuan, J. S., Reed, A., Chen, F. & Stewart, C. N., Jr. (2006), Statistical analysis of real-time PCR data. BMC Bioinformatics, *7*, 85.

Zhang, F., Phiel, C. J., Spece, L., Gurvich, N. & Klein, P. S. (2003), Inhibitory phosphorylation of glycogen synthase kinase-3 (GSK-3) in response to lithium. Evidence for autoregulation of GSK-3. J Biol Chem, *278*, 33067-77.

Zhang, J. & Byrne, C. D. (1997), A novel highly reproducible quantitative competitve RT PCR system. J Mol Biol, *274*, 338-52.

Zhu, K., Wang, H., Gul, Y., Zhao, Y., Wang, W., Liu, S. & Wang, M. (2011), Expression characterization and the promoter activity analysis of zebrafish hdac4. Fish Physiol Biochem.

Zhu, S., Wurdak, H., Wang, Y., Galkin, A., Tao, H., Li, J., Lyssiotis, C. A., Yan, F., Tu, B. P., Miraglia, L., et al. (2009), A genomic screen identifies TYRO3 as a MITF regulator in melanoma. Proc Natl Acad Sci U S A, *106*, 17025-30.

Ziegler, I. (2003), The pteridine pathway in zebrafish: regulation and specification during the determination of neural crest cell-fate. Pigment Cell Res, *16*, 172-82.

Appendices

Appendix 1

- **Evidence for the unsuitability of using a Mc1r morpholino (5'-AGTGATGGCGCGAAGAGTCGTTCAT-3') to test the role of the Mc1r pathway in melanocyte differentiation in zebrafish.**

Mc1r has been involved in pigmentation phenotypes in several species. In human, the pheomelanin:eumelanin ratio influences the skin's reaction to the sunlight resulting in the tanning reaction, as well as, changes in hair colour (Naysmith *et al.,* 2004). Activation or inhibition of Mc1r causes elevated or reduced levels of eumelanin and pheomelanin, respectively. In consequence, when the receptor is activated, a darker phenotype can be observed, and in contrast, inhibition of the receptor triggers a lighter phenotype (Garcia-Borron *et al.*, 2005, Benned-Jensen *et al.*, 2011). In mice, the cAMP levels regulate the activity of the melanogenic enzyme TYR in cells and therefore its controls the ratio eumelanin/pheomelanin in cells. In fish, Gross *et al.,* (2009) showed that Mc1r knockdown caused the reduction of melanisation in 48 hpf zebrafish. In horses, the chestnut coat colour has been shown to be associated with a single strand conformation polymorphism corresponding to a single missense mutation in the *mc1r* allele (Marklund *et al.,* 1996, Naysmith *et al.,* 2004, Metz *et al.,* 2006, Takahashi and Kawauchi, 2006). The Function of α-Msh in fish has most frequently been attributed to inducing rapid dispersal of melanin granules from clustering around the nucleus to dispersal throughout the cell body and dendritic extensions of the melanocytes (Metz *et al.,* 2006). Therefore, *mc1r* has also been shown to be involved in melanocyte differentiation as well as in regulation of the melanocyte shape and dendricity by regulating the production of catalase (Maresca *et al.*, 2010).

In contrast, in the blind Mexican cave fish *Astyanax mexicanus*, the brown phenotype was associated with reduced melanocyte pigmentation. This phenotype has been shown to be due to a 2-base-pair deletion in the extreme 5' end of the coding sequence, corresponding to the N-terminal domain of Mc1r (Gross *et al.*, 2009). In the study, Gross *et al.,* (2009) used the zebrafish model to recapitulate the brown phenotype observed in *Astyanax mexicanus.* Morpholino injections were used to knockdown the activity of Mc1r at one cell stage and the phenotype in melanocyte was observed in embryos at later stage. However, the post-translational knockdown of Mc1r by the morpholino was not assessed in cells so the functionality of the protein could not be estimated. Gross *et al.,* (2009) described a quantitative decrease of the melanin content in melanocyte and a decrease of eye pigmentation in embryos injected with the morpholino which were compared to control embryos. Because of its capacity to modulate the skin (and melanocyte) colouration in many species, but also because of its capacity to activate and regulate *Mitf*

expression, it is important to fully understand the role of *mc1r* in zebrafish, in melanocyte development

To confirm the results obtained by Gross *et al.,* (2009), and before further testing of the effects of Mc1r knockdown in *mitfa* expression in zebrafish, the experiments consisting of injecting Mc1r morpholino at 0.2 µM, were repeated by us. However, in contrast with the results related in Gross *et al.,* (2009), the staging of embryos was taken into account. Melanisation content changes rapidly and dynamically in embryos at early stages, therefore it is essential to compare embryos of the same stage to correctly analyse melanisation and pigment cell phenotypes. As there was no staged control in the Gross *et al.,* (2009) experiment, the first objective here, was to assess the pigmentation decrease phenotype by comparing the morpholino injected fish to a staged control embryo. If Mc1r was a crucial factor for melanin content modulation, or activation, blocking its activity should result in a marked decrease of cell pigmentation at 48 hpf, for example. The MO-Mc1r injected embryos showed developmental retardation compared to embryos injected with 0.2 µM non-sense construct at 48 hpf (data not shown). Head inclination, heart development and CNS development allowed to stage the injected embryos at 36 hpf (Kimmel *et al.,* 1995). Therefore, melanocyte pigmentation phenotype in morpholino injected embryos was not compared to 48 hpf embryos injected with the control non-sense construct, but instead, it was compared to the staged 36 hpf fish. Unexpectedly, comparing MO-Mc1r injected embryos to staged control embryos did not show any difference in melanocyte blackness, development or number. These results showed that the decrease of pigmentation observed in Gross *et al.,* (2009) was not clearly assessed. Furthermore, no test for activity of the morpholino was carried out, and consequently, it remains unclear if Mc1r could be important for melanocyte differentiation and pigmentation in fish.

Other mechanisms in cells could compensate for Mc1r knockdown by increasing the cAMP or MEK signalling for example. Indeed, the stress induced p38 pathway has also been involved with activation of the cAMP and the MEK pathways in melanocytes and it could be interesting to experimentally block or induce both MC1R and p38 pathways in embryos (Bellei *et al.*, 2010). This could be done by inducing Mc1r and p38 messengers ectopically in embryo, with or without, *sox10* and testing *mitfa* or *tyrosinase* expression. From this, an ectopic boost of expression when injecting both p38 and Mc1r.

Interestingly, *mc1r* has also been identified as a potential Mitfa target in microarray screens (Hoek *et al.,* 2008, Aoki and Moro, 2002). Further, comparing levels or *mc1r* in melanocyte in *mitfa* mutant to WT could show this interaction, suggesting the possibility of a regulatory loop activating *mitfa* expression. Other factors might be important for *mitfa* regulation and improving understanding of these factors will become a priority.

Appendix 2

- **Single cell qPCR results**

Three single cell samples (see Chapter 2, Material & Method for details of the method) could be analysed by RT-qPCR. Results are shown in Table A, and (Figure 7.01). Two of the cells show 322 and 275 copies of *dct* and the third shows 3087 copies of *dct*. These data on their own are not informative, and only give a sense of how many copies of the gene are detected at this exact time point. However, it would be interesting to collect more of these data for the four genes of interest (and more) at the five time points in order to provide numeric data for our mathematical modelling. More experimental optimisation would be required to improve the efficiency and the control of this experiment. More controls are required in order to test, by another method (e.g. single cell RT-nested PCR), the proportion of single cells expected to be positive for each gene. It would then be interesting to optimise the single cell RT-qPCR technique to match these results and inform us on expression levels for these genes in cells through specification and differentiation.

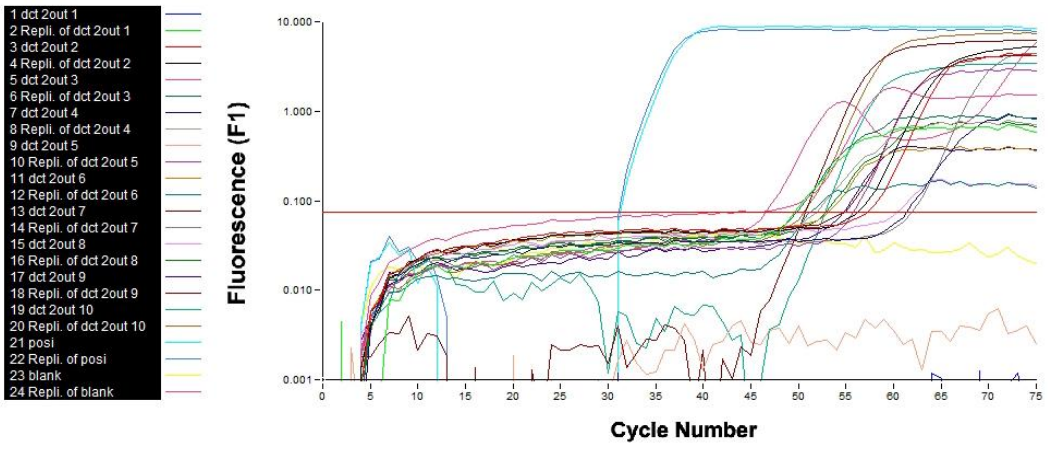

(A)

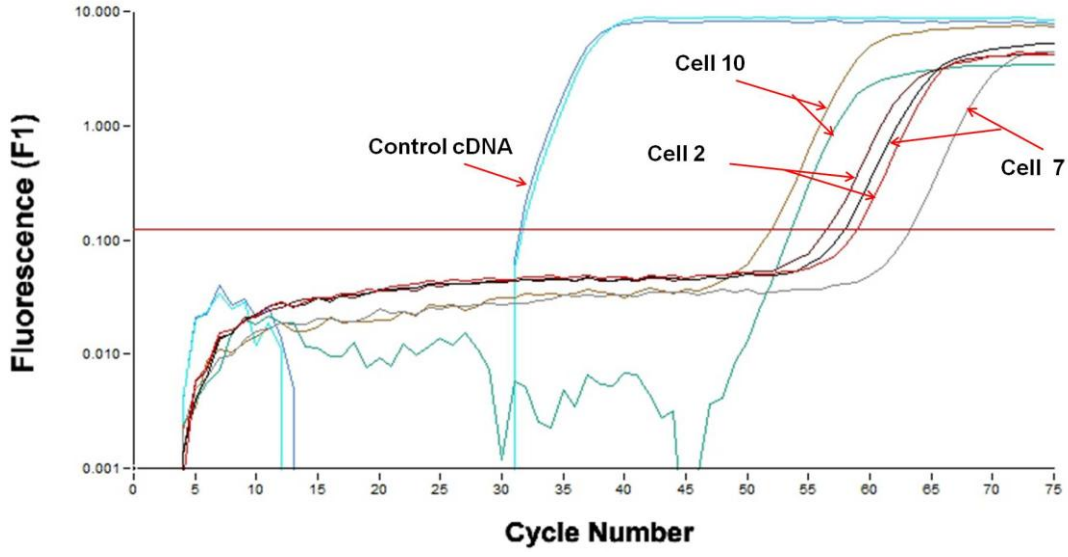

(B)

Figure 7.01: Single cell analysis of RT-qPCR looking at *dct* expression at 48 hpf.

Result of gene expression (*dct*) quantification in single melanocytes issued from 48 hpf zebrafish embryos. (A) Graph of Fluorescence signal (F1) as a function of the cycle number showing the *dct* amplification curve for each of the ten single cell samples in duplicate. The red line indicates the background levels. Three cells show the characteristic exponential linear increase of signal (cell 2, samples 3-4, cell 7, sample 13-14, cell 10,samples 19-20) the rest of samples do not . Graph showing the exponential linear increase of fluorescence signal (B) above the background (red line) for samples 3,4 (cell 2), 13,14 (cell 7), 19, 20 (cell 10) and the standard control (21,22). Cells 2, 7 and 10 show a clear exponential linear increase of signal

TABLE A: *dct* copy number in single cells at 48 hpf determined by qRT-PCR

Cell:	**2**	**7**	**10**
***dct* copy number**:	489	380	3364
	356	170	2811

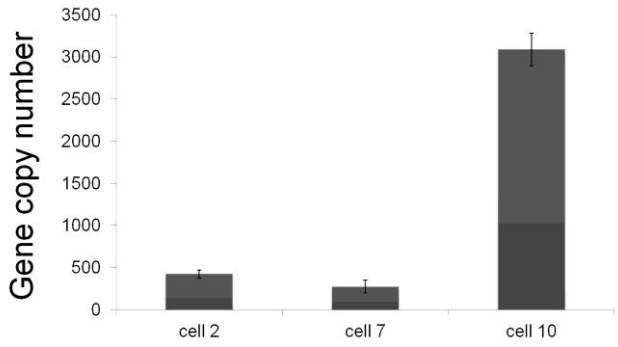

Figure 7.02: Graph related to TABLE A showing the *dct* copy number in single melanocytes at 48 hpf determined by qRT-PCR

dct copy number average in cell 2, 7 and 10 (± standard deviation).